Regulation of mitochondrial quality control in Parkinson's disease

Nicol Birsa

A thesis submitted to University College London for the degree of Doctor of Philosophy

15th September 2014

Department of Neuroscience, Physiology and Pharmacology
University College London

I, Nicol Birsa, confirm that the work presented in this thesis is my own. Where information has been derived from other sources, I confirm that this has been indicated in the thesis.

Abstract

Mitochondrial transport plays an important role in matching mitochondrial distribution to localised energy production and calcium buffering requirements. Miro is an outer mitochondrial membrane (OMM) protein that, via its interaction with the kinesin motors, mediates mitochondrial trafficking along the cytoskeletal tracks. Mitochondria, however, not only need to be delivered to specific cellular sites, but also need to be retrieved when not functional. PINK1 and Parkin are two Parkinson's disease (PD)-associated proteins that work in concert in a mitochondrial quality control system. PINK1 is a mitochondrial serine-threonine kinase generally present at low levels on the OMM. PINK1 selectively accumulates on the OMM of damaged mitochondria, and recruits Parkin, a cytosolic E3 ubiquitin ligase from the cytosol. Parkin then ubiquitinates several substrates on the OMM, leading to the initiation of mitophagy.

In this thesis Miro1 is shown to be a substrate of the PINK1/Parkin pathway in human dopaminergic neuroblastoma cells. Analysis of the kinetics of Miro1 ubiquitination, further demonstrates that mitochondrial damage triggers rapid K27-type ubiquitination of Miro1 on the OMM, dependent on PINK1 and Parkin. Proteasomal degradation of Miro1 is then seen on a slower timescale. Miro1 ubiquitination in dopaminergic neuroblastoma cells is found to be independent of Miro1 phosphorylation at serine 156, but dependent on the recently identified serine 65 residue within Parkin that is phosphorylated by PINK1. Interestingly, Miro1 can stabilise phospho-mutant versions of Parkin on the OMM, suggesting that Miro is also part of a Parkin receptor complex. These results provide new insights into the ubiquitination-dependent regulation of the Miro-mediated mitochondrial transport machinery by PINK1/Parkin and also suggest that disruption of this regulation may be implicated in PD pathogenesis.

Acknowledgements

I would like to thank Josef Kittler for being a great supervisor. Thank you for your support and enthusiasm throughout these four years. Thanks to all the present, past and honorary members of the Kittler lab, for discussion, help and for making the work in the lab much easier and fun. Thank you Nathalie for being such a good friend, for your constant support and occasional provision of gin. I really don't think we could have gone through that transfer report otherwise! Thank you Lorena, for your unlimited patience, help and for teaching me most of the molecular biology I know. Thank you Liz for teaching me lots and lots of English words, even though now I have to remember which ones are actually English and which ones are Liz-isms! Thank you Roz for helping with this project, proof reading this thesis and for your constant provision of music. And thanks Kate for teaching me that playing Lady Gaga results in better IP washes! Thanks Sheehan, because I know I can do things "on time" if you have to do them too. Thank you Sana. And thanks Georgina for your excellent PyMOL skills.

I also want to thank:

My friends at home: Annalisa, Anna, Mary, Jess, Pa and Roby. Thank you for always being there when I needed you.

And my Italian friends here: Vale, Fede, Mari and Elena.

My flatmates Ramona and Ellen. Thanks for your help and for coping with all the papers I left around the house.

Thank you to my mum and Walter.

And thank you to my dad.

And finally thank you Alessio. For being always present despite living in another country. For your incredible patience and constant support. And for spending the first long holiday in the last four years here, cooking for me, while I was writing this thesis.

This thesis is dedicated to my grandmother, nonna Rosa.

Publications

Publications related to this work:

Birsa N., Norkett R., Wauer T., Mevissen T.E., Wu H.C., Foltynie T., Bhatia K., Hirst W.D., Komander D., Plun-Favreau H., Kittler J.T. (2014) Lysine 27 ubiquitination of the mitochondrial transport protein Miro is dependent on serine 65 of the Parkin ubiquitin ligase. *Journal of Biological Chemistry.* 23; 289 (21): 14569-14582.

Other publications:

Birsa N., Norkett R., Higgs N., Lopez-Domenech G., Kittler J.T. (2013) Mitochondrial trafficking in neurons and the role of the Miro family of GTPase proteins. *Biochemical Society Transactions.* 41 (6): 1525-1531.

Contents

1 Introduction **18**

Mitochondrial structure 18

Oxidative phosphorylation and energy production 19

Mitochondria and calcium buffering 23

Mitochondria dynamics: fission and fusion 25

The mitochondrial transport machinery 28

Microtubule motor proteins 29

The kinesin motors 29

Kinesin adaptors 30

The dynein motors 31

Miro proteins 32

TRAKs 37

Static anchors 38

Mitochondria quality control 39

PINK1 40

The ubiquitination process 44

Parkin 45

PINK1 and Parkin in mitochondrial quality control 48

Regulators of Parkin recruitment onto damaged mitochondria 51

Mitophagy 53

Mitochondrial-derived vesicles (MDV) 55

PINK1 and Parkin independent mitophagy 57

Parkinson's disease 58

Aim of the thesis 60

2 Materials and Methods **61**

Antibodies 61

Constructs 62

Molecular Biology 63

Polimerase Chain Reaction (PCR) 63

Agarose gel 64

Digestion and purification 64

Ligation 64

Chemically competent cells 65

Transformation of competent cells 65

Site-directed mutagenesis by Reverse PCR 65
Maxi preparation of plasmid DNA 68
Molecular biology solutions 68
Cell culture 68
Cell lines 68
Neurons 69
Transient Transfection 70
Nucleofection (cell lines) 70
Electroporation 70
Calcium phosphate 70
Treatments 71
Cell culture media and reagents 72
Biochemistry 73
Cell lysis 73
Immunoprecipitation 73
Ubiquitin Chain Restriction (UbiCRest) Analysis 73
SDS-Polyacrylamide Gel Electrophoresis (PAGE) 74
PhosTag SDS-Polyacrylamide Gel Electrophoresis 74
Western blotting 75
Stripping 75
Biochemistry buffers and reagents 77

Immunofluorescence and Microscopy 77

Immunocytochemistry 77

Confocal Microscopy 78

Image processing 78

Immunohistochemistry solutions 78

Live cell imaging 79

Live imaging processing 79

Statistical analysis 80

3 Miro1 regulation by the ubiquitin ligase Parkin 81

Introduction 81

Results 83

PINK1 and Parkin regulate Miro loss upon mitochondrial damage in human dopaminergic neuroblastoma cells and fibroblasts 83

Ubiquitination of Miro by a PINK1 and Parkin complex upon mitochondrial damage 88

FCCP-dependent ubiquitination of endogenous Miro1/2 93

PINK1 dependency of Miro ubiquitination 93

Mitochondrial damage-dependent regulation of the interaction between Miro1 and the TRAKs 96

Discussion 99

4 Characterisation of Miro1 ubiquitination 103

Introduction . . . 103

Results . . . 105

Kinetics of Miro ubiquitination and degradation . . . 105

Miro1 degradation is VCP-independent . . . 108

Role of Miro1 phosphorylation in its damage-induced ubiquitination / degradation . . . 112

Contribution of Miro1 signalling domains in damage-induced Miro processing . . . 114

Lysine residues involved in Miro1 ubiquitination . . . 118

K27-type ubiquitination of Miro by a PINK1 and Parkin complex in dopaminergic neuroblastoma cells . . . 120

Discussion . . . 126

5 Parkin regulation and mitophagy 131

Introduction . . . 131

Results . . . 133

PINK1-dependent phosphorylation of Parkin on S65 results in impaired ligase function . . . 133

S65 on Parkin is important for the ligase recruitment to damaged mitochondria . . . 137

Role of Parkin S65 on mitochondrial trafficking . . . 149

Role of ubiquitin phosphorylation in Miro1 ubiquitination . . . 151

Discussion . . . 151

6 Final Discussion **157**

Summary 158

Mitochondrial damage-dependent regulation of the trafficking machinery . . . 159

Intracellular signalling leading to Miro ubiquitination 161

OMM proteins ubiquitination and mitophagy 163

Fusion and fission machinery 163

VDAC1 164

Miro 164

Minimal machinery required for the induction of mitophagy 166

Different types of mitophagy 168

FCCP model: advantages and disadvantages 168

Future directions 169

Concluding remarks 170

List of Figures

1.1 The mitochondrial compartments 20

1.2 Oxidative phosphorylation and the electron transport chain. 22

1.3 Mechanism of action of mitochondrial uncouplers. 24

1.4 The mitochondrial trafficking complex. 33

1.5 Mechanisms of mitochondrial arrest 36

1.6 Schematic of PINK1 and Parkin structure 43

1.7 Representation of a ubiquitin molecule structure. 46

1.8 Parkin ubiquitin alignment. 50

1.9 Model of PINK1-dependent Parkin activation and ubiquitination of mitochondrial proteins. 56

2.1 PCR protocol. 64

2.2 Oligonucleotide design for site directed mutagenesis. 66

3.1 Miro antibody characterisation. 84

3.2 Mitochondrial damage triggers Parkin-mediated Miro1 loss. 85

3.3 Miro1 loss is dependent on PINK1. 87

3.4 Miro1 degradation is impaired in patient-derived fibroblast lacking Parkin. 89

3.5 Miro1 interacts with the mitochondrial quality control proteins PINK1 and Parkin. 90

3.6 Miro1 is ubiquitinated by Parkin. 92

3.7 Miro1 ubiquitin chains are cleaved by vOTU and USP21. 94

3.8 Endogenous Miro1 is ubiquitinated upon mitochondrial damage. 95

3.9 Miro1 ubiquitination is dependent on the mitochondrial kinase PINK1. . 97

3.10 Mitochondrial damage regulation of Miro1 interaction with the TRAK proteins. 98

4.1 Temporal dynamics of Miro1 ubiquitination and degradation. 107

4.2 Miro1 degradation is blocked by proteasomal inhibition, but not by autophagy inhibition. 109

4.3 Mitochondrial damage-induced Miro1 degradation. 110

4.4 Quantification of FCCP-dependent ^{GFP}Miro1 loss from the OMM. . . . 111

4.5 Miro1 loss is VCP-independent. 113

4.6 Miro1 phosphorylation at S156 does not affect its ubiquitination dynamics. 115

4.7 S156 phosphorylation does not facilitate FCCP-dependent Miro1 ubiquitination/loss. 116

4.8 T298 T299 are not required for the regulation of FCCP-mediated Miro1 ubiquitination and loss. 117

4.9 Miro1 EF hand and GTPase domains do not influence the protein FCCP-induced ubiquitination. 119

4.10 Characterisation of allR ^{myc}Miro1. 121

4.11 Example of K-only and K-to-R ubiquitin mutants. 122

4.12 Analysis of Miro1 ubiquitin chains with K only ubiquitin mutants. . . . 123

4.13 Analysis of Miro1 ubiquitin chains with K-to-R ubiquitin mutants. . . . 125

4.14 DUB restriction analysis confirms K11, K27 and K29 contribution to Miro1 ubiquitin chains. 127

5.1 PhosTag™ technology. 135

5.2 Parkin is phosphorylated on S65. 136

5.3 Miro1 ubiquitination by Parkin S65 mutants in HeLa cells. 138

5.4 Miro1 ubiquitination by Parkin S65 mutants in neuronal SH-SY5Y cells. 139

5.5 The OMM protein TOM20 is stable after 1 hour FCCP treatment. . . . 140

5.6 Parkin mutants show delayed recruitment to damaged mitochondria after mitochondrial damage in HEK 293 cells. 142

5.7 Quantification of WT, S65A and S65E Parkin recruitment to damaged mitochondria in HEK 293 cells. 143

5.8 Miro1 facilitates the translocation of S65A and S65E Parkin mutants onto damaged mitochondria in HEK 293 cells. 144

5.9 WT, S65A and S65E ^{YFP}Parkin recruitment to damaged mitochondria after 2 hours FCCP treatment in HEK 293 cells overexpressing Miro1. . 145

5.10 Quantification of WT, S65A and S65E Parkin to damaged mitochondria in the presence of Miro1. 146

5.11 Miro1 promotes the translocation of S65E ^{YFP}Parkin onto damaged mitochondria in HeLa cells. 148

5.12 Regulation of mitochondrial trafficking by Parkin S65 mutants in hippocampal neurons. 150

5.13 Analysis of ubiquitin phospho-mutants incorporation in Miro1 ubiquitin chains. 152

6.1 Model of damage-dependent Miro1 processing and mitophagy initiation. 167

List of Tables

2.1 PCR reaction composition. 63

2.2 List of primers used for site-directed mutagenesis by reverse PCR. . . . 67

2.3 Bacterial culture and molecular biology solutions. 68

2.4 Cell culture and transfection solutions. 72

2.5 Cell lysis and biochemical assays buffers. 76

2.6 SDS-PAGE and western blotting buffers and solutions. 77

2.7 Immunohistochemistry solutions. 78

2.8 Live imaging solution. 79

Abbreviations

Ambra1	activating molecule in Beclin1 regulated autophagy
ATP	adenosine-5'-triphosphate
ATPIF1	ATPase inhibitory factor 1
BSA	bovine serum albumin
CMA	chaperone-mediated autophagy
CNS	central nervous system
DIV	days in vitro
DMEM	Dulbecco's Modified Eagle Medium
DMSO	dimethyl sulfoxide
Drp1	dynamin related protein 1
DUB	deubiquitinase
ER	endoplasmic reticulum
ERAD	ER-associated degradation
ETC	electron transport chain
EtOH	ethanol
FCCP	Carbonyl cyanide 4-(trifluoromethoxy)phenylhydrazone

HBS	HEPES buffered saline
HBSS	Hank's Balanced Salt Solution
HRP	horse radish peroxidase
IMM	inner mitochondrial membrane
IP	immunoprecipitation
LC3	MAP1 light chain 3
MAM	mitochondria-associated membranes
MCU	mitochondrial calcium uniporter
MDV	mitochondria derived vesicles
Mfn	mitofusin
mtDNA	mitochondrial DNA
MTS	mitochondria targeting sequence
MVB	multi-vesicular bodies
NMR	nuclear magnetic resonance
O-Glc-NAc	O-linked β-N-acetylglucosamine
O/N	over night
OGT	O-linked β-N-acetylglucosamine transferase
OMM	outer mitochondrial membrane
OPA1	optic atrophy protein 1
OXPHOS	oxidative phosphorylation
PAGE	polyacrylamide gel electrophoresis
PARL	presenilin-associated rhomboid like protease
PBS	phosphate buffered saline

PBS-T	phosphate buffered saline - tween
PD	Parkinson's disease
PDH E1α	pyruvate dehydrogenase E1 subunit alpha
PFA	paraformaldehyde
PI3K	phophatidylinositol 3-kinase
PINK1	PTEN-induced putative kinase 1
PLL	poly-L-Lysine
PTM	post translational modification
RBR	RING-in-between-RING
ROS	reactive oxygen species
RT	room temperature
SNpc	substantia nigra pars compacta
SNPH	syntaphillin
TMRM	tetramethylrhodamine methyl ester
TOM	translocase of the outer membrane
UbiCRest	ubiquitin chain restriction
VCP	valsolin containing protein
WT	wild type

Chapter 1

Introduction

First described in the XIX century, mitochondria are essential organelles for all eukaryotic cells. They provide cellular energy by generating adenosine-5'-triphosphate (ATP) and are therefore fundamental for all the metabolic activities within the cell. According to the endosymbiotic theory these organelles derive from aerobic bacteria that colonised anaerobic eukaryotic cells. These bacteria then evolved into mitochondria and the eukaryotic cells acquired the ability to metabolically use oxygen. Mitochondria not only provide cellular energy, but play crucial roles in a wide range of other processes, such as signalling and calcium buffering, cellular differentiation, cell death, as well as the control of the cell cycle and cell growth (Alberts, 2008).

Mitochondrial structure

Although mitochondria were first observed at the end of the XIX century, their structure and their role in the energy transduction started to be elucidated only in the mid 1900s (Palade, 1952; Sjostrand, 1953; Mitchell and Moyle, 1967). Mitochondria are characterised by an elaborate structure consisting of two highly specialised membranes (the outer mitochondrial membrane, OMM, and the inner mitochondrial membrane, IMM), a narrow intermembrane space and a much larger protein rich internal matrix (Fig. 1.1). On the OMM the presence of porins, integral membrane proteins, allows the diffusion of

ions and small molecules (<5 kDa) between the intermembrane space and the cytosol. The integrity of this membrane ensures the compartmentalisation of the intermembrane space proteins, such as cytochrome C, diffusion of which into the cytosol can initiate the apoptotic cascade (Martinou *et al.*, 2000).

The inner membrane is instead highly convoluted and forms many invaginations called cristae (Fig. 1.1). These structures extensively expand the surface area of the IMM, where the oxidative phosphorylation (OXPHOS) occurs, thus enhancing the mitochondrial ability to produce ATP (Mannella, 2006). Rather than being simple IMM folds, 3D reconstruction of electron microscopy images has shown that cristae are proper internal compartments that originate at narrow neck-like segments of the peripheral IMM portions, called cristae junctions (Fig. 1.1). These structures are highly dynamic and can change shape and distribution according to the metabolic state of the organelle. As already mentioned, the OMM is fairly permeable to ions and small molecules, instead diffusion across the IMM is tightly regulated to allow the complexes of the electron transport chain (ETC) to create the proton gradient necessary for the oxidative phosphorylation, but also to provide the segregation and buffering of calcium ions. The mitochondrial matrix is a dense compartment where the mitochondrial DNA (mtDNA) and the mitochondrial ribosomes reside. In fact, although most of the mitochondrial proteins are encoded by the genomic DNA, translated in the cytosol and only then imported in the mitochondria, 13 of the protein complexes involved in the ETC are encoded by mtDNA. Notably, the mtDNA is particularly susceptible to oxidative damage, due to its proximity to the respiratory chain, where reactive oxygen species (ROS) can be generated (Kotiadis *et al.*, 2014).

Oxidative phosphorylation and energy production

ATP production is achieved within the cell through glycolysis, Krebs cycle (or tricarboxylic acid -TCA- cycle) and oxidative phosphorylation. Glycolysis is an anaerobic process that takes place in the cytosol. Via a series of enzymatic reactions, glucose is converted into two molecules of pyruvate, resulting in the generation of two molecules of ATP. Pyruvate can then be oxidatively decarboxylated into acetyl CoA and transported inside the mitochondrial matrix, where the Krebs cycle takes place. Through this cycle

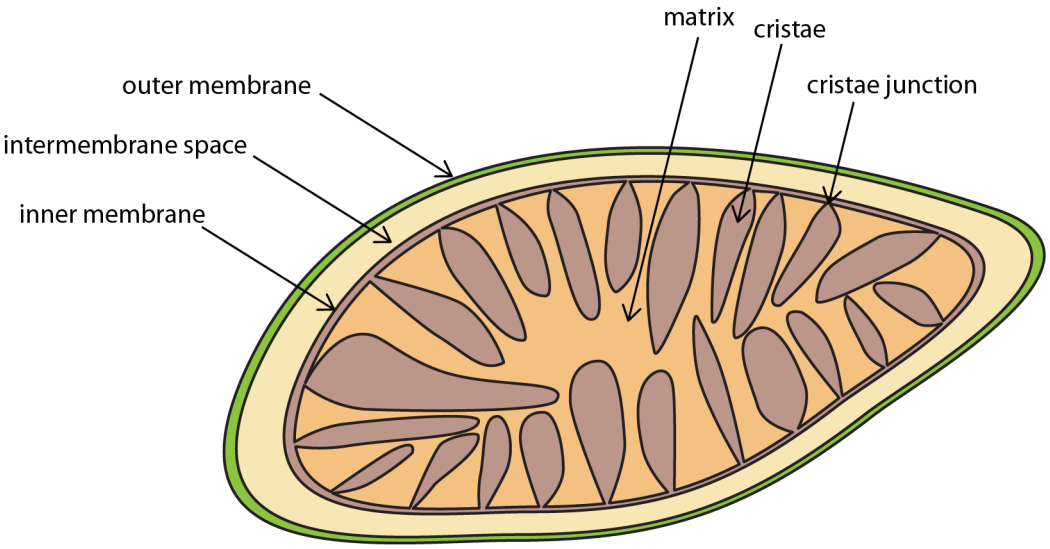

Figure 1.1: The mitochondrial compartments

Mitochondria are formed by an outer and an inner membrane (OMM and IMM) separated by the intermembrane space (IMS). The IMM is characterised by convoluted invaginations, the cristae, that surround the mitochondrial matrix, a protein rich compartment where the mitochondrial DNA (mtDNA) is located. The mitochondrial cristae, protrude into the matrix from bottle neck structures, called cristae junctions.

acetyl CoA is completely oxidised into two molecules of carbon dioxide, one molecule of GTP (or ATP) is produced and importantly three NAD^+ and one FADH are reduced to NADH and $FADH_2$. These are energy-rich molecules, carrying electrons with high transfer potential, that will be necessary in the ETC of the oxidative phosphorylation, the major source of ATP in aerobic organisms (Alberts, 2008).

The molecular machinery for energy production, the ETC, is organised within the mitochondrial cristae and consists of five protein complexes. The flow of electrons from the electron donors, NADH and $FADH_2$, to the electron acceptor O_2 through the ETC protein complexes leads to the pumping of protons out of the mitochondrial matrix. The resulting uneven distribution of protons across the cristae membrane generates a transmembrane electrical potential ($\Delta\psi_m$) which is utilised by the ATP synthase. In fact, the energy required for the synthesis of ATP is produced by the protons flowing back to the mitochondrial matrix through the ATPase protein complex.

The electron transport chain, as illustrated in Fig. 1.2, starts with the NADH dehydrogenase (complex I) or the succinate dehydrogenase (complex II) transferring electrons from respectively NADH or $FADH_2$ to ubiquinone. Although both processes can efficiently participate in the electron transfer, only complex I pumps protons out of the mitochondrial matrix, contributing to the generation of the proton gradient. The reduced ubiquinone, named ubiquinol, can freely diffuse across the cristae membrane. At the cytochrome C oxidoreductase (complex III), the electrons of the reduced ubiquinol are transferred both to the intermembrane space protein cytochrome C and to another site within the ubiquinol itself. This is coupled with the transfer of more protons to the intermembrane space. Subsequently the cytochrome C oxidase (complex IV) removes the electrons from cytochrome C to transfer them to molecular O_2 producing H_2O and further supporting the electrochemical proton gradient by pumping more protons into the intermembrane space. The movement of these ions back into the matrix through the F_0 subunit of the ATP synthase (complex V), is then used to produce ATP from ADP and phosphate (Alberts, 2008). The outcome of this mechanism is that the mitochondrial matrix generally has a negative potential compared to the cytoplasm estimated at between -150 to -180 mV, and that through oxidative phosphorylation between 30 and 38 molecules of ATP are generated per glucose molecule (Rich, 2003; MacAskill and Kittler, 2010). Most of these reactions are reversible, hence to maintain the proton gradient ATP can be hydrolysed (Campanella *et al.*, 2008). Notably, due to electron

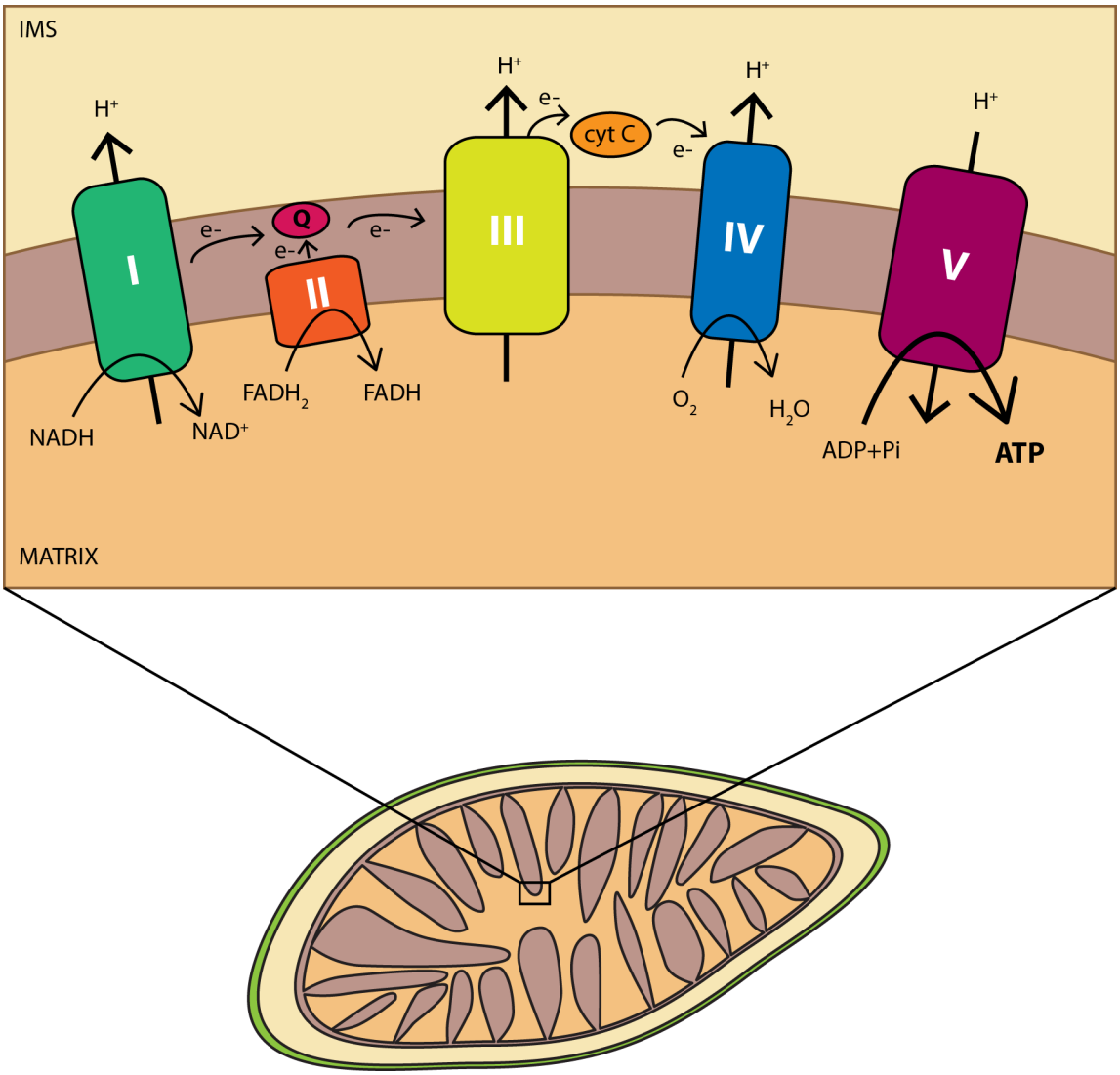

Figure 1.2: Oxidative phosphorylation and the electron transport chain.

The protein complexes involved in the electron transport chain (ETC) and the oxidative phosphorylation are located within the IMM cristae. Starting from NADH or $FADH_2$, via a series of oxidative reactions, electrons are transferred across the protein complexes of the ETC to produce H_2O. While transferring electrons, complex I, III and IV pump protons from the matrix into the intermembrane space, thus creating the proton gradient required by the F_OF_1 ATP synthase to produce ATP.

leakage (in particular at complex I and complex III) ROS can be produced. At low levels these reactive molecules are involved in cell signalling events, however when the ROS levels overcome the mechanisms that are in place to neutralise them, these by-products can damage the mtDNA, protein and lipids (Zhou *et al.*, 2008a).

Many drugs can selectively uncouple the mitochondrial membrane potential and ATP production as represented in Fig. 1.3. For example, carbonyl cyanide- p - trifluoromethoxyphenylhydrazone (FCCP) or its derivative carbonyl cyanide m-chlorophenyl hydrazone (CCCP), act as proton ionophores: after binding protons in the intermembrane space, these substances diffuse across the IMM and dissociate into the matrix, hence dissipating the mitochondrial $\Delta\psi_m$. In a similar way valinomycin, a potassium ionophore, dissipates the mitochondrial $\Delta\psi_m$ by determining a leak of potassium ions across the IMM. Antimycin A blocks the ETC by inhibiting complex III, whereas oligomycin directly affects mitochondrial function by blocking the flow of protons through the F_O subunit of the ATP synthase, thus inhibiting ATP production (Fig. 1.3, Bernardi, 1999; Kondapalli *et al.*, 2012). Overall these drugs have been extensively used to investigate the role mitochondria play within the cell.

Mitochondria and calcium buffering

Calcium signalling plays a crucial role in a variety cellular processes, from cell growth and differentiation, to neuronal signalling and apoptosis. Generally present at very low concentrations within cytoplasm (nanomolar range), calcium signals by spatio-temporally confined rises in the ion levels, that lead to the activation of several pathways. This signalling is tightly regulated and the increases in calcium concentration need to be quickly buffered, for the signal transduction to be regulated and to allow the transmission of consecutive stimuli. Moreover, prolonged increases in the calcium levels can lead to apoptosis, therefore multiple mechanisms are in place to bring the ion concentration back to steady-state levels (Berridge *et al.*, 2000).

In addition to their function in energy production, mitochondria have an important role in calcium buffering. These organelles were the first proposed to have a role in the sequestration of cytosolic calcium, function that was then directly demonstrated using isolated mitochondria in 1961 (DeLuca and Engstrom, 1961). Interestingly, these findings were

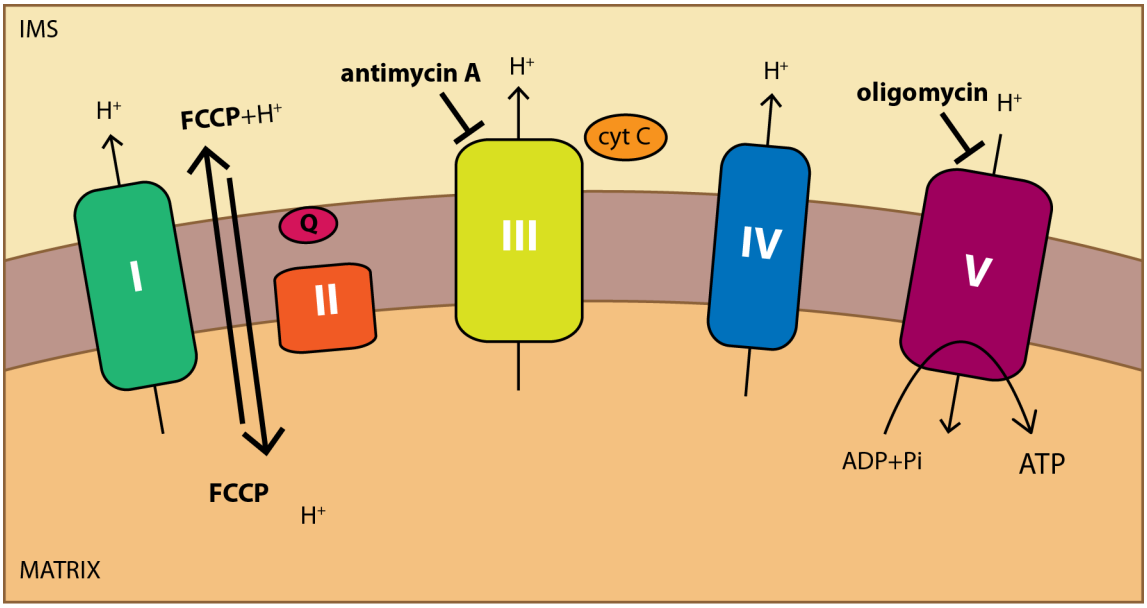

Figure 1.3: Mechanism of action of mitochondrial uncouplers.

Mitochondrial uncouplers impair mitochondrial oxidative phosphorylation and ATP production. FCCP (and CCCP) act as proton ionophores, being protonated in the intermembrane space, these molecules cross the IMM and release the protons into the matrix, thus impairing the proton gradient. Antimycin A instead blocks the Complex III function, whereas Oligomycin blocks the proton flow through the F_O subunit of the ATP synthase, inhibiting ATP production.

reported before the studies on the ETC and the discovery of the proton gradient across the IMM, which is indeed the driving force for the calcium uptake. Since the IMM is not permeable to ions, uniporters and exchangers are required for the selective import and release of calcium. The mitochondrial calcium uniporter (MCU), has long been pharmacologically and functionally described, however, the protein was only recently identified (Baughman *et al.*, 2011; De Stefani *et al.*, 2011). MCU has now been found to be part of a bigger complex that, sensing extracellular calcium (via the accessory proteins MICU1 and MICU2), mediates calcium intake into the mitochondrial matrix only when the cytosolic calcium levels are high, ensuring rapid calcium buffering and stimulation of the oxidative metabolism. Instead, when the calcium concentration in the cytosol is at resting levels, the activity of this uniporter is very low (De Stefani and Rizzuto, 2014). Once inside the mitochondrial matrix, calcium is likely to either combine with phosphate groups imported by the Pi carrier to form insoluble $(Ca^{2+})_x(PO_4)_y(OH)_z$ precipitates, or be transported back outside the mitochondrion via a Ca^{2+}/Na^+ antiporter. This is enabled by a sodium gradient set up by the Na^+/H^+ antiporter (Szabadkai and Duchen, 2008).

Mitochondria are often situated in close proximity to the endoplasmic reticulum (ER), another intracellular calcium store and increasing evidence suggests calcium exchanges between the two organelles (Malli *et al.*, 2005; Rizzuto *et al.*, 2009). The regions where the two organelles are tightly juxtaposed are called mitochondria-associated membranes (MAM) and interestingly, these contacts are regulated by cytoplasmic calcium levels, with resting calcium levels promoting their dissociation and higher calcium levels inducing their association, further suggesting a functional interchange between the two organelles (Wang *et al.*, 2000).

Mitochondria dynamics: fission and fusion

Rather than being separate units, mitochondria continuously move, fuse and divide creating a highly interconnected network that spreads within the cell. Mitochondrial shape can vary from spherical to tubular. It is not surprising that the word “mitochondrion” comes indeed from the Greek words for thread and granule. Morphology, size and number of mitochondria can change according to the cell type and its metabolic

status (Detmer and Chan, 2007). Fission and fusion are the processes that determine respectively the splitting of one mitochondrion into two smaller ones or the fusion of two mitochondria into one. These processes are not, however, solely responsible for controlling the number and size of the organelles, but they are thought to be important to maintain a functional mitochondrial population. In fact, a continuous interchange of mtDNA and metabolites is required to preserve the mitochondrial network functional. In agreement with this, mouse embryonic fibroblasts lacking core components of the fusion machinery have reduced respiratory capacity and individual mitochondria show great heterogeneity in shape and membrane potential (Chen *et al.*, 2005, 2010).

Mitochondrial fusion involves the coordinated fusion of both the outer and inner mitochondrial membranes. In mammalian cells the core components of the fusion machinery are three dynamin-related GTPases: Mitofusin1 and Mitofusin2 (Mfn1 and Mfn2) for the outer membrane and the optic atrophy protein 1 (OPA1) for the inner membrane. The Mitofusins are located on the OMM, and are characterised by a N-terminal GTPase domain, two hydrophobic heptad repeats (HR) and two transmembrane domains that mediate the insertion of the proteins into the OMM. They can form homo- or hetero-oligomers that initially tether adjacent mitochondria and then mediate their fusion. The GTPase activity of these fusion proteins provides the biochemical energy needed to overcome the energy barrier and initiate the mixing of the two lipid bilayers (Westermann, 2010). Besides mitochondrial fusion, Mfn2 has also been shown to be implicated in mitochondrial trafficking and in the mitochondria-ER tethering (Misko *et al.*, 2010; de Brito and Scorrano, 2008), suggesting a more complex role for this GTPase. The inner membrane fusion requires the dynamin-related GTPase OPA1 and it is dependent on the mitochondrial membrane potential. OPA1 is located on the intermembrane space side of the IMM, to which it is anchored by a N-terminal transmembrane domain. In humans, OPA1 exists in 8 different splice variants which in turn can undergo proteolytic cleavage. The model that has been proposed involves the m-AAA protease, paraplegin (active on the matrix side of the IMM), or the i-AAA protease, Yme1L (active on the intermembrane space side of the IMM), to produce shorter forms of OPA1, which are subsequently cleaved by the rhomboid protease PARL. These bi-cleaved products are then released in the intermembrane space. Little is known about how OPA1 mediates fusion, however, interestingly this process requires the presence of both uncleaved and cleaved forms of the protein, suggesting that they act in a complex. In addition to its role in mitochondrial fusion, the GTPase OPA1 also plays a central role in the main-

tenance of the IMM structure, in fact, its down-regulation results in abnormal cristae structure in addition to the widening of the cristae junctions (Scorrano, 2013).

Mitochondrial fission involves the synergicistic activity of the cytosolic dynamin-related protein 1 (Drp1) and its mitochondrial receptors (hFis1, the mitochondrial fission factor Mff, or the mitochondrial division proteins MiD, MiD49 and MiD51). Drp1, a cytosolic protein characterised by a N-terminal GTP binding domain and a C-terminal GTPase effector domain (GED), is recruited by its mitochondrial anchors to discrete areas onto the OMM, where fission is initiated. Interestingly such foci have been reported to be often juxtaposed to ER structures, which are thought to promote the remodelling of the organelle (Friedman *et al.*, 2011), further supporting a functional coupling between the two organelles. Once stabilised on the OMM, Drp1 oligomerises and forms spiral chains that constrict the mitochondrion leading to its fission (Mozdy *et al.*, 2000). Drp1 can be subjected to post translational modifications to regulate its localisation. For example mTOR-mediated activation of PKA during starvation induces the phosphorylation of Drp1 at serine 637, promoting the cytosolic localisation of the protein and consequent mitochondrial elongation (Gomes *et al.*, 2011). On the other hand calcineurin-dependent dephosphorylation of serine 637 has been associated with its translocation to the OMM, which is particularly relevant for mitochondrial remodelling following heart ischaemia and in Huntington's disease (Slupe *et al.*, 2013). Interestingly, calcium/calmodulin-dependent protein kinase (CaMK) Iα has also been reported to phosphorylate serine 637, however this modification was suggested to have the opposite effect and to induce Drp1 translocation onto mitochondria (Han *et al.*, 2008). Drp1 can also be phosphorylated by cyclin-dependent kinase 1 (cdk1) on serine 616, which promotes mitochondrial fission during mitosis. Moreover, stabilisation on the mitochondrion can be promoted by Drp1 SUMOylation, suggested to impede the protein degradation by the proteasome (Harder *et al.*, 2004), and by S-nitrosylation (Cho *et al.*, 2009).

Other components of this machinery include endophilin B1 and MTP18, both involved in maintenance of mitochondrial morphology by promoting mitochondrial fission (Tondera *et al.*, 2005; Karbowski *et al.*, 2004). However the components of the machinery involved in this process and the steps leading to mitochondrial constriction remain to be fully elucidated.

The mitochondrial transport machinery

"By far the most important and interesting are the observations on the living cells. The mitochondria are almost never at rest, but are continually changing their position and also their shape" - Mitochondrial transport was first documented by Lewis and Lewis 100 years ago (Lewis and Lewis, 1914). Within the cell, mitochondria respond to spatio-temporally localised metabolic needs, and to do so they have to be actively transported to areas of high energy demand or calcium buffering requirements. Mitochondrial trafficking is therefore an important process to allow proper mitochondrial function in every cell type. In neurons however, due to their complex architecture, comprising of an extensive dendritic arborisation and a very long axonal process, transport of mitochondria has an even more crucial role. In fact, in these cells, mitochondria need to be transported long distances (up to one meter in the human sciatic nerve) in order to be able to exert their function where needed. Mitochondria are generally found at locations with high metabolic demand such as pre- and post-synaptic domains, the axon initial segment, nodes of Ranvier and growth cones (Hollenbeck and Saxton, 2005). However, these organelles are not only delivered to axons and dendrites, but they are also retrieved and therefore transported back to the cell soma. This highlights the need for a fine mechanism to control mitochondrial localisation and transport.

Among the mitochondrial population, about 20-30% of mitochondria move in cultured hippocampal neurons (Overly *et al.*, 1996; MacAskill *et al.*, 2009b). Long range mitochondrial trafficking is principally mediated by motor proteins (kinesin and dyneins) that transport the organelles along the microtubules, whereas the actin cytoskeleton is believed to be more important for anchoring mitochondria and for short range movements via the myosin motors. Mitochondrial movement along the cytoskeletal tracks is fast and bi-directional, with transport velocities that mostly fall in the range of 0.3–1.0 μm/second, with rates observed *in vivo* comparable with those of some neuronal culture studies. These organelles move, stop, start again and switch direction. It is generally believed that plus end-directed movement is mediated by the kinesin motors, whereas minus end-directed movement is mediated by the dyneins (MacAskill and Kittler, 2010).

Microtubule motor proteins

The kinesin motors

Kinesin motors mediate plus end-directed movement on the microtubules. In axons or distal dendrites, where the microtubules are polarised, kinesin-mediated transport is referred as anterograde, from the soma to the periphery. Instead, in proximal dendrites microtubules have mixed polarity, hence kinesin-mediated transport can traffick cargoes towards and from the soma. The kinesin motors are formed by a globular motor domain, generally at the N-terminus of the protein and a globular cargo binding domain, generally at the C-terminus. These two domains are connected by a linker coiled-coil that mediates the dimerisation of the protein. Kinesin movement is achieved by the sequential hydrolysis of ATP which induces a conformational change in the motor domain, making one domain swing ahead of the other one and resulting in a "walking" mechanism. The most well studied family of kinesin heavy chains is the kinesin family 1 (KIF5). Kinesin family 1 members are generally associated with two kinesin light chains, which are thought to play a role in cargo binding. There are currently 45 different kinesin genes divided into 15 families, and they have distinct localisation, transport properties and adaptors. Cargo binding to the kinesins is mostly mediated by trafficking adaptors and scaffolds, that determine the kinesin/cargo selectivity (Hirokawa *et al.*, 2009).

The best characterised kinesin motor involved in mitochondrial trafficking is KIF5. In *Drosophila* there is only one isoform of KIF5, in contrast, in mammalian cells, this family comprises of three different isoforms, KIF5A, KIF5B and KIF5C. KIF5B is widely expressed, while KIF5A and KIF5C are neuronal specific. However whether these motors have isoform-specific roles or share similar pathways is still unclear. KIF5 mutations in *Drosophila* neurons disrupt anterograde axonal mitochondrial transport (Pilling *et al.*, 2006), similarly in non-neuronal mouse cells deletion of KIF5B inhibits the transport of mitochondria to the periphery, resulting in their perinuclear clustering (Tanaka *et al.*, 1998). Further supporting the role of KIF5 in the trafficking of mitochondria, expression of KIF5 dominant-negative mutants disrupts mitochondrial trafficking in axons of rat hippocampal neurons (Cai *et al.*, 2005). In dendrites however, the role of kinesin-mediated trafficking is less clear. Antibodies that specifically block the kinesin motor function were found to inhibit mitochondrial transport in both directions in mixed polarity microtubules (MacAskill *et al.*, 2009b), however in a recent study, expression of

dominant-negative KIF5 constructs had little effect on mitochondrial mobility in primary proximal dendrites (van Spronsen *et al.*, 2013). In mammalian neuronal cells KIF1B (a member of the kinesin family 3) was also found to have a role in mitochondrial trafficking. This motor was localised on immunopurified mitochondria and, in contrast to the KIF5 family members, it was shown to mediate transport in a monomeric form (Nangaku *et al.*, 1994). More recently also Klp6 (kinesin like protein 6) has been also proposed to play a role in the transport of mitochondria. Dominant negatives of Klp6 were in fact found to reduce the number of moving mitochondria and silencing of the protein affected mitochondrial trafficking velocity in neuronal differentiated cell lines (Tanaka *et al.*, 2011).

Kinesin adaptors

Several kinesin adaptors associated with mitochondrial trafficking have been identified to date. These include syntabulin, FEZ1 (fasciculation and elongation protein ζ - 1), RanBP2 (Ran-binding protein 2), TRAKs (trafficking protein kinesin-binding) and Miro (mitochondrial Rho). Syntabulin, was first discovered as an adaptor linking syntaxin containing synaptic vesicles to the kinesin motors (Su *et al.*, 2004). Later this adaptor protein was also reported to associate with mitochondria. Syntabulin silencing was shown to affect both the anterograde movement of mitochondria (and synaptic vesicles) and the density of the mitochondria in the distal processes of rat hippocampal neurons (Cai *et al.*, 2005). FEZ1, another adaptor found in a complex with the kinesin motor proteins, was shown to promote mitochondrial transport in hippocampal neurons and to induce the presence of mitochondria in the developing processes in NGF stimulated PC12 cells (Ikuta *et al.*, 2007; Fujita *et al.*, 2007). Moreover, selective knock down of FEZ1 was shown to inhibit mitochondrial movement only in the anterograde direction, further suggesting a role for this adaptor protein in the anterograde transport of mitochondria (Blasius *et al.*, 2007). RanBP2, a scaffold protein previously associated with nucleocytoplasmic transport, protein biogenesis and mitosis (Yokoyama *et al.*, 1995), was more recently associated with mitochondrial function in the central nervous system (CNS) and then found to bind specifically KIF5A and KIF5B (but not C, Aslanukov *et al.*, 2006; Cho *et al.*, 2007). This suggests the possibility of different roles for these motor proteins in neurons. Genetic screens in *Drosophila* have identified the kinesin binding protein Milton (the *Drosophila* orthologue of the TRAK proteins) and the atypical GTPase

dMiro (*Drosophila* Miro) as being crucial for anterograde transport of mitochondria along axons in fruitflies (Stowers *et al.*, 2002; Guo *et al.*, 2005). Miro and the TRAKs have emerged as key conserved regulators of mitochondrial trafficking in neurons and will be discussed in further detail in the sections respectively on page 32 and 37.

The dynein motors

Dynein motors mediate movement of cargoes towards the minus end of microtubules, which corresponds to retrograde transport (from the periphery to the cell soma) in axons and distal dendrites, where microtubules are polarised. In contrast to the extensive kinesin family, there are relatively few dynein heavy chains. The cytoplasmic dynein 1 heavy chain (encoded by *DYNC1H1* in humans, and hereafter referred as cytoplasmic dynein) is used for nearly all of the minus end-directed transport in the cytoplasm of most eukaryotic cells, whereas cytoplasmic dynein 2 (encoded by *DYNC2H1* in humans) is specifically localised in cilia and flagella. The cytoplasmic dynein consists of two heavy chains, two intermediate chains, two light intermediate chains and a variable number of light chains. The heavy chains are formed by a C-terminal motor domain and an N-terminal tail domain. The motor domain contains six AAA+ ATPase domains arranged in a ring, from which the microtubule binding domain protrudes. The tail domain mediates the oligomerization of the heavy chains and serves as a platform for the binding of several associated subunits, which in turn mediate the interaction with the cargoes either via direct binding or through the recruitment of other adaptor proteins. Dynein transport requires the presence of dynactin, a multisubunit complex necessary for dynein activity. Dynein and dynactin exist as a complex and it has been proposed that dynactin could mediate the interaction between the dynein motors and the cargoes, as antibodies that inhibit binding of the largest subunit of dynactin, p150$^{\text{Glued}}$ to dynein heavy chain, inhibit dynein mediated retrograde transport of cargo, without altering dynein processivity along microtubules (Waterman-Storer *et al.*, 1997; Roberts *et al.*, 2013).

Both dynein and the dynactin components p50 and p150$^{\text{Glued}}$ have been detected on purified mitochondria in *Drosophila* extracts and mutating the dynein heavy chain or p150$^{\text{Glued}}$ has been shown to inhibit axonal mitochondrial trafficking in both directions (Pilling *et al.*, 2006; Martin *et al.*, 1999). Moreover, dynein has been localized on both

anterogradely and retrogradely moving axonal mitochondria (Hirokawa *et al.*, 1990). A few proteins have been suggested to link mitochondria to dynein-mediated transport. The dynein light chain Tctex1, involved in the dynein-mediated transport of rhodopsin channels in photoreceptors (Tai *et al.*, 1999), has been shown to interact with the mitochondrial voltage-dependent anion channels (VDAC) located on the OMM (Schwarzer *et al.*, 2002). Another putative adaptor is APLIP1 (APP -amyloid precursor protein-like protein interacting protein 1), a *Drosophila* homologue of the mammalian JIP (JNK - c-Jun N-terminal kinase- interacting protein). Generally involved in cargo-mediated kinesin activation (Horiuchi *et al.*, 2007; Blasius *et al.*, 2007), APLIP1 mutations were found to selectively disrupt retrograde mitochondrial transport, while both retrograde and anterograde vesicle transport was inhibited (Horiuchi *et al.*, 2005). Recently, dynein was also found to interact with the TRAK adaptors, raising the possibility that the kinesin adaptor Miro, which binds the TRAKs, is also the adaptor that recruits dynein motors to these organelles to coordinate dynein-mediated mitochondrial transport (van Spronsen *et al.*, 2013; Russo *et al.*, 2009). This suggests that Miro proteins may be important for mediating the cross-talk between dynein and kinesin transport.

Miro proteins

Miro proteins were originally identified as mitochondrial atypical Rho-like small GTPases (Fransson *et al.*, 2003). Evolutionary conserved (Gem1 is Miro's yeast orthologue), Miro exists in two isoforms in mammals (Miro1 and Miro2, which are 60% identical) and one in *Drosophila* (dMiro). As shown in Fig. 1.4 A, these proteins are characterised by the presence of several signalling domains: two GTPase domains flank two calcium sensing EF hands and a C-terminal transmembrane domain. The first evidence of Miro being involved in mitochondrial trafficking came from studies in flies where knock out of the protein resulted in a defect in the transport of mitochondria into neuronal axons (Guo *et al.*, 2005). These studies were then confirmed by experiments showing that Miro can bind the kinesin proteins, coupling the mitochondria to the molecular motors, and overexpression or silencing of Miro were respectively correlated to increased and decreased transport of mitochondria (MacAskill *et al.*, 2009b; Wang and Schwarz, 2009). Mitochondrial transport has been known to be negatively regulated by increased calcium levels within the cell which can arise from a variety of stimuli such as glutamate receptor activation, action potentials, calcium release from the ER (Rintoul *et al.*, 2003; Yi *et al.*,

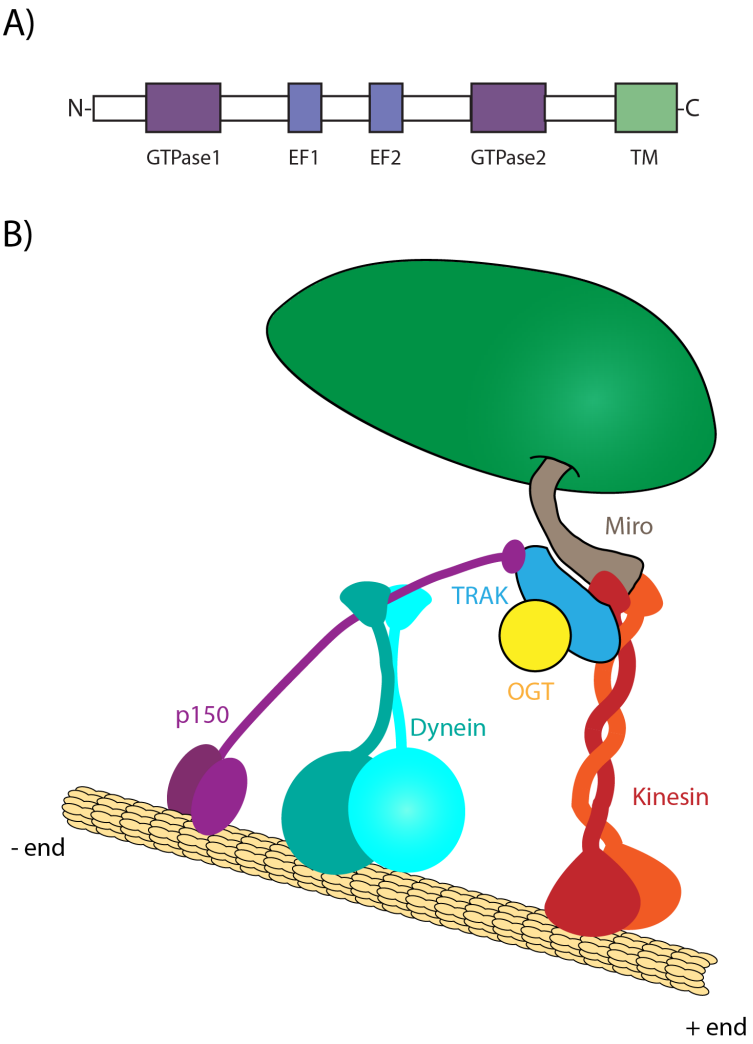

Figure 1.4: The mitochondrial trafficking complex.

(A) Schematic representation of Miro1 domains. The protein is characterised by two GTPase domains flanking two EF calcium-binding domains. At the C-terminus a transmembrane domain locates Miro in the OMM. (B) Representation of the mitochondrial trafficking complex. Miro binds the kinesin motors and the TRAK adaptor molecules directly, whereas dynein-dependent transport is mediated by the interaction between the dynactin subunit $p150^{Glued}$ and TRAK. The TRAK adaptors also bind OGT(O-linked β-N-acetylglucosamine transferase).

2004). However, the mechanism underlying calcium-dependent mitochondrial stopping was long unknown. EF hand-containing Miro proteins were a good candidate for this. EF hand domains are helix-loop-helix domains characterised by a conserved sequence comprising a negatively charged residue in the loop that is involved in the calcium binding. These domains are often present in tandem in calcium sensors such as calmodulin (Lewit-Bentley and Réty, 2000). Calcium binding to Miro1 has been shown to determine mitochondrial arrest, in fact, expression of calcium insensitive ΔEF (where the calcium binding ability is lost by the double mutation E208K and E328K) prevented calcium-dependent mitochondrial arrest (Saotome *et al.*, 2008; MacAskill *et al.*, 2009b; Wang and Schwarz, 2009). This process is particularly relevant in neurons where localised calcium rises, following synaptic activation, can promote the stopping of mitochondria. In these areas of high energy demand, mitochondria play a crucial role by providing the ATP needed to revert the ion fluxes. Moreover, by buffering the calcium these organelles can shape the calcium-dependent signalling cascades. Although the role of Miro in calcium-dependent mitochondrial arrest is generally agreed, the mechanism underlying this process is debated. MacAskill and colleagues have shown that glutamate-dependent calcium increase determines the loss of the kinesin motors from purified neuronal mitochondria, suggesting that a conformational change, due to calcium binding on Miro, impairs its ability to interact with the kinesin motors (Fig. 1.5 A, MacAskill *et al.*, 2009b), whereas Wang and Schwarz have shown that mitochondrial arrest is due to the motor domain of the kinesin binding Miro in between its two EF hands, resulting in the detachment of the motor from the microtubules. Moreover, in this model the cargo binding domain of the kinesins motors does not interact directly with Miro, but the interaction is mediated by the TRAK adaptors (Fig. 1.5 B, Wang and Schwarz, 2009). Both mechanisms, however, involve a fine regulation that determines the stopping of the organelles where the calcium concentration is higher. A newly reported protein, Alex3, was recently shown to regulate mitochondrial trafficking in axons and to interact with Miro and TRAK2 in a calcium-dependent manner. Alex3 is unique to Eutherian mammals and although the exact mechanism of function of this protein is not yet known, its identification provides another potential level of regulation of the mitochondrial transport machinery and suggests an increased regulatory complexity in the mitochondrial dynamics in the most evolved mammals (López-Doménech *et al.*, 2012).

In addition to the calcium-dependent regulation, Miro1 can be modulated by its GTPase function. Miro proteins are able recruit the adaptors TRAK1 and TRAK2 (also known

as OIP106 and Grif-1 or OIP98) to the mitochondria (Fransson *et al.*, 2006). This is dependent on the first GTPase domain of Miro, since expression of constitutively active GTPase1 Miro1 mutant (V13, equivalent to GTP-bound Miro1), prevents the recruitment of TRAK2 (MacAskill *et al.*, 2009a). Since the TRAK adaptors can bind both Miro and the kinesin motors (Brickley *et al.*, 2005), these data suggest that TRAK2, recruited to GDP-bound Miro, might promote mitochondria coupling to the molecular motors. Moreover, the loss of interaction between Miro1 and TRAK2 (caused by the expression of a peptide containing the TRAK2 Miro binding domain, which acts as a dominant negative) leads to a decreased number of mitochondria in neuronal processes, indicating the importance of the functional coupling between Miro, the TRAKs and the kinesins in mitochondrial trafficking (MacAskill *et al.*, 2009a).

Little is known about the role of Miro1 in retrograde, dynein-mediated transport. Tuning Miro1 levels regulates mitochondrial transport in both directions, however it is arguable that increased anterograde transport, due to Miro1 overexpression, could homeostatically promote the retrograde transport of the organelles (independently of Miro). Interestingly however, Miro1 has been recently shown to mediate the coupling between mitochondria and dynein motor complex in lymphocytes (Morlino *et al.*, 2014), suggesting that this mitochondrial adaptor could indeed have a role in the tuning between anterograde, kinesin-mediated and retrograde, dynein-dependent, mitochondrial transport.

Although in mammals Miro has two isoforms, most studies have focused on Miro1 function. The two proteins have been suggested to have a similar function (Fransson *et al.*, 2006), however some differences have emerged from the work of Misko and colleagues, that have found knock down of Miro2, but not of Miro1, to affect axonal transport of mitochondria (Misko *et al.*, 2010).

Miro1, Miro2 and Milton have been recently found to interact with PINK1, a Parkinson's disease-associated protein involved in mitochondrial quality control, raising the possibility that the Miro trafficking molecules can have a role in the recognition and processing of damaged mitochondria (Weihofen *et al.*, 2009).

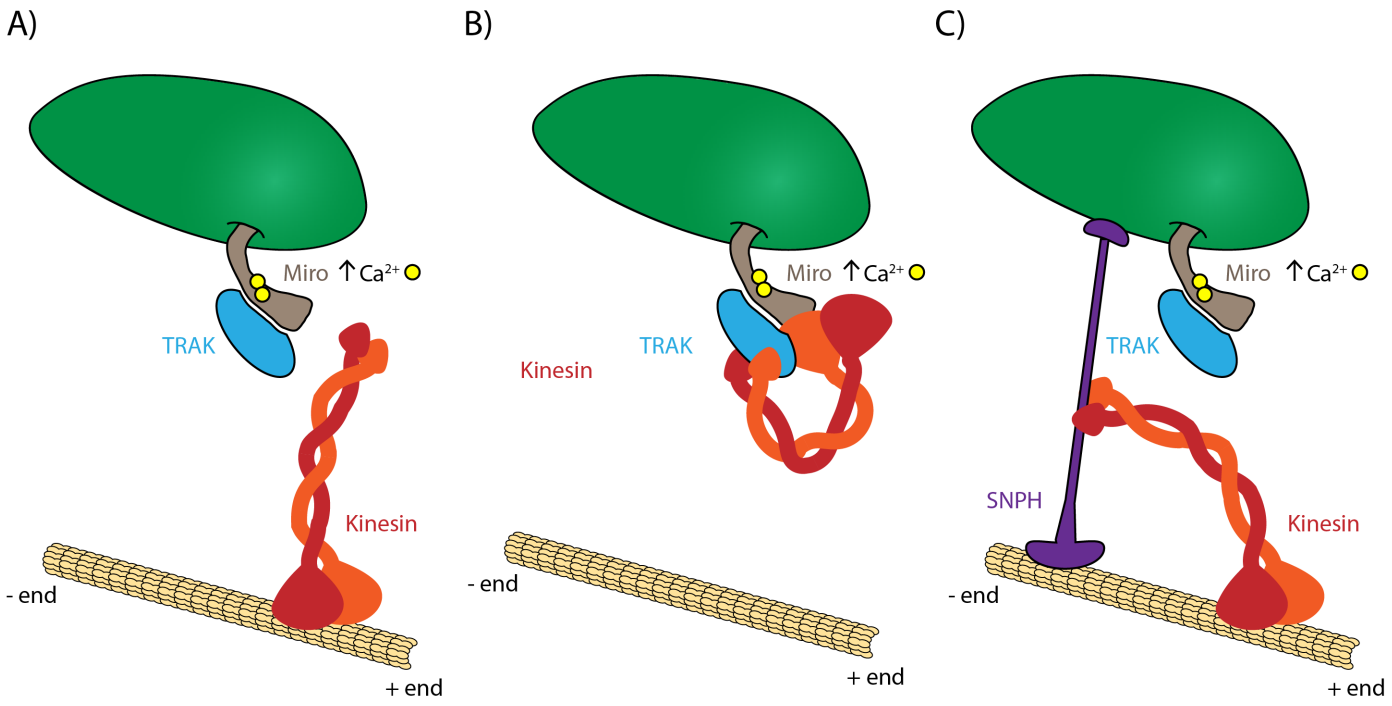

Figure 1.5: Mechanisms of mitochondrial arrest

According to the first model (A), calcium binding to Miro causes the protein release from the kinesin motors, determining the detachment of the mitochondrion from the microtubule tracks (MacAskill *et al.*, 2009b). In the second model (B), calcium binding to Miro EF-hand domains promotes the detachment of the kinesin motors from the microtubules and the interaction of their motor domains with Miro, causing mitochondrial arrest (Wang and Schwarz, 2009). A third model (C) shows both the detachment of kinesin from Miro and its subsequent interaction with the mitochondrial tether syntaphilin (SNPH, Chen and Sheng, 2013) .

TRAKs

Milton, the *Drosophila* homolog of the TRAK proteins, was first identified as a mitochondrial adaptor in a genetic screen (Stowers *et al.*, 2002). Milton mutant flies exhibited no mitochondria in the axons of photoreceptors, indicating that the protein was involved in the transport of mitochondria into the neuronal processes. Milton was then shown to be associated with purified mitochondria and to bind the kinesin motors (Stowers *et al.*, 2002; Brickley *et al.*, 2005). Two mammalian homologues of Milton, the trafficking protein kinesin binding (TRAK) 1 and 2 were then identified. These proteins are 48% identical and share respectively 33.5 % and 35.3 % sequence similarity with Milton. As their *Drosophila* orthologue, the TRAK proteins bind the kinesins and this interaction occurs via the C-terminal cargo binding domain of the motor (Brickley *et al.*, 2005; Smith *et al.*, 2006). The TRAKs are characterised by a N-terminal coiled-coil region, which shows high homology to the trafficking adaptor HAP1 (huntington associated protein 1), and is involved in the kinesin binding (residues 124-283), a Hrs (hepatocyte growth factor-regulated tyrosine kinase substrate) binding region, which links these proteins to the endo-lysosomal pathway, and the Miro binding domain at the C-teminal (residues 476-913, Smith *et al.*, 2006; Kirk *et al.*, 2006; MacAskill *et al.*, 2009a). Possibly due to the presence of different domains, the TRAKs have been shown to exert several functions, for example transport of ion channels (Beck *et al.*, 2002; Smith *et al.*, 2006; Grishin *et al.*, 2006), endosomes (Kirk *et al.*, 2006; Webber *et al.*, 2008) as well as mitochondria (MacAskill *et al.*, 2009a; Smith *et al.*, 2006; Brickley and Stephenson, 2011). Via the interaction with Miro and the kinesin motors, the TRAKs have been shown to modulate mitochondrial trafficking. Disruption of the TRAK/KIF interaction by expression of a peptide with dominant negative function or silencing of TRAK1 reduces the number of moving mitochondria in axons (Brickley and Stephenson, 2011), however, since Miro itself can bind the kinesins and promote mitochondrial transport, the contribution of each protein should be further investigated. Interestingly, the levels of the TRAK acceptors (Miro1 or Hrs) have been shown to shift the localisations of these proteins (i.e. from mitochondria to endosomes), suggesting that the availability of these binding partners can influence the TRAKs function (MacAskill *et al.*, 2009a). Recently van Spronsen and collaborators have demonstrated for the first time that TRAK1 and TRAK2 exhibit a distinct localisation in neurons, with TRAK1 being more prominent in axons and TRAK2 in dendrites. This segregation was suggested to be due to a different

affinity to the kinesin motors, in fact although both TRAK1 and TRAK2 could bind the dynein/dynactin complex, TRAK2 interaction with the kinesin motors was prevented, possibly due to a folded head-to-tail conformation that TRAK2 preferentially adopts. The model proposed by the authors suggests TRAK1 to be delivered to the axons by the kinesins, whereas TRAK2 can only be trafficked to the dendritic compartment in a dynein-mediated mechanism (van Spronsen *et al.*, 2013). These results agree with previous work showing that TRAK1, but not TRAK2, silencing inhibits mitochondrial trafficking in axons (Brickley and Stephenson, 2011), however these studies do not take into consideration the TRAK-independent Miro contribution to mitochondrial trafficking.

TRAK1 and TRAK2 have been shown to interact with O-linked β-N-acetylglucosamine (O-Glc-NAc) transferase (OGT, Iyer *et al.*, 2003), an enzyme that catalyses O-linked glycosylation of serine and threonine residues. O-Glc-NAcylation is a reversible post translational modification that has been compared to phosphorylation (Wells *et al.*, 2003). OGT has been shown to be an integral component of the TRAK/kinesin trafficking complex (Brickley *et al.*, 2011) and since the the levels of O-Glc-NAcylation can be linked to glucose levels, this suggests a possible association between mitochondrial trafficking and the availability of mitochondrial substrates. Pekkurnaz and colleagues have indeed recently demonstrated that, in the presence high glucose (30 mM), mitochondrial trafficking is reduced and this is dependent on TRAK1 O-Glc-NAcylation since mutation of key O-Glc-NAcylated serine residues blocks this glucose-dependent mitochondrial stopping (Pekkurnaz *et al.*, 2014).

Static anchors

Over two thirds of neuronal mitochondria are stationary, ideally serving as constant energy suppliers in metabolically active areas within the neuron. This lack of movement could be simply due to the organelles not being bound to the transport machinery, or it could be an actively regulated mechanism, involving docking proteins and static anchors. The actin cytoskeleton has been shown to have a role in the mitochondrial sequestration into the stationary component either by direct anchoring or by delivery of the mitochondria to docking areas, in fact disruption of the actin filaments prevents the NGF-dependent arrest of mitochondria (Chada and Hollenbeck, 2004). Stationary

mitochondria can also be tethered by the intermediate filaments. Interestingly this process was reported to be dependent on the organelles membrane potential, suggesting that only fully functional organelles can be docked to locally provide energy and buffer calcium (Wagner *et al.*, 2003). More recently Plectrin 1b, a intermediate filament bound protein, was found to link the filaments to the mitochondria in fibroblasts, however knock out of the protein did not affect mitochondrial movement in these cells (Winter *et al.*, 2008). Another protein was recently found to have a role in mitochondrial docking: syntaphilin (SNPH). This protein was shown to bind both mitochondria, via its C-terminal transmembrane domain, and axonal microtubules, via its N-terminal domain. Moreover, interaction with the dynein light chain LC8, was reported to stabilise the syntaphilin/microtubule interaction (Chen *et al.*, 2009). Syntaphilin was shown to be specifically localised to axonal stationary mitochondria and over expression of the protein resulted in stopping of axonal mitochondria. Conversely syntaphilin knock out resulted in a reduction of the mitochondrial density in axons and a substantially increased number of moving mitochondria in these processes (Kang *et al.*, 2008). More recently syntaphilin was also proposed to play a key role in Miro-dependent calcium-induced mitochondrial arrest in a revised 'engine-switch and brake' model. In this model, following the calcium-triggered uncoupling of the Miro/kinesin complex, sytaphilin not only docks the mitochondrion to the axonal microtubules, but also binds the kinesin, keeping the whole complex stably tethered (Fig. 1.5 C, Chen and Sheng 2013).

Mitochondria quality control

Increased ROS production, disrupted calcium homeostasis and defective protein turnover can affect mitochondrial functionality. When mitochondrial damage is limited, mechanisms are in place to repair the organelles, such as ROS scavengers that convert and neutralise the radicals, heat shock proteins that prevent the aggregation of unfolded proteins and promote their degradation (Kotiadis *et al.*, 2014). However, when the damage is extensive, the mitochondrial membrane potential drops, the proton gradient dissipates and the mitochondrial functionality is lost. Fusion of these impaired organelles with functional mitochondria in the long term will lead to a diffusion of the damage, which ultimately will be detrimental for the whole mitochondrial network. To prevent this scenario a mitochondrial quality control system is in place to recognise, isolate and

clear damaged mitochondria via a pathway called mitophagy (mitochondrial autophagy). The key players in the quality control of mitochondria are the proteins PINK1 (PTEN-induced putative kinase 1) and Parkin. PINK1 is a mitochondrial kinase that, upon mitochondrial depolarisation, accumulates on the OMM and recruits Parkin, a cytosolic E3 ubiquitin ligase, onto the damaged organelles. Parkin-dependent ubiquitination of OMM proteins is a crucial step in mitochondrial clearance. PINK1 and Parkin are both associated with autosomal recessive forms of Parkinson's disease, indicating the importance of this system in cellular physiology (Youle and Narendra, 2011).

PINK1

Encoded by the gene *PARK6,* PINK1 is a mitochondrial serine/threonine kinase. This protein is characterised by an N-terminal mitochondrial targeting sequence (MTS), a transmembrane domain and a C-terminal serine/threonine kinase domain with homology to the calcium/calmodulin family (Fig. 1.6). The subcellular localisation of PINK1 has long been debated, since the protein has been found on the OMM, in the IMM and in the cytosol. Recent work has elucidated several aspects of the complex regulation of this kinase. PINK1 has been reported to be initially targeted to the OMM, where it interacts with and is rapidly imported by the TOM (translocase of the outer membrane) complex in a membrane potential-dependent manner (Lazarou *et al.*, 2012). Once inside the mitochondrion PINK1 has been reported to be processed by several proteases including the mitochondrial processing peptidase (MPP), the presenilin-associated rhomboid-like protease (PARL), m-AAA and ClpXP (Greene *et al.*, 2012). MPP, a protease responsible for cleaving the MTS of precursor proteins imported into the mitochondrion, has been shown to cleave the PINK1 MTS. Interestingly, knock down of MPP has been associated with the accumulation of full length PINK1 on the OMM, suggesting that MPP-dependent cleavage promotes PINK1 import into the mitochondria. Although unexpected, MPP-dependent processing of newly imported proteins has been previously shown to be coupled with the protein import, and the protease itself has been suggested to be important for the protein import. The mechanism by which this occurs has however remained elusive (Greene *et al.*, 2012). Within the mitochondrion PINK1 has been shown to be further processed. Lin and Kang have demonstrated that within three minutes from the protein synthesis PINK1 is cleaved into an primary unstable peptide (Δ1-PINK1, 53 kDa), which has a half life of 30 minutes and is degraded by the

proteasome, or into a secondary smaller product (Δ2-PINK1, 45 kDa) which has been shown to be more stable due to its interaction with the chaperone Hsp90 (Lin and Kang, 2008). The Δ1-PINK1 53 kDa product is formed by the IMM protease PARL (presenilin-associated rhomboid like protease), which cleaves PINK1 at A103 (Deas *et al.*, 2011; Jin *et al.*, 2010). Identification of Δ1-PINK1 cleavage sites allowed further investigations in the role of the full length versus the Δ1 cleaved protein. Interestingly, accumulation of full-length PINK1 (due to the cleavage site mutation) was shown to cause the loss of membrane potential, increased ROS production and altered mitochondrial network, suggesting that this cleaved product is involved in the maintenance of mitochondrial homeostasis (Deas *et al.*, 2011). The lack of stability of Δ1-PINK1 has been shown to be due to the phenylalanine 104 (F104), which is the first residue of the PARL-cleaved Δ1-PINK1. According to the N-terminal rule for degradation the presence of specific amino acids at the (cleaved) N-terminus of a polypeptide can promote the degradation of the protein via the proteasome. These destabilising residues are arginine, lysine and histamine for type-1 degradation, and phenylalanine, tryptophan, tyrosine, isoleucine and leucine for type-2 (type-1 and type-2 protein degradation differ on the enzymes involved in the recognition and ubiquitination of the N-terminus). These residues promote the ubiquitination by specific E3 ubiquitin ligases and the consequent degradation of the protein (Tasaki *et al.*, 2012). Mutation of F104 to more stable residues increases the stability of Δ1-PINK1, which is found in the cytosol, in agreement with the cleaved product being released from the intermembrane space into the cytosol and processed by the proteasome (Yamano and Youle, 2013). Although the function of cytosolic PINK1 under basal conditions has been long unknown, recent evidence has shown it to potentially regulate the cytosolic pool of Parkin, maintaining the ligase in an inactive state (Fedorowicz *et al.*, 2014). Moreover, experiments using PINK1 lacking its MTS have shown that this cytosolic form of the kinase promoted PKA-dependent neurite outgrowth and dendritic extension (Dagda *et al.*, 2014). The physiological role of the more stable secondary product Δ2-PINK1 is not clear to date. This smaller polypeptide does not seem to compensate for Δ1-PINK1 protective role against oxidative stress, however via its interaction with Hsp90 it has been suggested to regulate the full lengh/Δ-PINK1 ratio (Lin and Kang, 2008).

Due to its rapid import within the mitochondrion PINK1 levels on the OMM are very low in basal conditions. However, since this process is dependent on the membrane potential, mitochondrial damage results in the accumulation of PINK1 on the OMM,

a crucial step in the initiation of mitophagy which will be described in the mitophagy section on page 48.

PINK1 was originally found to be linked to autosomal recessive Parkinson's disease in 2004 (Valente *et al.*, 2004). The first evidences of PINK1 function came from studies in *Drosophila*, where PINK1 knock out resulted in loss of dopaminergic neurons, male sterility, muscle degeneration, defective locomotion, altered mitochondrial morphology (including fragmented cristae) and increased sensitivity to multiple stress (i.e. oxidative stress). Interestingly, in these experiments it was reported that Parkin overexpression in PINK1 mutant flies rescued the male sterility and mitochondrial morphology defects of PINK1 mutants (Clark *et al.*, 2006; Yang *et al.*, 2006; Park *et al.*, 2006), however, in mammalian cells Parkin overexpression does not compensate for PINK1 loss, suggesting the existence of non conserved mechanisms between species. Since the discovery of PINK1 as a PD-related gene in 2004, several disease-associated mutations in this protein have been identified. Most PINK1 mutations affect the kinase activity or the stability of the protein, resulting in a decreased function of the kinase. PINK1 mutants have been associated with increased oxidative stress, decreased respiratory activity and ATP production, mitochondrial calcium overload and synaptic deficits (Deas *et al.*, 2009; Gandhi *et al.*, 2009; Exner *et al.*, 2012). PINK1 disease-linked mutations and knock out have been associated with a reduction in complex I function, leading to a decrease in membrane potential, however the mechanism underlying this was elusive (Morais *et al.*, 2009). Recently Morais and colleagues have shown that PINK1 is associated with the phosphorylation of a subunit of complex I, and this modification is crucial to promote the ubiquinone reduction, which is required for the ETC, thus providing a mechanism for PINK1-dependent complex I malfunction (Morais *et al.*, 2014). PINK1 has also been suggested to protect against oxidative stress by phosphorylating the mitochondrial chaperone TRAP1 (tumor necrosis factor receptor-associated protein 1)/Hsp75. Upon phosphorylation, this protein has a pro-survival effect, preventing cytochrome C release and H_2O_2-induced apoptosis (Pridgeon *et al.*, 2007). Moreover, PINK1 has been shown to interact with and regulate the mitochondrial protease HtrA2/Omi, a Parkinson's disease-associated protein. The protease activity of HtrA2/Omi is dependent on its phosphorylation state and is regulated by PINK1, although evidence of direct phosphorylation is missing. This protease has been suggested to be involved in a quality control system within the mitochondrion, possibly involving the degradation of misfolded proteins, and to promote the resistance to mitochondrial stess (Plun-Favreau *et al.*, 2007).

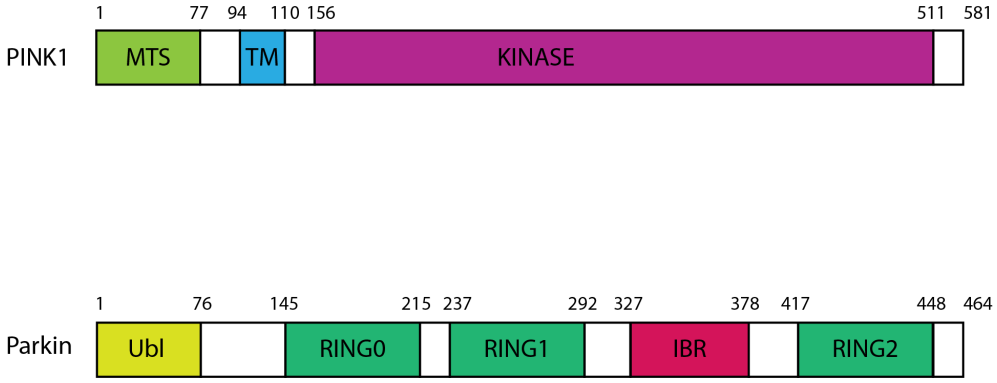

Figure 1.6: Schematic of PINK1 and Parkin structure

PINK1 is characterised by a N-terminal mitochondrial targeting sequence (MTS), a transmembrane domain (TM) and a C-terminal kinase domain. Parkin is formed by a N-terminal ubiquitin-like domain (Ubl), a RING0 domain, RING1 domain, a in-between-ring (IBR) domain and a RING2 domain at the C-terminus.

The ubiquitination process

Ubiquitination requires the sequential action of three different enzymes: ubiquitin-activating E1, ubiquitin-conjugating E2, and ubiquitin ligating E3. E1-mediated ubiquitin activation is a two-step reaction dependent on ATP. First the E1 binds to ATP and ubiquitin to catalyse the acyl-adenylation of the C-terminus of ubiquitin, thus creating a ubiquitin-adenylate intermediate. Then the AMP is released and ubiquitin is transferred to a cysteine residue in the E1 active site, to form a high energy thioester intermediate (between ubiquitin's C-terminal carboxyl group and the cysteine sulphydryl group). Ubiquitin is then trans-thiolated from the E1 to the active-site cysteine of a E2 enzyme. Ubiquitin transfer to the ε-amino group of a substrate lysine occurs in a E3 type-dependent manner. There are several types of E3 ligases, mainly HECT (homologous to the E6AP carboxyl terminus)-type, RING (really interesting new gene)-type and RING-related E3s. HECT E3-mediated ubiquitination involves the formation of a thioester intermediate between ubiquitin and a E3 catalytic cysteine prior to substrate ubiquitination, whereas RING-type and U-box E3s act as scaffolds that bring ubiquitin-conjugated E2s and target proteins into close proximity, allowing the formation of an isopeptide bond between the two molecules (Metzger *et al.*, 2012). Substrates can be modified by the addition of a single ubiquitin moiety on one or more sites (mono-ubiquitination and multi-mono-ubiquitination) or can be tagged with chains of ubiquitin (poly-ubiquitination). Chain formation can occur through one of the seven lysines within ubiquitin (K6, K11, K27, K29, K33, K48 and K63) or via ubiquitin's N-terminal methionine (M1; Fig. 1.7). The type of ubiquitin modification specifies the cellular outcome of ubiquitination, and among the eight different chain types, only a few (referred as typical) have been extensively characterised. K48-mediated linkage, for example, has been strongly associated with proteasomal degradation (Mallette and Richard, 2012), whereas K63-linked chains have been shown not to have a degradative function, and to be primarily associated with signalling and protein-protein interaction (Chen and Sun, 2009). The remaining chain types are often referred as atypical, due to their poor characterisation. Only recently these atypical chains are starting to be studied, K6-type linkage has been suggested to have a non-degradative role, whereas K11-mediated ubiquitination seems to be associated with protein degradation. K27-mediated ubiquitin chains have been found to accumulate on damaged mitochondria, while K29 and K33 have been associated with both degradative and non-degradative roles (Kulathu and

Komander, 2012).

In humans there are two E1 enzymes, roughly forty E2s and more than six hundred E3s (of which thirty are HECT-type, Li *et al.*, 2008). Since E3 ligases recruit the substrates and mediate the transfer of ubiquitin from the E2, it is highly likely that these enzymes determine the specificity of ubiquitination. However, whether particular combinations of activated E2s and E3s are required is not clear and would bring the ubiquitination process to another level of complexity. Moreover, it is still to be clarified how the chain linkage is determined. When RING domain or U-Box ligases are involved, it is likely that the conjugating E2 enzyme defines the linkage type, whereas with HECT domain ligases, which form a thioester intermediate with the ubiquitin molecules, the ligases themselves are believed to determine the chain composition (Komander and Rape, 2012).

Parkin

Parkin (coded by the gene *PARK2*) is a cytosolic E3 ubiquitin ligase. This protein comprises of a N-terminal Ubiquitin like (Ubl) domain, a RING0 domain, a RING1 domain, an in-between-rings (IBR) domain and a RING2 domain (Fig. 1.6). RING domains are characterised by several cysteines and histidines involved in the coordination of zinc ions and crucial for the structure and folding of the ligase, moreover in RING-type E3 these structures facilitate the transfer of ubiquitin from the E2 to the substrate (Lorick *et al.*, 1999). Due to the presence of these domains Parkin was initially considered a RING-like E3 ligase, however further investigations classified the protein as part of the newly reported family of RING in-between-RING RING (RBR), which have been described as a hybrid between RING and HECT E3 ligases. In fact, in addition to the presence of RING domains, RBR-type ligases also have a catalytic cysteine (that in Parkin is C431, within the RING2 domain) that forms a thioester intermediate with ubiquitin in a HECT-like fashion (Lazarou *et al.*, 2013).

Parkin, normally exists in a closed, autoinhibited conformation. Structural analysis has shown that the Ubl domain binds the RING1 domain, possibly hindering the E2 binding site, while the RING0 domain blocks the catalytic C431 residue, that is located on the RING2 domain, and is crucial for the ligase activity (Trempe *et al.*, 2013; Wauer and Komander, 2013; Riley *et al.*, 2013). Activation of this ligase is therefore a tightly regulated multi-step process which will be described in the following section.

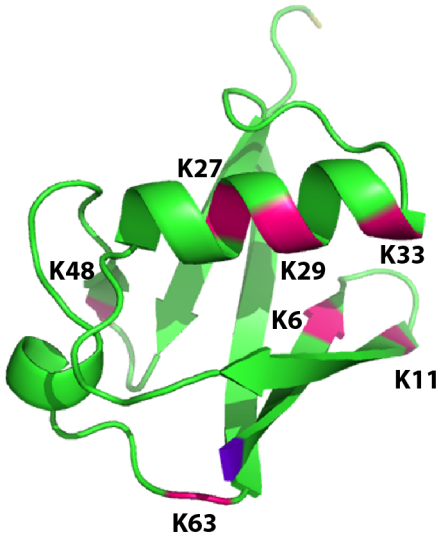

Figure 1.7: Representation of a ubiquitin molecule structure.

3D structure of a ubiquitin molecule generated with PyMOL (PDB=1UBQ). Lysine residues (K6, K11, K27, K29, K33, K48, K63), that mediate ubiquitin chain linkages, are represented in pink, the initial methionine in purple and the C-terminal glycine in yellow.

Parkin has been first associated with early onset autosomal recessive Parkinson's disease in 1998 (Kitada *et al.*, 1998). Since then, many PD-associated mutations have been found and Parkin is now considered the most common cause of inherited early onset PD. Since 1998 Parkin's function and localisation have been extensively studied. Similar to PINK1 deficient flies, Parkin mutants exhibit locomotor defects, muscle degeneration and male sterility (Greene *et al.*, 2003). Moreover, mitochondria from Parkin mutant flies have been described as morphologically abnormal, hyperfused, swollen and with indistinct cristae and this phenotype was reported to be rescued by favouring mitochondrial fission (by overexpression of Drp1 or down regulation of the Mfns or OPA1; Deng *et al.*, 2008; Greene *et al.*, 2003; Yang *et al.*, 2008; Poole *et al.*, 2008). Mouse knock out animals for PINK1 or Parkin have a milder phenotype and do not reproduce the common symptoms of PD, however, mitochondria from these models show defects in respiration and sensitivity to oxidative stress (Chen and Chan, 2009; Pogson *et al.*, 2011). Since their discovery, many groups have investigated the role of PINK1 and Parkin in mitochondrial physiology and pathophysiology, and the role of these proteins has become clearer, even though there are still some open questions in the dissection of their regulation.

Although cytosolic, Parkin has been shown to be efficiently recruited (Narendra *et al.*, 2008) and activated (Kondapalli *et al.*, 2012; Shiba-Fukushima *et al.*, 2012) by the kinase PINK1 onto damaged mitochondria, where the ligase mediates the ubiquitination of more than 100 substrates, as reported by a proteomic study (Sarraf *et al.*, 2013). Parkin has been reported to catalyse K27-, K48- and K63-type ubiquitin linkages (Chan *et al.*, 2011; Geisler *et al.*, 2010; Narendra *et al.*, 2010a), and this process is believed to be a key step in the initiation of the autophagosome formation and in mitochondrial clearance by mitophagy. Disease-associated Parkin mutations not only impact on the protein's ligase activity, but also on its recruitment dynamics, since both a lower activity and delayed recruitment onto damaged mitochondria will affect Parkin-mediated ubiquitination.

Along with its important function in mitophagy, Parkin has also been shown to promote cell survival, in fact overexpression of the ligase limits the translocation of pro-apoptotic Bax to the mitochondrial surface (Johnson *et al.*, 2012) and increases the threshold for cytochrome C release from mitochondria (Berger *et al.*, 2009). Furthermore, Parkin has been associated with neuronal physiology, although its role is debated. Staropoli and colleagues had initially found Parkin to protect neurons from kainate-triggered ex-

citotoxicity by blocking cyclin E accumulation and apoptosis (Staropoli *et al.*, 2003), while Helton and coworkers have reported Parkin to negatively regulate the number and strength of glutamatergic synapses (Helton *et al.*, 2008).

Notably Parkin also stimulates mitochondrial biogenesis, in fact upon depolarization, Parkin promotes the degradation of the transcriptional repressor PARIS, which causes the release of the mitochondrial biogenesis transcription factor PGC1α (Shin *et al.*, 2011), possibly to replace the damaged mitochondria with functional ones.

PINK1 and Parkin in mitochondrial quality control

As previously described, PINK1 processing includes the kinase import from the OMM through the TOM complex and the subsequent proteolytic cleavage of the kinase by several mitochondrial proteases followed by proteasomal-dependent degradation of the protein. Since PINK1 import occurs in a membrane potential-dependent manner, when mitochondria are impaired and their membrane potential is low, PINK1 accumulates on the OMM (Fig. 1.9 A). This is a crucial step in the activation of the mitophagy cascade. Once stabilised on the OMM, PINK1 recruits Parkin from the cytosol and promptly activates it by phosphorylation of serine 65 within the Ubl domain (Fig. 1.9 B). Parkin phosphorylation has been detected within 10 minutes from mitochondrial damage, it is maximal after 40 minutes and it is sustained up to 6 hours from mitochondrial uncoupling. Parkin S65 phosphorylation is thought to release the ligase Ubl domain, thus allowing Parkin to be active (Kondapalli *et al.*, 2012; Shiba-Fukushima *et al.*, 2012).

Supporting this theory phosphorylated Parkin has been shown to catalyse the formation of free ubiquitin chains (Kondapalli *et al.*, 2012) and oxyester intermediates were found between ubiquitin and wild type and phospho-mimic, but not phospho-null Parkin (on a C431S backbone to allow the formation of a stable oxyester bond, Iguchi *et al.*, 2013). However, no studies have shown the role of this phosphorylation on substrate ubiquitination. Interestingly, previous experiments by Lazarou and colleagues aimed to understand the role of PINK1 in Parkin activation have taken advantage of a rapalog-induced heterodimerisation system to force the recruitment of Parkin to polarised mitochondria. This system uses a FKBP (FK506 binding protein) and FRB (a portion of FRAP/mTOR sufficient to bind the FKBP/rapalog complex) domains, which are used

as tags to the proteins of interest, and the drug rapalog (homologue of rapamycin). Exposure to this drug promotes the stable interaction of the two domains. Lazarou and colleagues have elegantly shown that Parkin translocation to functional mitochondria was not sufficient to induce ubiquitination of the organelles and mitophagy. Oppositely, rapalog-dependent translocation and accumulation of PINK1 (lacking its MTS) on the mitochondria induced Parkin recruitment, ubiquitination of the organelles and mitophagy (Lazarou *et al.*, 2012), therefore suggesting that PINK1 not only physically recruits Parkin, but it is also necessary for the ligase activation.

Recruitment and activation of Parkin are not, however, the only steps controlled by the mitochondrial kinase PINK1. Three independent reports have recently identified PINK1 as the first kinase to phosphorylate ubiquitin (Fig. 1.9 A and B; Koyano *et al.*, 2014; Kazlauskaite *et al.*, 2014b; Kane *et al.*, 2014), adding another level of complexity to the regulation of mitophagy. Once accumulated at the OMM, PINK1 phosphorylates both Parkin and ubiquitin at the same conserved serine 65 (in the Ubl on Parkin, Fig. 1.8). Koyano and colleagues have shown that expression of phospho-mimic S65D ubiquitin promotes the activity of phospho-mimic S65E Parkin by analysing its auto-ubiquitination state *in vitro* and *in vivo*. However expression of the ubiquitin phospho-mimic mutant failed to recruit Parkin to mitochondria in the absence of mitochondrial damage (Koyano *et al.*, 2014). These data suggest that PINK1 promotes the activation of Parkin and ubiquitin only surrounding damaged mitochondria (just 0.05% of total ubiquitin is in fact phosphorylated upon damage, Koyano *et al.*, 2014) to promote the ubiquitination of the OMM proteins and therefore mitophagy. Ubiquitin phosphorylation is yet another step in the complex activation of Parkin, but whether this modification is also crucial for ubiquitin incorporation into multimeric chains, or whether specific ubiquitin chains can be favoured by this post-translational modification has not been explored to date.

Once Parkin is fully activated and stabilised on damaged mitochondria, it can ubiquitinate its substrates. Proteomic studies revealed that Parkin may directly or indirectly regulate ubiquitination of more than 100 mitochondrial proteins upon mitochondrial depolarisation (Sarraf *et al.*, 2013), of which the most well characterised are the Mfn1 and Mfn2, VDAC1, Drp1, Tom20 and 40 (Geisler *et al.*, 2010; Wang *et al.*, 2011a; Ziviani *et al.*, 2010; Yoshii *et al.*, 2011; Poole *et al.*, 2010; Sarraf *et al.*, 2013). Recent studies have found two deubiquitinases (DUBs), enzymes that hydrolyse ubiquitin chains, to

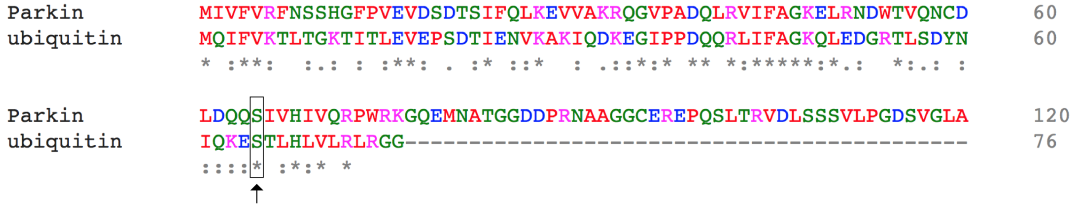

Figure 1.8: Parkin ubiquitin alignment.

Clustal Ω alignment of human Parkin (first 120 residues) and ubiquitin amino acid sequences. The conserved serine 65, target of PINK1-dependent phosphorylation on both proteins, is indicated by an arrow.

counteract Parkin function: USP30, a mitochondrial DUB and USP15 a cytosolic enzyme (Bingol *et al.*, 2014; Cornelissen *et al.*, 2014). Silencing of both proteins favours Parkin-mediated ubiquitination and mitochondrial clearance upon damage, hence these enzymes can be good targets to promote the ubiquitination mediated by defective, PD-associated Parkin mutants.

Whether ubiquitination of specific proteins exerts a distinctive function during mitophagy or it is the overall ubiquitination of the mitochondrion to be essential for the autophagic signalling cascade is not clear. The presence of several ubiquitinated proteins on the mitochondrion drives the recruitment of elements of the autophagic machinery and the formation of autophagosome-like structures, that will result in the formation and maturation of the autophagosome. This autophagic organelle will then fuse with acidified lysosomes causing the degradation of the mitochondrion. Parkin-mediated protein ubiquitination on damaged mitochondria, has however also been associated with protein degradation by the proteasome. For example ubiquitination of the mitofusins, one of the most well characterised targets of Parkin, determines their retrotranslocation from the damaged mitochondria by the ATPase valsolin containing protein (VCP or p97), followed by their degradation by the proteasome (Tanaka *et al.*, 2010). This is a key step in the initiation of mitophagy, since on one hand the damaged mitochondria are unable fuse with the functional mitochondrial network, and on the other hand the elimination of the fusion proteins favours the fragmentation of the mitochondria, thus promoting their clearance. Recent studies have shown that several proteins are degraded in a proteasome-dependent manner, and in addition proteasomal subunits have been shown to be recruited to damaged mitochondria (Tanaka *et al.*, 2010; Chan *et al.*, 2011). This raises the interesting question on whether the mitochondrial ubiquitinated proteins are required to recruit the autophagic machinery, but are also needed to be degraded before the formation/maturation of the phagosome. Or more specifically if specific proteins (i.e. Mfn) need to be rapidly degraded to allow another subset of proteins to induce the formation of the autophagosome.

Regulators of Parkin recruitment onto damaged mitochondria

Since the importance of the mitochondrial quality control system, there is a great interest in thoroughly investigating this pathway and finding its possible regulators. Recently

Hasson and colleagues via a high throughput screen have identified several positive and negative regulators of mitophagy. In particular, TOMM7 (a component of the TOM complex) and HSPA1L (a member of the Hsp70 family) are two positive regulators of Parkin recruitment to mitochondria, and BAG4, SIAH3 are two negative ones. TOMM7 was shown to be essential for depolarisation-dependent PINK1 accumulation on the OMM, suggesting that this protein might sense the mitochondrial membrane potential and block PINK1 import, however how HSPA1L, BAG4 and SIAH3 regulate this pathway is yet to be investigated (Hasson *et al.*, 2013).

Moreover the Bcl family of proteins has been recently shown to affect mitophagy. Bcl family members are both pro- and anti-apoptotic. Interestingly, overexpression of pro-survival Bcl proteins such as Bcl-XL and Mcl1 inhibit the translocation of Parkin to damaged mitochondria, whereas overexpression of pro-apoptotic members of the family such as Bad, Bim, Nox or Puma favour the translocation of the ligase and therefore mitochondrial clearance (Hollville *et al.*, 2014). Although Hollville and coworkers did find Beclin1, another member of the pro-survival Bcl proteins known to promote the autophagosome formation, to have a role in the regulation of mitophagy, Choubey and colleagues have shown that this protein interacts with the cytosolic pool of Parkin and its knock down inhibits Parkin translocation to impair mitochondria (Choubey *et al.*, 2014; Hollville *et al.*, 2014). Moreover, Mcl1 has been shown to be a target of Parkin, in fact following extensive mitochondrial damage, Parkin, together with PINK1, promotes apoptosis by ubiquitinating this anti-apoptotic protein (Zhang *et al.*, 2014). This suggests that these pathways are intimately linked. It would be interesting to investigate whether the level of mitochondrial damage makes one or the other pathway prevail, and what mechanism could act as a sensor to determine the switch from survival to apoptosis.

Treatment of mitochondria with uncouplers and toxins drives extensive mitochondrial depolarization. It is likely, however, that mitochondria often undergo variations in their membrane potential in physiological conditions, for example mitochondrial calcium uptake has been associated with mitochondrial depolarisation (Duchen *et al.*, 1998), and autonomous pacemaking activity of dopaminergic neurons of the substantia nigra pars compacta (SNpc), has been associated with transient and slight mitochondrial depolarisation (Guzman *et al.*, 2010). To recover the mitochondrial membrane potential, the mitochondrial ATP synthase complex reverts its function to hydrolyse ATP and sustain

the proton gradient. However, to avoid the risk of depleting the ATP reservoir to sustain the proton gradient of severely impaired mitochondria, the ATPase inhibitory factor 1 (ATPIF1) blocks this ATPasic activity of complex V. Although it is not clear how ATPIF1 is activated or how it senses the level of damage, by blocking the rescue of the mitochondrial membrane potential, ATPIF1 favours PINK1 stabilisation on the OMM, Parkin recruitment and ultimately mitophagy of the damaged organelle. Mitochondrial damage of ATPIF1 knock down cells results in higher mitochondrial membrane potential (compared to control) associated with the lack of accumulation of PINK1 (Lefebvre *et al.*, 2013).

In addition to mitochondrial damage, an increased amount of mitochondrial unfolded proteins activates the unfolded protein response. This generally promotes the expression of chaperones (Hsp60 and Hsp70) and mitochondrial proteases to counteract and process the unfolded proteins, thus providing an inner mitochondrial quality control. It has been recently shown that accumulation in the mitochondrial matrix of unfolded proteins (due to the expression of a non cleavable mutant of ornithine carbamyl transferase) activates the PINK1/Parkin pathway on polarised mitochondria (Jin and Youle, 2013). The mechanism by which PINK1 accumulates on the OMM of polarised organelles is unclear, however it is interesting that different levels of quality control cooperate to segregate and remove dysfunctional mitochondria.

Mitophagy

There are three main types of autophagy: microautophagy, chaperone-mediated autophagy (CMA), and macroautophagy. Microautophagy involves invaginations of the lysosomal membrane to directly engulf molecules from the cytoplasm. CMA instead requires the chaperone Hsc70 to recognise and unfold substrate proteins characterised by the specific sequence KFERQ (Dice, 1990). These substrates bind to the lysosomal protein LAMP-2A, are translocated within the lysosome and degraded . Macroautophagy is often directly referred to as autophagy, this process has been firstly described in yeast and it is highly conserved. Non specific macroautophagy is often used by the cell as a catabolic reaction to rescue nutrients and amino acids by digesting cytosolic cargoes, for example during starvation (Schneider and Cuervo, 2014). However, macroautophagy

can be selective and in this case it is used by the cell to clear damaged or malfunctional organelles such as mitochondria. Mitochondrial autophagy is termed mitophagy (Kim *et al.*, 2007). During this process a bilayered isolation membrane is formed, it expands and engulfs the targeted organelle, forming a structure called the autophagosome. This autophagosome then matures and eventually fuses with a lysosome, promoting the degradation of its content by the lysosomal proteases. The latest stages of mitophagy generally take place at perinuclear level. This process has been shown to involve the coordinated action of up to 30 distinct proteins which, in yeast, are named autophagy-related proteins, ATGs. Specifically, knocking down ATG3, ATG5 or ATG7 prevents degradation of impaired mitochondria (Narendra *et al.*, 2008).

Parkin-dependent mitochondrial ubiquitination triggers the induction of mitophagy by the recruitment of several adaptors that bind both poly-ubiquitinated proteins and autophagy-related adaptors, such as p62 and HDAC6. P62, also known as sequestosome1, has been reported to accumulate on depolarised mitochondria, and due to its ability to bind the autophagosomal protein LC3 (MAP1 light chain 3, homologue of the yeast Atg8), has been suggested to promote the autophagosome formation. However whether p62 is or is not dispensable for mitochondrial clearance is debated (Geisler *et al.*, 2010; Narendra *et al.*, 2010a). A possibility is that the newly described protein NBR1, by binding LC3 and ubiquitinated cargoes compensates for p62 loss (Kirkin *et al.*, 2009). The histone deacetylase HDAC6 also binds ubiquitinated proteins and links them to the dynein motors. Recruitment of this protein to damaged mitochondria suggests a possible link between mitochondrial transport and mitophagy. Interestingly, p62, NBR1 and HDAC6 have all been found to be upregulated in mitophagy (Chan *et al.*, 2011). Moreover Parkin could itself promote the autophagosome formation. Van Humbeek and colleagues have found by mass spectrometry the autophagy promoting protein Ambra1 (activating molecule in Beclin1-regulated autophagy) to interact with Parkin. Ambra1 activates the class III phophatidylinositol 3-kinase (PI3K) complex, which is essential for the formation of the autophagosome, and interestingly the interaction between Ambra1 and Parkin increases following mitochondrial damage, suggesting that the ligase itself may have a role in the recruitment of the autophagic machinery (Van Humbeeck *et al.*, 2011). Similarly, full length PINK1 has been found to interact with Beclin1, that together with its interactor class III PI3K, is required for the initiation of the autophagosome (Michiorri *et al.*, 2010). More recently, Yamano and colleagues have shown that TBC1D15 and TBC1D17, two members of of the TBC (Tre-2/Bub2/Cdc16) family, that

function as Rab GTPase activating proteins (RabGAP) act together with Fis1 to control the autophagosome formation following mitochondrial damage. In particular these RabGAPs bind Fis1 and LC3 homologue proteins (LC3 and GABARAP) and regulate the activity of Rab7, a key protein involved in the shaping of the forming phagosome (Yamano *et al.*, 2014).

Most of the investigations on the mitophagic pathway have been done in morphologically simple, non neuronal cells, however an important question is where mitophagy occurs in complex cells such as neurons. In neuronal cells most of the mature acidified lysosomes are localised in the somatic region, therefore in order to degrade their components autophagosomes need to be actively transported to the soma to fuse with these degradative organelles. Accordingly, Maday and colleagues have shown that in axons, peripheral autophagosomes mature while trafficked back from the neuronal periphery to the cell soma, where they fuse with acidified lysosomes (Maday *et al.*, 2012). In agreement, Cai and collaborators have shown that damaged mitochondria colocalise with the autophagosomal marker LC3 only in the somatic compartment (Cai *et al.*, 2012). However, recently Ashrafi and colleagues have shown that damaged mitochondria can be cleared at axonal level (Ashrafi *et al.*, 2014). It is possible that both mechanisms occur, likely depending on the extent of damage and on the overall health of the cell.

Mitochondrial-derived vesicles (MDV)

More recently a new type of mitochondrial quality control has been described, the mitochondrial-derived vesicles (MDV, Sugiura *et al.*, 2014; Soubannier *et al.*, 2012; Neuspiel *et al.*, 2008). These are small vesicles (between 70 and 150 nm) that originate from the mitochondria and can either contain only OMM, or both mitochondrial membranes and matrix portions. These vesicles are formed in a Drp1-independent manner and often contain oxidised cargoes. MDV were reported to be formed under oxidative stress and to precede the induction of mitophagy, suggesting that this could be an early type of quality control. More importantly MDV generation does not require membrane depolarisation, and PINK1 and Parkin have been shown to be necessary for the formation of these vesicles (Mclelland *et al.*, 2014). It has been proposed that this mechanism involves PINK1 activity at a very localised level. Local damage (i.e. local protein aggregation, impairment of the import machinery, limited protein oxidation) would cause the

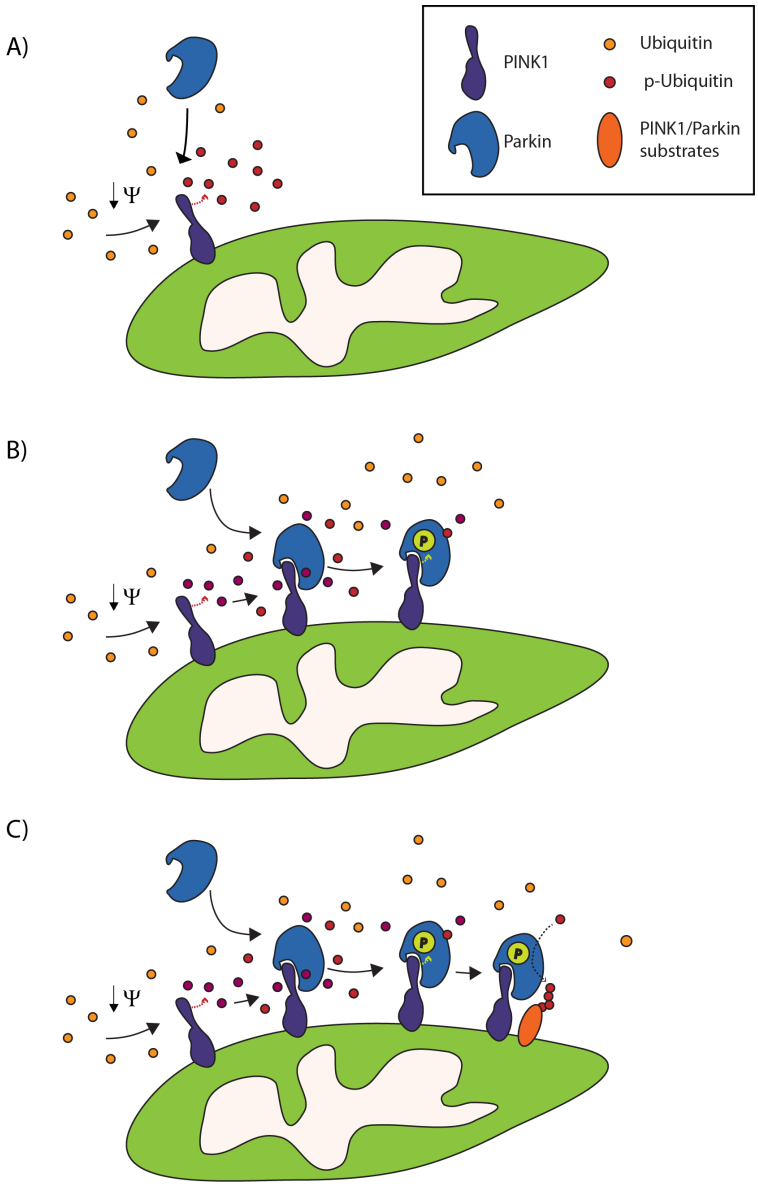

Figure 1.9: Model of PINK1-dependent Parkin activation and ubiquitination of mitochondrial proteins.

(A) Upon mitochondrial damage the kinase PINK1 accumulates on the OMM, triggers the recruitment of the cytosolic E3 ubiquitin ligase Parkin and phosphorylates the ubiquitin molecules surrounding the mitochondrion (Narendra *et al.*, 2008; Kane *et al.*, 2014; Kazlauskaite *et al.*, 2014b; Koyano *et al.*, 2014). (B) Parkin translocates on the damaged mitochondrion, is activated by PINK1-dependent phosphorylation of S65 and further stabilised/activated by the interaction with phospho-ubiquitin (Kondapalli *et al.*, 2012; Shiba-Fukushima *et al.*, 2012). (C) Fully activated Parkin ubiquitinates its mitochondrial substrates, such as Mfns and VDAC1 (Geisler *et al.*, 2010; Gegg *et al.*, 2010; Poole *et al.*, 2010; Ziviani *et al.*, 2010).

accumulation of PINK1 at specific import sites, causing the local recruitment of Parkin. Although the budding mechanism is not known, it has been suggested that protein oxidation could promote protein aggregation and curvature of the mitochondrial membrane. MDV have been shown to be integrated into multi-vesicular bodies (MVB), or directly fuse with lysosomes for degradation. According to this mechanism being parallel to (and preceding) mitophagy, MDV degradation is independent from the autophagic proteins ATG5 and LC3 (Soubannier *et al.*, 2012; Sugiura *et al.*, 2014). MDV have also been shown to be delivered to peroxisomes although the function of this is unknown (Sugiura *et al.*, 2014). Likely, upon complete depolarisation of the mitochondrion, there would be a switch from local removal to general mitochondrial clearance, with PINK1 and Parkin taking part not only in mitophagy, but also in the physiological removal of damaged parts of the mitochondrion.

Parkin independent mitophagy

Most of the studies conducted so far on mitochondrial quality control and mitophagy have converged on the critical function of PINK1 and Parkin. Recently however, some reports have described a Parkin-independent mitophagy. Fu and colleagues have identified gp78 (or AMFR, autocrine motility factor receptor), a ER anchored E3 ubiquitin ligase, generally involved in the ER-associated degradation (ERAD), to play a role in mitophagy. Gp78, localised on mitochondria-associated ER domains (MAMs), has been shown to induce the degradation of the mitochondrial OMM fusion machinery (Mfn1 and Mfn2) and to promote the recruitment of the autophagosomal marker LC3 upon mitochondrial damage. Moreover gp78 function in mitophagy resulted to be dependent on the expression of Mfn1, but not of Mfn2 (Fu *et al.*, 2013). Although the authors show that gp78-mediated mitophagy is Parkin independent, since knock down of Parkin or usage of HeLa cells where the ligase is not expressed did not alter this process, it is puzzling why gp78-mediated mitophagy is not able to compensate for the loss of Parkin function in PD. Notably however, gp78 is only expressed on the ER membranes its function might depend on the number of ER/mitochondria contacts, which can vary according to local calcium levels and cellular stressors (Wang *et al.*, 2000; Raturi and Simmen, 2013). Moreover overexpression of the protein could impact on the number of these contacts favouring its function in mitophagy. Another report demonstrated that

iron chelation can induce PINK1/Parkin-independent mitophagy in fibroblasts. This process was detected by LC3 decoration of mitochondria and quenching of GFP signal in a GFP-mCherry tandem reporter (GFP fluorescence, but not the mCherry one is quenched by the low pH of the autophagosomes) often used to study autophagy. The mechanism by which loss of iron induces mitophagy and how the autophagy machinery is recruited to the mitochondria is not clear, however this seem to be dependent on a decrease in the mitochondrial respiration and on the switch to a glycolytic metabolism (Allen *et al.*, 2013).

Parkinson's disease

Parkinson's disease was first described by James Parkinson in "An Essay of the Shaking Palsy", 1817. PD is the second most common neurodegenerative disorder, affecting 1-2% of the population over the age of 60. While palliative treatments exist, up to date there is no cure available. Clinical features of PD include motor impairment such as resting tremor, bradykinesia, postural instability and rigidity, and non-motor symptoms, comprising autonomic, cognitive and psychiatric problems. The pathological hallmarks of Parkinson's are characterized by the progressive loss of neuromelanin-containing dopaminergic neurons in the substantia nigra pars compacta (SNpc). Cytoplasmic proteinaceous inclusions named Lewy bodies, and dystrophic Lewy neurites are often found in surviving neurons. Notably however, there are cases of PD patients which do not display such aggregates, while Lewy bodies can be found in patients carrying other diseases (e.g. Lewy body dementia) as well as clinically normal people. Although, neuronal loss in SNpc is pronounced, there is a widespread neurodegeneration in the central nervous system (CNS) with the pars compacta being the most affected (Corti *et al.*, 2011).

The majority of Parkinson's disease cases are sporadic, with only $<10\%$ of the cases being inherited. The pathophysiological basis for the progressive cellular dysfunction that causes Parkinson's disease have long remained elusive, however age, use of drugs (exposure to MPTP is capable of inducing parkinsonism) and pesticides (rotenone and paraquat) have been described as risk factors for the disease. Although the inherited cases are rare, the discovery of genes linked to these familial forms of PD have provided

a huge progress in understanding molecular pathogenesis of PD, leading to the identification of several molecular pathways that are affected in the disorder (Corti *et al.*, 2011).

Genetic studies in families with mendelian inheritance of Parkinson's disease have lead to the discovery and cloning of several disease-associated genes. The first reported gene associated with autosomal dominant PD was *PARK1* (encoding α-synuclein, a major component of Lewy bodies, Polymeropoulos *et al.*, 1996). Since then, at least 16 loci (*PARK1* to *PARK16*) and 11 genes have been associated with inherited forms of parkinsonism. *PARK1* together with *PARK8* (LRRK2), are associated to autosomal dominant PD. While *PARK2* (Parkin), *PARK6* (PINK1), *PARK7* (DJ-1) and *PARK9* (ATP13A2) are associated with the autosomal recessive form of the disease (Martin *et al.*, 2011).

Mitochondrial dysfunction was first associated with PD in the early 1980s following the discovery of the mechanism of action of the MPTP, which causes parkinsonism. Once through the blood brain barrier, MPTP is converted into MPP+ in glial cells, which is then taken up by the dopamine transporter of monoaminergic neurons. In these cells it concentrates in mitochondria, where it specifically inhibits complex I of the respiratory chain, leading to ATP depletion, oxidative stress, and apoptotic cell death (Langston *et al.*, 1984; Martinez and Greenamyre, 2012).

From cellular to animal models mitochondrial dysfunction, oxidative stress and impaired clearance of misfolded proteins and damaged organelles have emerged as common features of familial PD, and increasing evidence shows that mitochondrial impairment is associated with both inherited (particularly in the recessive forms) and sporadic PD (Trancikova *et al.*, 2012).

Aim of the thesis

Mitochondrial dysfunction, impaired trafficking and calcium homeostasis have been associated with several neurodegenerative diseased, including Parkinson's. Miro, a key component of the mitochondrial trafficking complex, has been shown to interact with PINK1, a PD-associated protein, playing a major role in the mitochondrial quality control. This suggests that Miro could be a substrate of the PINK1 and Parkin pathway, and more importantly raises the possibility of it being important for the retrieval and clearance of damaged mitochondria.

The aim of this thesis is therefore to investigate the contribution of Miro in mitochondrial quality control, and in particular to study:

- The role Miro1 as a substrate of the PINK1/Parkin pathway following mitochondrial damage
- The characterisation of the Parkin-dependent Miro1 ubiquitination
- The role of Miro1 in the recruitment and stabilisation dynamics of Parkin on damaged mitochondria

Chapter 2

Materials and Methods

Antibodies

The following primary antibodies were used: anti-Miro1 (cat. no. HPA010687, recognising Miro1 and 2, 1:1000), anti-Miro2 (cat. no. HPA012624. 1:1000) and anti-TRAK1 (cat. no. HPA005853, 1:500) antibodies were from Atlas (rabbit), anti-Mfn1 and Apo-Track™ Cytochrome C Apoptosis WB Antibody Cocktail (CValpha, PDH E1alpha, cytochrome C, GAPDH) were from Abcam (1:1000, mouse), anti-Actin (1:2000, rabbit) and anti-Flag (1:1000, rabbit) were from Sigma, anti-Tom20 (1:500, rabbit) was from Santa Cruz Biotechnology, anti mono- and poly-ubiquitinylated conjugates (FK2) was from Enzo Life Sciences (1:1000, mouse), anti-green fluorescent protein (GFP) antibody was from Neuromab (clone N86/8, 1:100, mouse) or Nacalai tesque (1:2000, rat).

The monoclonal antibodies 9E10 (recognising myc) and 12CA5 (recognising HA) were obtained from 9E10 and 12CA5 hybridomas respectively and used directly as supernatant for western blotting and immunofluorescence (1:100). Monoclonal 9E10 and 12CA5 antibodies were produced by growing hybridoma cultures in Integra CL350 flasks. Cells were maintained in the cell compartment in DMEM containing 20 % foetal bovine serum and 0.1 % Gentamicin. The nutrient compartment contained serum free DMEM containing 0.1 % Gentamicin. Cells were harvested every 3-5 days by removal of 4/5 of the media from the cell compartment and its replacement with fresh media. Cells

were pelleted and the antibody containing supernatant was kept, filtered through a 0.45 µm filter and frozen at -20°C. 9E10 and 12CA5 antibodies were produced by Alison Twelvetrees and Rosalind Norkett.

Horseradish peroxidase (HRP) conjugated secondary antibodies were purchased from Rockland and used at 1:5000. Light chain specific HRP conjugated secondary antibodies were from Jackson Immunoresearch (1:5000). Secondary antibodies Alexa-488, Alexa-564 and Alexa-633 or Alexa-647 were purchased from Invitrogen and used at 1:1000. Dylight-405 was from Jackson ImmunoResearch and used at 1:500.

Constructs

cDNA constructs encoding mtDsRed2, ^{GFP}Miro1 and ^{myc}Miro1 have been previously described ((MacAskill *et al.*, 2009a; Fransson *et al.*, 2003, 2006)). ^{GFP}Miro1 S156A and S156E mutations were made by site-directed mutagenesis on the ^{GFP}Miro1 backbone, ^{GFP}TRAK1 was cloned by insertion of the mouse TRAK1 sequence in the EGFP-C1 vector. mito-LSS-mKate2-N1 (large stokes shift mKate2) [plasmid # 31879 (Piatkevich *et al.*, 2010)], pRK5-Parkin-myc [plasmid #17612 (Zhang *et al.*, 2000)], EYFP-Parkin [plasmid #23955 (Narendra *et al.*, 2008)], pRK5-HA-Ubiquitin [plasmid #17608 (Lim *et al.*, 2005)] and Ubiquitin K27 [plasmid #22902 (Livingston *et al.*, 2009)], K29 [plasmid #22903 (Livingston *et al.*, 2009)], K33 [plasmid #17607 (Lim *et al.*, 2005)], K48 [plasmid # 17605 (Lim *et al.*, 2005)], K63 [plasmid # 17606 (Lim *et al.*, 2005)], K48R [plasmid # 17604 (Lim *et al.*, 2005)], K29R [plasmid # 17602 (Lim *et al.*, 2005)] mutants were from Addgene. ^{HA}Ubiquitin K6, K11, K6R, K11R, K27R and K27R-K29R mutants were made by site-directed mutagenesis on the pRK5-HA-Ubiquitin or on the pRK5-HA-Ubiquitin KO [plasmid # 17603 (Lim *et al.*, 2005)] backbone. ^{HA}Ubiquitin S65A and S65E mutants were made by site-directed mutagenesis on the pRK5-HA-Ubiquitin backbone. ^{YFP}Parkin S65A and S65E mutations were made by site-directed mutagenesis on the ^{YFP}Parkin backbone. EGFP-C1 was from Clontech. pcDNA4-PINK1-myc was a gift from Hélène Plun-Favreau and pSC2-mCherry-Miro1 was a gift from John Carroll.

Molecular Biology

Polymerase Chain Reaction (PCR)

PCR was carried out using Phusion polymerase (Finnzymes) following the manufacturer's instructions. The PCR reaction was assembled as described in Table 2.1, and then subjected to a PCR programme with appropriate annealing temperature and extension time depending on the experiment (annealing time is 30 seconds/kb for normal PCR and 1 minute/kb for reverse PCR).

PCR reaction - components:	Final concentrations:
10 µL 5x HF-buffer	1x
2.5 µL forward primer	0.5 µM
2.5 µL reverse primer	0.5 µM
1 µL dNTPs mix	200 µM each
1 µL template DNA (50 ng/µL)	1 ng/µL
32.5 µL milliQ water	–
0.5 µL Phusion	0.02 U/µL

Table 2.1: PCR reaction composition.

5 µL of the resulting PCR product was run on an agarose gel to check for the quality of the amplification. If the PCR product consisted in one single band the remaining PCR was purified using a PCR purification kit (Qiagen) following the manifacturer's instructions. If the PCR amplification resulted in multiple bands, 20-40 µL of the PCR were run on an agarose gel, the DNA band at the correct weight was excised, the DNA was extracted and purified with a gel extraction kit (Qiagen) following the manufacturer's instructions.

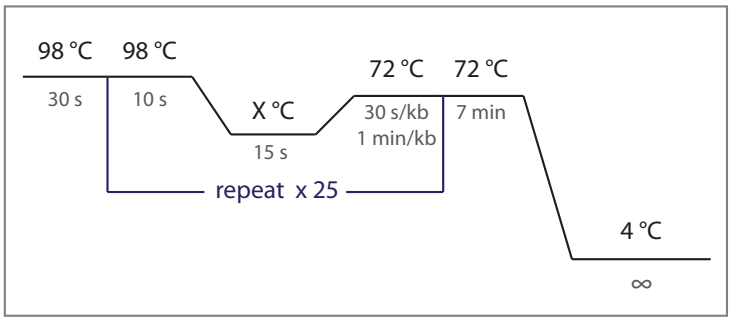

Figure 2.1: PCR protocol.

Agarose gel

Agarose gels were made by melting 1% agarose in 1x TBE buffer. 1 µL of ethidium bromide or 5 µL of StarSafe (Lonza) was added to visualise the DNA. Gels were let to set, and then loaded with DNA samples and DNA ladder (Hyperladder I, Bioline) and resolved at 90-100V for the required time (approximately 1 hour).

Digestion and purification

5 µL of the purified insert and 1 µg of the vector were digested with the selected restriction enzymes (NEB) in the appropriate digestion buffer (NEB), supplemented with BSA for 1 hour. Digests were resolved on an agarose gel and insert and vector bands were excised and purified using gel extraction kit (Qiagen) following the manufacturer's instructions.

Ligation

Purified insert and vector were combined at a 3:1 ratio and incubated with 2 µL of T4 ligase buffer and 1 µL of T4 ligase (total reaction volume 20 µL) at room temperature (RT) for 30 minutes and at 4°C O/N.

Chemically competent cells

Competent cells were prepared by the Inoue method (Inoue *et al.*, 1990) by Katharine Smith and Nathalie Higgs.

Transformation of competent cells

Competent cells were thawed on ice. 50 µL of cells were transferred to a 14 mL round bottom falcon tube (BD). Following incubation for 30 minutes on ice with the appropriate amount of DNA (3 µL of ligations or 10 pg of plasmid DNA), bacteria were heat shocked at 42°C for 45 seconds. Cells were then incubated on ice for 2 minutes, 200 µL of RT LB media supplemented with 0.4% glucose were added, and cells incubated in a bacterial shaker (230 rpm) at 37°C for 1 hour before plating onto agar plates with the appropriate resistance. Plates were then incubated O/N at 37°C.

The next day, colonies were picked and grown O/N in 10 mL of LB media with the appropriate resistance. DNA was extracted with a mini prep kit (Sigma) and sequenced. Positive bacterial clones were stored as glycerol stocks (750 µL of bacteria supplemented with 250 µL of 60% glycerol) at -80°C.

Site-directed mutagenesis by Reverse PCR

Site-directed mutagenesis was achieved by reverse PCR. Primers used for mutagenesis are listed in Table 2.2, and were designed as shown in Fig. 2.2. The PCR reaction was assembled as described in Table 2.1. The purified PCR product was subjected to phosphorylation to allow the ligase activity. 16 µL of the purified PCR was linearised by incubation at 60°C for 5 minutes. The DNA was then incubated on ice for 2 minutes and 2 µL of T4 ligase buffer and 1 µL of T4 polynucleotide kinase (PNK) were added. The reaction carried out by incubation at 37°C for 30 minutes. 1 µL of T4 ligase was added and the sample was incubated at RT for 30 minutes and at 4°C O/N.

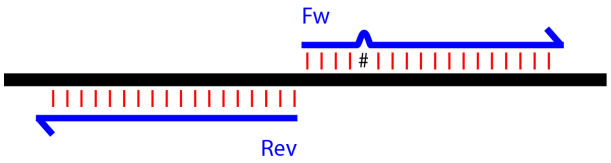

Figure 2.2: Oligonucleotide design for site directed mutagenesis.

Forward and reverse primers were designed so that the forward one carried the mutation of interest between the nucleotides +4 and +6. Primers were ~20nt long, with a GC content of 50% when possible, and with similar melting temperatures (Tm, between 58-70^{o}C).

Mutation	sense	sequence 5' -> 3'
Miro1 S156A	forward	ataGCAgagctcttttattacgc
	reverse	gttcttcaggtttttcgct
Miro1 S156E	forward	ataGAAgagctcttttattacgc
	reverse	gttcttcaggtttttcgct
Parkin S65A	forward	cagGCcattgttcacattgt
	reverse	ctgatccaggtcacaattct
Parkin S65E	forward	caggAAattgttcacattgt
	reverse	ctgatccaggtcacaattct
R6K ubiquitin (on K0)	forward	gtcaAaacgttaaccggtaga
	reverse	gaagatctgcatggtcga
R11K ubiquitin (on K0)	forward	ggtaAaaccataactctagaagt
	reverse	ggttaacgttctgacgaa
K6R ubiquitin	forward	cgtgaGgaccctgactggtaag
	reverse	aagatctgcatggtcgaccc
K11R ubiquitin	forward	ggtaGgaccatcactctcga
	reverse	agtcagggtcttcacgaag
K27R ubiquitin	forward	gtcaGggcaaagatccaagaca
	reverse	attctcaatggtgtcactcggc
K27R ubiquitin (on K29R)	forward	gtcaGggcaaGgatccaagaca
	reverse	attctcaatggtgtcactcggc
S65A ubiquitin	forward	agGccaccctgcacctgg
	reverse	ctttctggatgttgtagtcagaca
S65E ubiquitin	forward	agGAAaccctgcacctgg
	reverse	ctttctggatgttgtagtcagaca

Table 2.2: List of primers used for site-directed mutagenesis by reverse PCR.

Maxi preparation of plasmid DNA

Plasmid DNA was purified from bacterial cultures with Pure Yield Maxi prep Kit (Promega) following the manufacturer's instructions.

Molecular biology solutions

Luria-Bertani Broth (LB)	10 g NaCl 10 g Tryptone 5 g Yeast extract H_2O up to 1 L
Luria Broth Agar (LBA)	10 g NaCl 10 g Tryptone 5 g Yeast extract 10 g Agar H_2O up to 1 L
Ampicillin	100 µg/mL
Kanamycin	30 µg/mL
TBE	89 mM Tris 89 mM Boric acid pH 8.3 2 mM Na_2EDTA
Loading dye (6x)	40% sucrose 0.25% bromophenol blue H_2O

Table 2.3: Bacterial culture and molecular biology solutions.

Cell culture

Cell lines

SH-SY5Y, COS-7, HeLa and HEK 293 cells were maintained in Dulbecco's Modified Eagles Medium (DMEM, Gibco) supplemented with 10% heat inactivated FBS, penicillin and streptomycin (2 µg/mL puromycin was added to the SH-SY5Y non-silencing

or PINK1 shRNA overexpressing cells media as a selection antibiotic). Cells were incubated at 37 °C, in a humidified 5% CO_2 atmosphere. When 80-100% confluent cell cultures were divided. Cells were first washed with PBS and then allowed to detach by incubation with trypsin solution at 37 °C. Cells were pelleted by centrifugation and resuspended in complete DMEM for plating onto new dishes. ^{Flag}Parkin stably overexpressing SH-SY5Y cells were a gift from Dr. Helen Ardley (Leeds Institute of Molecular Medicine) and were previously described (Ardley *et al.*, 2003). VCP scrambled and specific shRNAi overexpressing cells were a gift from Helene Plun-Favreau and were previously described (Bartolome *et al.*, 2013). PINK1 and non-silencing shRNA stably expressing SH-SY5Y were previously described (Wood-Kaczmar *et al.*, 2008; Gandhi *et al.*, 2009). Human fibroblasts were derived from punch biopsies taken with informed consent from a control patient or from a patient carrying a homozygous deletion of exons 3 and 4 of the *PARK2* gene by Thomas Foltynie and Kailash Bhatia (Institute of Neurology, UCL, London). The ethics for this study were approved by the London – City Road and Hampstead REC committee. The tissue was dissected by Hsiu-Chuan Wu and fibroblasts cultured in Dulbecco's modified Eagle medium (DMEM) supplemented with 10% heat inactivated FBS, penicillin and streptomycin. Cells were kept in 5% CO_2 at 37°C, in a humidified incubator.

Neurons

Neuronal cultures were prepared from E18 Sprague Dawley rat embryos. Time pregnant rats were killed following United Kingdom regulations. Embryos of either sex were removed and placed onto ice-cold dissection media (HEPES-buffered Hank's Balanced Salt Solution HBSS, Invitrogen). Brains were isolated, meninges were removed and hippocampi were dissected. Hippocampi were incubated in 0.125% trypsin diluted in dissection media (5 mL) for 15 minutes at 37°C. Neurons were cleared from further trypsin enzymatic activity by three washes in pre-warmed attachment media (Minimum Essential Medium supplemented with 10% horse serum, 1 mM sodium pyruvate, and 33 mM glucose). Hippocampi were gently triturated with a fire-polished glass pasteur pipette, followed by trituration with a second fire-polished pipette with a 60% diameter of the first one. Cells were counted using a Neubauer Haemocytometer and cell viability was assessed by erythrosin B exclusion. 350.000 hippocampal neurons were plated in 6 cm dishes containing 13 mm coverslips coated with 500 µg/mL (PLL). Neurons were

allowed to attach and 4 to 6 hours after plating, media was replaced with neuronal maintenance media (Neurobasal supplemented with 2% B27, 1% glutamine, and 33 mM glucose) and cultures were kept in 5% CO_2 at 37°C, in a humidified incubator.

Transient Transfection

Nucleofection (cell lines)

Pelleted cells obtained after trypsinization were resuspended in 100 µL of WT-EM solution, the appropriate amount of DNA was added (1 µg per 3 cm dish, 2-3 µg per 6 cm dish, 4-5 µg per 10 cm dish), cells were transferred in cuvettes and nucleofected using the appropriate Amaxa program. Nucleofected cells were then immediately plated into DMEM complete media-containing plates and left to express for 48 hours.

Electroporation

Pelleted COS-7 cells obtained after trypsinization were washed in Opti-MEM® (Gibco). After re-pelleting cells were resuspended in 500 µL Opti-MEM®/transfection and 5 µg of DNA was added (10 cm dish). Cells were transferred into a cuvette and electroporated using a Capacitance Extender II accessory module. Voltage was set at 400 mV and high capacitance at 125 µF. Cells were then plated in DMEM complete media and left to express for 24-48 hours.

Calcium phosphate

7-9 days in vitro (DIV) hippocampal neurons were transfected by calcium phosphate method (Graham and Van Der Eb, 1973). 2.5 µg DNA were diluted in 27 µL of MilliQ water. 3 µL of 2.5 M $CaCl_2$ were added and this mixture was transferred in a new tube containing 30 µL of 2x HBS. This was added dropwise to the neuronal culture (on coverslips) previously placed in a 3 cm dish containing 1 mL of prewarmed neurobasal media. The DNA precipitates were checked on a light microscope and neurons were placed in the incubator for 7-15 minutes. The media was removed and replaced with

conditioned maintenance media. Cells were left to express for 24-48h unless otherwise stated.

Treatments

Carbonyl cyanide 4-(trifluoromethoxy) phenylhydrazone (FCCP, Sigma) was used at 10 µM, MG-132 (Cayman Chemical) was used at 30 µM for 30 minutes before and during FCCP treatment, Bafilomycin 1A (Biovitica) was used at 1 µM for 30 minutes before and during FCCP treatment, valinomycin (Sigma) was used at 2 µM in neurobasal medium (Gibco) supplemented with 0.6% D-glucose.

Cell culture media and reagents

PBS	137 mM NaCl 2.7 mM KCl 10 mM Na_2HPO_4 2 mM KH_2PO_4
Trypsin solution	137 mM NaCl 2.7 mM KCl 8 mM Na_2HPO_4 1.5 mM KH_2PO_4 2.5 g/L trypsin (from porcine pancreas) 200 mg/L EDTA
Dissection media	HBSS (Gibco) 10 mM HEPES
Attachment media	MEM (Gibco) 10% horse serum 1 mM sodium pyruvate, and 33 mM glucose
Maintenance media	Neurobasal (Gibco) 2% B27 supplement (Gibco) 1% glutamine
WT-EM	15 mM NaH_2PO_4 35 mM Na_2HPO_4 5 mM KCl 10 mM $MgCl_2$ 11 mM Glucose 100 mM NaCl 20 mM HEPES
2x HBS pH 7.11	274 mM NaCl 10 mM KCl 1.4 mM Na_2HPO_4 15 mM D-Glucose 42 mM HEPES

Table 2.4: Cell culture and transfection solutions.

Biochemistry

Cell lysis

For protein analysis confluent cells were lysed in the appropriate buffer. Briefly, cells were washed twice in PBS to remove the media, lysis solution was added (Laemmli sample buffer, radioimmunoprecipitation assay -RIPA- buffer or Tris-based Triton-X buffer) and cells were scraped from the plate. When whole protein lysates were analysed cells were directly lysed in 1x Laemmli sample buffer, transferred in Eppendorf tubes and genomic DNA was broken down by homogenization with a 1 mL syringe provided with a 25 Gauge needle prior to protein denaturation at 95°C. When proteins needed to be immunopurified either for post-translational modification (PTM) analysis or for protein-protein interaction analysis, cells were lysed in RIPA (PTM analysis) or Tris-based Triton-X 100 buffer (protein-protein interaction analysis). Lysates were transferred into new Eppendorf tubes and were then incubated on a rotating wheel at 4°C for 1 hour prior to nuclei and cellular debris elimination by centrifugation at 20000 g for 10 minutes.

Immunoprecipitation

To immunopurify endogenous proteins, nuclei-cleared cell lysates were incubated with 0.5 µg of primary antibody (Miro1, rabbit) in parallel with a non immune rabbit IgG control antibody for 1.5-2 hours. Protein/antibody complexes were then precipitated for 1.5 hours with 15 µL of a 50% protein A-Sepharose bead slurry (Generon). When GFP-tagged or myc-tagged proteins were to be immunopurified, nuclei-free lysates were incubated with 10 µL of a 50% slurry of either GFP-TRAP beads (Chromotek) or anti-myc beads (Sigma) at 4°C for 2 hours. Bound material was washed three times (co-immunopurification) or five times (immunopurification) in the appropriate lysis buffer before elution with 3x Laemmli sample buffer. Protein samples were then denatured at 100°C for 5 minutes.

Ubiquitin Chain Restriction (UbiCRest) Analysis

UbiCRest assays were performed as previously described (Mevissen *et al.*, 2013). Briefly, ubiquitinated ^{GFP}Miro1 (expressed in ^{Flag}Parkin overexpressing cells, treated with 10

µM FCCP for 1 hour) was immunopurified on GFP-TRAP beads and resuspended in 2x deubiquitinase (DUB) reaction buffer (100 mM Tris pH 7.4, 100 mM NaCl, 10 mM DTT). USP21, OTUD2 and Otulin (produced and purified by Tycho Mevissen, David Komander lab, LMB, Cambridge, UK), diluted in 2x DUB dilution buffer (50 mM Tris pH 7.4, 300 mM NaCl, 20 mM DTT), were incubated for 10 minutes at RT. DUBs were then added to equal amounts of the immunoprecipitated ^{GFP}Miro1 and the reaction was carried out for 30 minutes at 37°C. The reaction was stopped by the addition of Laemmli sample buffer, and samples were separated on a half 8% and half 15% SDS-PAGE gel and blotted on PVDF membrane (Amersham Biosciences).

SDS-Polyacrylamide Gel Electrophoresis (PAGE)

Polyacrylamide gels were generally made using 10% separating gels and 5% stacking gels in Novex 1.5 mm cassettes. Gels were submerged in running buffer in a Novex XCell SureLock Mini-Cell system. Samples resuspended in Laemmli sample buffer and denatured (5 minutes, 100°C) were loaded on the gel and were run at 130-150 V until the dye front reached the end of the cassette.

PhosTag™ SDS-Polyacrylamide Gel Electrophoresis

PhosTag™(Wako), a phosphate binding tag, was used to detect phosphorylated proteins. As illustrated in Fig. 5.1 Chapter 5, this technique is based on a mobility shift caused by binding of the phosphate groups of phosphorylated proteins to the PhosTag™, which determines a slower migration of these proteins and consequent separation from the unphosphorylated species. 20 µM PhosTag™and 20 µM $MnCl_2$ were added to 7% acrylamide gels and solution poured in in Novex 1.5 mm cassettes. 5% stacking gels were cast onto the PhosTag™ resolving gels. Gels were submerged in running buffer in a Novex XCell SureLock Mini-Cell system. Samples, lysed in Laemmli sample buffer, were denatured (5 minutes, 100°C) and loaded on the gel the day of the preparation. Gels were resolved at 140 V until the dye front reached the end of the cassette. Cassettes were opened and the gel submerged in transfer buffer supplemented with 10 mM EDTA for 10 minutes in agitation to remove the $MnCl_2$. Gels were subsequently western blotted.

Western blotting

Gels were transferred onto a Hybond-ECL nitrocellulose membrane (GE Healthcare) or polyvinylidene difluoride (PVDF) membrane (when small proteins such as mono-ubiquitin needed to be detected, Amersham Biosciences) using the Novex system. PVDF membranes were pre-activated in methanol and membrane/gel sandwiches were soaked in transfer buffer. Transfer was carried out at 30 V for 2 hours. Membranes were probed with Ponceau staining and then blocked for 1 hour with 4% milk in PBS-T (1x PBS - 0.05% Tween). Blocked membranes were incubated O /N at 4°C with primary antibodies, then washed 3 times (5 minutes each) with 4% milk PBS-T and incubated for 1 hour with secondary antibodies. After 3 washes (10 minutes each) with 4% milk PBS-T, a final wash with PBS-T was done and membranes were incubated with the Luminata Crescendo or Forte substrate (Millipore) for 1 minute. Bands were then detected using an ImageQuant LAS 4000 CCD camera system (GE Healthcare) and analysed using the QuantityOne Biorad software.

Stripping

Membranes were first washed two times with PBS-T for 10 minutes and then incubated in pre-warmed (37°C) stripping buffer for 20 minutes. Membranes were washed in PBS-T 3 times for 10 minutes and blocked in 4% milk in PBS-T for 1 hour before incubation with the primary antibody.

RIPA buffer	50 mMTris pH 7.4 150 mM NaCl 1 mM EDTA 2 mM EGTA 0.5% deoxycholic acid 1% NP40 0.1% SDS 1 mM PMSF (phenylmethylsulfonyl fluoride) 10 µg/mL antipain 10 µg/mL leupeptin 10 µg/mL pepstatin
Tris/Triton buffer	50 mMTris pH 7.4 150 mM NaCl 1 mM EDTA 0.5% Triton X-100 1 mM PMSF 10 µg/mL antipain 10 µg/mL leupeptin 10 µg/mL pepstatin
3x Lammli sample buffer	150 mM Tris pH 8.0 6% SDS 300 mM dithiothreitol (DTT) 30% glycerol 0.3% bromophenol blue
DUB reaction buffer	100 mM Tris pH 7.4 100 mM NaCl 10 mM DTT

Table 2.5: Cell lysis and biochemical assays buffers.

Biochemistry buffers and reagents

10% resolving gel	10% Protogel (acrylamide solution) 375 mM Tris pH 8.8 1% SDS 1% ammonium persulphate (APS) 0.04% TEMED
Stacking gel	5% Protogel (acrylamide solution) 125 mM Tris pH 6.8 1% SDS 1% APS
10x Running buffer	250 mM Tris 1.92 M glycine 1% SDS
10x Transfer buffer	250 mM Tris 1.92 M glycine 20% methanol 0.35% SDS
Ponceau stain	5% acetic acid 0.1% Ponceau S
Membrane blocking solution	4% non fat milk 0.05% Tween in 1x PBS
Stripping buffer	6.25 mM Tris pH 6.8 2% SDS 0.7% β-mercapto-ethanol in 1x PBS

Table 2.6: SDS-PAGE and western blotting buffers and solutions.

Immunofluorescence and Microscopy

Immunocytochemistry

For fixed imaging, cells grown on coverslips were washed in 1x PBS, and fixed in 4% paraformaldehyde (PFA) solution (4% PFA, 4% sucrose in 1x PBS, pH 7.0) for 10

minutes. After 3 further washes in 1x PBS coverslips were incubated for 10 minutes in blocking solution (0.5% bovine serum albumine (BSA), 10% Horse serum, 0.2% Triton X-100 in 1x PBS). Coverslips were then incubated for 1 hour with primary antibodies diluted in blocking solution, washed 5 times in 1x PBS and incubated with secondary antibodies. After further 5 washes in 1x PBS coverslips were mounted on glass slides using ProGold anti fade reagent (Invitrogen) and later sealed with nail varnish.

Confocal Microscopy

Cells were imaged on a Zeiss LSM700 upright confocal microscope, with an Achroplan 63× oil-immersion lens with 1.4 numerical aperture. Images were digitally captured using ZEN 2010 software.

Image processing

Images were processed in ImageJ for fluorescence intensity quantification, or in Metamorph for colocalisation analysis. For colocalisation studies, cells displying similar fluorescence (indicating comparable transfection levels) were considered. Images were taken with comparable Hi (red)/Low (blue) ratio and then arbitrarily thresholded. The integrated colocalisation function was used to measure the colocalisation.

Immunohistochemistry solutions

PFA solution pH 7.0	4% PFA 4% sucrose in 1x PBS
IF blocking solution	10% horse serum 0.5% bovine serum albumine (BSA) 0.2% Triton X-100 in 1x PBS

Table 2.7: Immunohistochemistry solutions.

Live cell imaging

For neuronal imaging of mitochondria, primary hippocampal neurons were transfected at 7-8 DIV and imaged at 9-10 DIV under continuous perfusion with imaging media warmed to 37°C and flowed at a rate of 1-2 mL/minute throughout the duration of the experiment. For acquisition, fluorescence was captured using an Olympus microscope (BX60M) with a 60× Olympus objective coupled to an EM-CCD camera (Ixon, Andor). Excitation was provided by a mercury arc lamp (Cairn) with the appropriate filters. Images were acquired at 1 frame per second for two minutes throughout. Axonal regions were acquired at a distance of 100 to 200 µm from the cell body. The length of process assayed was ≈ 150 µm.

Imaging solution (ACSF) pH 7.4	125 mM NaCl 10 mM HEPES 10 mM glucose 5 mM KCl 2 mM $CaCl_2$ 1 mM $MgCl_2$

Table 2.8: Live imaging solution.

Live imaging processing

Mitochondrial movement was analysed utilising kymographs, which allow the projection of the spatial displacement along a line-scan of a particle (mitochondrion) across time. The x axis therefore represents the position of particles within the process, and the y axis plots their position changes over time. Live imaging recording files were opened in ImageJ, curved processes were straightened using the "straighten" plug-in and kymographs created by the "multiple kymograph" plug-in. Straight vertical lines represent stationary mitochondria, while oblique lines represent moving mitochondria. Mobility was assessed by counting the percentage of mitochondria moving during the imaging

recording (2 minutes). Mitochondria in a field of view were classed as moving if they moved more than 2 μm.

Statistical analysis

All data were obtained using cells from at least three different preparations. Numbers of cells studied are given in the text or figure legends. Statistical significance across groups was analysed using one-way ANOVA and Dunnett's post hoc test to compare the data groups to their reference group or the Bonferroni's post hoc test to compare all data groups. Individual differences were assessed using individual student's t-tests. Data are shown as mean ± SEM.

Chapter 3

Miro1 regulation by the ubiquitin ligase Parkin

Introduction

Mitochondria are dynamic organelles, they fuse, divide and are actively transported within the cell to areas of high energy demand and calcium buffering requirements. When damaged, these organelles lose functionality and their fusion with the mitochondrial network would cause an overall dilution of the damage, that would ultimately turn into the impairment of the whole mitochondrial network. To prevent this scenario a set of tightly regulated proteins act as a mitochondrial quality control system that recognises, segregates and clears impaired mitochondria, preventing their fusion with the cell's functional mitochondrial network. The principal proteins involved in the detection of damaged mitochondria are PINK1 and Parkin, two proteins associated with early onset autosomal recessive Parkinson's disease (PD). PINK1 is a mitochondrial serine threonine kinase. Although being located on the OMM, the kinase is rapidly imported within the mitochondrion through the TOM complex (Lazarou *et al.*, 2012), cleaved by several proteases including PARL and the fragment degraded by the proteasome (Deas *et al.*, 2011; Jin *et al.*, 2010). Thus, in basal conditions, due to its rapid processing and turnover the levels of PINK1 on the OMM are very low. However, when mitochondria are damaged, their membrane potential drops and PINK1 import is blocked. PINK1

therefore accumulates on the OMM and this is a crucial step in the targeting of damaged mitochondria. Once accumulated, PINK1 recruits Parkin, a cytosolic E3 ubiquitin ligase, and activates it by phosphorylation of serine 65 on its N-terminal Ubl domain. Parkin is then activated and stabilised on damaged mitochondria to ubiquitinate several proteins (including Mfns, VDAC1, Tom20, Drp1; Geisler *et al.*, 2010; Wang *et al.*, 2011a; Ziviani *et al.*, 2010; Yoshii *et al.*, 2011; Poole *et al.*, 2010; Sarraf *et al.*, 2013.). Ubiquitination of these proteins not only prevents mitochondrial fusion with neighbouring mitochondria, but also signals to ubiquitin binding proteins, such as p62, to induce the formation of the autophagosome, a crucial step for mitochondrial autophagy.

In recent years there has been a great interest in further understanding this pathway, and in particular the mechanisms by which malfunctional mitochondria are retrieved from the cell periphery and degraded. In 2009 Weihofen and collaborators have shown by mass spectrometry the interaction between PINK1, Miro and TRAK1, two key proteins of the mitochondrial transport machinery (Weihofen *et al.*, 2009). Miro is a mitochondrial atypical Rho GTPase that, via its interaction with the kinesin motors, mediates mitochondrial trafficking along the cytoskeletal tracks (MacAskill *et al.*, 2009b; Wang and Schwarz, 2009), whereas TRAK1 is a trafficking adaptor that binds both Miro the kinesin and dynein motors (Brickley *et al.*, 2005; Glater *et al.*, 2006; van Spronsen *et al.*, 2013). The interaction between the mitochondrial quality control protein, PINK1 and the trafficking proteins, Miro and TRAK1, suggests the interesting possibility of a functional cross-talk between the two machineries. In fact, mitochondrial damage could induce a PINK1/Parkin-dependent modulation of Miro and/or the TRAKs to favour the transport of the organelles towards the cell soma, in agreement with the directionality of mitochondrial transport being coupled to the functionality of the organelles (Miller and Sheetz, 2004). Another possibility is that damaged mitochondria need to be isolated, which could occur by their uncoupling from the molecular motors. Therefore by modifying Miro, PINK1 and Parkin could induce mitochondrial arrest, in conjunction with the recruitment of the autophagic machinery.

In this Chapter Miro regulation upon mitochondrial damage will be discussed. Analysis of the dynamics of Miro ubiquitination and degradation and the dependency on the kinase PINK1 and the E3 ubiquitin ligase Parkin will be investigated in neuronal dopaminergic SH-SY5Y cell line as well as in human fibroblasts derived from a Parkinson's disease patient carrying a homozygous deletion of exons 3 and 4 of the *PARK2*

gene encoding Parkin. Moreover the stability of the trafficking adaptors, TRAK1 and TRAK2, and their interaction with Miro upon mitochondrial damage will be analysed.

Results

PINK1 and Parkin regulate Miro loss upon mitochondrial damage in human dopaminergic neuroblastoma cells and fibroblasts

To investigate the role of PINK1 and Parkin in the regulation and processing of Miro proteins in neuronal cells, human derived dopaminergic neuroblastoma SH-SY5Y cells were used. In these cells Parkin has been shown to translocate to mitochondria following mitochondrial damage, and to promote their clearance by mitophagy (Geisler *et al.*, 2010). To study the damage-induced regulation of Miro, SH-SY5Y cells, in which endogenous Parkin levels are relatively high (Zhou *et al.*, 2008b), were incubated with the mitochondrial uncoupler FCCP, a proton ionophore that disrupts the mitochondrial membrane potential, therefore causing extensive mitochondrial damage. Cells were treated for increasing amounts of time (from 1 hour to 6 hours) with FCCP (10 μM), lysates were then collected and resolved by SDS-PAGE. Following western blotting, membranes were probed with different antibodies. Miro was detected with an anti-Miro1 antibody (Atlas, cat. no. HPA010687) which is the best available to detect the protein, even though it cross-reacts with Miro2 (Fig. 3.1). Analysis of these time-course experiments, showed a loss of endogenous Miro1/2 protein at its expected molecular weight (70 kDa) within 2 hours of FCCP treatment (Fig. 3.2 A, top panel and B, Miro1/2 normalised mean intensity after 2 hours FCCP 0.53 ± 0.13 compared to Miro1/2 intensity in control conditions 1.0, n=6), while the mitochondrial matrix protein, pyruvate dehydrogenase E1, subunit alpha (PDH E1α), used as control, was unaffected.

To specifically investigate the role of Parkin in the loss of Miro proteins following mitochondrial damage, previously characterised SH-SY5Y cells that stably overexpressed ^{Flag}Parkin (^{Flag}Parkin OE, Ardley *et al.*, 2003) were used. Analysis of the degradation of Miro1/2 over time in experiments performed using ^{Flag}Parkin overexpressing cells and compared to control SH-SY5Y cells, showed that Miro1/2 loss was significantly facilitated by the increased expression of Parkin (Fig. 3.2, Miro1/2 normalised mean

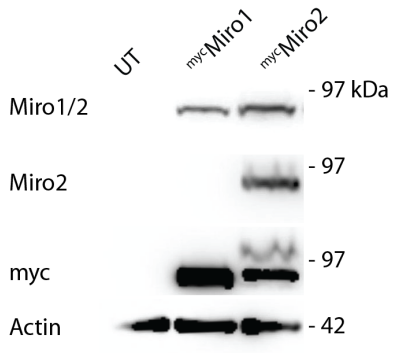

Figure 3.1: Miro antibody characterisation.

COS-7 cells either untransfected (UT) or expressing ^{myc}Miro1 or ^{myc}Miro2 were lysed, proteins resolved by SDS-PAGE and western blotted. Samples were probed with an anti-Miro1 antibody (Atlas, cat. no. HPA010687, top blot), an anti-Miro2 antibody (Atlas, cat. no. HPA012624, second blot from top), and an anti-myc antibody to confirm expression of the two constructs (third blot from top). As shown in the top blot the anti-Miro1 antibody recognised both Miro1 and Miro2 (Miro1/2), while the anti-Miro2 antibody is isoform specific. Both antibodies failed to recognise the endogenous protein in COS-7 cells. Similar loading is confirmed by actin staining.

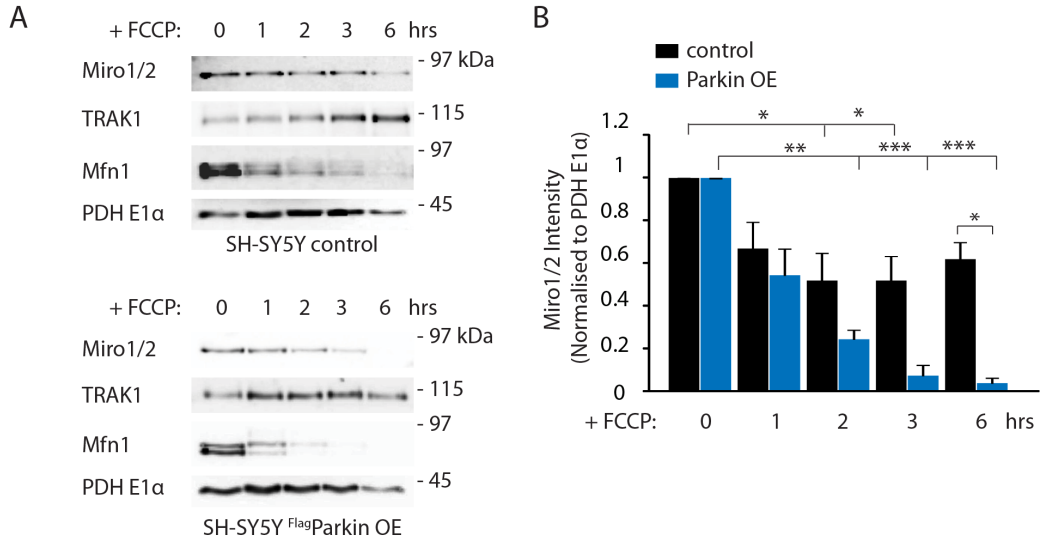

Figure 3.2: Mitochondrial damage triggers Parkin-mediated Miro1 loss.

Control SH-SY5Y cells or cells stably overexpressing ^{Flag}Parkin SH-SY5Y (^{Flag}Parkin OE) cells were incubated with FCCP (10 μM) for the indicated time. (A) shows a FCCP time course experiment indicating the loss of the outer membrane proteins Miro1/2 and Mfn1, but not of the trafficking adaptor TRAK1 or the mitochondrial matrix protein PDH E1α. Loss of Miro1/2 and Mfn1 is favoured by Parkin overexpression. (B) Quantification of Miro1/2 bands (ctr n=6, Parkin OE n=3 independent experiments, *$p<0.05$, **$p<0.01$, ***$p<0.001$).

intensity in control SH-SY5Y cells at 1 hour FCCP 0.67 ± 0.12 SEM, at 2 hours 0.52 ± 0.13 SEM, at 3 hours 0.52 ± 0.12 SEM, at 6 hours 0.62 ± 0.08 SEM; n=6. Miro1/2 mean intensity in ^{Flag}Parkin OE SH-SY5Y cells at 1 hour FCCP 0.54 ± 0.12 SEM, at 2 hours 0.24 ± 0.04 SEM, at 3 hours 0.07 ± 0.05, at 6 hours 0.04 ±0.02 SEM; n=3, *p<0.05, **p<0.01, ***p<0.001).

Since Miro proteins are part of a mitochondrial trafficking machinery, the stability of other key proteins, following FCCP treatment, was analysed. TRAK1, a trafficking adaptor which is known interact with Miro and is part of the transport complex (Brickley *et al.*, 2005; Wang and Schwarz, 2009; MacAskill *et al.*, 2009a) and the mitochondrial fusion GTPase Mfn1, a key regulator of mitochondrial dynamics and known substrate of the PINK1/Parkin pathway (which also interacts with Miro Misko *et al.*, 2010), was monitored. FCCP-induced Mfn1 loss was observed to occur rapidly upon mitochondrial damage and was facilitated by Parkin overexpression similar to previous reports (Ziviani *et al.*, 2010; Gegg *et al.*, 2010). However, TRAK1 protein levels did not decrease under these conditions, rather a trend to increase was observed (Fig. 3.2 A).

As previously described, PINK1 acts upstream of Parkin to recruit the ligase to the OMM of damaged mitochondria (Narendra *et al.*, 2010b). To investigate whether PINK1 was involved in damage-induced Miro loss, SH-SY5Y cells expressing PINK1 shRNA or a non silencing shRNA were used. PINK1 down regulation in these cells was previously characterised (Wood-Kaczmar *et al.*, 2008; Gandhi *et al.*, 2009). Similar to the progressive loss of Miro1/2 detected in Fig. 3.2, FCCP treatment induced a decrease in Miro1/2 levels in non silencing shRNA expressing SH-SY5Y cells transiently transfected with ^{YFP}Parkin, however this effect was blocked by the expression of PINK1 RNAi (Fig. 3.3, Miro1/2 normalised mean intensity in non silencing shRNA in control 1.0, at 1 hour FCCP 0.50 ± 0.15, 2 hours FCCP 0.37 ± 0.16, 3 hours FCCP 0.39 ± 0.20, 6 hours FCCP 0.31 ± 0.12; Miro1/2 mean intensity in PINK1 shRNA expressing cells in control 1.0, at 1 hour FCCP 0.84 ± 0.22, at 2 hours FCCP 0.80 ± 0.30, at 3 hours FCCP 0.78 ± 0.30, at 6 hours FCCP 0.58 ± 0.23, n=4, p<0.05). As expected also Mfn1 loss was inhibited in PINK1 knock down cells, whereas TRAK1 levels showed a trend to increase in both PINK1 and non silencing shRNA expressing cells (Fig. 3.3 A).

To further investigate the impact on Miro regulation in pathological conditions, human patient-derived fibroblasts carrying a homozygous deletion of exons 3 and 4 of the *PARK2* gene encoding Parkin were used. Control fibroblasts and PD patient-derived

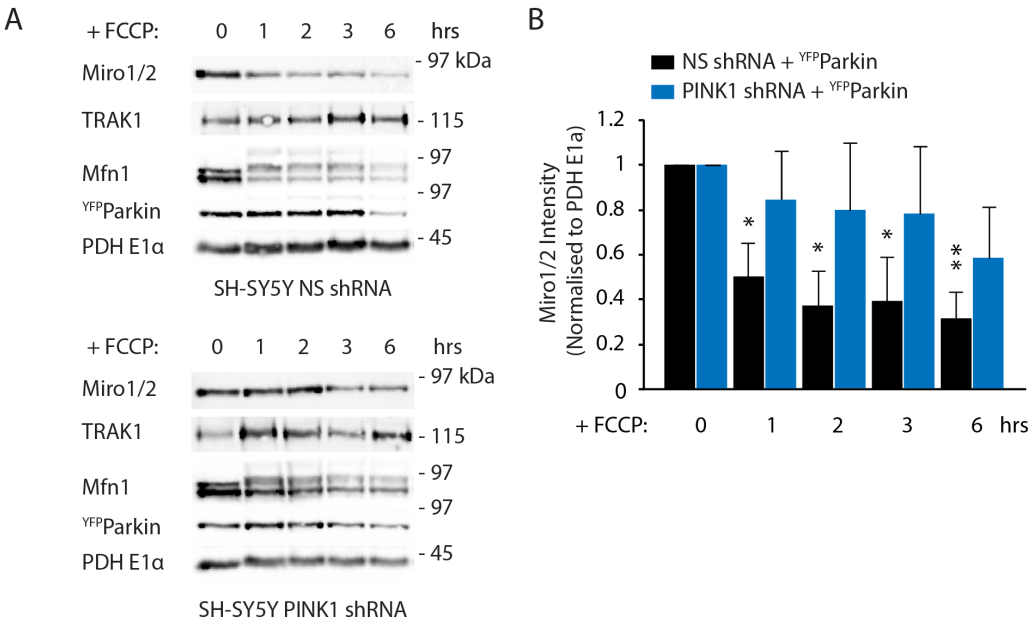

Figure 3.3: Miro1 loss is dependent on PINK1.

SH-SY5Y cells stably expressing either non silencing (NS) shRNA or PINK1 specific shRNA and transfected with ^{YFP}Parkin were treated with FCCP (10 μM) for the indicated time points. In (A) is shown a representative western blot of a FCCP time course experiment. Miro1/2 loss is inhibited by the specific knock down of PINK1. (B) Quantification of this effect (n=4, significance is calculated comparing treated samples to control, 0h. *$p<0.05$, **$p<0.01$).

cells, lacking Parkin, were subjected mitochondrial disruption with FCCP (1 to 6 hours treatment) and the loss of Miro 1/2 was investigated by western blotting. Compared to control fibroblasts, where treatment with FCCP induced a progressive loss of Miro 1/2, in Parkin deficient fibroblasts Miro 1/2 levels were unchanged (Fig. 3.4). Furthermore, as in the dopaminergic SH-SY5Y cells, in the control fibroblasts the levels of Mfn1 decreased, whereas the levels of TRAK1 remained stable over time. Thus Miro levels upon mitochondrial damage, in dopaminergic neuroblastoma cells and in human fibroblasts, are controlled by the PINK1/Parkin pathway. Moreover, the regulation of Miro levels is disrupted in fibroblasts derived from a patient with PD and lacking the E3 ubiquitin ligase Parkin.

Ubiquitination of Miro by a PINK1 and Parkin complex upon mitochondrial damage

The previously described results support a key role for the PINK1/Parkin pathway in regulating Miro levels upon mitochondrial damage in human dopaminergic SH-SY5Y cells and fibroblasts. To examine whether Miro interacts with the key proteins of this pathway, co-immunoprecipitation experiments were performed in $^{\text{Flag}}$Parkin overexpressing SH-SY5Y cells. These cells were transiently transfected with GFP, GFP tagged Miro1 ($^{\text{GFP}}$Miro1), or $^{\text{GFP}}$Miro1 together with myc tagged PINK1 (PINK1$^{\text{myc}}$). FCCP (10 μM, 1 hour) or vehicle (DMSO) treated cells were lysed and $^{\text{GFP}}$Miro1, or GFP (as control) were immunopurified. Complexes were resolved on a SDS-PAGE, western blotted and probed with antibodies to recognise the proteins of interest. The interaction between Miro and PINK1 could be readily detected, as previously reported in HEK 293 cells (Weihofen *et al.*, 2009; Wang *et al.*, 2011b; Liu *et al.*, 2012). Moreover, in agreement with Parkin being recruited to the mitochondrial membrane only upon mitochondrial damage, the formation of a complex between Miro and Parkin could only be observed when PINK1 was overexpressed and upon FCCP-induced mitochondrial damage (Fig. 3.5).

The loss of Miro1/2 at its expected molecular weight upon mitochondrial damage (as shown in Fig. 3.2 and Fig. 3.3) is likely due to Miro ubiquitination by Parkin. Since protein ubiquitination implies the addition of one or several ubiquitin molecules to lysine residues of a protein, this post translational modification (PTM) results in a progressive

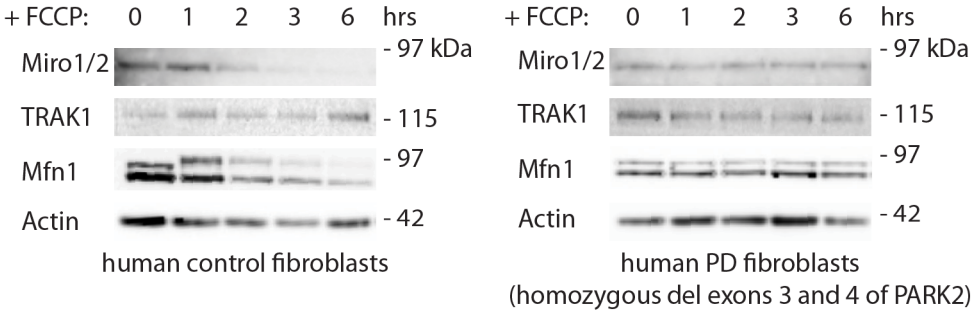

Figure 3.4: Miro1 degradation is impaired in patient-derived fibroblast lacking Parkin.

FCCP treatment (10 μM) of human control fibroblasts triggers the loss of Miro1/2 as well as Mfn1 (left panel), however FCCP-induced mitochondrial damage in human fibroblasts derived from a PD patient carrying a deletion of exons 3 and 4 of the PARK2 gene does not cause loss of Miro1/2 or Mfn1 (right panel).

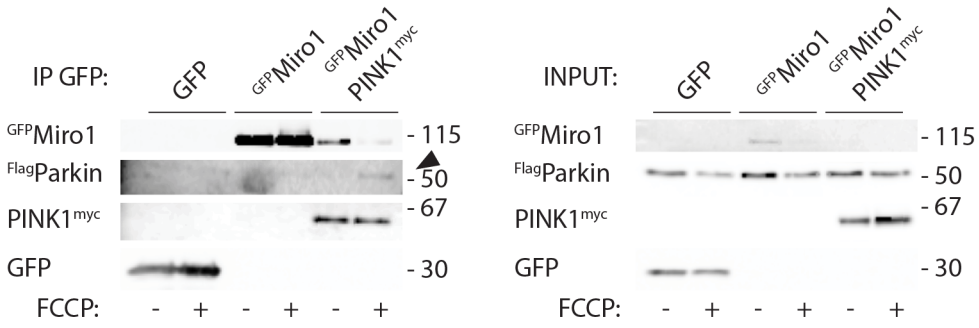

Figure 3.5: Miro1 interacts with the mitochondrial quality control proteins PINK1 and Parkin.

Co-immunoprecipitation experiments carried out in SH-SY5Y cells stably overexpressing ^{Flag}Parkin and transfected with GFP, ^{GFP}Miro1, ^{GFP}Miro1 and PINK1^{myc}. Following FCCP (10 μM, 1 hour) or vehicle, cells were lysed and GFP (as a control) or ^{GFP}Miro1 were immunoprecipitated. Samples were resolved by SDS-PAGE and western blotted. Membranes were probed for Flag (^{Flag}Parkin), myc (PINK1^{myc}) and GFP (GFP or ^{GFP}Miro1). PINK1^{myc} is shown to co-immunoprecipitate with Miro1 in control and treated conditions, but mitochondrial depolarisation is needed for Parkin to participate in the complex.

increase of the protein's molecular weight, which, in a western blot, determines a high molecular weight smear (or laddering) of the protein of interest. To investigate whether Miro1 was indeed ubiquitinated by Parkin upon mitochondrial damage, COS-7 cells were transfected with ^{GFP}Miro1, ^{GFP}Miro1 and ^{myc}Parkin, ^{GFP}Miro1 and PINK1^{myc}, or ^{GFP}Miro1, PINK1^{myc} and ^{myc}Parkin along with ^{HA}ubiquitin.^{GFP}Miro1 was immunoprecipitated from FCCP (10 μM, 1 hour) or vehicle (DMSO) treated samples in a stringent buffer (RIPA), samples were resolved, western blotted and immunoprecipitates were probed with an anti HA antibody to detect ^{HA}ubiquitin conjugated to the immunopurified Miro. Ubiquitination assays show a robust increase in ^{GFP}Miro1 ubiquitination, which can be seen as a high molecular weight smear in the ^{GFP}Miro1 immunoprecipitates, upon FCCP treatment in cells overexpressing Parkin alone, but not PINK1 alone. Co-expression of Parkin together with PINK1 led to a further significant potentiation of ^{GFP}Miro1 ubiquitination, suggesting a cooperative role of the two proteins (Fig. 3.6, ubiquitinated Miro1 when no Parkin or PINK1 are expressed with FCCP 0.88 ± 0.23, and DMSO 1.0, when Parkin is OE with FCCP 2.17 ± 0.33, and DMSO 1.0, *p=0.027, when PINK1 is OE with FCCP 0.88 ± 0.18, and DMSO 1.0, not significant, when PINK1 and Parkin are OE with FCCP 3.85 ± 0.48, and DMSO 1.0, **p=0.006, n=4).

To confirm that the ^{HA}ubiquitin positive high molecular smear was indeed Miro1 ubiquitination, purified ubiquitinated Miro1 samples were subjected to digestion with deubiquitinases (DUBs), a class of enzymes that specifically hydrolyses poly-ubiquitin chains. To this aim the enzymes vOTU (viral Ovarian Tumor Ubiquitinase) and USP21 (Ubiquitin Specific Protease 21) were used. vOTU is a DUB that can cleave ubiquitin chains (but not mono-ubiquitin attached to substrate proteins) whereas USP21 is a very active, chain aspecific DUB (Ye *et al.*, 2011; Akutsu *et al.*, 2011). Ubiquitinated ^{GFP}Miro1 samples extracted and purified from Parkin OE SH-SY5Y previously treated with the mitochondrial uncoupler FCCP (10 μM, 1 hour), were subjected to digestion with either vOTU or USP21. Samples were resolved on a dual acrylamide percentage SDS-PAGE (8 and 15%) and western blotted on PVDF membrane (which has smaller pores than nitrocellulose) due to the small size of mono-ubiquitin (8 kDa). Western blot analysis showed that incubation with USP21 resulted in the complete cleavage of ^{GFP}Miro1 ubiquitin chains, rescue of the protein at its expected molecular weight (100 kDa) and release of mono-ubiquitin. Incubation with vOTU, instead, resulted in an incomplete cleavage of the ^{GFP}Miro1 bound ubiquitin chains, with the long ones being cleaved, and residual short chains, likely mono- or multi-mono-ubiquitination. A partial rescue of the protein

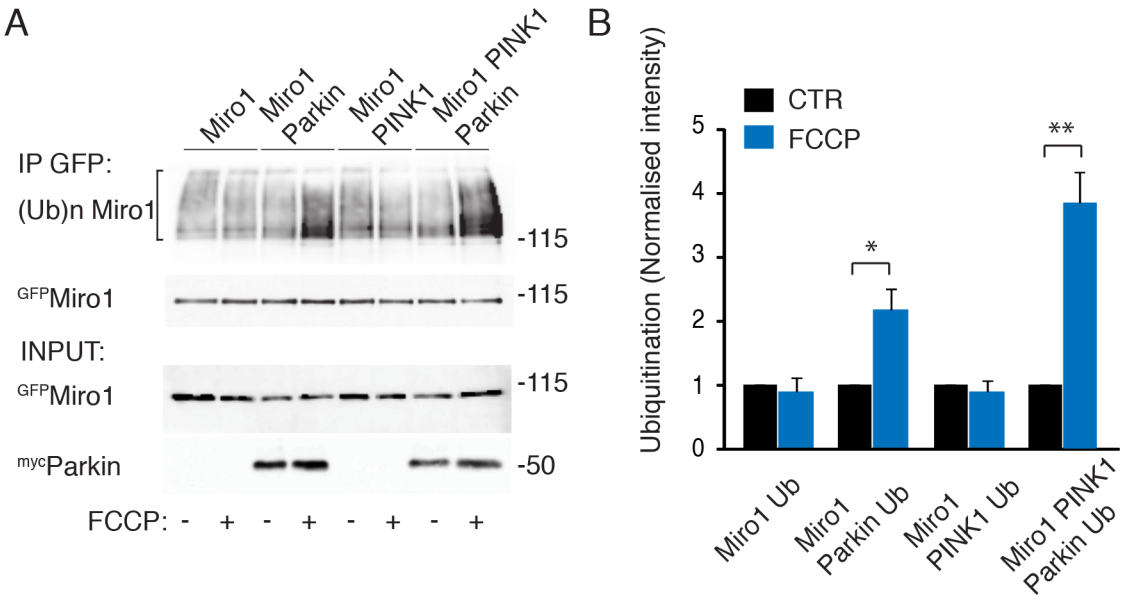

Figure 3.6: Miro1 is ubiquitinated by Parkin.

COS-7 cells transfected with ^{GFP}Miro1, ^{GFP}Miro1 and ^{myc}Parkin, ^{GFP}Miro1 and PINK1^{myc}, or ^{GFP}Miro1, PINK1^{myc} and ^{myc}Parkin along with ^{HA}ubiquitin. Cells were treated with FCCP (10 µM, 1 hour) or vehicle (DMSO), lysed and ^{GFP}Miro1 was immunopurified. Samples were resolved by SDS-PAGE. Membranes were probed with anti-HA, anti-GFP and anti-myc antibodies. Western blot analysis shows that FCCP treatment triggers Miro1 ubiquitination detected as a HA positive high molecular weight smear, when ^{myc}Parkin or PINK1^{myc} and ^{myc}Parkin were overexpressed, but not with PINK1^{myc}overexpression only (*p=0.027, **p=0.006, n=4 independent experiments).

at 100 kDa and release of free ubiquitin were also observed. These data further confirm that the ^{HA}ubiquitin positive smear is exclusively Miro1 poly-ubiquitination (Fig. 3.7).

FCCP-dependent ubiquitination of endogenous Miro1/2

To further characterise Miro1 ubiquitination, damage-induced modification of endogenous Miro1/2 was examined. Neuronal dopaminergic SH-SY5Y cells were transfected with ^{YFP}Parkin and ^{HA}ubiquitin. FCCP (10 μM, 1 hour) or vehicle (DMSO) treated samples were lysed and either incubated with non specific IgG (to control for non specific binding) or with an antibody that specifically recognises Miro1 and 2. Antibody/antigen complexes were then purified by incubation with protein A-conjugated beads and resolved by SDS-PAGE. Western blot analysis showed that endogenous Miro1/2 was robustly ubiquitinated (Fig. 3.8 A), in a similar fashion to heterologously expressed ^{GFP}Miro1.

Moreover, a similar experiment was carried out to confirm that endogenous ubiquitin takes part in Parkin-mediated Miro1/2 ubiquitination. Dopaminergic SH-SY5Y cells stably overexpressing ^{Flag}Parkin were treated with FCCP (10 μM, 1 hour) or vehicle (DMSO). Samples were subjected to immunoprecipitation by incubation with a Miro1/2 specific antibody or non specific IgG as a control, followed by the addition of protein A-conjugated beads to purify the protein complexes. Samples were resolved by SDS-PAGE and western blotted. Membranes were probed with an antibody that specifically detects endogenous mono- and poly-ubiquitin (FK2), which confirmed the presence of endogenous ubiquitin in the FCCP-induced Miro1/2 ubiquitination smear. Whole lysates (inputs) were probed Miro1/2, ^{Flag}Parkin and actin antibodies to confirm similar loading (Fig. 3.8 B).

PINK1 dependency of Miro ubiquitination

PINK1 is known to act upstream of Parkin and, as previously shown in Fig. 3.3, specific knock down of PINK1 blocks Parkin-dependent degradation of Miro1 and Mfn1. Moreover overexpression of this mitochondrial serine threonine kinase potentiates Parkin-dependent ubiquitination of Miro1 in COS-7 cells (Fig. 3.6). To examine whether

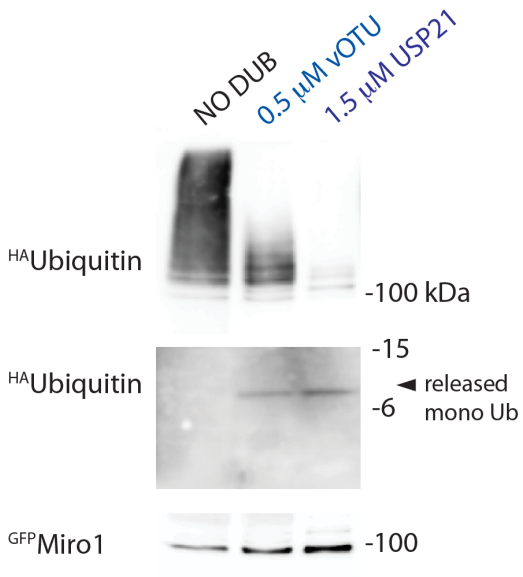

Figure 3.7: Miro1 ubiquitin chains are cleaved by vOTU and USP21.

vOTU and USP21 digested ^{GFP}Miro1, purified from FCCP treated (10 μM, 1 hour) Parkin OE SH-SY5Y cells. Samples were resolved by SDS-PAGE, western blotted, and membranes were probed with anti-HA and anti-GFP antibodies. Incubation with vOTU results in shortening of Miro1 ubiquitin chains to small chains, likely mono- or multi-mono-ubiquitination, whereas incubation with USP21 results in the complete cleavage of Miro1 ubiquitination. In both cases there is a rescue of ^{GFP}Miro1 at 100 kDa and release of free ubiquitin (8 kDa).

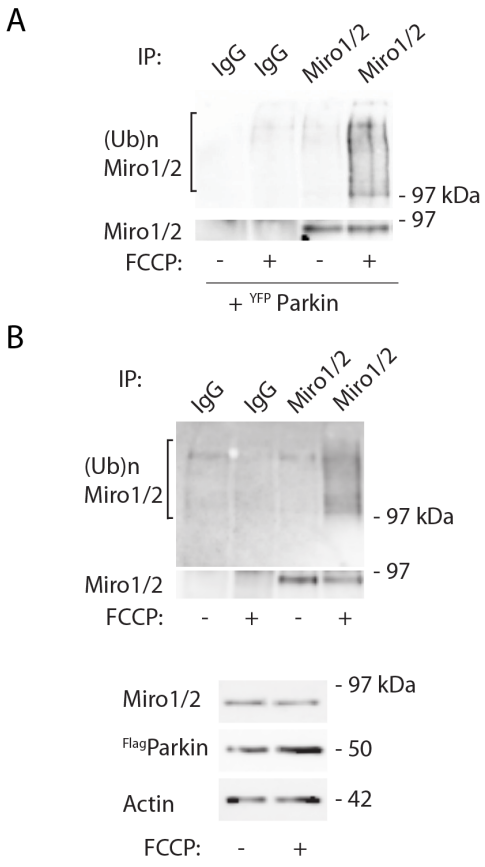

Figure 3.8: Endogenous Miro1 is ubiquitinated upon mitochondrial damage.

(A) Ubiquitination assay of endogenous Miro1/2 in SH-SY5Y cells, heterologously expressing ^{YFP}Parkin and ^{HA}ubiquitin. Following FCCP (10 μM, 1 hour) or vehicle (DMSO) treatment, cells were lysed and incubated with either an antibody recognising Miro1/2 or a non specific IgG as a control. Following incubation with protein A-conjugated beads to purify the antibody/antigen complexes, samples were resolved by SDS-PAGE and western blotted. Mitochondrial depolarisation induced robust ubiquitination of Miro1/2 as visualised by the increase in the HA positive smear. The membrane was stripped and reprobed with anti-Miro1/2 antibody to confirm the presence of the immunopurified protein (n=3 independent experiments). (B) Parkin OE SH-SY5Y cells were treated with FCCP (10 μM, 1 hour) or DMSO. Lysates were subjected to immunoprecipitation with Miro1/2 or IgGs. Immunopurified samples and whole lysates were run on a SDS gel and western blotted. FCCP treatment induces Parkin-dependent ubiquitination of endogenous Miro1/2, which can be detected with an antibody against endogenous mono- and poly-ubiquitin (FK2). Immunopurified samples were reprobed with anti-Miro1/2 antibody to confirm the IP, and whole lysates (bottom panel) were probed for Miro1/2, ^{Flag}Parkin and Actin to confirm similar loading (n=3 independent experiments).

PINK1 is necessary for Parkin-mediated ubiquitination of Miro1, ubiquitination assays were performed in control shRNA or PINK1 specific shRNA expressing SH-SY5Y cells transiently transfected with ^{YFP}Parkin to enhance mitophagy. Analysis of endogenous Miro1/2 ubiquitination by western blotting showed that FCCP-dependent, Parkin-mediated Miro1/2 ubiquitination was drastically blocked when PINK1 was silenced, further confirming the essential role of the kinase in the recruitment and activation of Parkin on damaged mitochondria (Fig. 3.9, ubiquitinated Miro mean intensity in PINK1 shRNA cells 0.16 ± 0.07 compared with ubiquitinated Miro1 intensity in non silencing shRNA expressing cells 1.0; **, p = 0.006; ***, p = 0.0008, n=3 independent experiments).

Mitochondrial damage-dependent regulation of the interaction between Miro1 and the TRAKs

Since Miro1 together with the TRAK adaptors form a complex that couples the mitochondria to the cellular motors, to investigate the impact of Miro1 ubiquitination on mitochondrial transport, Miro1 binding to the kinesin adaptors TRAK1 and TRAK2 following mitochondrial damage was investigated. Parkin OE SH-SY5Y cells were heterologously transfected with either ^{GFP}TRAK1 or ^{GFP}TRAK2, alone (to control for aspecific binding) or together with ^{myc}Miro1. Co-immunoprecipitation experiments from FCCP (10 μM, 1 hour) or vehicle (DMSO) treated samples were analysed by western blotting. Mitochondrial damage triggered ^{myc}Miro1 laddering (as seen in the immunoprecipitated sample and in the inputs), but did not affect its interaction with ^{GFP}TRAK1 (Fig. 3.10 ^{GFP}TRAK1/Miro1 co-immunoprecipitation upon FCCP treatment 1.17 ± 0.11, compared to 1.0 in control). Unexpectedly, an increase in the levels of overexpressed ^{GFP}TRAK2 upon FCCP treatment was consistently observed (Fig. 3.10, ^{GFP}TRAK2 levels upon FCCP treatment 1.90 ± 0.09, compared to 1.0 in control conditions, **p=0.01, n=3). This mirrored an increase in the binding of ^{myc}Miro1 to TRAK2, possibly due to the higher levels of the protein (Fig. 3.10, ^{GFP}TRAK2/Miro1 coIP upon FCCP treatment 3.18 ± 0.79, compared to 1.0 in control, *p=0.04, n=3 independent experiments).

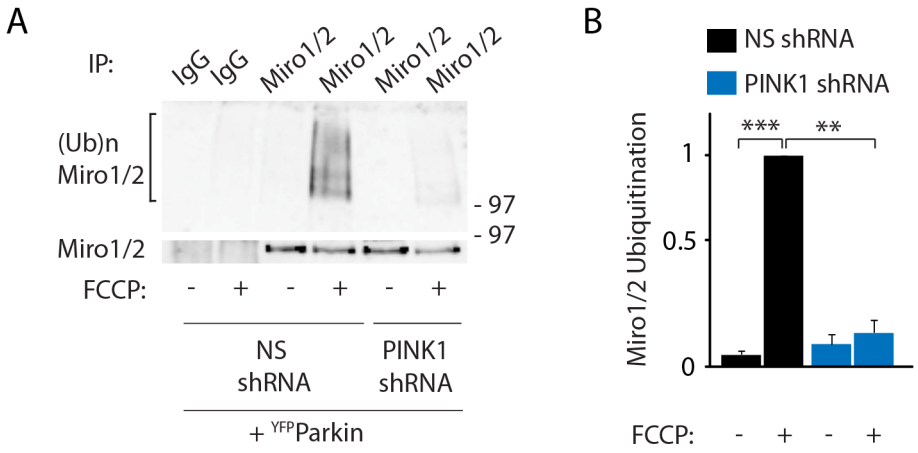

Figure 3.9: Miro1 ubiquitination is dependent on the mitochondrial kinase PINK1.

Endogenous Miro1/2 ubiquitination assays in SH-SY5Y cells stably expressing either a non silencing (NS) shRNA or a PINK1 specific shRNA and transiently transfected with ^{YFP}Parkin and ^{HA}ubiquitin. Following treatment with FCCP (10 μM, 1 hour) or DMSO, cells were lysed and incubated with either an antibody against Miro1/2 or non specific IgGs to control for aspecific binding. Protein complexes were purified by incubation with protein A-conjugated beads, resolved by SDS-PAGE and western blotted. As visualised by the increase in the HA positive smear, FCCP treatment induced robust ubiquitination of Miro1/2 in non silencing shRNA expressing cells, but not in PINK1 shRNA expressing SH-SY5Y cells. The membrane was stripped and reprobed with anti-Miro1/2 antibody to confirm the presence of the immunopurified protein (**p = 0.006; *** p = 0.0008, n=3 independent experiments).

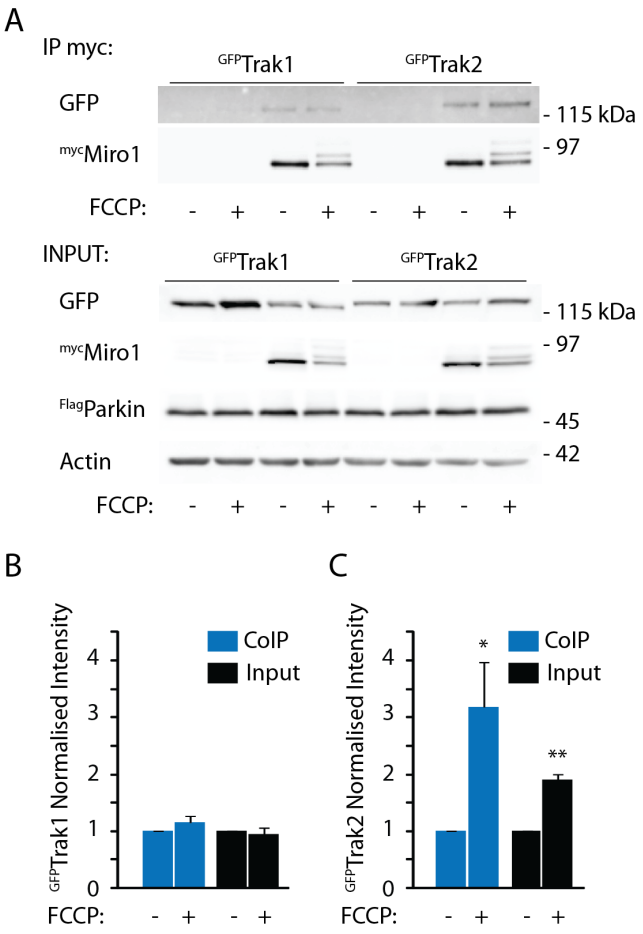

Figure 3.10: Mitochondrial damage regulation of Miro1 interaction with the TRAK proteins.

(A) Co-immunoprecipitation experiments carried out in Parkin OE SH-SY5Y cells transiently transfected with ^{GFP}TRAK1 or ^{GFP}TRAK2, alone or with ^{myc}Miro1. Samples were resolved, western blotted and membranes probed with anti-GFP, anti-myc, anti-Flag and anti-actin antibodies. Treatment with FCCP (10 μM, 1 hour) determined ^{myc}Miro1 laddering, but did not affect its interaction with ^{GFP}TRAK1. ^{GFP}TRAK2 levels were instead altered by FCCP treatment, this increase mirrored an increased interaction with ^{myc}Miro1. (B, C) Quantification of TRAKs levels in the co-immunoprecipitation and in the input after FCCP treatment were normalised to their control (n=3 independent experiments, *p=0.04, **p=0.01).

Discussion

In this Chapter multiple experiments have demonstrated the mitochondrial damage-induced turnover and ubiquitination of the Miro mitochondrial trafficking complex. Using neuronal dopaminergic SH-SY5Y cells as a model system, a robust loss of Miro was detected upon mitochondrial impairment. This process was found to be facilitated by Parkin overexpression and inhibited by PINK1 down regulation (Fig. 3.2 and Fig. 3.3), similar to recent reports in HEK 293 cells (Wang *et al.*, 2011b; Liu *et al.*, 2012) and in agreement with the current model that places PINK1 and Parkin as master regulators of mitophagy. In fact, if PINK1 is essential for Parkin translocation, activation and possibly stabilisation on the OMM, Parkin is necessary for the initiation of mitophagy and the recruitment of the autophagic machinery. Miro1 regulation following mitochondrial impairment was found to be disrupted in a PD patient-derived fibroblasts, which lack functional Parkin, indicating that this pathway might be affected in PD.

Miro loss at its expected molecular weight corresponded to a robust increase in the ubiquitination of the protein which determined its shift to higher molecular weights. In this Chapter the damage-induced loss of Miro was examined and an initial characterisation of its ubiquitination was carried out, however, an in depth analysis of Miro1 processing following ubiquitination will be analysed in Chapter 4. The Mitofusins, key GTPases involved in mitochondrial fusion, are one of the first described substrates of the PINK1/Parkin pathway. Damage-induced degradation of these proteins following their ubiquitination by Parkin is believed to promote the segregation of damaged mitochondria from the functional mitochondrial network by targeting their fusion machinery. It is possible that Miro ubiquitination/degradation has a similar role in the isolation of impaired organelles. Wang and collaborators have shown that Parkin-dependent degradation of Miro causes mitochondrial arrest (Wang *et al.*, 2011b). However, it is still unclear whether ubiquitination of Miro has a role *per sé* in the regulation of mitochondrial transport or it is solely a necessary step in the protein's degradation. Miro is a key protein in the mitochondrial transport machinery, coupling mitochondria to the cellular motors and trafficking adaptors, Miro mediates mitochondrial transport. Miro ubiquitination could directly impact on the trafficking of mitochondria, for example facilitating retrograde versus anterograde mitochondrial trafficking, or the ubiquitin chains could sterically hinder Miro association (or functional interaction) with the microtubule motor proteins leading to mitochondrial arrest. Ubiquitination of Miro1 could

also mediate novel protein-protein interactions which could promote the regulation of mitochondrial trafficking or mitophagy. For example HDAC6 has been shown to bind poly-ubiquitinated proteins and link them to the dynein motors, mediating their trafficking to the cell soma (Kawaguchi *et al.*, 2003). HDAC6 was also reported to promote the activation of an actin-remodelling machinery that favours autophagosome–lysosome fusion. P62 instead links poly-ubiquitinated proteins to LC3, a key component of the autophagosome, thus promoting autophagy (Lee *et al.*, 2010).

Once damaged mitochondria are isolated, an appropriate machinery should be in place to promote their degradation. This is likely to be particularly important in very complex cells like neurons, where mitochondria can be damaged in the periphery (at the tip of the axon, or in the dendritic arborization). Although in neurons, autophagosomes have been shown to form distally and mature on their way to the cell soma where they can then fuse with the lysosomes and degrade their cargo (Maday *et al.*, 2012), Cai and colleagues have reported that, in cortical neurons, mitochondrial damage-induced mito-autophagosomes are only formed in the neuronal soma, where they are then degraded (Cai *et al.*, 2012). Recently, however, Ashrafi and colleagues have shown that damaged mitochondria can be cleared at a peripheral level in neurons (Ashrafi *et al.*, 2014), suggesting that both mechanisms can occur, possibly depending on the extent of damage and on the overall health of the cell. When peripheral isolated damaged mitochondria need to be carried back to the cell soma, an appropriate machinery that identifies them and transports them should be in place. It would be interesting to know whether ubiquitination of Miro could have a role in this mechanism, possibly switching the transport directionality upon damage (before Miro1 is degraded) or, for example, moving from a Miro1-based transport to a Miro2-based transport. Miro2 has half the amount of lysine residues compared to Miro1, suggesting the possibility of a different ubiquitination-dependent regulation between the two proteins. Miro2-mediated mitochondrial trafficking has not been thoroughly studied, however, it would be interesting to investigate whether the two mechanisms are different.

Recent reports have shown that mitochondria-derived vesicles (MDV) can be targeted to lysosomes and peroxisomes (Soubannier *et al.*, 2012; Neuspiel *et al.*, 2008). Formation of these vesicles is promoted by oxidative stress. Interestingly MDVs are formed in a Drp1 and mitochondrial membrane potential independent way, and can contain both inner and outer mitochondrial membranes, preserving membrane polarization. MDVs

are also found to be engulfed in multivesicular bodies (MVB), that in turn deliver them to lysosomes for degradation (Soubannier *et al.*, 2012). MDVs generation was found to be associated with local and restricted accumulation of PINK1 and Parkin recruitment (Mclelland *et al.*, 2014), therefore it would be interesting to investigate whether formation of these structures could mediate the degradation of distal mitochondria by delivering them to the lysosomes.

Interestingly, TRAK1 levels were found to be stable following mitochondrial damage (Fig. 3.2 and Fig. 3.4). TRAK1 and TRAK2 are known not to be only restricted to mitochondria, but also to be associated with other cellular compartments, such as endosomes (Kirk *et al.*, 2006; Webber *et al.*, 2008; MacAskill *et al.*, 2009a). Thus mitochondrial damage could, in principle, relocate these proteins to other cellular compartments and promote mitochondrial arrest. According to this, a previous report has found TRAK1 to be removed from the mitochondria when PINK1 and Parkin were co-expressed (Wang *et al.*, 2011b), however, in the experiments described in this Chapter variations in the levels of PINK1 or Parkin did not impact on Miro1 or TRAK1 levels as described in the above cited report. FCCP-triggered mitochondrial damage induced Miro1 ubiquitination, yet this did not affect the Miro1/TRAK1 interaction (Fig. 3.10). This suggests that, at least one hour after mitochondrial damage, the levels of TRAK1 on the mitochondria are unaffected. Unexpectedly, heterologously expressed ^{GFP}TRAK2 levels were found to be increased upon FCCP treatment in the neuronal, Parkin OE SH-SY5Y cells. This increase in the protein amount mirrored an increased interaction with Miro1 following mitochondrial damage. The enhanced TRAK2 levels could be either due to increased translation (which is unlikely since the protein is heterologously expressed, hence the mRNA lacks its UTR domains necessary for the translation regulation), or to decreased degradation, which could be favoured by stabilising post-translational modifications or changes in protein interactions. The role of TRAK1 and TRAK2 post-translational modifications in their stability has not been investigated, however, both TRAKs have several phosphorylation sites and are known to be O-GlcNAcylated by OGT on conserved serine residues (Iyer *et al.*, 2003; Trinidad *et al.*, 2012). Recently Pekkurnaz and colleagues have shown that glucose-induced O-GlcNAcylation of TRAK1 reduces mitochondrial trafficking (Pekkurnaz *et al.*, 2014), therefore increased TRAK levels on the mitochondria does not necessarily translate to positive regulation of mitochondrial trafficking.

Following one hour incubation with FCCP Miro1 is ubiquitinated but not degraded (see Chapter 4), in addition, the TRAK adaptors can still bind the protein. The current model of the mitochondrial transport machinery predicts Miro to bind the kinesin motors and the TRAKs to bind to both Miro and the kinesins (MacAskill and Kittler, 2010). It would be interesting to investigate whether, when Miro is degraded, the TRAKs can be still localised to the mitochondria, or they are recruited to other cellular compartments. Moreover if the TRAKs can be bound to the mitochondria in the absence of Miro, it would be interesting to know whether they are able to mediate mitochondrial trafficking and whether this can be promoted in both antero- and retrograde directions. Alternatively, due to their dual localisation (mitochondria/endosomes) these proteins could promote the delivery of damaged mitochondria to the endosomal/lysosomal pathway (Webber *et al.*, 2008).

Overall in this Chapter the damage-induced, PINK1/Parkin-dependent regulation of Miro has been analysed. Although Miro1 ubiquitination and degradation has been established and has been confirmed by other groups, many open questions remain concerning how this modification can affect mitochondrial trafficking and processing of the damaged mitochondrion. The functional consequence of the increase in TRAK2 is unclear and further work will be needed to shed light on the role of this protein in mitophagy.

Chapter 4

Characterisation of Miro1 ubiquitination

Introduction

As shown in Chapter 3 mitochondrial damage triggers PINK1 and Parkin-dependent Miro1 ubiquitination. However, whether this modification only results in the rapid degradation of the protein and consequent mitochondrial arrest, or it is an active signalling component of a cascade that initiates with mitochondrial damage and leads to correct mitochondrial disposal is still unclear. Wang and collaborators have shown that, upon mitochondrial damage, Miro was found to be phosphorylated on serine 156, threonine 298 and threonine 299. However, only serine 156 phosphorylation was shown to be required for Miro degradation by Parkin (Wang *et al.*, 2011b). Nevertheless, whether Miro1 phosphorylation by PINK1 is crucial for its recognition and ubiquitination by Parkin is still under debate (Liu *et al.*, 2012).

As previously described Miro proteins are characterised by several signalling domains: two EF-hand calcium binding domains flanked by two GTPase domains. Miro EF-hands have been shown to have a crucial role in sensing calcium levels. In fact calcium binding to these domains is likely to induce a change in the protein's conformation, that leads to the uncoupling of Miro (and the mitochondrion) from the kinesin motor proteins

(MacAskill *et al.*, 2009b). The GTPase domains function is instead less clear. Constitutively active or inactive GTPase domain 1 has been associated with distinct recruitment capabilities of the trafficking adaptor TRAK2 (MacAskill *et al.*, 2009a), possibly affecting the transport directionality. Whether regulation of these Miro signalling domains, either by calcium binding to the EF-hands or GTP/GDP binding to the GTPase domains, could modulate Miro processing and therefore mitochondrial transport following damage, would be interesting to explore.

Ubiquitination can target one (e.g. PCNA) or more (e.g. Arc, EGFR) specific lysines within a protein, or more broadly can target lysines within a specific protein domain (e.g. p53) (Hoege *et al.*, 2002; Mabb *et al.*, 2014; Haglund *et al.*, 2003b; Carter *et al.*, 2007). Human Miro1 comprises of approximately 40 lysines (and Miro2 20) and the identification of which lysine residue(s) on Miro are targeted by ubiquitination, would be extremely important to further study the role of this post-translational modification in mitochondrial transport and mitophagy.

Ubiquitin can be attached to a substrate protein as a single molecule or as a polymeric chain. In fact, ubiquitin contains seven lysines (K6, K11, K27, K29, K33, K48, K63) and one methionine (M1) that can act as acceptor sites for further ubiquitination, resulting in the formation of poly-ubiquitin chains (see Fig. 1.7 in the introduction). Protein mono-ubiquitination is often associated with endocytosis and signalling (Haglund *et al.*, 2003a), whereas, more complex long ubiquitin chains are often linked to different cellular processes. Depending on which residue within the ubiquitin molecule mediates the chain formation, this will determine the topology of the chain. In fact, structural and NMR analysis of polymeric chains has shown that K6 and K48-mediated chains display a compact structure (where adjacent moieties interact with each other), whereas K63 and M1-linked chains are linear. Interestingly K11-mediated linkage can be found in both open and closed conformations (Komander and Rape, 2012). Moreover ubiquitin chains can be either homogeneous, when the same linkage-type is repeated across the whole chain, or mixed, when multiple linkages are involved in the chain elongation. The different chain conformations determined by the specific linkages are likely to determine interaction with specific partners which ultimately will result in specific cellular outcomes. Among the eight different chain types, only a few (referred as typical) have been extensively characterised. K48-mediated linkage, for example, has been strongly associated with proteasomal degradation (Mallette and Richard, 2012), whereas K63-

linked chains have been shown not to have a degradative function, but to be primarily associated with signalling and protein-protein interaction (Chen and Sun, 2009). The remaining chain types are often referred as atypical, due to their poor characterisation. Only recently these atypical chains are starting to be studied, K6-type linkage has been suggested to have a non-degradative role, whereas K11-mediated ubiquitination seems to be associated with protein degradation. K27-mediated ubiquitin chains have been found to accumulate on damaged mitochondria, while K29- and K33-type chains have been associated with both degradative and non-degradative roles (Kulathu and Komander, 2012).

An open question remains as to what determines the chain type. When RING domain or U-Box ligases are involved, it is likely that the conjugating E2 enzyme defines the linkage type, whereas with HECT and RING-in-between-RING (RBR) domain ligases, such as Parkin, that form a thioester intermediate with ubiquitin molecules, the ligases themselves are believed to determine the chain composition (Komander and Rape, 2012).

In this Chapter the temporal dynamics of Miro1 ubiquitination/degradation upon mitochondrial damage in the dopaminergic cell line SH-SY5Y have been analysed by biochemical and immunocytochemistry experiments. The role of S156, T298 and T299 phosphorylation in Miro1 ubiquitination and degradation has been investigated using phospho-null and phospho-mimic (only for S156) Miro1 constructs. The possible interplay between Miro1 signalling domains and its ubiquitination has been analysed using ΔEF mutant Miro1 (lacking the calcium binding ability) and GTPase active (V13), or inactive (N18) mutants. In order to characterise further the role of Miro1 ubiquitination, ubiquitin mutants that allow either one specific chain type, or every chain type apart from a specific one have been used. Data on ubiquitin chain linkage have been further corroborated by restriction analysis with specific deubiquitinases (UbiCRest).

Results

Kinetics of Miro ubiquitination and degradation

Miro ubiquitination could lead to its rapid degradation and removal from the OMM, alternatively Miro could remain on the mitochondrial membrane in an ubiquitinated form

where it may act in other ubiquitination-mediated processes such as signalling. To better understand the dynamics of Miro1 ubiquitination and degradation, ubiquitination assays were performed where Parkin OE SH-SY5Y cells, transiently transfected with ^{GFP}Miro1 and ^{HA}ubiquitin, were incubated for several time points, from 5 minutes to 3 hours with the mitochondrial uncoupler FCCP (10 μM). Cell lysates were collected, ^{GFP}Miro1 was immunopurified and samples were resolved by SDS-PAGE. Western blot analysis showed that the HA positive ubiquitination smear of ^{GFP}Miro1 could be detected as little as 20 minutes after mitochondrial damage, and appeared to remain stable for at least one hour, reaching its maximum intensity at 40-60 minutes after FCCP treatment. This increase in the protein ubiquitination corresponded to a loss of GFP positive Miro1 at its expected molecular weight, 100kDa. Thus, at 1 hour of FCCP treatment Miro1 appears to be fully ubiquitinated, hence undetectable at 100 kDa. At later time points (120-180 minutes) HA positive ^{GFP}Miro1 ubiquitination smear decreased, corresponding to the actual degradation of the protein by proteasomal activity. This effect could in fact be blocked by pre-incubation of the samples with the proteasomal inhibitor MG-132 (30 μM, 30 minutes pre-incubation, Fig. 4.1. In (B) the mean intensities of ubiquitinated ^{GFP}Miro1 at 0 minutes 0.12 ± 0.08, at 5 minutes 0.08 ± 0.03, at 10 minutes 0.09 ± 0.04, at 20 minutes 0.41 ± 0.09, at 40 minutes 1.24 ± 0.23, at 60 minutes 1.0 ± 0.0, at 120 minutes 0.52 ± 0.09, at 180 minutes 0.37 ± 0.08; immunoprecipitated ^{GFP}Miro1 at 0 minutes 1.0 ± 0.0, at 5 minutes 1.09 ± 0.14, at 10 minutes 0.95 ± 0.10, at 20 minutes 0.71 ± 0.18, at 40 minutes 0.16 ± 0.10, at 60 minutes 0.05 ± 0.03, at 120 minutes 0.02 ± 0.01, at 180 minutes 0.01 ± 0.01; n=3, ***$p<0.005$. In (C) mean intensity of ^{GFP}Miro1 ubiquitination at 180 minutes with MG-132 1.33 ± 0.24 compared to 0.37 ± 0.08 at 180 min without MG-132, immunoprecipitated ^{GFP}Miro1 at 180 minutes with MG-132 0.15 ± 0.05, compared to immunoprecipitated ^{GFP}Miro1 at 180 minutes without MG-132 0.01 ± 0.01, n=3, **$p=0.006$).

MG-132 treatment has been reported not only to block proteasomal activity, but also to affect mitophagy (Tanaka *et al.*, 2010). Inhibition of Miro1 degradation by MG-132, instead of being specifically caused by proteasomal impairment, could therefore be due to an overall block of mitophagy. To better understand which pathway was involved in Miro1 degradation, the effect of proteasomal block was compared to that of autophagy inhibition by Bafilomycin 1A. Bafilomycin 1A is an inhibitor of the vacuolar type H^+-ATPase (V-ATPase) which blocks the acidification of the lysosomes, therefore inhibiting autophagy. Parkin OE SH-SY5Y cells heterologously expressing ^{GFP}Miro1 and

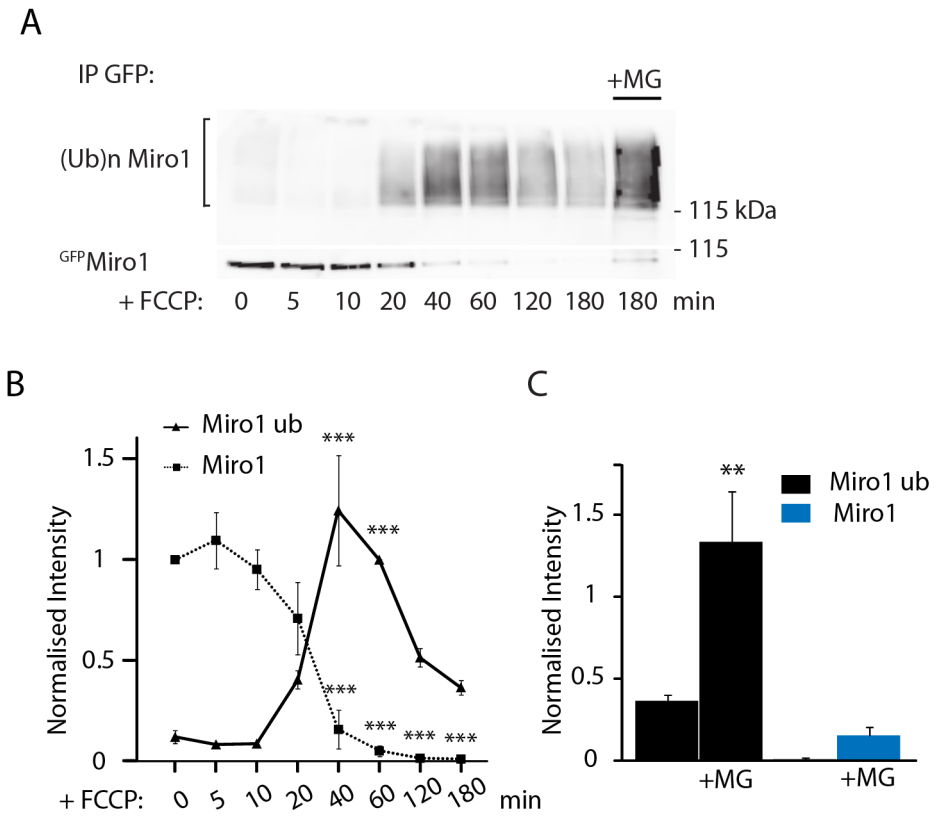

Figure 4.1: Temporal dynamics of Miro1 ubiquitination and degradation.

(A) ^{Flag}Parkin stably overexpressing SH-SY5Y cells were incubated with FCCP (10 μM) for several time points before ubiquitination assays were performed. Samples were resolved and western blotted, membranes were probed for HA and GFP. HA positive ^{GFP}Miro1 ubiquitination can be detected after 20 minutes incubation with the mitochondrial uncoupler and peaks after 40-60 minutes. Although the GFP positive Miro1 band disappears at 60 minutes, an actual decrease in the higher molecular weight species (ubiquitinated ^{GFP}Miro1) indicating protein degradation is detected only after 120 minutes (2 hours). Pre-treatment with the proteasomal blocker MG-132 (30 μM, 30 minutes) resulted in the accumulation of ubiquitinated Miro1. (B) Graph quantifying GFP positive Miro1 bands (immunoprecipitated, dashed line) and HA positive ubiquitination smear intensity (full line) in (A). Average intensities of ^{GFP}Miro1 (IP) are normalised to ^{GFP}Miro1 (IP) at 0 minutes, while Miro1 ubiquitination smear intensities are normalised to the smear intensity at 60 minutes, n=3 independent experiments, ***$p<0.005$. (C) Bar graph showing the quantification of the effect of MG-132 in (A), n=3 independent experiments, **$p=0.006$.

^{HA}ubiquitin were pre-incubated with either MG-132 (30 μM, 30 minutes), Bafilomycin 1A (1 μM, 30 minutes), or their respective vehicles (EtOH or DMSO) and treated with FCCP (10 μM) for 3 hours to allow ^{GFP}Miro1 ubiquitination and degradation. Western blot analysis of the samples revealed that MG-132 treatment, but not Bafilomycin 1A treatment, blocked Miro1 degradation, resulting in an accumulation of the ubiquitinated form (HA positive ubiquitination smear) of ^{GFP}Miro1 (Fig. 4.2). This result confirms that ubiquitinated ^{GFP}Miro1 is processed by the proteasome.

To further investigate Miro stability on the OMM upon mitochondrial damage, immunohistochemical experiments were performed. ^{GFP}Miro was expressed together with the mitochondrial intermembrane space-targeted fluorescent protein mito-LSS (Large Stoke Shift)-mKate2 in Parkin OE SH-SY5Y cells. Cells were treated for several time points (1-6 hours), fixed and imaged with a laser scanning confocal microscope. Fluorescence in both channels was quantified with ImageJ and the levels of ^{GFP}Miro1 were normalised to mito-LSS-mKate2. In agreement with the biochemical results (Fig. 4.1), ^{GFP}Miro1 levels were found to be stable on the OMM for at least 60 minutes after induction of mitochondrial damage with FCCP and well beyond the initial fast ubiquitination, as can be observed by the relatively stable levels of ^{GFP}Miro1 fluorescence signal. Only at later stages (after 2 hours) ^{GFP}Miro1 fluorescence intensity began to decrease (Fig. 4.3 and Fig. 4.4, ^{GFP}Miro1 intensity normalised to mito-LSS-mKate2 intensity at 0 hours 1.0, at 1 hour 0.83 ± 0.14, at 2 hours 0.52 ± 0.09, at 3 hours 0.35 ± 0.003, at 6 hours 0.33 ± 0.01, n=3, **$p<0.01$, ***$p<0.005$), correlating closely with the observed delayed degradation of ubiquitinated Miro (Fig. 4.1). These results demonstrate that in human dopaminergic neuroblastoma cells Miro is initially rapidly ubiquitinated on the OMM where it appears to remain in an ubiquitinated form before undergoing a slower degradation and removal, dependent on proteasomal activity.

Miro1 degradation is VCP independent

Similar to Miro, Parkin-dependent ubiquitination of the Mitofusins has been shown to lead to the degradation of the proteins by the proteasome. In particular valsolin containing protein (VCP) or p97, an ATPase that generally participates in the extraction of ubiquitinated proteins from the ER to promote their clearance, has been shown to mediate the extraction of poly-ubiquitinated Mitofusins from damaged mitochondria,

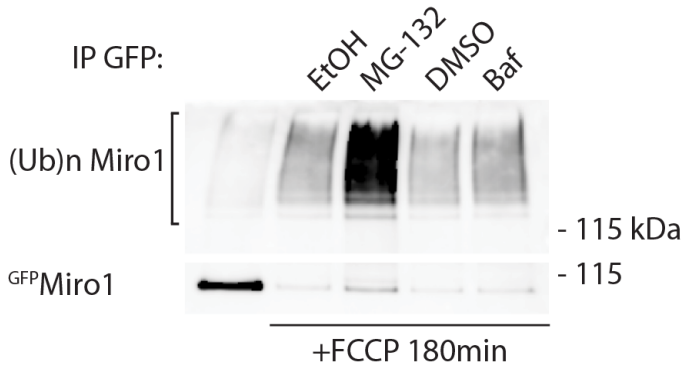

Figure 4.2: Miro1 degradation is blocked by proteasomal inhibition, but not by autophagy inhibition.

Ubiquitination assay of Parkin OE SH-SY5Y cells transiently overexpressing ^{GFP}Miro1 and ^{HA}ubiquitin. Treatment with FCCP (10 µM, 180 minutes) was preceded by incubation with the proteasomal inhibitor MG-132 (30 µM, 30 minutes), the lysosomal inhibitor Bafilomycin 1A (1 µM, 30 minutes), or the respective vehicles (EtOH and DMSO). Miro1 degradation is blocked by MG-132 pre-treatment, but not by the pre-treatment with the lysosomal inhibitor Bafilomycin 1A, as shown by the HA positive Miro1 ubiquitination smear (n=1).

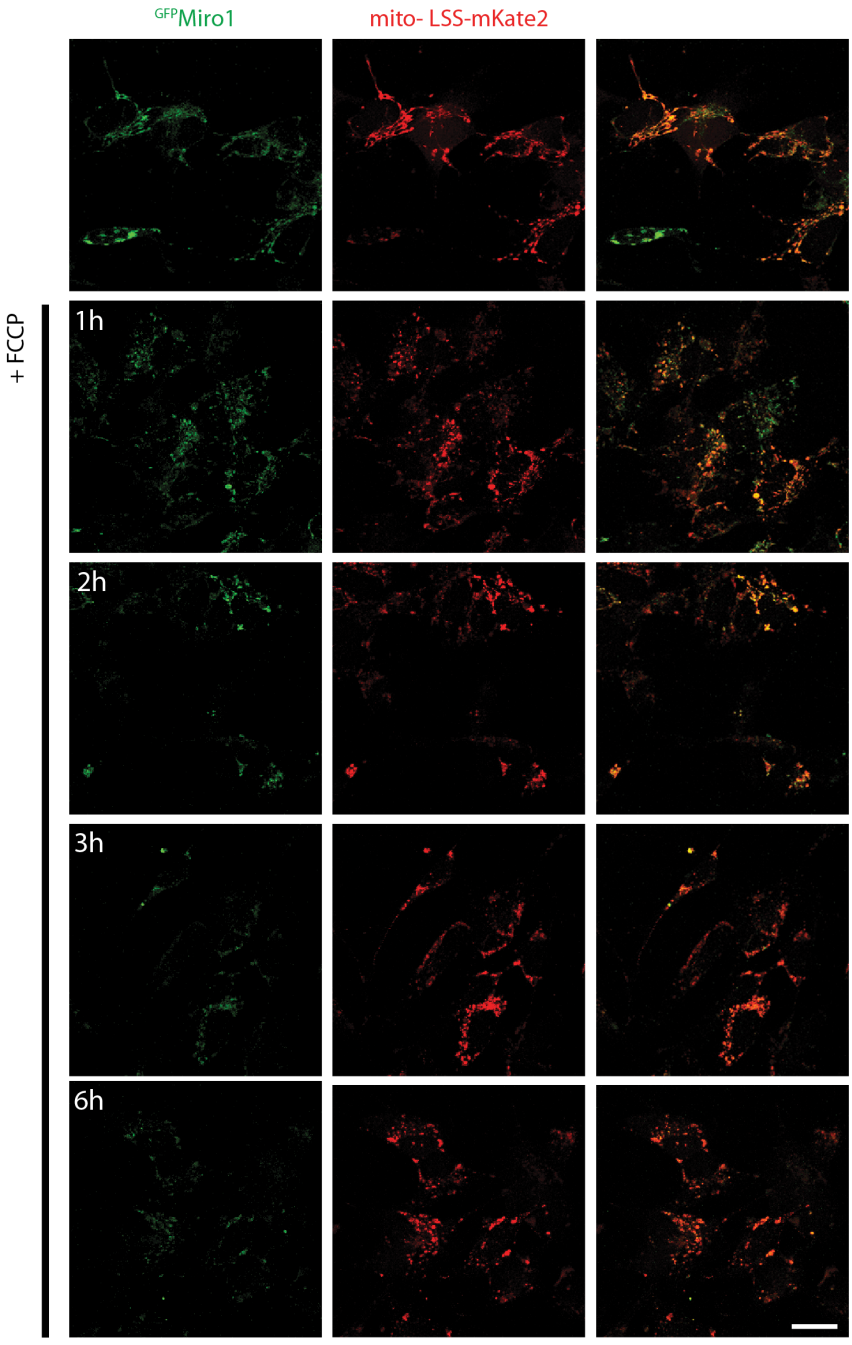

Figure 4.3: Mitochondrial damage-induced Miro1 degradation.

FlagParkin OE SH-SY5Y cells co-transfected with GFPMiro1 and the mitochondrial marker mito-LSS-mKate2. Confocal imaging of a FCCP (10 µM) time course experiment (0-6 hours) shows a decrease over time of the GFPMiro1 fluorescence compared to signal of mito-LSS-mKate2, scale bar = 20 µm.

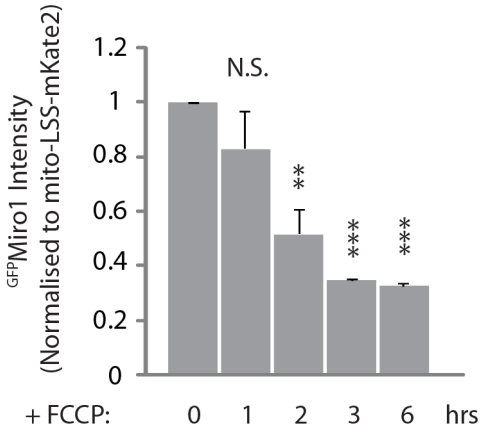

Figure 4.4: Quantification of FCCP-dependent ^{GFP}Miro1 loss from the OMM.

Quantification of the ^{GFP}Miro1 fluorescence intensity normalised to the fluorescence of the mitochondrial intermembrane space-targeted mito-LSS-mKate2 as shown in Fig. 4.3. Miro1 starts to be degraded only after 2 hours of FCCP (10 μM) treatment n=3 independent experiments, **p<0.01, ***p<0.005.

allowing their degradation by the proteasome (Tanaka *et al.*, 2010). VCP could therefore be involved in the retrotranslocation of ubiquitinated Miro1 from the mitochondrial membrane. To address this idea, previously characterised SH-SY5Y cells stably overexpressing a control shRNA or a VCP specific shRNA were used (Bartolome *et al.*, 2013). ^{myc}Miro1, ^{Flag}Parkin and ^{HA}ubiquitin transfected cells were subjected to a FCCP (10 μM) time course (0, 1 and 3 hours) to allow the protein ubiquitination and consequent degradation. Cells were then lysed and ^{myc}Miro1 was immunopurified. Samples were resolved by SDS-PAGE and western blotted. If VCP was necessary for Miro1 retrotranslocation, knock down of the ATPase would result in a accumulation of Miro1 ubiquitinated species. However, analysis of the HA positive ^{myc}Miro1 ubiquitination smear showed that the protein was equally degraded in control and VCP shRNA expressing cells (Fig. 4.5, n=3), indicating that VCP does not contribute to Miro1 processing. However, as detected in the whole cell lysates, Mfn1 loss did not appear to be drastically blocked by the knock down of VCP (Fig. 4.5), suggesting that other mechanisms could be in place for the extraction of these ubiquitinated proteins from damaged mitochondria in neuroblastoma SH-SY5Y cells.

Role of Miro1 phosphorylation in its damage-induced ubiquitination / degradation

Wang and collaborators have demonstrated that PINK1 can phosphorylate Miro1 on serine 156, threonine 298 and threonine 299 in *in vitro* kinase assays. Moreover, they showed that PINK1-dependent Miro1 phosphorylation at S156 was required for its degradation (Wang *et al.*, 2011b). However, whether S156 has a crucial role in the PINK1/Parkin-dependent processing of Miro1 is currently under debate (Liu *et al.*, 2012). To study the role of this residue in the ubiquitination and degradation of Miro1, S156 was mutated to phospho-null Miro1 (S156A), which cannot be phosphorylated due to the lack of an hydroxyl group on its side chain, and phospho-mimic Miro1 (S156E), which mimics the negative charge given by the phosphate group with the negative charge present on the glutamic acid side chain. Phospho-null and phospho-mimic ^{GFP}Miro1 mutants were transfected along with ^{HA}ubiquitin into Parkin OE SH-SY5Y cells. Cells were treated with FCCP (10 μM, 1 hour) or vehicle (DMSO) and ubiquitination assays were performed in order to investigate the contribution of this residue in the damage-induced processing of Miro1. Western blot analysis revealed no difference in the ubiquitination of

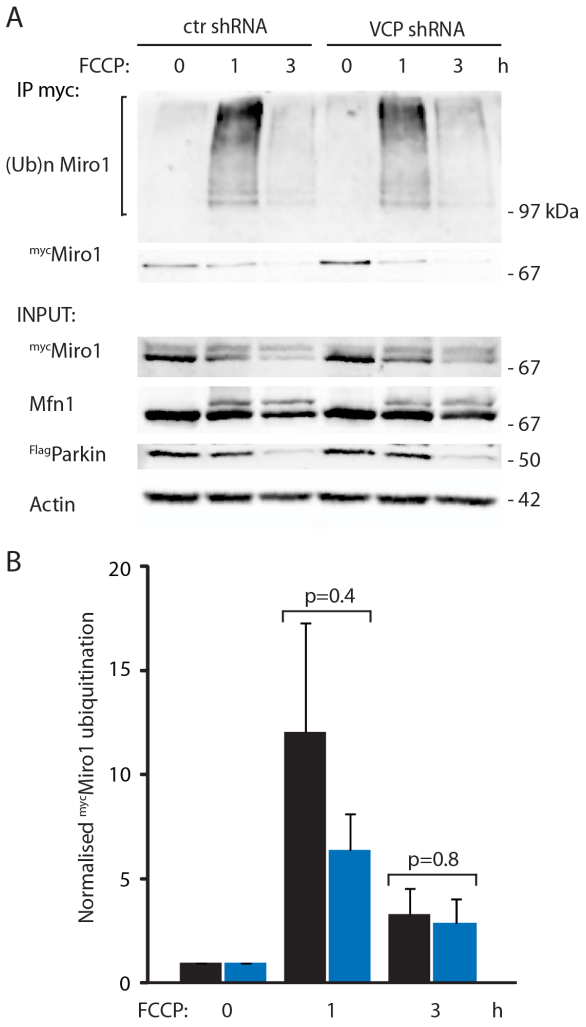

Figure 4.5: Miro1 loss is VCP-independent.

(A) Control or VCP shRNA overexpressing SH-SY5Y cells were transfected with ^{myc}Miro1, ^{Flag}Parkin and ^{HA}ubiquitin. Cells were subjected to a FCCP (10 μM) time course (0, 1, 3 hours), lysed and ^{myc}Miro1 was immunopurified. Immunopurified samples and whole lysates were resolved by SDS-PAGE and western blotted. Miro1 HA positive ubiquitination smear was similar in control or VCP shRNA overexpressing cells, indicating that VCP is not required for ubiquitinated Miro1 processing. Parkin expression is confirmed in the whole cell lysates. (B) Quantification of Miro1 HA positive ubiquitination smear. Values are normalised to control (n=3 independent experiments).

S156A or S156E Miro1 mutants compared to WT. Moreover, both mutants were readily lost at their expected molecular weight (100kDa, Fig. 4.6).

Even though it did not affect Miro1 ubiquitination or loss upon 1 hour FCCP treatment (10 μM), PINK1-dependent phosphorylation of Miro1 at S156 could modulate the stability of the protein, for example by facilitating the temporal dynamics of Miro1 ubiquitination/degradation. To investigate this, a time course experiment was performed, where WT or phospho-null S156A ^{GFP}Miro1 were transiently transfected into Parkin OE SH-SY5Y cells. Cells were then treated for several time points (20, 40, 60 minutes) with FCCP (10 μM), so that a delay in ubiquitination of the phospho-null mutant could be detected. However, also at early stages no difference could be detected in the ubiquitination dynamics between WT and phospho-null S156A ^{GFP}Miro1 (Fig. 4.7, ubiquitinated S156A Miro1 mean intensity at 0 minutes 0.19 ± 0.08, at 20 minutes 0.57 ± 0.17, at 40 minutes 1.75 ± 0.47, at 60 minutes 1.0, ubiquitinated wild type Miro1 mean intensity at 0 minutes 0.04 ± 0.004, at 20 minutes 0.29 ± 0.08, at 40 minutes 0.96 ± 0.22, at 60 minutes 1.0; n=3 independent experiments), suggesting that in this model system the phosphorylation of Miro1 at S156 is not required for its FCCP-triggered ubiquitination/degradation.

Since Miro1 was found to be phosphorylated on T298 and T299 in the presence of PINK1 (Wang *et al.*, 2011b), the role of these residues in the damage-induced regulation of Miro1 was also analysed. To this end a double phospho-null construct was made where both threonines were mutated to alanines (^{GFP}Miro1 T298A/T299A). Parkin OE SH-SY5Y cells were transiently transfected with WT or T298A/T299A ^{GFP}Miro1 and ubiquitination assays were performed following FCCP-induced mitochondrial damage (10 μM, 1 hour). Analysis of the western blot experiments revealed that mutation of threonines 298 and 299 to alanines did not impact on Miro1 ubiquitination or loss as can be seen comparing the WT or T298A/T299A ^{GFP}Miro1 ubiquitination smear or inputs (Fig. 4.8, n=3 independent experiments).

Contribution of Miro1 signalling domains in damage-induced Miro processing

Miro1 is characterised by the presence of several signalling domains. Two EF calcium binding hands, essential for the calcium dependent regulation of mitochondrial traffick-

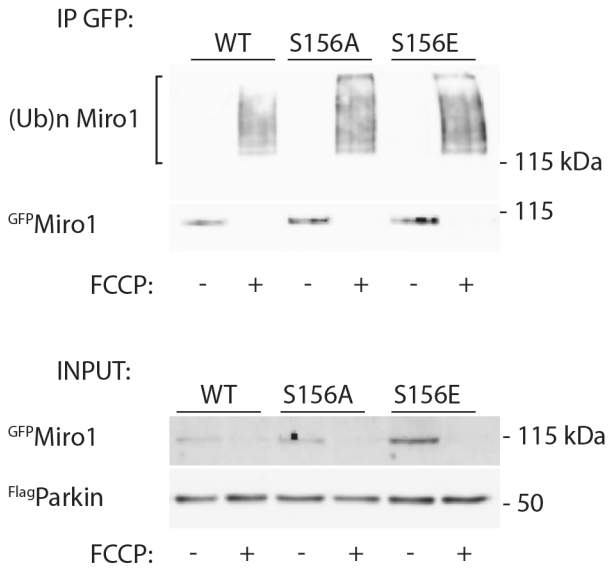

Figure 4.6: Miro1 phosphorylation at S156 does not affect its ubiquitination dynamics.

Ubiquitination assays of Parkin OE SH-SY5Y cells transiently transfected with WT, phospho-null S156A, or phospho-mimetic S156E ^{GFP}Miro1 along with ^{HA}ubiquitin. Cells were treated with FCCP (10 μM) or vehicle (DMSO) for 1 hour, ^{GFP}Miro1 was immunopurified and samples analysed by western blot. Membranes were probed with anti GFP, HA and Flag antibodies. S156A and S156E ^{GFP}Miro1 mutants show no difference in ubiquitination (HA positive smear) compared to WT ^{GFP}Miro1 (n=3 independent experiments).

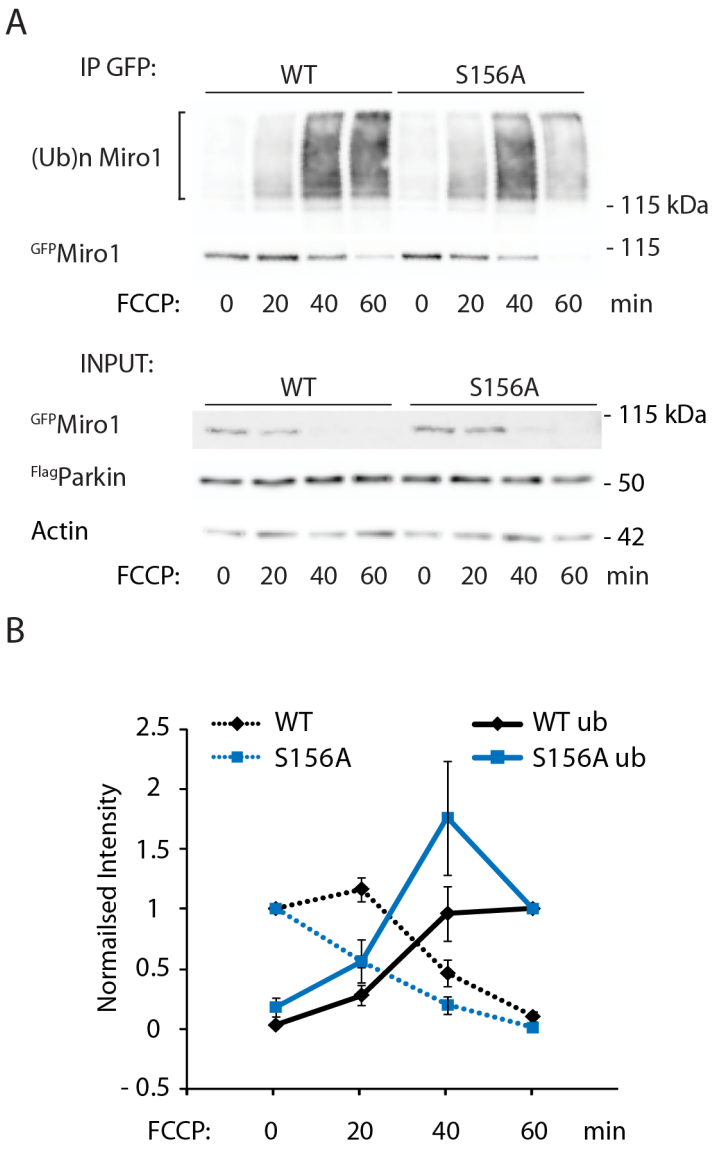

Figure 4.7: S156 phosphorylation does not facilitate FCCP-dependent Miro1 ubiquitination/loss.

(A) Parkin OE SH-SY5Y cells transiently transfected with WT or S156A ^{GFP}Miro1 and ^{HA}ubiquitin were subjected to a FCCP (10 μM) time course before the ubiquitination assay was carried out. Samples were resolved western blotted and membranes were probed with anti GFP, HA Flag and actin antibodies. Analysis of the intensities of the samples treated with FCCP (10 μM) for 20, 40 and 60 minutes revealed no significant difference in the ubiquitination dynamics of S156A mutant compared to WT ^{GFP}Miro1. (B) Quantification of this effect, full lines represent the quantification of the HA positive ubiquitination smear, whereas dashed lines represent the quantification of the GFP positive immunopurified protein (n=3 independent experiments).

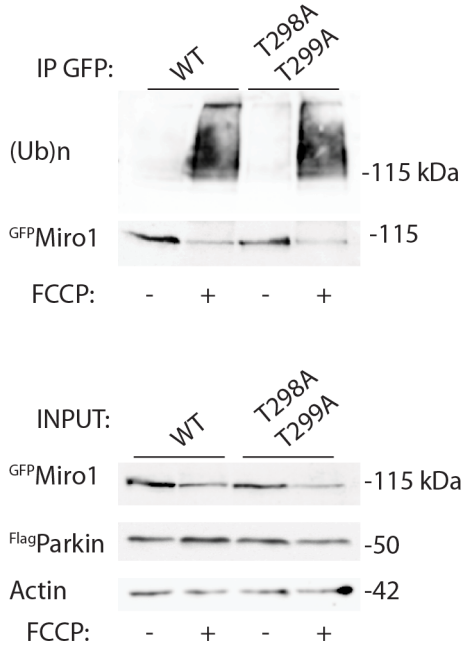

Figure 4.8: T298 T299 are not required for the regulation of FCCP-mediated Miro1 ubiquitination and loss.

Parkin OE SH-SY5Y cells transfected with WT or T298A/T299A ^{GFP}Miro1 along with ^{HA}ubiquitin, were treated with FCCP (10 μM, 1 hour) or vehicle (DMSO) before ubiquitination assays were carried out. Western blot analysis shows no difference in the ubiquitination of WT or T298A/T299A mutant ^{GFP}Miro1 detected by the HA positive high molecular weight smear, or in the loss of the protein detected by GFP in the immunoprecipitated samples or in the inputs. Similar loading is confirmed by actin immunoreactivity (n=3 independent experiments).

ing, are flanked by two GTPase domains, whose function is less well characterised. To investigate whether the regulation of Miro via its signalling domains could affect the damage-induced ubiquitination of the protein, previously described ^{GFP}Miro1 mutants lacking the calcium sensitivity (ΔEF, with the double mutation E208K and E328K), constitutively active GTPase1 (V13) and inactive (N18) were used (Fransson *et al.*, 2003, 2006). Parkin OE SH-SY5Y cells transfected with ΔEF, V13, N18 or WT ^{GFP}Miro1 were FCCP (10 μM, 1 hour) or vehicle (DMSO) treated, ^{GFP}Miro1 was immunopurified from the samples and ubiquitination was tested by western blotting. Analysis of ^{GFP}Miro1 ubiquitination smears revealed no difference between WT and the mutant forms of Miro1 (Fig. 4.9, n=2).

Lysine residues involved in Miro1 ubiquitination

Identifying the lysine residues within Miro1 that mediate its ubiquitination would be of crucial importance in the study of the damage-induced regulation of this protein. Mass spectrometry reports have found a few Miro1 lysine residues to be ubiquitinated, in particular K153, K182, K187, K194 and more recently K572 (Wagner *et al.*, 2011; Sarraf *et al.*, 2013; Kazlauskaite *et al.*, 2014a). In order to investigate the importance of these different residues, a lysine-null Miro1 construct was created, where all the lysines (41 residues) were substituted by arginines (Miro1 allR, synthesised by Invitrogen) to then reintroduce by site-directed mutagenesis the single lysines of interest. Since the extensive mutagenesis could affect the protein folding and/or subcellular localisation and the lack of lysines would impede allR Miro1 processing by the ubiquitin-proteasome system, this mutated construct expression and localisation were tested by immunocytochemistry and western blotting. AllR ^{myc}Miro1 was expressed in HeLa cells and its subcellular localisation was analysed and compared with that of WT ^{myc}Miro1. Although the cells where the expression of the construct was higher exhibited an altered and aggregated mitochondrial network, when allR ^{myc}Miro1 was expressed at lower levels, the mitochondrial network appeared normal, and allR ^{myc}Miro1 showed a mitochondrial localisation similar to WT ^{myc}Miro1 (Fig. 4.10 A). To further test the construct expression and Parkin-mediated processing, WT or allR ^{myc}Miro1 were expressed in HeLa cells together with ^{YFP}Parkin. Following FCCP (10 μM, 1 hour) or vehicle (DMSO) treatment, cells were lysed, samples resolved by SDS-PAGE and western blotted. AllR ^{myc}Miro1 was expressed at lower levels compared to WT, however, FCCP treatment did not induce

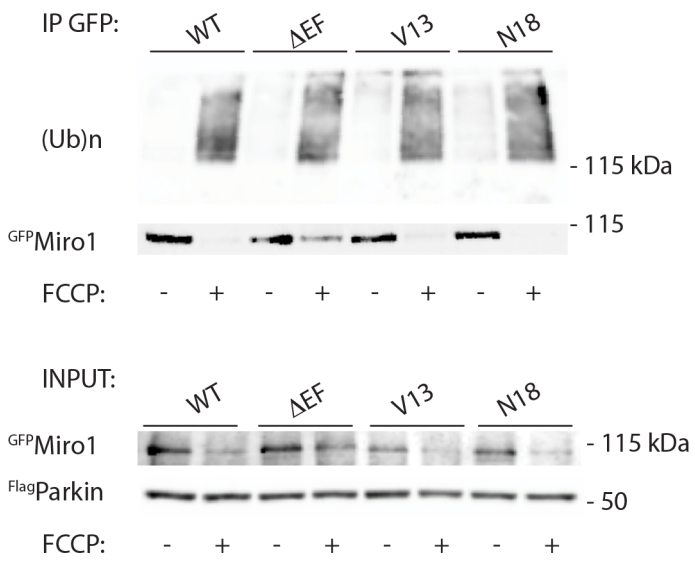

Figure 4.9: Miro1 EF hand and GTPase domains do not influence the protein FCCP-induced ubiquitination.

Parkin OE SH-SY5Y cells transiently transfected with WT, ΔEF, V13 or N18 ^{GFP}Miro1 together with ^{HA}ubiquitin were subjected to FCCP (10 μM, 1 hour) or vehicle (DMSO) treatment. Western blotted samples were probed with anti HA, GFP and Flag antibodies. Analysis of immunopurified ^{GFP}Miro1 showed no difference in the HA positive ubiquitination smear of the mutants compared to WT (n=2 independent experiments).

a loss of the protein at its expected molecular weight or its laddering as with the WT protein. To control that the expression of allR Miro1 does not alter the processing of other PINK1/Parkin substrates the levels of Mfn1 were tested. FCCP induced a loss in the fusion protein when coexpressed with both Miro1 constructs, indicating that allR ^{myc}Miro1 does not affect Parkin mediated ubiquitination of other substrates (Fig. 4.10 B).

K27-type ubiquitination of Miro by a PINK1 and Parkin complex in dopaminergic neuroblastoma cells

Ubiquitin can be bound to lysine residues of a substrate protein as a single molecule or in the form of a polymeric chain. In fact, the initial methionine or one of the seven lysines within ubiquitin can act as acceptor sites for the attachment of successive ubiquitin moieties. Depending on which residue within ubiquitin mediates the formation of the chain, it will lead to different chain conformations that will, affect the functional outcome of ubiquitination. To further investigate the role of Miro ubiquitination, chain composition was initially studied taking advantage of ubiquitin mutants where six of the seven lysines were mutated to arginines (referred as K only, Fig. 4.11 on the left), therefore permissive of only one chain type. Parkin OE SH-SY5Y cells were transfected with WT ^{HA}ubiquitin, or the different ubiquitin mutants (K6, K11, K27, K29, K33, K48, K63). Cells were treated with the mitochondrial uncoupler FCCP (10 μM, 1 hour) and cell lysates were subjected to immunoprecipitation with either IgG (to control for aspecific binding) or anti Miro1/2 specific antibody. Immunopurified samples and inputs were resolved on a SDS-PAGE and western blotted. Analysis of the HA positive Miro1/2 high molecular weight smear revealed that K27 ubiquitin was the K only ubiquitin mutant most prominently incorporated in endogenous Miro1/2 chains, K11 and K29 ^{HA}ubiquitin mutants also took part in Miro1/2 chain formation, whereas there was very little K6, K33, K48 and K63-mediated Miro1/2 ubiquitination found (Fig. 4.12, n=3 independent experiments).

To further confirm the contribution of K27 linkage in Miro1 ubiquitin chains, ^{HA}ubiquitin mutants in which only one lysine was mutated to arginine (referred as K-to-R mutants, Fig. 4.11 on the right), and therefore blocking a specific chain type, were used. In particular Parkin OE SH-SY5Y cells were heterologously transfected with WT, K6R,

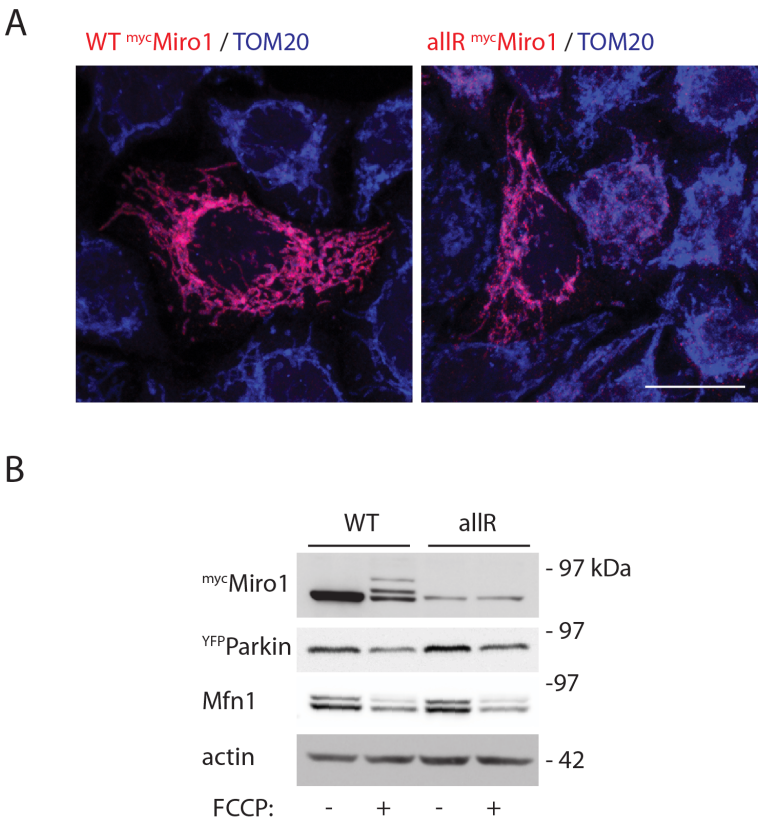

Figure 4.10: Characterisation of allR ^{myc}Miro1.

A) Representative images of HeLa cells overexpressing either WT ^{myc}Miro1 or allR ^{myc}Miro1 (low expression - unaltered mitochondrial network). Cells were fixed and immunostained for ^{myc}Miro1 (red) and the mitochondrial marker TOM20 (blue). When expressed at low levels AllR^{myc}Miro1 showed a mitochondrial localisation similar to WT. Scale bar = 20 μm. B) WT or allR ^{myc}Miro1 were overexpressed along with ^{YFP}Parkin in HeLa cells. Following FCCP treatment (10 μM, 1 hour) cells were lysed, samples resolved by SDS-PAGE and western blotted. Myc immunoreactivity shows that, although allR ^{myc}Miro1 is expressed at lower levels compared to WT, mitochondrial damage does not cause laddering of the mutated protein. Mfn1 loss is triggered by FCCP treatment when coexpressed both with WT and allR ^{myc}Miro1. Actin bands confirm similar loading (n=2).

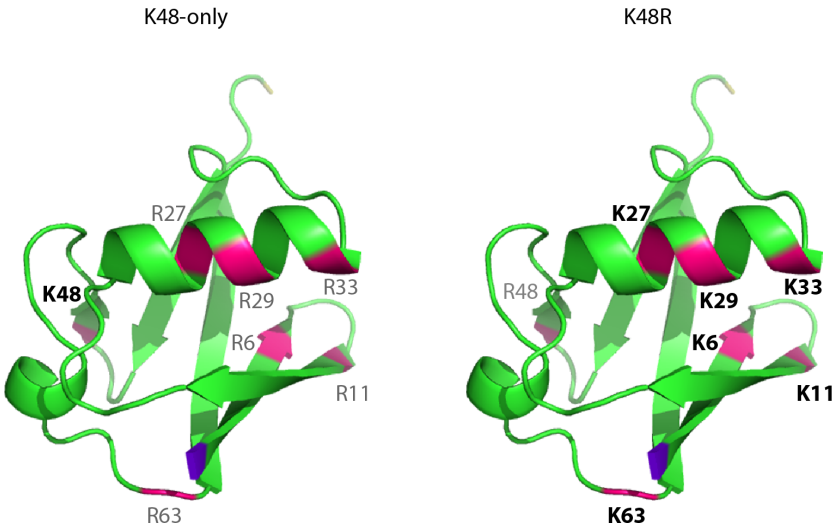

Figure 4.11: Example of K-only and K-to-R ubiquitin mutants.

On the left a representation of a K48 ubiquitin only mutant, where every lysine apart from K48 is mutated to arginine. This mutant is only permissive of K48-linked chains. On the right, a representation of a K-to-R (K48R) ubiquitin mutant, where only lysine 48 is mutated to R. This mutant allows the formation of every chain apart from the K48-mediated ones. The 3D structure of ubiquitin was generated with PyMOL (PDB=1UBQ).

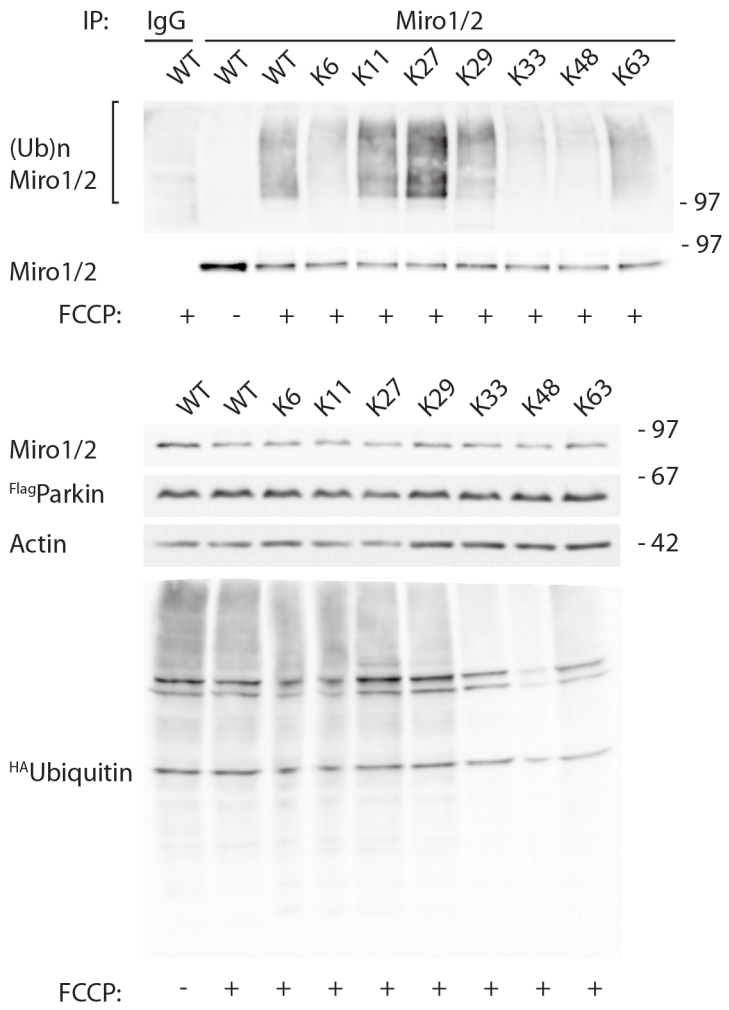

Figure 4.12: Analysis of Miro1 ubiquitin chains with K only ubiquitin mutants.

Ubiquitination assays performed in SH-SY5Y cells stably overexpressing ^{Flag}Parkin and transfected with either wild type ^{HA}ubiquitin or several K only ubiquitin mutants, that allow only specific chain types (K6, K11, K27, K29, K33, K48, K63). Endogenous Miro1/2 was immunopurified from control or FCCP treated cells (10 μM, 1 hour), samples were resolved by SDS-PAGE and western blotted. Membranes were probed with anti HA, Miro1/2, Flag and actin antibodies. Analysis of the HA positive Miro1/2 high molecular weight smear reveals that endogenous Miro1/2 is primarily ubiquitinated in a K27-dependent manner, and that K11 and K29 can also take part in Miro1/2 chain formation (top panel). Inputs show similar expression of the ^{HA}ubiquitin mutants (bottom panel, n=3 independent experiments).

K11R, K27R, the double mutant K27R/K29R or K48R. Following mitochondrial damage triggered with FCCP (10 μM, 1 hour), cell lysates were collected and subjected to immunoprecipitation with a non specific IgG or a Miro1/2 specific antibody. Samples were resolved by SDS-PAGE and western blotted. Interestingly, analysis of the HA positive Miro1 smear showed that only the K27R and K27R/K29R mutants were able to reduce endogenous Miro1/2 ubiquitination, confirming the results obtained with the K only ^{HA}ubiquitin mutants. No difference was detected comparing WT ^{HA}ubiquitin to K6R, K11R and K48R mutants (Fig. 4.13, n=3).

Ubiquitin mutants are a tool to investigate chain linkage composition, however, overexpression of these mutants could bias the chain formation favouring the specific linkages permitted. Moreover K mutations on ubiquitin could alter the conformation of the protein, possibly affecting the interaction of these mutants with E2 enzymes, E3 ligases, or altering the chain conformation itself and consequently the interaction with ubiquitin binding proteins or deubiquitinases (DUBs). To further investigate Miro1 ubiquitin chain composition without affecting the chain formation, chain specific DUBs were used in ubiquitin chain restriction (UbiCRest) analysis (Mevissen *et al.*, 2013). To this end Parkin OE SH-SY5Y cells were transiently transfected with ^{GFP}Miro1 and ^{HA}ubiquitin. After FCCP treatment (10 μM, 1 hour), ubiquitinated ^{GFP}Miro1 was immunopurified on high affinity GFP-TRAP beads and incubated with several DUBs of distinct specificities. Reactions were stopped by addition of denaturing Laemmli sample buffer and proteins resolved on a dual acrylamide percentage gel (8%-15%). Proteins were transferred onto a PVDF membrane and probed with anti HA and anti GFP antibodies. USP21 is a highly active, ubiquitin-specific, but linkage-aspecific DUB (Ye *et al.*, 2011). As seen in the previous chapter (Fig. 3.7), western blot analysis of the USP21 reaction showed that this enzyme efficiently cleaves ^{GFP}Miro1 ubiquitin chains, generating unmodified ^{GFP}Miro1 (100 kDa), mono-ubiquitin (8 kDa, white arrowhead) and a small amount of mono-ubiquitinated ^{GFP}Miro1. An enzyme that specifically recognizes and cleaves K27 linkages has not been identified to date. However, OTUD2, an enzyme from the ovarian tumor ubiquitinases, shows linkage-preference for K11, K27, K29, and K33 linkages and is the only DUB cleaving K27 chains efficiently (Mevissen *et al.*, 2013). Incubation of ^{GFP}Miro1 with increasing concentrations of OTUD2 results in a progressive shortening of high-molecular weight ^{GFP}Miro1 ubiquitination, partial rescue of ^{GFP}Miro1 at its expected molecular weight and the formation of HA positive bands at 20 and 30 kDa (black arrowheads), which are likely to be ubiquitin dimers or trimers. The latter

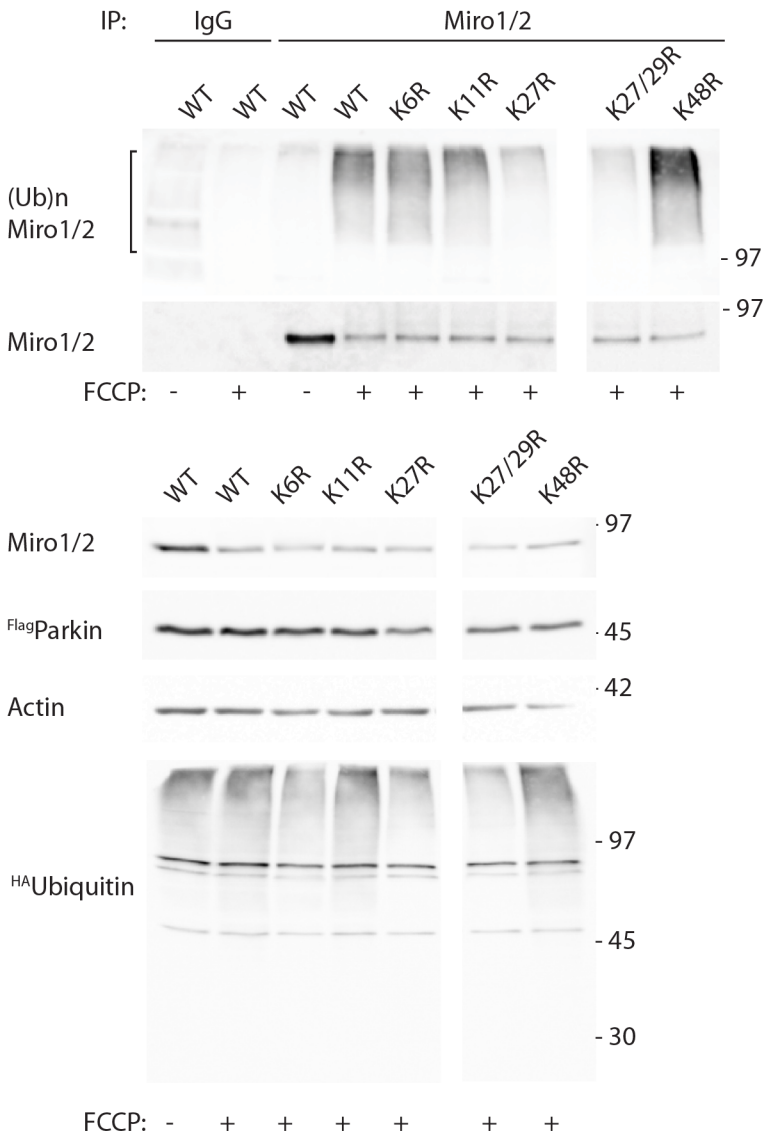

Figure 4.13: Analysis of Miro1 ubiquitin chains with K-to-R ubiquitin mutants.

Ubiquitination assays performed in SH-SY5Y cells stably overexpressing ^{Flag}Parkin and transfected with either wild type ^{HA}ubiquitin or several K-to-R ubiquitin mutants, which block one specific chain type (K6R, K11R, K27R, K27R/K29R, K48R). Endogenous Miro1/2 was immunopurified from control or FCCP treated cells (10 µM, 1 hour), samples were resolved by SDS-PAGE and western blotted. Membranes were probed with anti HA, Miro1/2, Flag and actin antibodies. Analysis of the HA positive Miro1/2 high molecular weight smear reveals that only the K27R and the K27R/K29R ^{HA}ubiquitin mutants affect endogenous Miro1/2 ubiquitination (top panel). Inputs show similar expression of the ^{HA}ubiquitin mutants (bottom panel, n=3 independent experiments).

could be released from mixed-linkage chains on ^{GFP}Miro1. In contrast, incubation of ^{GFP}Miro1 with the highly active, but Met1/linear chain specific DUB Otulin (Keusekotten *et al.*, 2013), does not affect ^{GFP}Miro1 ubiquitination (Fig. 4.14). This confirms that ^{GFP}Miro1 comprises atypical polyubiquitin chain linkages, most likely K27-chains.

Discussion

In this Chapter the ubiquitination of Miro1 has been extensively investigated. Both biochemical and immunohistochemical time course experiments, performed in neuronal dopaminergic SH-SY5Y cells, have shown that, although Miro1 ubiquitination occurs rapidly (within 20 minutes), its degradation is delayed to later time points (2-3 hours). This suggests that the protein, which is stable in its ubiquitinated form on the OMM for at least one hour, may participate in the regulation of damaged mitochondria. The role of S156 and T298/T299 has been studied, however, in the model used, PINK1-dependent phosphorylation of these residues did not impact on Miro1 turnover. Finally, Miro1 chain type was characterised using several ubiquitin mutants (both K only and K-to-R) and DUB restriction analysis (UbiCRest).

According to the current model, damage-induced degradation of Miro results in the block of mitochondrial transport (Wang *et al.*, 2011b). Whilst the data described in the previous Chapter support the PINK1/Parkin-dependent loss of Miro, the analysis of the kinetics of Miro ubiquitination described in this Chapter, shows that the loss of Miro at its expected molecular weight is primarily due to a shift of the ubiquitinated protein to higher weight species. Moreover immunohistochemical experiments confirm that this ubiquitinated form of Miro1 is stable on the OMM for at least one hour before being degraded by the proteasome, suggesting that Miro ubiquitination, rather than ubiquitination-induced Miro degradation, may directly act as a rapid signal on the OMM for mitochondrial arrest. Various mechanisms could underpin this, as mentioned in the discussion of Chapter 3. Ubiquitination of Miro could mediate the recruitment of other factors such as p62 and/or HDAC6 to the mitochondrial trafficking complex to promote the transport to the cell soma and clustering of damaged mitochondria prior to their clearance by mitophagy. Moreover, Miro ubiquitination may also either directly, or by recruitment of HDAC6 and/or p62, impede its association with the motor proteins leading to mitochondrial arrest.

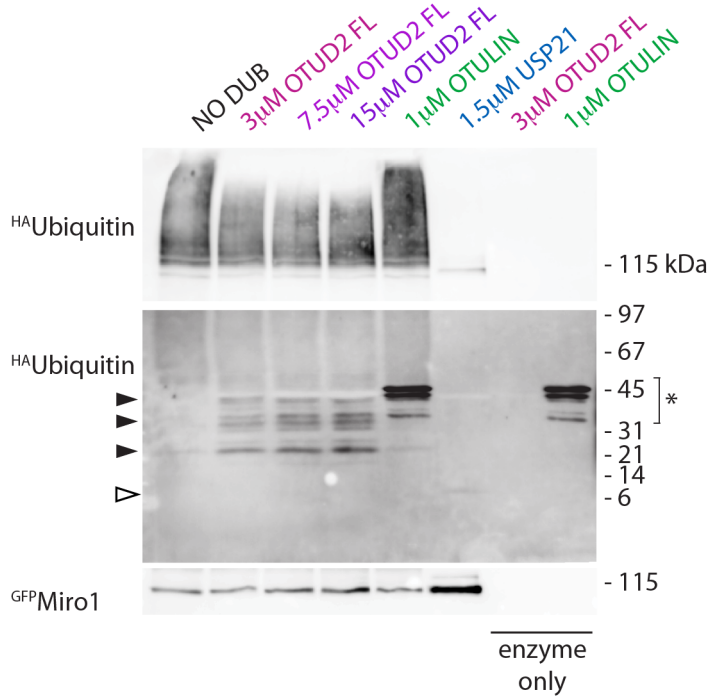

Figure 4.14: DUB restriction analysis confirms K11, K27 and K29 contribution to Miro1 ubiquitin chains.

Parkin OE SH-SY5Y cells were transfected with ^{GFP}Miro1 and ^{HA}ubiquitin. Mitochondrial damage was triggered with FCCP (10 μM, 1 hour) and ubiquitinated ^{GFP}Miro1 was immunopurified. ^{GFP}Miro1 retained on GFP-TRAP beads was then incubated with increasing amounts of OTUD2 (that specifically cleaves K11, K27, K29 and K33 mediated ubiquitin linkages), Otulin (cleaves Met-linked chains) or USP21 (chain type aspecific DUB). Samples were first probed with anti-HA antibody to visualise ^{GFP}Miro1 ubiquitination smear and ubiquitin released from the chains and, after stripping, re-probed with anti-GFP antibody to detect ^{GFP}Miro1. OTUD2 triggers the shortening of ^{GFP}Miro1 ubiquitination, releases HA positive 20-30kDa species (black arrowheads), probably ubiquitin trimers and dimers, and results in a partial rescue of the GFP positive Miro1 at 100kDa. Incubation with Otulin does not alter ^{GFP}Miro1 ubiquitination smear, asterisk indicates cross-reactivity between Otulin and the anti-HA antibody due to a high homology sequence. USP21 cleaves ^{GFP}Miro1 ubiquitin chains almost completely, releasing mono-ubiquitin (8 kDa, white arrowhead) and rescuing unmodified ^{GFP}Miro1.

At later time points (after 2 hours from damage induction) Miro is finally degraded by the proteasome. The mechanism by which Miro1 degradation occurs has not yet been explored. Valsolin containing protein (VCP) or p97, an ATPase that normally participates in the extraction of misfolded ubiquitinated proteins from the ER to promote their clearance in a process called ERAD (endoplasmic-reticulum-associated protein degradation), has been shown to mediate the extraction of poly-ubiquitinated Mitofusins from damaged mitochondria (Tanaka *et al.*, 2010). In a similar way VCP could promote the extraction from the mitochondrion and subsequent degradation of Miro1, however, results presented in Fig. 4.5 do not support the role of this protein in Miro1 processing and degradation. Nevertheless a few reports have shown the recruitment of proteasomal subunits to damaged mitochondria, indicating that this complex could be directly shuttled to the damaged organelles to degrade the OMM proteins (Shiba-Fukushima *et al.*, 2012; Chan *et al.*, 2011). The reason why the selective degradation of the OMM proteins is needed for the autophagic clearance of damaged mitochondria to occur is still unclear, yet it would be interesting to selectively block the degradation of specific proteins (for example by targeting key lysine residues that mediate ubiquitination) to understand how this would affect mitophagy.

Wang and colleagues have shown that PINK1 phosphorylates Miro on S156 and that this phosphorylation is crucial for the subsequent Parkin-dependent degradation of the protein (Wang *et al.*, 2011b). Mutation of this key residue should therefore block Miro ubiquitination and could be used to study the role of this post-translational modification in mitophagy. However, in Parkin OE dopaminergic neuroblastoma SH-SY5Y cells, mutation of S156 to non phosphorylatable alanine (S156A) neither blocked Miro loss nor it delayed its ubiquitination kinetics (Fig. 4.6 and Fig. 4.7). Phosphorylation of Miro1 by PINK1 to regulate Miro stability and ubiquitination may, therefore, be cell specific, possibly due to different expression levels of PINK1, Parkin, or of other regulatory factors such as Miro protein phosphatases. In a similar way, PINK1-dependent phosphorylation of T298 and T299 on Miro1 was found not to affect the ubiquitination dynamics of the protein (Fig. 4.8). These data are in agreement with a more recent study (Liu *et al.*, 2012) and, in addition, in a screen of 16 putative PINK1 substrates (including Miro2) only Parkin was found to be robustly phosphorylated by PINK1 *in vitro* (Kondapalli *et al.*, 2012).

With two EF hand domains and two GTPase domains Miro1 can be defined as a sig-

nalling hub. Miro's two EF hands determine the calcium-dependent mitochondrial stop (Wang and Schwarz, 2009; MacAskill *et al.*, 2009b), whereas the function of the two GTPase domains is less clear. The first GTPase domain has been associated with different affinities to the trafficking adaptor TRAK2, possibly affecting mitochondrial transport or directionality (MacAskill *et al.*, 2009a). However whether there is a signalling cross-talk among these domains or they work separately is yet to be investigated. Since Miro1 ubiquitination is likely to modulate the protein's functionality and consequently mitochondrial trafficking, a cross-talk mechanism could be in place between Miro1 signalling domains and its ubiquitination. Using calcium insensitive ΔEF, constitutively active (V13) or inactive (N18) GTPase1 Miro1 mutants, Miro1 ubiquitination was analysed, however these mutants did not interfere with Parkin-dependent Miro1 ubiquitination (Fig. 4.9).

The identification of Miro1 lysine residues ubiquitinated by Parkin is essential to further investigate the role of this modification in mitochondrial trafficking and mitophagy. Recently, Miro1 was found to be ubiquitinated on K152, K182, K187, K194 and K572 (Wagner *et al.*, 2011; Sarraf *et al.*, 2013; Kazlauskaite *et al.*, 2014a). To investigate role of these residues, a Miro1 construct where all the lysines were mutated into arginines (allR Miro1) will be used. The lack of lysine residues could affect many aspects of this mutant protein processing, from its subcellular localisation, to its function and turn over. AllR Miro1 was shown to be localised on mitochondria, however whether the presence of this mutant affects mitochondrial functionality should be tested with a membrane potential-dependent dye, such as TMRM. Moreover the processing and functionality of this ubiquitination-deficient construct should be analysed. By interfering with Parkin-mediated ubiquitination allR Miro1 may allow the study of the role of Miro1-dependent mitochondrial trafficking in mitophagy.

Ubiquitin chain topology can determine the cellular outcome of ubiquitination. To characterise further Parkin-dependent Miro processing, the composition of its ubiquitin chains was analysed utilising ubiquitin mutants and UbiCRest experiments. Miro1 was found to be mainly modified with atypical K27-linked ubiquitin chains as seen with both K only and K-to-R ubiquitin mutants, moreover, a partial contribution of K11 and K29 was detected in the K only experiments (Fig. 4.12 and Fig. 4.13). Miro1 chain composition was also tested taking advantage of linkage specific DUBs. Since a K27-linkage specific DUB has not been found to date, OTUD2, a deubiquitinase of

the family of the ovarian tumor ubiquitinases, which shows a preference for K11, K27, K29 and K33-type linkages was used (Mevissen *et al.*, 2013). This enzyme was able to cleave Miro1 ubiquitin chains confirming the contribution of the K27, K11 and K29 linkage (Fig. 4.14). OTUD2-dependent cleavage of Miro1 chains was not, however, complete. This could be due to the fact that the enzyme OTUD2 is not very active, but it could also suggest that other chain-linkages, could be involved in the formation of Miro1 ubiquitin chains. A recent report showed Miro1 to be ubiquitinated, *in vitro*, in a K6, K11, K33, K48 and K63 manner by mass spectrometry (Kazlauskaite *et al.*, 2014a). Such a different result might be due to the difference between an *in vitro* versus an *in vivo* system. Within cells, in fact, Miro1 is ubiquitinated at the mitochondrion and many co-factors (or different E2s) could favour specific chain types. Thus a more extensive DUB restriction assay, or mass spectrometry experiments will be required to fully characterise Parkin-mediated Miro1 ubiquitin chains.

Interestingly, K27-linked ubiquitin chains have so far only been observed in connection with Parkin (Geisler *et al.*, 2010). Moreover, the modification with this chain type does not seem to lead to Miro1 immediate degradation, which is consistent with previous proteomic analysis showing that K27 chains are not significantly enriched when the proteasome is inhibited, in contrast to K48 or K11 chains (Kim *et al.*, 2011). This suggests that this chain type may have other roles. For example, K27-linked poly-ubiquitin chains have previously been correlated to p62 translocation to damaged mitochondria (Geisler *et al.*, 2010). An interesting question is whether ubiquitin chains are stable, or they can be remodelled over time. For example, protein ubiquitination could switch from a pro-signalling to a pro-degradative linkage. To this end analysis of Miro1 ubiquitination could be analysed immediately after damage as well as prior to degradation.

In this Chapter, Miro1 ubiquitination was thoroughly characterised. Miro1 was found to be ubiquitinated rapidly upon mitochondrial damage, however its degradation was delayed. The protein is therefore stable on the OMM in its ubiquitinated form for at least one or two hours, suggesting an alternative signalling role for this post-translational modification. Moreover atypical K27-linked ubiquitin chains, previously associated with mitophagy, were found on Miro, suggesting that this chain-type could have a peculiar role in the targeting of damaged mitochondria for mitophagy. Mass spectrometry analysis of Miro1 ubiquitin chains is however needed to further confirm these results.

Chapter 5

Parkin regulation and mitophagy

Introduction

Mitochondrial damage triggers a cascade of events that ultimately results in mitochondrial clearance by mitophagy. As previously described, following the loss of the mitochondrial membrane potential, PINK1 accumulates on the OMM. This is a crucial step in the activation of the mitophagy cascade. Once stabilised at the OMM, PINK1 not only recruits Parkin, a cytosolic E3 ubiquitin ligase, to the mitochondrion, but also promptly activates (within 10 minutes after mitochondrial damage) the ligase by phosphorylation of serine 65 at the N-terminal Ubl domain (Kondapalli *et al.*, 2012; Shiba-Fukushima *et al.*, 2012). Parkin, normally exists in a closed, autoinhibited conformation. Structural analysis has shown that the Ubl domain binds the RING1 domain, possibly hindering the E2 binding site, while the RING0 domain blocks the catalytic C431 residue, that is located on the RING2 domain, and is crucial for the ligase activity (Trempe *et al.*, 2013; Wauer and Komander, 2013; Riley *et al.*, 2013). Activation of this ligase is therefore a tightly regulated multi-step process. Phosphorylation at S65 has been suggested to release Parkin N-terminal Ubl domain, allowing the ligase to be active. Indeed phosphorylated Parkin was shown to catalyse the formation of free ubiquitin chains (Kondapalli *et al.*, 2012) and oxyester intermediates were found between ubiquitin and wild type and phospho-mimic, but not phospho-null Parkin (on a C431S backbone to allow the formation of a stable oxyester bond) (Iguchi *et al.*, 2013). Even though these assays prove the

activation of Parkin in principle, further experiments are needed to investigate the role of serine 65 phosphorylation in the ubiquitination of Parkin substrates. Since defects in the translocation to damaged mitochondria would impact on the ligase activity, Parkin enzymatic function needs to be studied alongside its subcellular localisation, which is indeed controversial. Sarraf and colleagues have in fact found Parkin phospho-null and phospho-mimic mutants to exhibit recruitment dynamics to damaged mitochondria similar to WT Parkin, whereas Shiba-Fukushima and collaborators reported a translocation defect for these mutants (Shiba-Fukushima *et al.*, 2012; Sarraf *et al.*, 2013).

Recruitment and activation of Parkin are not, however, the only steps controlled by the mitochondrial kinase, PINK1. Three reports have in fact recently demonstrated that PINK1 is the first kinase to phosphorylate ubiquitin (Koyano *et al.*, 2014; Kazlauskaite *et al.*, 2014b; Kane *et al.*, 2014). A post translational modification of a post translational modification that adds another level of complexity to the regulation of mitophagy. Once accumulated at the OMM, PINK1 phosphorylates both Parkin and ubiquitin at the same conserved serine 65 (in the Ubl on Parkin). Koyano and colleagues have shown that expression of phospho-mimic S65D ubiquitin promotes the activity of phospho-mimic S65E Parkin by analysing its auto-ubiquitination state *in vitro* and *in vivo*. However expression of the ubiquitin phospho-mimic mutant failed to recruit Parkin to mitochondria in the absence of mitochondrial damage (Koyano *et al.*, 2014). These data suggest that PINK1 promotes the formation of a "cloud" of activated Parkin and ubiquitin surrounding damaged mitochondria (only 0.05% of total ubiquitin is in fact phosphorylated upon damage, Koyano *et al.*, 2014) to promote the ubiquitination of the OMM proteins and therefore mitophagy. Ubiquitin phosphorylation is yet another step in the complex activation of Parkin, but whether this modification is also crucial for ubiquitin incorporation into multimeric chains, or whether specific ubiquitin chains can be favoured by this post-translational modification has not yet been explored.

Once Parkin is fully activated and stabilised on damaged mitochondria, it can ubiquitinate its substrates. Several proteins have been shown to be ubiquitinated by this E3 ligase: for example the Mitofusins (1 and 2), VDAC1, Drp1, TOM20 and 40 and, as described in the previous chapters, Miro (Geisler *et al.*, 2010; Wang *et al.*, 2011a; Ziviani *et al.*, 2010; Yoshii *et al.*, 2011; Poole *et al.*, 2010; Liu *et al.*, 2012; Sarraf *et al.*, 2013; Wang *et al.*, 2011b). Whether ubiquitination of each single protein exerts a specific function during mitophagy or it is the overall ubiquitination of the mitochondrion

that is essential for the autophagic signalling cascade is debated. Nevertheless, the presence of several ubiquitinated proteins on the mitochondrion drives the recruitment of elements of the autophagic machinery and the formation of autophagosome-like structures, that will result in the formation and maturation of the autophagosome. This autophagic organelle will then fuse with acidified lysosomes causing the degradation of the mitochondrion.

In this Chapter the role of serine 65 phosphorylation on Parkin ligase activity will be investigated by analysing the levels of Miro1 ubiquitination, using phospho-null (S65A) and phospho-mimic (S65E) Parkin mutants in HeLa and SH-SY5Y cells. Moreover, an in depth analysis of phospho-null and phospho-mimic Parkin recruitment dynamics to damaged mitochondria and the role of Miro1 as part of an acceptor complex for Parkin will be investigated by immunofluorescence experiments. Finally the role of PINK1-dependent ubiquitin phosphorylation on Parkin activity will be studied.

Results

PINK1-dependent phosphorylation of Parkin on S65 results in impaired ligase function

Several reports have recently shown that PINK1 phosphorylates Parkin on its serine 65. This modification is thought to determine a conformational change that promotes the activation of the protein, as shown by the formation of ubiquitin chains *in vitro* or by the detection of oxyester intermediates between ubiquitin and wild type and phospho-mimic, but not phospho-null Parkin (on a C431S backbone) (Kondapalli *et al.*, 2012; Shiba-Fukushima *et al.*, 2012; Iguchi *et al.*, 2013). Shiba-Fukushima and colleagues have shown that mutation of S65 on Parkin to phospho-null S65A delays the degradation of OMM proteins (Shiba-Fukushima *et al.*, 2012), however, whether the phosphorylation of this residue is important for substrate ubiquitination by Parkin in response to mitochondrial damage, has not been tested. To this aim, ^{YFP}Parkin was mutated to phospho-null S65A and phospho-mimic S65E. PINK1-mediated phosphorylation of Parkin upon mitochondrial damage was tested taking advantage of the PhosTag™ technology. PhosTag™ is a compound that is added together with $MnCl_2$ to the SDS-PAGE gel solution. While

being resolved on the gel, phosphorylated proteins bind to PhosTag™, which causes a delay in the migration of these species. As a result, phosphorylated proteins will run slower than their unphosphorylated counterparts and antibodies will recognise unphosphorylated/faster moving bands and phosphorylated/slower moving bands (Fig. 5.1).

HeLa cells, which do not express endogenous Parkin (Denison *et al.*, 2003), were transiently transfected with WT or S65A ^{YFP}Parkin. Cells were treated with FCCP (10 μM, 1 hour) to induce mitochondrial damage or vehicle (DMSO), lysed and proteins resolved either on a conventional SDS-PAGE gel or on a PhosTag™ gel. Proteins were then western blotted on a PVDF membrane and probed with an anti-GFP antibody. Upon FCCP treatment a slow migrating GFP positive band could be detected in the PhosTag™ gel, but not in the conventional SDS-PAGE gel (Fig. 5.2). Moreover this band was prevented by the S65A mutation in Parkin, indicating that this slower migrating band is phosphorylated Parkin at S65. FCCP treatment also induced the formation of another GFP positive WT ^{YFP}Parkin band which could be detected in both conventional and PhosTag™ gels, but is absent in the ^{YFP}Parkin^{S65A} samples. This band is likely to represent an auto-ubiquitinated form of Parkin, which is prevented by the S65A mutation (Fig. 5.2).

To investigate the role of serine 65 on Parkin ligase activity on impaired mitochondria, Miro1 ubiquitination was studied. HeLa or SH-SY5Y cells were transfected with WT, phospho-null S65A or phospho-mimic S65E ^{YFP}Parkin along with ^{myc}Miro1 and ^{HA}ubiquitin. Cells were treated with FCCP (10 μM, 1 hour) or vehicle (DMSO), lysed, and ^{myc}Miro1 was immunoprecipitated. Immunoprecipitated samples and inputs were resolved by SDS-PAGE, western blotted and ubiquitination of ^{myc}Miro1 was detected with an anti-HA antibody. In contrast to the robust ^{myc}Miro1 ubiquitination triggered by FCCP when WT ^{YFP}Parkin was expressed, ^{myc}Miro1 ubiquitination was greatly reduced when ^{YFP}Parkin^{S65A} was expressed both in HeLa and in SH-SY5Y cells (Fig. 5.3 and Fig. 5.4), similar to recent data obtained with *in vitro* assays (Kazlauskaite *et al.*, 2014a), and supporting a key role for PINK1-dependent phosphorylation of Parkin in Miro1 ubiquitination.

Although ^{YFP}Parkin^{S65E} expression led to reduced FCCP-dependent ubiquitination of Miro1 compared to WT, Miro expression levels appeared reduced under basal conditions with this mutant (Fig. 5.3 and Fig. 5.4), suggesting constitutive activity of phospho-mimic S65E Parkin to regulate Miro. This could be potentially due to impaired

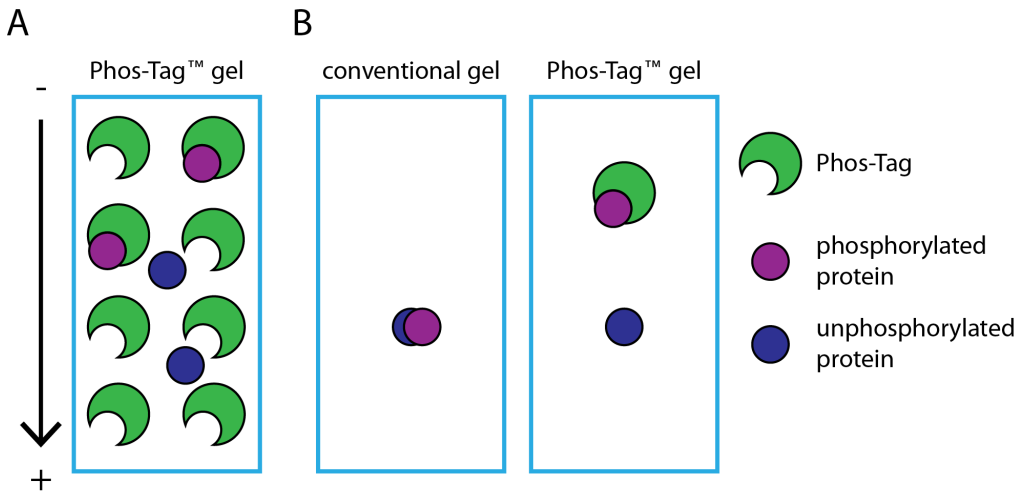

Figure 5.1: PhosTag™ technology.

(A) Addition of the phosphate binding PhosTag™ to acrylamide gels results in the slower migration of phosphorylated proteins. (B) With conventional acrylamide gels phosphorylated and unphosphorylated forms of a protein run according to their molecular weight and cannot be distinguished, however, these different species can be separated and visualised as two separate bands on PhosTag™ gels. Modified from Wako Chemicals.

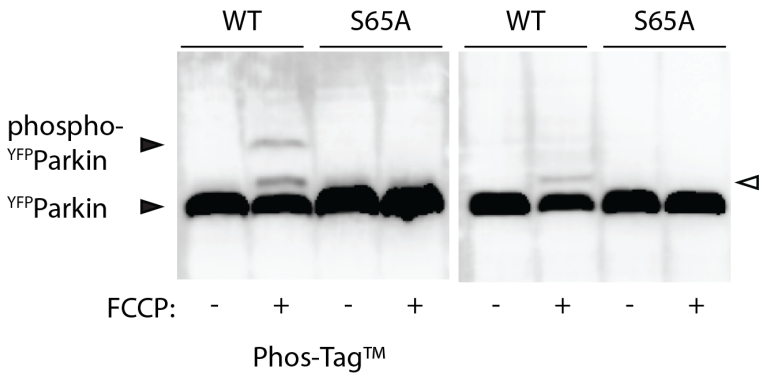

Figure 5.2: Parkin is phosphorylated on S65.

WT or S65A ^{YFP}Parkin transfected HeLa cells were treated with FCCP (10 μM, 1 hour) or vehicle (DMSO). Lysates were either resolved on a PhosTag™ gel (left panel) or on a conventional SDS-PAGE gel (right panel) and probed with an anti GFP antibody. FCCP treatment (10 μM, 1 hour) triggers the phosphorylation of ^{YFP}Parkin WT, but not S65A, as can be visualised by the high molecular weight GFP positive band in the PhosTag™ gel. An extra band, slightly lower than phospho-Parkin, is present both in the PhosTag™ and conventional gel (white arrowhead) and is likely to be an ubiquitinated form of Parkin (n=1).

Ubl domain-mediated inhibition of the ligase (Chaugule *et al.*, 2011). In Parkin S65E overexpressing cells mitochondrial damage induced further Miro loss and ubiquitination suggesting that additional regulatory mechanisms may contribute to mitochondrial damage-induced activation of Parkin (Fig. 5.3 and Fig. 5.4).

S65 on Parkin is important for the ligase recruitment to damaged mitochondria

The role of Parkin in mitophagy is not only dependent on its ubiquitin ligase activity, but also on its ability to be recruited to damaged mitochondria, where it exerts its function. Consequently regulation of both processes needs to be studied in order to examine the effect of Parkin mutations in mitophagy. In addition to the characterisation of the ligase activity of phospho-null and phospho-mimic ^{YFP}Parkin mutants on Miro1 ubiquitination, the recruitment and stabilisation of these mutants onto mitochondria was also investigated. For this aim a good mitochondrial marker was needed. Since Chan and colleagues have shown that several OMM proteins, including TOM20 (often used as a mitochondrial marker), are degraded upon induction of mitophagy (Chan *et al.*, 2011), TOM20 stability following mitochondrial damage was assessed. In particular HEK 293 cells transiently transfected with ^{YFP}Parkin, were treated with the mitochondrial uncoupler FCCP (10 μM, 1 hour) or DMSO. Lysates were collected, resolved on a SDS-PAGE gel and western blotted. The levels of TOM20 were similar after mitochondrial damage (1 hour, Fig. 5.5), in agreement with the data reported by Chan and colleagues, where 30 μM CCCP triggered Parkin-dependent TOM20 loss only after 4 hours (Chan *et al.*, 2011). TOM20 was therefore used as a mitochondrial marker within this time period.

To investigate the recruitment dynamics of the Parkin mutants to damaged mitochondria, HEK 293 cells were transiently transfected with WT, phospho-null or phospho-mimic ^{YFP}Parkin. Mitochondrial damage was triggered with FCCP (10 μM, 1 hour), cells were fixed and representative images were taken with a confocal microscope from previously blinded samples. The recruitment of ^{YFP}Parkin mutants to mitochondria was analysed as integrated fluorescence colocalisation of ^{YFP}Parkin and the OMM TOM20. Following 1 hour FCCP treatment nearly 80% of wild type ^{YFP}Parkin was recruited to the damaged mitochondria, however this translocation was inhibited by the phospho-null S65A mutation and reduced by the phospho-mimic S65E mutant (Fig. 5.6 A and

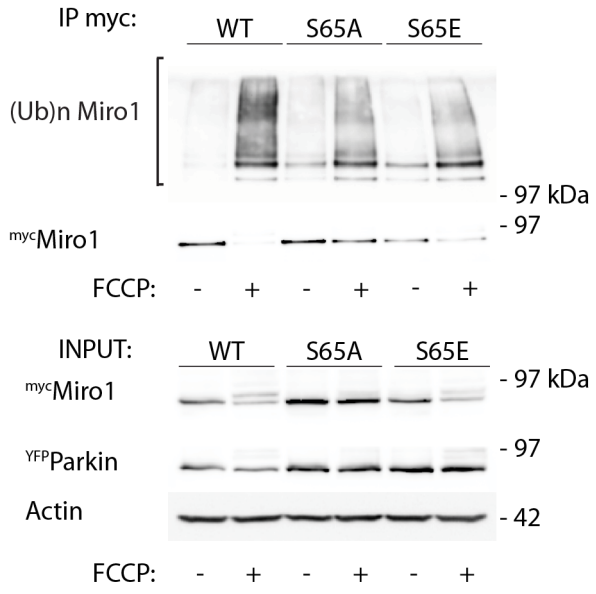

Figure 5.3: Miro1 ubiquitination by Parkin S65 mutants in HeLa cells.

HeLa cells transfected with WT, S65A or S65E ^{YFP}Parkin, ^{myc}Miro1 and ^{HA}ubiquitin, were treated with FCCP (10 μM, 1 hour) or vehicle (DMSO), and ^{myc}Miro1 was immunopurified. Western blotted samples were probed with anti HA, myc, GFP and actin antibodies. Expression of the phospho-null ^{YFP}Parkin^{S65A} mutant reduces the FCCP-induced ^{myc}Miro1 HA positive ubiquitination smear and blocks the subsequent loss of the protein, detected with an anti myc antibody. When phospho-mimetic ^{YFP}Parkin^{S65E} is expressed ^{myc}Miro1 levels are lower, as detected by the myc positive bands in the inputs and in the immunoprecipitated sample, however mitochondrial damage results in a further decrease of the protein (n=3 independent experiments).

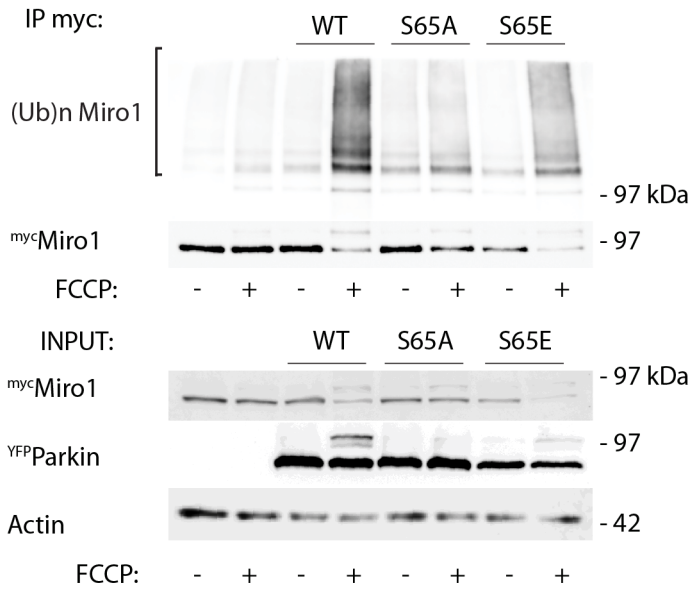

Figure 5.4: Miro1 ubiquitination by Parkin S65 mutants in neuronal SH-SY5Y cells.

Neuronal SH-SY5Y cells transfected with WT, S65A or S65E ^{YFP}Parkin, ^{myc}Miro1 and ^{HA}ubiquitin, were treated with FCCP (10 μM, 1 hour) or vehicle (DMSO). ^{myc}Miro1 was immunopurified and samples western blotted. Expression of the phospho-null ^{YFP}Parkin^{S65A} mutant reduces the FCCP-induced ^{myc}Miro1 HA positive ubiquitination smear and the protein loss. When phospho-mimetic ^{YFP}Parkin^{S65E} is expressed, some residual HA positive Miro1 ubiquitination smear can be detected. Myc positive Miro1 levels are lower, as detected in the inputs and in the immunoprecipitated samples, moreover mitochondrial damage results in a further decrease of the protein.

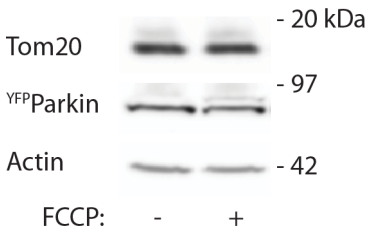

Figure 5.5: The OMM protein TOM20 is stable after 1 hour FCCP treatment.

HEK 293 cells were transfected with ^{YFP}Parkin and treated with FCCP (10 μM, 1 hour) to induce mitochondrial damage or DMSO as a control. Western blot analysis of the lysates shows that the levels of TOM20 are unaltered after 1 hour of mitochondrial damage (n=1).

Fig. 5.7, percentage of S65A Parkin on mitochondria 33.27 ± 1.46%, percentage of S65E Parkin on mitochondria 52.97 ± 4.68 %, compared to wild type Parkin on mitochondria 78.19 ± 4.86 %, n=9-14, #p<0.05, ###p<0.005. * indicates significance between treated/untreated samples, # indicated significance within a treatment group, #p<0.05, **p<0.01, ###/***p<0.005).

The lack of recruitment of Parkin phospho-mutants could be due to either a block or a delay of Parkin translocation onto damaged mitochondria. To address this HEK 293 cells transfected with WT S65A or S65E ^{YFP}Parkin and treated for 2 hours with the mitochondrial uncoupler FCCP (10 μM) were analysed. After 2 hours of mitochondrial damage both mutants were recruited to the OMM to the same extent as WT Parkin. This suggests that the translocation dynamics are delayed or the stability of these mutants on the OMM is reduced (Fig. 5.6 B and Fig. 5.7, percentage of S65A Parkin on mitochondria 53.97 ± 6.57%, percentage of S65E Parkin on mitochondria 60.90 ± 7.62%, compared to wild type Parkin on mitochondria 71.33 ± 6.98%, n=9-14 from 3 independent experiments, *** p<0.005), in agreement with a previous report (Shiba-Fukushima *et al.*, 2012).

To investigate whether Miro1 had a role in regulating phospho-null and phospho-mimic ^{YFP}Parkin translocation and stabilisation on the OMM, HEK 293 cells were transfected with ^{mCherry}Miro1 together with WT, S65A or S65E ^{YFP}Parkin. Mitochondrial damage was triggered by incubation with FCCP (10 μM) for 1 or 2 hours prior to fixation. Interestingly ^{mCherry}Miro1 was found to significantly increase the recruitment and stabilisation of both the S65A and S65E mutants at early time points to an extent similar to WT Parkin, as seen by the increase in integrated colocalisation of the YFP signal with TOM20 fluorescence (Fig. 5.8 and Fig. 5.10, percentage of S65A Parkin on mitochondria at 1 hour when Miro1 is OE 63.55 ± 5.24%, percentage of S65E Parkin on mitochondria 72.82 ± 4.85% compared to wild type Parkin on mitochondria 61.69 ± 2.55%, n=12-14 from 3 independent experiments, ***p<0.005). A similar translocation was also detected after 2 hours of mitochondrial damage (Fig. 5.9 and Fig. 5.10, percentage of S65A Parkin on mitochondria 61.63 ± 6.56 %, percentage of S65E Parkin on mitochondria70.53 ± 4.97%, compared to wild type Parkin on mitochondria 67.41 ± 4.86%, n=12-13 from 3 independent experiments, ***p<0.005).

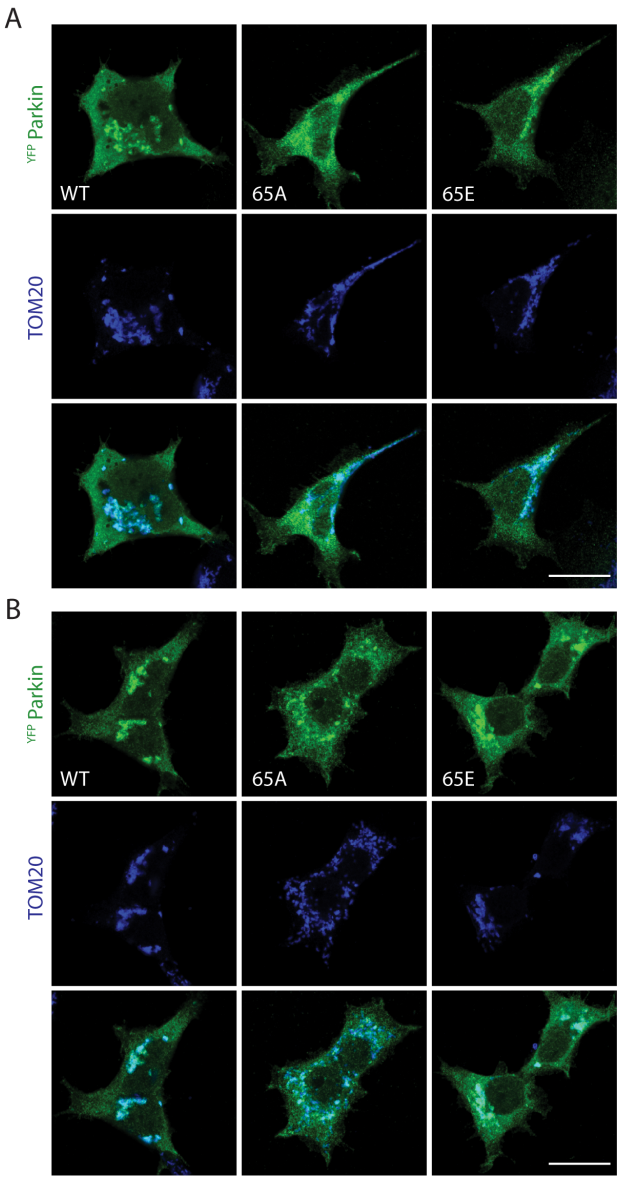

Figure 5.6: Parkin mutants show delayed recruitment to damaged mitochondria after mitochondrial damage in HEK 293 cells.

Confocal images of HEK 293 cells transfected with WT, S65A or S65E ^{YFP}Parkin, and treated with FCCP (10 μM) for 1 (A) or 2 (B) hours.^{YFP}Parkin fluorescent signal is represented in green and TOM20 positive mitochondria are represented in blue. Scale bar = 20 μm.

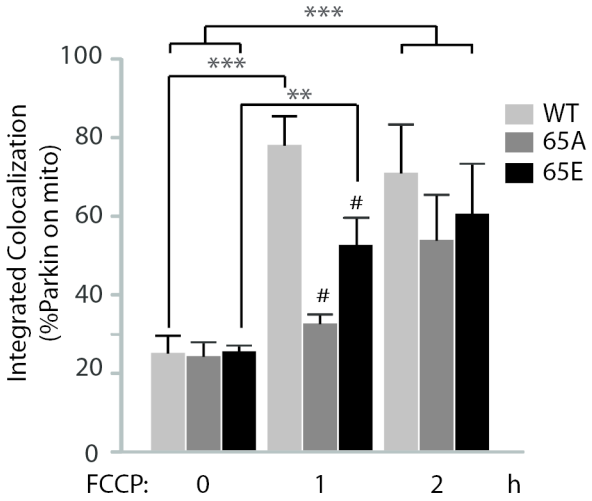

Figure 5.7: Quantification of WT, S65A and S65E Parkin recruitment to damaged mitochondria in HEK 293 cells.

Graph showing the quantification of Parkin translocation onto mitochondria following 1 and 2 hours FCCP treatment (10 μM), as shown in Fig. 5.6. Translocation was measured as integrated colocalisation of the ^{YFP}Parkin signal with the mitochondrial marker TOM20 signal, n=9-14 from 3 independent experiments, #p<0.05, ###p<0.005. * indicates significance between treated/untreated samples, # indicated significance within a treatment group, #p<0.05, **p<0.01, ###/***p<0.005.

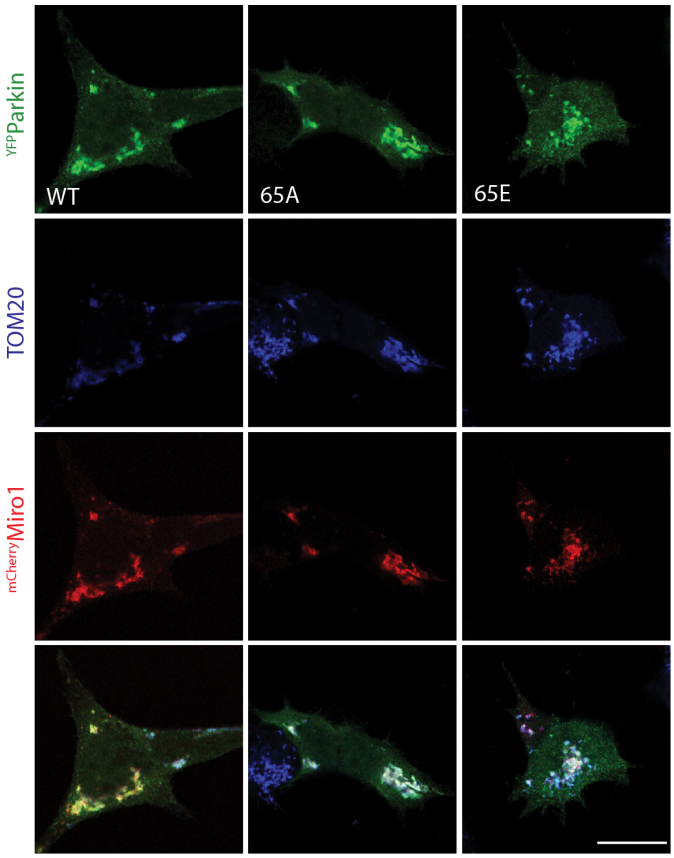

Figure 5.8: Miro1 facilitates the translocation of S65A and S65E Parkin mutants onto damaged mitochondria in HEK 293 cells.

Overexpression of $^{\text{mCherry}}$Miro1 (red) together with $^{\text{YFP}}$Parkin or the S65A and S65E mutants (green) facilitates Parkin recruitment to the TOM20 positive mitochondria (blue) after 1 hour FCCP treatment in HEK 293 cells. Scale bar = 20 μm.

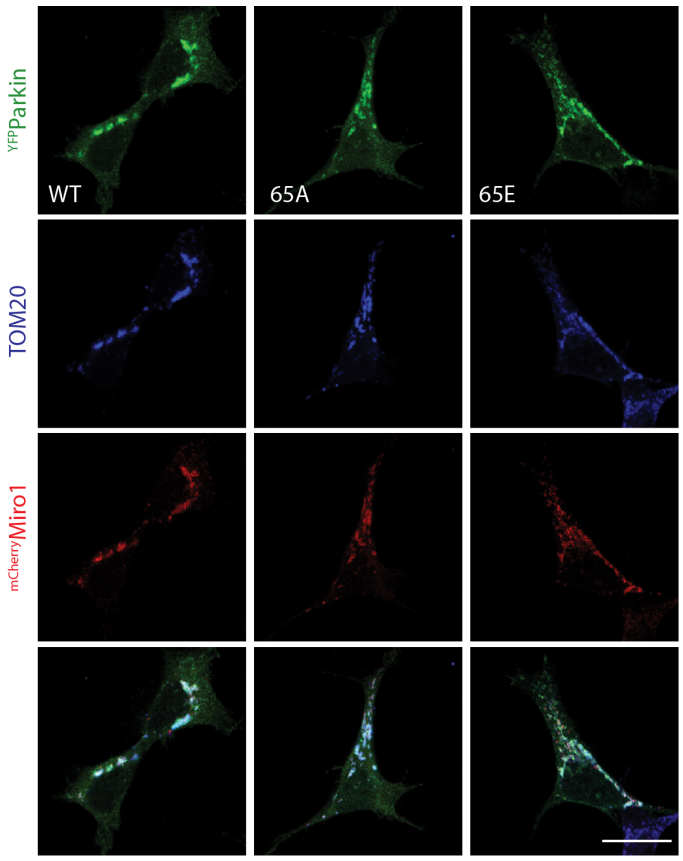

Figure 5.9: WT, S65A and S65E ^{YFP}Parkin recruitment to damaged mitochondria after 2 hours FCCP treatment in HEK 293 cells overexpressing Miro1.

HEK 293 cells overexpressing WT, S65A and S65E ^{YFP}Parkin (green) together with ^{mCherry}Miro1 (red), were treated with FCCP (10 μM, 2 hours) before fixation. Mitochondria were labelled with the mitochondrial marker TOM20 (blue). Scale bar = 20 μm.

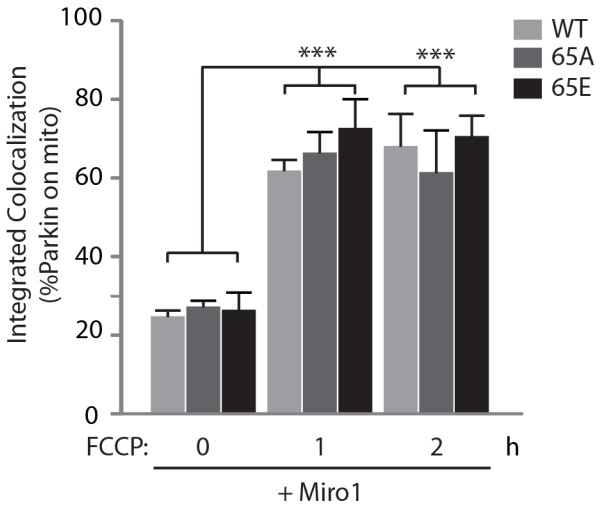

Figure 5.10: Quantification of WT, S65A and S65E Parkin to damaged mitochondria in the presence of Miro1.

Graph showing the quantification of Parkin translocation onto damaged mitochondria following 1 and 2 hours FCCP treatment (10 μM) in HEK 293 cells overexpressing Miro1, as shown in Fig. 5.8 and Fig. 5.9. Recruitment is measured as integrated colocalisation of ^{YFP}Parkin fluorescence with the mitochondrial marker TOM20 fluorescence. n=12-14 from 3 independent experiments, ***$p<0.005$.

To further confirm the role of Miro1 in the recruitment and stabilisation of Parkin phospho-null and phospho-mimic mutants, HeLa cells were used to exclude the possibility of a contribution of endogenous Parkin. Cells were transfected with WT, S65A or S65E ^{YFP}Parkin with or without ^{mCherry}Miro1. Mitochondrial damage was triggered with FCCP (10 μM, 1 hour), cells were fixed, stained and imaged on a confocal microscope. Similar to HEK 293 cells, S65A and S65E Parkin mutants exhibited impaired recruitment to damaged mitochondria in HeLa cells (Fig. 5.11). Moreover, even though ^{mCherry}Miro1 overexpression promoted the translocation onto damaged mitochondria of the Parkin mutants, this appeared to happen only in a subset of cells, rather than with different degrees of translocation like in HEK 293 cells. To quantify the percentage of cells displaying Parkin recruitment to damaged mitochondria, blinded samples were then manually scored (recruitment Vs no recruitment). When WT ^{YFP}Parkin was expressed, mitochondrial damage induced the translocation of Parkin onto damaged mitochondria in the totality of transfected cells in the presence or absence of ^{mCherry}Miro1 overexpression. However, both phospho-null (S65A) and phospho-mimic (S65E) ^{YFP}Parkin failed to translocate onto damaged mitochondria. Importantly, like in HEK 293 cells, co-expression of ^{mCherry}Miro1 in HeLa cells promoted the recruitment and stabilisation of Parkin phospho-mutants. In particular phospho-null (S65A) translocation onto mitochondria was detected in a subpopulation of the transfected cells, whereas S65E translocated in the majority of transfected cells (Fig. 5.11, 100% of WT ^{YFP}Parkin transfected cells showed Parkin enrichment on damaged mitochondria in the presence or absence of ^{mCherry}Miro1 overexpression, no translocation was observed when S65A or S65E Parkin mutants were expressed in the absence of Miro1 coexpression, whereas 16.42 ± 2.0% of S65A Parkin expressing cells and 88.83 ± 5.0% of S65E Parkin expressing cells showed Parkin translocation on mitochondria when Miro1 was co-expressed; 44-79 cells from 3 independent experiments, #$p<0.05$, **$p<0.01$, ***/###$p<0.005$). These data further suggest that following mitochondrial damage Miro1 could act as a component of a Parkin acceptor complex on the OMM.

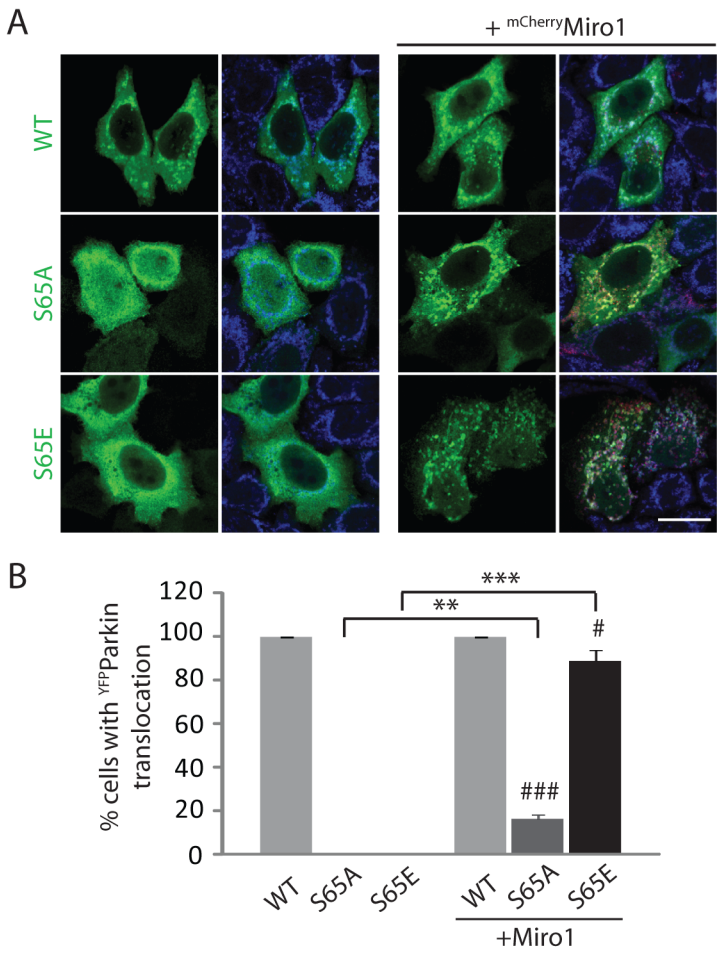

Figure 5.11: Miro1 promotes the translocation of S65E ^{YFP}Parkin onto damaged mitochondria in HeLa cells.

(A) Confocal images of HeLa cells transfected with WT, S65A or S65E ^{YFP}Parkin with or without ^{mCherry}Miro1. Mitochondrial damage was triggered with FCCP (10 μM, 1 hour) prior to fixation. In green ^{YFP}Parkin fluorescence, in blue the mitochondrial marker TOM20, in red ^{mCherry}Miro1. FCCP treatment did not trigger S65A or S65E ^{YFP}Parkin recruitment to mitochondria (left panels), however ^{mCherry}Miro1 overexpression promoted this translocation in a subpopulation of S65A expressing cells and in the majority of S65E transfected cells (right panels). Scale bar = 20 μm (B) Cells that exhibited WT or mutant ^{YFP}Parkin recruitment to mitochondria were scored manually from previously blinded samples (44-79 cells from 3 independent experiments, #$p<0.05$, **$p<0.01$, ***/###$p<0.005$).

Role of Parkin S65 on mitochondrial trafficking

Parkin S65E phospho-mimic mutant was shown to facilitate Miro1 turnover in basal conditions, suggesting that expression of this mutant could influence mitochondrial transport. To address this question mitochondrial trafficking in hippocampal neurons was analysed. Neuronal cultures were transfected at 8 days in vitro (DIV) with the mitochondrial marker mtDsRed2 together with either GFP, WT ^{YFP}Parkin, S65A ^{YFP}Parkin or S65E ^{YFP}Parkin. At 10 DIV axons of GFP/YFP and mtDsRed2 positive cells were morphologically identified (thin process at least 3 times longer than the other thicker processes - dendrites), and mtDsRed2 labelled mitochondria imaged over 2 minutes. The percentage of moving mitochondria was analysed. Expression of WT, S65A or S65E ^{YFP}Parkin caused no difference in the mitochondrial motility, compared to GFP expression (Fig. 5.12 A, B, 21.2 ± 4.4% of moving mitochondria with GFP overexpression, 20.0 ± 5.7% with WT ^{YFP}Parkin , 26.0 ± 3.8% with S65A ^{YFP}Parkin and 25.4 ± 2.7% with S65E ^{YFP}Parkin; n=8-11 from 3 independent experiments). Since ubiquitin, in its phosphorylated form, was recently found to further activate Parkin (Kane *et al.*, 2014; Kazlauskaite *et al.*, 2014b; Koyano *et al.*, 2014), mitochondrial trafficking in hippocampal neurons was investigated in cells overexpressing S65E ^{YFP}Parkin with or without ^{HA}ubiquitin. Hippocampal cultures were transfected at 8 DIV with the mitochondrial marker mtDsRed2 together with S65E ^{YFP}Parkin with or without ^{HA}ubiquitin. At 10 DIV axons mtDsRed2 labelled mitochondria of YFP positive neurons, were imaged over 2 minutes. The percentage of moving mitochondria was analysed and ^{HA}ubiquitin co-expression with phospho-mimic S65E ^{YFP}Parkin was found to reduce the number of moving mitochondria compared to control (Fig. 5.12 C and D, 17.6 ± 3.3 % of moving mitochondria when S65E ^{YFP}Parkin and ^{HA}ubiquitin were expressed, while 29.9 ± 3.0% of mitochondria were moving when S65E ^{YFP}Parkin only was expressed, n=9-11 from 3 independent experiments, p=0.015). After being imaged, cells were fixed and ^{HA}ubiquitin expression was confirmed by immunofluorescence. Although exciting these experiments are preliminary. In fact, whether this effect can be blocked by phospho-null Parkin mutant, and whether ubiquitin expression itself can influence mitochondrial trafficking need to be investigated.

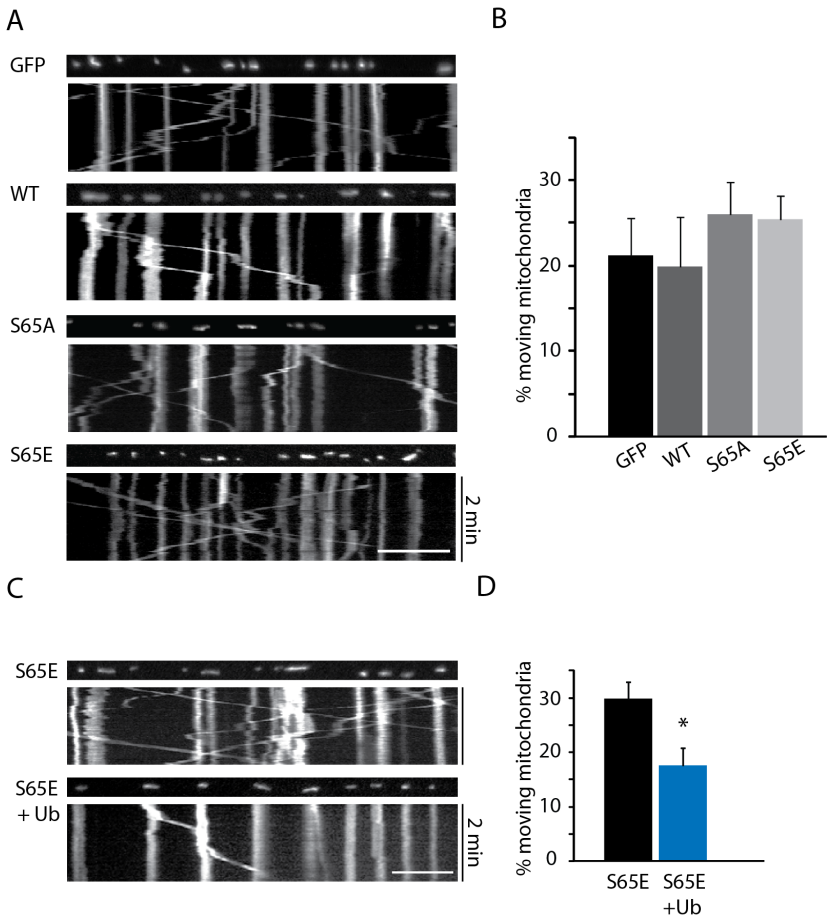

Figure 5.12: Regulation of mitochondrial trafficking by Parkin S65 mutants in hippocampal neurons.
(A) Hippocampal neurons were transfected with GFP, WT ^{YFP}Parkin, S65A ^{YFP}Parkin or S65E ^{YFP}Parkin, together with the mitochondrial marker mtDsRed2 at 8 DIV. MtDsRed2 live imaging was performed at 10 DIV in GFP/YFP positive axons. In each condition static images and kymographs are represented. Kymographs were created by projecting sequential line scans through the process of interest onto the y-axis, so that stationary mitochondria are seen as straight lines and moving mitochondria as diagonal lines. Mitochondrial movement was imaged for 2 minutes. Scale bar = 20 μm. (B) Bar graph quantifying the percentage of moving mitochondria shows that expression of Parkin or its phospho-mutants does not affect mitochondrial motility (n=8-11, from 3 independent experiments). (C) Hippocampal neurons were transfected with S65E ^{YFP}Parkin and mtDsRed2 with or without ^{HA}ubiquitin at 8 DIV. At 10 DIV mitochondrial trafficking was imaged in axons. Static images and kymographs are shown for each condition. Scale bar = 20 μm. (D) Graph quantifying the percentage of moving mitochondria shows that ^{HA}ubiquitin overexpression inhibits mitochondrial trafficking (n=9-11 axons from 3 independent experiments, *p=0.015).

Role of ubiquitin phosphorylation in Miro1 ubiquitination

Three reports have recently demonstrated that upon mitochondrial damage ubiquitin is phosphorylated by PINK1 on conserved serine 65, and that this modification is a further step in the complex activation of Parkin during mitophagy (Kane *et al.*, 2014; Kazlauskaite *et al.*, 2014b; Koyano *et al.*, 2014). Phospho-ubiquitin was found to promote the activation/auto-ubiquitination of phospho-mimic 65E Parkin, and oxyester bonds were found between Parkin (C431S, to allow the formation of the oxyester bond) and phospho-mimic 65D ubiquitin, suggesting the activation of the E3 ligase (Kazlauskaite *et al.*, 2014b; Koyano *et al.*, 2014). However, the role of ubiquitin phosphorylation in Parkin-dependent substrate ubiquitination has not been explored to date. To investigate whether by promoting the activation of Parkin, phosphorylation of ubiquitin regulates the rate of ubiquitination of the OMM proteins, WT, phospho-null S65A or phospho-mimic S65E ubiquitin were heterologously expressed in Parkin OE SH-SY5Y cells together with ^{myc}Miro1. Cells were subjected to mitochondrial damage with the ionophore FCCP (10 μM, 1 hour), ^{myc}Miro1 was immunopurified, samples were resolved by SDS-PAGE and western blotted. Unexpectedly, the incorporation of phospho-mimic S65E mutant in Miro1 ubiquitin chains (HA positive high molecular weight smear) upon FCCP treatment was drastically reduced, whereas phospho-null S65A ubiquitin showed a similar incorporation in Miro1 ubiquitination to WT ubiquitin (Fig. 5.13, n=3). This suggests that phosphorylation of ubiquitin could have a role in the structural activation of Parkin, but not in the ubiquitin chain elongation.

Discussion

A complex, multi-step regulation controls Parkin function. Upon mitochondrial damage, this E3 ubiquitin ligase is recruited by PINK1 from the cytosol to damaged mitochondria, PINK1 then induces the release of Parkin auto-inhibition by phosphorylating the ligase Ubl domain at S65 and, by phosphorylating ubiquitin, PINK1 promotes a further activation of Parkin. In this Chapter the role of S65-dependent activation and regulation of the E3 ubiquitin ligase Parkin has been investigated. In particular the role of this residue on Parkin ligase activity and recruitment dynamics to damaged mitochondria has been explored with phospho-null and phospho-mimic Parkin constructs in HeLa,

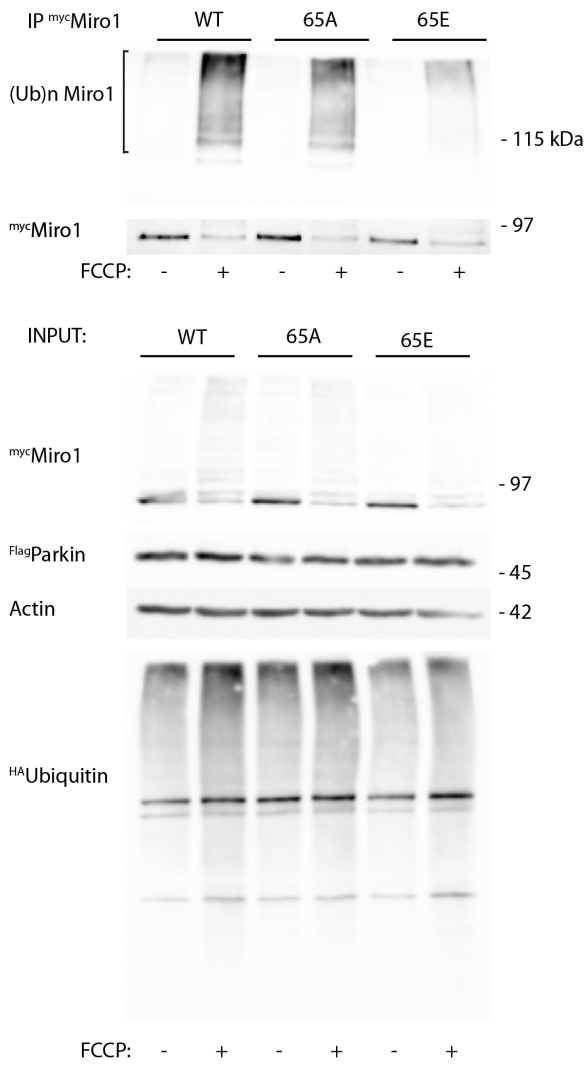

Figure 5.13: Analysis of ubiquitin phospho-mutants incorporation in Miro1 ubiquitin chains.

Parkin OE SH-SY5Y cells were transiently transfected with ^{myc}Miro1 together with WT, 65A or 65E ^{HA}ubiquitin. Cells were treated with FCCP (10 μM, 1 hour) or vehicle (DMSO), ^{myc}Miro1 was immunopurified and samples were run on a SDS-PAGE gel. Western blotted samples were probed with anti HA, myc, Flag and actin antibodies. HA positive Miro1 ubiquitination smear was similar when WT or phospho-null S65A mutant were expressed, whereas phospho-mimic S65E ubiquitin was less incorporated in Miro1 ubiquitin chains. Expression of the ubiquitin mutants, as shown in the inputs, is similar (bottom panel, n=3 independent experiments).

SH-SY5Y and HEK 293 cells. Following mitochondrial damage phospho-mimic Parkin was shown to ubiquitinate Miro to a smaller extent than WT, however, this mutant was still able to promote the protein turnover. Oppositely, expression of phospho-null Parkin blocked FCCP-dependent Miro1 loss. Moreover, both mutants were shown to have delayed translocation dynamics onto damaged mitochondria and interestingly, Miro was found to facilitate the stabilisation of the Parkin mutants on the OMM. Lastly, the role of phospho-ubiquitin in Parkin ligase activity has been studied by analysing Miro1 ubiquitination. Although phosphorylation of ubiquitin was reported to activate Parkin, phospho-mimic 65E ubiquitin was found to be less prominent in Miro1 ubiquitin chains.

PINK1-dependent phosphorylation of serine 65 on Parkin has been suggested to activate Parkin by causing the release of the autoinhibitory Ubl domain, favouring the ligase active conformation. In fact S65 phosphorylation of Parkin has been shown to promote the ligase self-ubiquitination and the formation of free ubiquitin chains (Shiba-Fukushima *et al.*, 2012; Kondapalli *et al.*, 2012), however, little is known on the effect of this crucial residue on the ubiquitination of Parkin substrates during mitophagy. Taking advantage of phospho-null and phospho-mimic Parkin mutants, Miro1 ubiquitination was studied in HeLa cells and in neuronal SH-SY5Y cells. Mutation of serine 65 to non phosphorylatable alanine resulted in decreased Miro1 ubiquitination, and the consequent stabilisation of the protein after mitochondrial damage (Fig. 5.3 and Fig. 5.4), in agreement with a recent study *in vitro* (Kazlauskaite *et al.*, 2014a). In contrast, despite having a decreased ubiquitin ligase activity following FCCP treatment, expression of phospho-mimic S65E Parkin caused a reduction in the levels of Miro1, which was further enhanced by mitochondrial damage, suggesting an increased basal activity of this mutant. These data agree with a recently published report, where reduced Miro and Mitofusin levels were detected upon expression of a phospho-mimic Parkin mutant *in vivo* in *Drosophila* (Shiba-Fukushima *et al.*, 2014). It is possible that the negative charge given by the phospho-mimic glutamate causes a conformational change in Parkin that might induce an "activated" state of the protein in the absence of mitochondria damage. S65E Parkin could therefore more easily interact with and ubiquitinate its substrates leading to an increase in their turnover and a consequent decrease in their steady state levels.

Among the various disease-associated Parkin mutants, many are characterised by impaired ligase function, however others are unable to be recruited to the mitochondria and cannot, therefore, promote mitophagy. Parkin function is in fact, not only depen-

dent on its enzymatic activity, but also on its spatial regulation. For this reason, to better understand the role of Parkin phosphorylation in the ligase function, the translocation of Parkin S65 mutants to damaged mitochondria was investigated. Although S65E Parkin was found to be enriched on damaged mitochondria, both mutants showed impaired recruitment dynamics compared to WT Parkin at early time points in HEK 293 cells (Fig. 5.6 A and Fig. 5.7). The translocation of phospho-null and phospho-mimic Parkin was not however blocked, but rather delayed to later time points (Fig. 5.6 B and Fig. 5.7). Unexpectedly, when expressed in HeLa cells phospho-null and phospho-mimic Parkin mutants completely failed to be recruited onto damaged mitochondria, unlike what was previously reported by Shiba-Fukushima and colleagues (who documented a partial recruitment) or by Sarraf and collaborators (who did not detect any difference in the translocation of WT, phospho-null or phospho-mimic Parkin) (Shiba-Fukushima *et al.*, 2012; Sarraf *et al.*, 2013). This effect might be possibly due to different expression levels of the Parkin constructs and/or the OMM proteins in the different HeLa cell lines used. Altogether these results suggest that PINK1-dependent phosphorylation of Parkin could have a role in the stabilisation of the ligase onto the mitochondria, possibly favouring its interaction with PINK1 or its substrates. Alternatively, mutations at S65 could affect Parkin self association, which has been suggested to promote its activation and stabilisation onto mitochondria (Lazarou *et al.*, 2013).

Interestingly, Miro levels were found to stabilise phospho-null and phospho-mimic Parkin mutants onto damaged mitochondria both in HEK 293 and in HeLa cells (Fig. 5.8, Fig. 5.9, Fig. 5.10 and Fig. 5.11). Unlike HEK 293 cells, where Parkin mutants showed different levels of recruitment (in the absence of Miro), HeLa cells either displayed a clear recruitment of Parkin onto the mitochondria or the ligase appeared to remain cytosolic, possibly due to the lack of endogenous Parkin that might facilitate the mutants translocation. These results suggest that Miro, and potentially other OMM Parkin substrates such as Mfn2 (Chen and Dorn II, 2013), may play an additional role in stabilising Parkin on the OMM. Therefore substrate binding by Parkin in conjunction with its phosphorylation, could work together to stabilise the E3 ligase on the OMM of damaged mitochondria, providing a mechanism to regulate Parkin levels to the levels of its substrates on the mitochondria.

Parkin overexpression has been previously described to induce Miro degradation, thus promoting a decrease in mitochondrial transport (Wang *et al.*, 2011b). In this work

however, expression of ^{YFP}Parkin did not drastically affect Miro1 levels (for example in Fig. 5.4 ^{myc}Miro1 levels are similar in untreated cells, transfected or not with Parkin) or impaired mitochondrial transport (Fig. 5.12 A and B). This lack of Parkin-mediated regulation of Miro in control conditions could be due to the fact that the ligase, although overexpressed, is not recruited to polarised mitochondria. S65E phospho-mimic Parkin, suggested to exhibit an activated conformation, was shown to facilitate Miro1 basal turnover (Fig. 5.3 and Fig. 5.4), suggesting that this mutant could affect mitochondrial transport. Analysis of mitochondrial motility in the presence of phospho-mimic S65E Parkin, however, showed no difference compared to WT Parkin or GFP control (Fig. 5.12 A and B). Recently, however, three reports showed that ubiquitin, in its phosphorylated form, further activates Parkin (Kane *et al.*, 2014; Koyano *et al.*, 2014; Kazlauskaite *et al.*, 2014b). Indeed, preliminary experiments showed that overexpression of ubiquitin together with S65E phospho-mimic Parkin caused a reduction of mitochondrial transport in axons of hippocampal neurons (Fig. 5.12 C and D), in agreement with the idea of ubiquitin to promote Parkin S65E basal activity.

PINK1-mediated ubiquitin phosphorylation on the conserved S65 was recently found to be an additional step in the tight regulation of mitochondrial quality control. Phosphorylated ubiquitin was shown to promote phospho-mimic S65E Parkin auto-ubiquitination *in vitro*, and oxyester bonds were found between Parkin C431S (to allow the formation of stable oxyester bonds) and phospho-mimic 65D ubiquitin in the absence of mitochondrial depolarization (Kane *et al.*, 2014; Koyano *et al.*, 2014), suggesting that ubiquitin phosphorylation could promote Parkin activation/function. Unexpectedly, in Parkin OE SH-SY5Y cells Miro1 was ubiquitinated in a comparable way when WT or S65A ^{HA}ubiquitin were expressed. Additionally, its ubiquitination was drastically reduced in the presence of phospho-mimic S65E ^{HA}ubiquitin (Fig. 5.13). Koyano and colleagues have shown that Parkin is able to conjugate both phosphorylated and unphosphorylated ubiquitin molecules (Koyano *et al.*, 2014), therefore it is possible that when phospho-null ubiquitin was expressed, phosphorylation of endogenous ubiquitin was sufficient to fully activate Parkin, which in turn could conjugate S65A ubiquitin. Meanwhile, if ubiquitin phosphorylation is a key process in Parkin activation, but not in the incorporation of ubiquitin into polymeric chains, S65E ^{HA}ubiquitin could bind and activate Parkin, but not necessarily take part in the assembly of Miro1 ubiquitin chains, which could be formed by the endogenous protein (that would not be detected by the anti-HA antibody). For this reason, it would be interesting to test the contribution of endogenous

ubiquitin in Miro1 ubiquitination when the phospho-null and phospho-mimic ubiquitin mutants are expressed to investigate whether phospho-ubiquitin-dependent Parkin activation and phospho-ubiquitin incorporation into chains are two separate processes. Moreover, phospho-mimic S65D ubiquitin should be used instead of S65E, since it has been shown to promote phospho-mimic Parkin self-ubiquitination (Koyano *et al.*, 2014). An open question is whether phosphorylation of ubiquitin can influence the ubiquitin chain linkage. In this case the the selective activation of ubiquitin kinases or phosphatases could either favour or impede specific chain types, affecting the outcome of ubiquitination.

Overall in this Chapter the phosphorylation-dependent regulation of Parkin and mitophagy have been studied. Parkin phosphorylation at S65 has been found to be crucial both for the prompt recruitment of the ubiquitin ligase to damaged mitochondria and for its enzymatic function. Interestingly Miro1 was found to promote the translocation of the Parkin mutants onto impaired mitochondria, suggesting that Miro could be part of a Parkin acceptor complex that promotes the stabilisation of Parkin on the OMM, although mitochondrial damage was necessary for this to happen. Finally phospho-mimic ubiquitin, recently shown to activate Parkin, was found not to take part in Miro1 ubiquitination, however further experiments will be needed to thoroughly investigate the function of this phosphorylation in the ubiquitin chain assembly process and in the linkage preference.

Chapter 6

Final Discussion

Mitochondria play a central role within the cell. These organelles provide energy, buffer calcium and they are involved in several cellular processes from cell differentiation and growth to apoptosis. Mitochondria are not just randomly distributed within the cell, but they are actively transported across the cytoplasm to areas of high energy demand and calcium buffering requirements. Mitochondrial trafficking is accomplished by a set of proteins that forms the mitochondrial transport machinery. Miro proteins are atypical Rho GTPases localised on mitochondria. By the interaction with the kinesin motors these proteins mediate mitochondrial trafficking along the cytoskeletal tracks (MacAskill *et al.*, 2009b). Miro also interacts with the TRAK adaptors, that have been reported to bind both kinesin and dynein motors (Brickley *et al.*, 2005; Brickley and Stephenson, 2011; Glater *et al.*, 2006; van Spronsen *et al.*, 2013), suggesting that this motor complex regulates mitochondrial transport in both antero and retrograde directions. Mitochondria however, not only need to be trafficked where necessary, but also need to be retrieved when dysfunctional. Work from Miller and Sheetz has shown that in neurons mitochondrial transport is linked to mitochondrial functionality (Miller and Sheetz, 2004). The authors have in fact showed that anterogradely moving mitochondria were characterised by higher membrane potential than retrogradely moving ones. Moreover, treatment with antimycin A, which inhibits complex III of the ETC, resulting in ROS formation and inhibition of the ATP production, favoured retrograde transport of the axonal organelles, thus suggesting that mitochondrial damage induces a switch in the

transport directionality. Damaged, depolarised mitochondria need to be isolated from the functional mitochondrial network and then cleared by mitophagy.

In the last decade our knowledge on the role of PINK1 and Parkin in mitochondrial quality control and mitophagy has greatly improved. PINK1 and Parkin have been shown to orchestrate recognition, isolation and mitophagy-targeting of damaged mitochondria. However, less is known on how mitochondrial clearance is regulated, the fate of ubiquitinated proteins and the steps that determine and follow the formation of the autophagosome. In particular, mitophagy was assumed to occur at somatic level (Maday *et al.*, 2012; Cai *et al.*, 2012), and an open question remains as to what mechanism underlies the retrieval of damaged mitochondria. Miro, that together with TRAK was found in a complex with PINK1 (Weihofen *et al.*, 2009), represents an optimal candidate to play a role in cross-talk between mitochondrial trafficking and quality control.

Summary

In this thesis the role of Miro as a substrate of the PINK1/Parkin pathway has been investigated. Mitochondrial damage was shown to trigger PINK1/Parkin-dependent Miro loss in dopaminergic SH-SY5Y cells. To further confirm the role of Parkin in this pathway, damage-induced Miro degradation was shown to be disrupted in human fibroblasts derived from a PD patient lacking Parkin. Moreover, Miro was found to interact with and be ubiquitinated by Parkin upon mitochondrial damage. To investigate whether Miro1 ubiquitination affected its interaction with other components of the trafficking machinery, Miro binding to the TRAKs was tested. Interestingly, however, no change was detected, suggesting that the complex was preserved.

Miro ubiquitination could lead to its rapid degradation, or alternatively the protein could be retained on the OMM in its ubiquitinated form. Further analysis of Miro1 ubiquitination and degradation dynamics demonstrated that although the protein was found to be rapidly ubiquitinated (20 minutes FCCP), it appeared to be stable on the OMM for at least one hour following treatment with the mitochondrial uncoupler FCCP, suggesting that ubiquitinated Miro1 could have a signalling role prior to its degradation by the proteasome. While working on this project a paper came out from the

Schwarz lab, showing that mitochondrial damage leads to the prompt block of mitochondrial transport caused by the rapid degradation of Miro1. Moreover, they showed that Parkin-dependent Miro1 loss was induced by PINK1-mediated phosphorylation of serine 156 (Wang *et al.*, 2011b). To further analyse Miro1 ubiquitination and potentially study the role of a ubiquitination-deficient mutant, Miro1 serine 156 phospho-null and phospho-mimic mutants were made. These mutants, however, were shown to have similar ubiquitination and degradation dynamics, in agreement with another study (Liu *et al.*, 2012). Depending on the chain linkage, poly-ubiquitination can have several cellular outcomes. Miro1 ubiquitination was therefore studied using ubiquitin mutants and chain-specific deubiquitinases. Interestingly, Miro1 was found to be ubiquitinated primarily in a K27-linked manner, but also K11 and K29-linkages were detected, whereas no K48 chain type contribution was found, in agreement with the slower degradation of the protein.

Recent studies have reported the crucial role that PINK1 plays in the recruitment and activation of Parkin. PINK1 in fact, not only binds and phosphorylates Parkin on serine 65 to promote the activation of the ligase, but also phosphorylates ubiquitin, which further activates Parkin. To investigate the role of serine 65 in Parkin ligase activity, Miro1 ubiquitination following mitochondrial damage was studied using phospho-null and phospho-mimic Parkin contructs. Both mutants exhibited a lower activity compared to wild type, however, interestingly, expression of phospho-mimic S65E Parkin seemed to regulate steady-state Miro1 levels, suggesting a constitutive role of this mutant. Parkin mutants also exhibited a delayed recruitment onto damaged mitochondria, however, expression of Miro1 promoted their recruitment and stabilisation, suggesting that Miro is part of a Parkin acceptor complex on damaged mitochondria. Incorporation of phospho-null and phospho-mimic ubiquitin mutants in Miro1 ubiquitin chains was also analysed, however in this assay phospho-mimic S65E ubiquitin was not found to be enriched in Miro1 ubiquitin chains.

Mitochondrial damage-dependent regulation of the trafficking machinery

Miro1, a key component of the mitochondrial trafficking complex, was found to interact with the mitochondrial quality control protein PINK1 (Weihofen *et al.*, 2009).

This raised the interesting possibility of Miro being a substrate of the PINK1/Parkin pathway, and mitochondrial trafficking being regulated upon damage. In this work the regulation of Miro1 upon mitochondrial depolarisation was studied, and Miro was found to be rapidly and consistently ubiquitinated in a PINK1/Parkin dependent manner. While working on this, a paper from Thomas Schwartz lab was published and showed that Parkin overexpression or mitochondrial damage triggered a drastic loss in Miro1 content (although no ubiquitination was reported) and this loss was associated with mitochondrial arrest. The authors consequently suggested a model whereby mitochondrial damage triggers the rapid degradation of Miro, which results in the uncoupling of the organelles from the cytoskeletal tracks (Wang *et al.*, 2011b). In Chapter 4, combined analysis of Miro1 ubiquitination and degradation dynamics in dopaminergic SH-SY5Y cells, revealed that Miro was rapidly ubiquitinated by Parkin, nevertheless the protein resulted to be stable on the OMM for at least one hour following mitochondrial damage, before being turned over by the proteasome. Hence mitochondrial arrest could be determined by a change in the Miro1 interactome following ubiquitination, rather than its degradation. For example Miro ubiquitination could result in a change in the protein affinity with the mitochondrial trafficking complex, or determine the recruitment of other proteins to promote mitochondrial arrest (see model in Fig. 6.1). The affinity of ubiquitinated Miro1 with the trafficking adaptors TRAK1 and TRAK2 was analysed, and the interaction with TRAK1 resulted unchanged, whereas binding to TRAK2 was increased. Interestingly TRAK2 levels were found to be also increased following FCCP treatment. Since the TRAKs have been previously reported to facilitate the delivery of endosomes to lysosomes (Webber *et al.*, 2008; Kirk *et al.*, 2006), this result hints at the possibility of these proteins having a role in the delivery of damaged mitochondria to the autophagic pathway. Due to their binding to the kinesins, dyneins and Miro, the TRAK adaptors are key components of the mitochondrial transport machinery, however the interaction between Miro itself and the motor proteins should be analysed to investigate the stability of the complex upon mitochondrial damage.

In general mitochondrial stopping can be promoted by uncoupling of the organelles from the microtubules, but could also be favoured by their interaction with docking molecules as discussed in the introduction. No anchor has been reported so far to participate in damage induced mitochondrial arrest, however it would not be surprising if this could partly account for mitochondrial arrest.

Intracellular signalling leading to Miro ubiquitination

In their report Wang and collaborators showed that PINK1 phosphorylates Miro on serine 156 and threonines 298 and 299, making Miro1 a PINK1 substrate. Moreover, phosphorylation of serine 156 in particular, was shown to be required for the protein recognition/degradation by Parkin, suggesting a mechanism whereby PINK1 primes substrates for Parkin to ubiquitinate (Wang *et al.*, 2011b). By utilising phospho-null and phospho-mimic contracts, the role of serine 156 in Miro1 ubiquitination was studied, however no difference in the ubiquitination and loss of Miro was found in this work (Fig. 4.6, Chapter 4), in agreement with another report (Liu *et al.*, 2012). Moreover, since Miro1 phosphorylation could influence its ubiquitination/degradation dynamics, rendering the protein more prone to a rapid turn over, the ubiquitination dynamics of phospho-null Miro1 were assessed, however mutant Miro1 appeared to be ubiquitinated and degraded in a similar way to WT Miro in these experiments (Fig. 4.7, Chapter 4). This could be due to different expression levels of Miro and/or Parkin, or to possible additional regulators which could be cell specific (i.e. phosphatases).

In the last couple of years a huge progress has been made in the understanding of PINK1 and Parkin regulation. Initially, two independent groups demonstrated that Parkin is activated on damaged mitochondria by PINK1, via the phosphorylation of serine 65. Phosphorylation of this residue on Parkin's Ubl domain leads to a switch from an autoinhibited to an active conformation of the ligase (Kondapalli *et al.*, 2012; Shiba-Fukushima *et al.*, 2012). Does Parkin phosphorylation affect the protein recruitment and stabilisation to damaged mitochondria? In Chapter 5 the dynamics of Parkin phospho-null and phospho-mimic mutants translocation on damaged mitochondria were analysed. Interestingly these mutants exhibited a delayed recruitment, with phospho-null Parkin being less recruited than phospho-mimic at earlier time points (Fig. 5.6 and Fig. 5.7, Chapter 5), in HEK 293 cells (similarly in HeLa cells) both mutants were not translocated following 1 hour FCCP. More importantly however, Miro1 was found to promote the recruitment and stabilisation of phospho-null and phospho-mimic Parkin in both cell types. This suggests that the presence of Parkin substrates on the OMM acts as an acceptor complex to stabilise the protein onto damaged mitochondria. Recently Mfn2 was found to act in a similar way, stabilising Parkin on the OMM (Chen and Dorn II, 2013), suggesting the possibility that tuning the levels of Parkin substrates on the OMM could favour the recruitment of Parkin mutants exhibiting a

translocation defect. In Chapter 5 the activity of these mutants was also tested, by analysing their ability to ubiquitinate Miro1 upon mitochondrial damage in both HeLa and dopaminergic SH-SY5Y cells. Phospho-null Parkin leads to substantially reduced Miro ubiquitination which correlates with increased stability of the protein, whereas the phospho-mimic mutant had the opposite effect, apparently increasing Miro turnover under basal conditions. This leads to the interesting idea that phospho-mimic S65E Parkin could reside in the cytoplasm in a partly activated conformation, likely to regulate its substrates at steady-state levels. Although mitochondrial transport was not affected by the expression of WT, phospho-null or phospho-mimic Parkin in primary hippocampal neurons, preliminary results suggest that ubiquitin co-expression with phospho-mimic Parkin could determine a reduction in the number of moving mitochondria, promoting Parkin S65E basal activity (Fig. 5.12, Chapter 5).

Following the finding that established PINK1 as a Parkin kinase, three reports have shown that PINK1 not only phosphorylates Parkin, but it also phosphorylates ubiquitin on the same conserved serine 65. This implies that upon PINK1 accumulation on the OMM, damaged mitochondria become surrounded by phosphorylated ubiquitin, which has been proposed to promote Parkin activity and possibly stabilisation (Kane *et al.*, 2014; Kazlauskaite *et al.*, 2014b; Koyano *et al.*, 2014). This adds a completely new level of complexity to the regulation of the ubiquitination process, hinting at the possibility of further kinases and phosphatases to regulate this post-translational modification. Moreover the control of ubiquitin phosphorylation in response to the activation of different pathways suggests an even more stringent spatial control of the ubiquitination process. In addition, phosphorylation of ubiquitin could either facilitate or block the formation of specific chain-linkages, for example due to the proximity of S65 to K63, K63-type ubiquitin chain formation could be impaired following phosphorylation. In this study the role of phospho-ubiquitin in the potentiation of Parkin ligase activity has been investigated by analysing Miro ubiquitination in the presence of phospho-null and phospho-mimic ubiquitin constructs in dopaminergic SH-SY5Y cells overexpressing Parkin. Unexpectedly, phospho-mimic S65E ubiquitin was not found to be incorporated into Miro1 ubiquitin chains upon mitochondrial damage, whereas phospho-null S65A was incorporated at the same level as WT ubiquitin. This, however, could reflect the fact that S65E might not act as a proper phospho-mimic, or phosphorylated ubiquitin could bind and activate Parkin, but not take part in the chain elongation.

OMM proteins ubiquitination and mitophagy

Parkin-dependent ubiquitination of mitochondrial proteins induces mitophagy by promoting the recruitment of autophagy adaptors, such as p62 and HDAC6. However, in addition to this bulk recruitment of autophagy-related proteins, ubiquitination of distinct proteins can have specific effects in the regulation of the mitophagic cascade. Notably, protein ubiquitination on the mitochondria is not only dependent on Parkin, but also on the counteracting activity of protein deubiquitinases such as USP30, which has been shown to promote the deubiquitination of Miro1 and TOM20, and USP15 (Bingol *et al.*, 2014; Cornelissen *et al.*, 2014). Interestingly, USP30 was reported to counteract Parkin activity, but it was also found to be ubiquitinated and degraded in a Parkin-dependent manner (Bingol *et al.*, 2014). This suggests that when mitochondrial damage is limited, a balance between Parkin-mediated ubiquitination and USP30/15-dependent deubiquitination is in place, however increased stabilisation of Parkin on mitochondria following extensive damage shifts this balance letting the ubiquitination process to prevail.

Fusion and fission machinery

The first and most well characterised proteins reported to be ubiquitinated and degraded by Parkin upon mitochondrial damage were the Mitofusins (Gegg *et al.*, 2010; Poole *et al.*, 2010; Ziviani *et al.*, 2010; Glauser *et al.*, 2011; Rakovic *et al.*, 2011). Prior to Parkin-dependent ubiquitination, Mfn2 was recently found to be phosphorylated by PINK1, which in turn facilitates its interaction with Parkin and the ligase recruitment to impaired mitochondria, ultimately favouring mitophagy (Chen and Dorn II, 2013). Once ubiquitinated, the Mitofusins were shown to be extracted from the mitochondrial membrane by the VCP/p97 retrotranslocase, and to be then degraded by the proteasome (Tanaka *et al.*, 2010). Depletion of Mitofusins from the OMM of depolarised mitochondria, is thought to promote the segregation of these organelles by preventing their fusion with the functional network. Additionally, mitochondrial fragmentation has been shown to be required for the elimination of depolarised mitochondria (Twig *et al.*, 2008). In agreement with this, analysis of the mitochondrial proteome following mitochondrial damage showed a decrease in the OMM fusion machinery and an increase in Drp1, the

major fission protein (Chan *et al.*, 2011). Notably however Drp1 was also found to be a substrate of Parkin (Wang *et al.*, 2011a), so the initial increase in the protein stability might be followed by a Parkin-dependent degradation of the protein.

VDAC1

Another target of the PINK1/Parkin pathway is the voltage-gated anionic channel VDAC1. This protein has been shown to be ubiquitinated in a K27-dependent manner by Parkin, associating for the first time this atypical ubiquitin chain linkage to Parkin-dependent regulation of impaired mitochondria. K27-type VDAC1 ubiquitination was reported to favour the recruitment of p62 onto damaged mitochondria (Geisler *et al.*, 2010), which in turn would promote the translocation of LC3 and the autophagosome formation. However, whether this protein is or is not necessary for the selective clearance of damaged mitochondria is debated (Geisler *et al.*, 2010; Narendra *et al.*, 2010a).

Miro

In this thesis Miro1 was reported to be a substrate of the PINK1/Parkin pathway. To further understand the cellular outcome of Miro1 ubiquitination, in Chapter 4 the ubiquitin chain linkage was investigated. Similar to VDAC1, Miro1 ubiquitination was found to include atypical K27-linked ubiquitin chains (Fig. 4.12, Fig. 4.13 and 4.14, Chapter 4), further supporting the idea of this chain linkage having a role in mitophagy, possibly promoting the recruitment of p62 (Fig. 6.1 B). Moreover, Miro1 ubiquitination did not lead to Miro1 immediate degradation, which is consistent with previous proteomic analysis showing that K27 chains are not significantly enriched when the proteasome is inhibited, in contrast to K48 or K11 chains (Kim *et al.*, 2011). This suggests that the chain type may have other more specific roles, such as mediating mitophagy. In addition, at later stages, Miro was shown to be degraded by the proteasome (Fig. 4.1 and Fig. 4.2, Chapter 4 and Fig. 6.1 C), similar to the Mitofusins (Tanaka *et al.*, 2010). This step however, appeared to be independent of the retrotranslocase VCP (Fig. 4.5). Proteasomal block has been reported to impair mitophagy (Tanaka *et al.*, 2010), suggesting that specific protein degradation mediated by the ubiqutin-proteasome system is required for subsequent mitochondrial clearance.

Whilst working on this project three other papers reported Miro1 to be ubiquitinated in a PINK1/Parkin-dependent manner (Liu *et al.*, 2012; Sarraf *et al.*, 2013; Kazlauskaite *et al.*, 2014a). In particular, Kazlauskaite and colleagues have also investigated Miro1 ubiquitin chain composition and reported that by mass spectrometry of *in vitro* ubiquitination assays they detected K6, K11, K33, K48 and K63 chains linkages associated with Miro1 (Kazlauskaite *et al.*, 2014a). The lack of K27 and K29 linkages in these experiments might be due to the difference between *in vitro* and *in vivo* systems, since mitochondria-associated cofactors or different E2 enzymes could promote specific chain types. Mass spectrometry experiments to detect Parkin-mediated Miro1 ubiquitin chains *in vivo* will be required to complete the characterisation of this post translational modification.

Further dissecting the role of Miro1 in mitophagy Liu and collaborators have analysed the effect of Miro1 and Miro2 knock down in mitophagy. Interestingly the authors found that in HeLa cells depletion of the Miro proteins favoured the perinuclear aggregation of damaged mitochondria and OMM protein degradation, suggesting that the Miro proteins could oppose the early stages of mitophagy, possibly by promoting mitochondria movement towards the periphery. However, by impairing Miro-dependent mitochondrial motility, knock down of the Miro proteins could itself promote a more perinuclear localisation of mitochondria, therefore facilitating mitochondrial aggregation and mitophagy. In addition, in Chapter 5, it was shown that tuning the levels of Miro1 expression could promote the recruitment and stabilisation of Parkin S65A and S65E mutants onto damaged mitochondria (Fig. 5.8 and Fig. 5.10, Chapter 5), suggesting that Miro is part of an acceptor complex for Parkin (similar to Mfn2).

To further address the role of Miro in mitophagy, degradation deficient forms of the protein could be helpful. A few reports have identified specific lysine residues within Miro, K153, K182, K187, K194 and K572 to be targeted by Parkin (Wagner *et al.*, 2011; Sarraf *et al.*, 2013; Kazlauskaite *et al.*, 2014a), with K572 being the more prominent (Kazlauskaite *et al.*, 2014a). Studying mitophagy dynamics in the presence of Miro mutants where these residues have been mutated into arginines, or in cells expressing Miro allR mutant, will shed more light on the role of this protein in mitochondrial clearance, and specifically it may allow the dissection between Miro1 role in mitochondrial trafficking and in mitophagy. More generally, this assay would allow the analysis of the role of mitochondrial trafficking in mitophagy, by determining whether Miro ubiquitination-

dependent mitochondrial stopping is required for mitophagy to occur.

Minimal machinery required for the induction of mitophagy

The identification of each player in the PINK1/Parkin-dependent mitochondrial clearance, as well as the dissection of every step that leads to mitophagy are of crucial importance to target and modulate this process in PD. After the initial reports showing that Parkin-dependent ubiquitination of OMM proteins of damaged mitochondria triggered the recruitment of p62 and induced mitophagy (Geisler *et al.*, 2010; Narendra *et al.*, 2010a), Narendra and colleagues attempted to induce mitophagy by targeting ubiquitin molecules to polarised mitochondria with the FRB/FKBP heterodimerisation system. However, accumulation of ubiquitin on functional organelles did not promote the recruitment of the autophagic machinery and trigger mitophagy, suggesting that protein poly-ubiquitination is probably needed for this process (Narendra *et al.*, 2010a). Subsequently, Tanaka and collaborators targeted Parkin itself with the same FRB/FKBP system to mitochondria, failing again to induce mitophagy. Interestingly however, mitophagy was found to be induced by the FRB/FKBP-mediated accumulation of PINK1 (lacking its MTS domain), that in turn recruits Parkin to ubiquitinate its OMM substrates (Lazarou *et al.*, 2012). This agrees with the recent finding that Parkin is activated by PINK1-dependent S65 phosphorylation (Kondapalli *et al.*, 2012; Shiba-Fukushima *et al.*, 2012). More recently also PINK1-dependent ubiquitin phosphorylation has been shown to promote Parkin activation, in particular phospho-mimic S65D ubiquitin was reported to promote phospho-mimic S65E Parkin self-ubiquitination (Koyano *et al.*, 2014). In Chapter 5 the transport of mitochondria in the presence of S65E Parkin together with WT ubiquitin was shown to be reduced, although preliminary and needing further controls, this experiment suggests that the presence of ubiquitin can boost phospho-mimic Parkin basal activity to regulate mitochondrial trafficking. However, more experiments are needed to assess whether ubiquitin contribution is blocked by phospho-null Parkin expression and whether ubiquitin itself can affect mitochondrial transport. Using the FRB/FKBP system, it would be interesting to target polarised, functional mitochondria with phospho-mimic S65E Parkin, in the presence of S65D ubiquitin to see whether these components of the PINK-Parkin system are sufficient to trigger OMM protein ubiquitination and to therefore induce mitophagy. Moreover, it

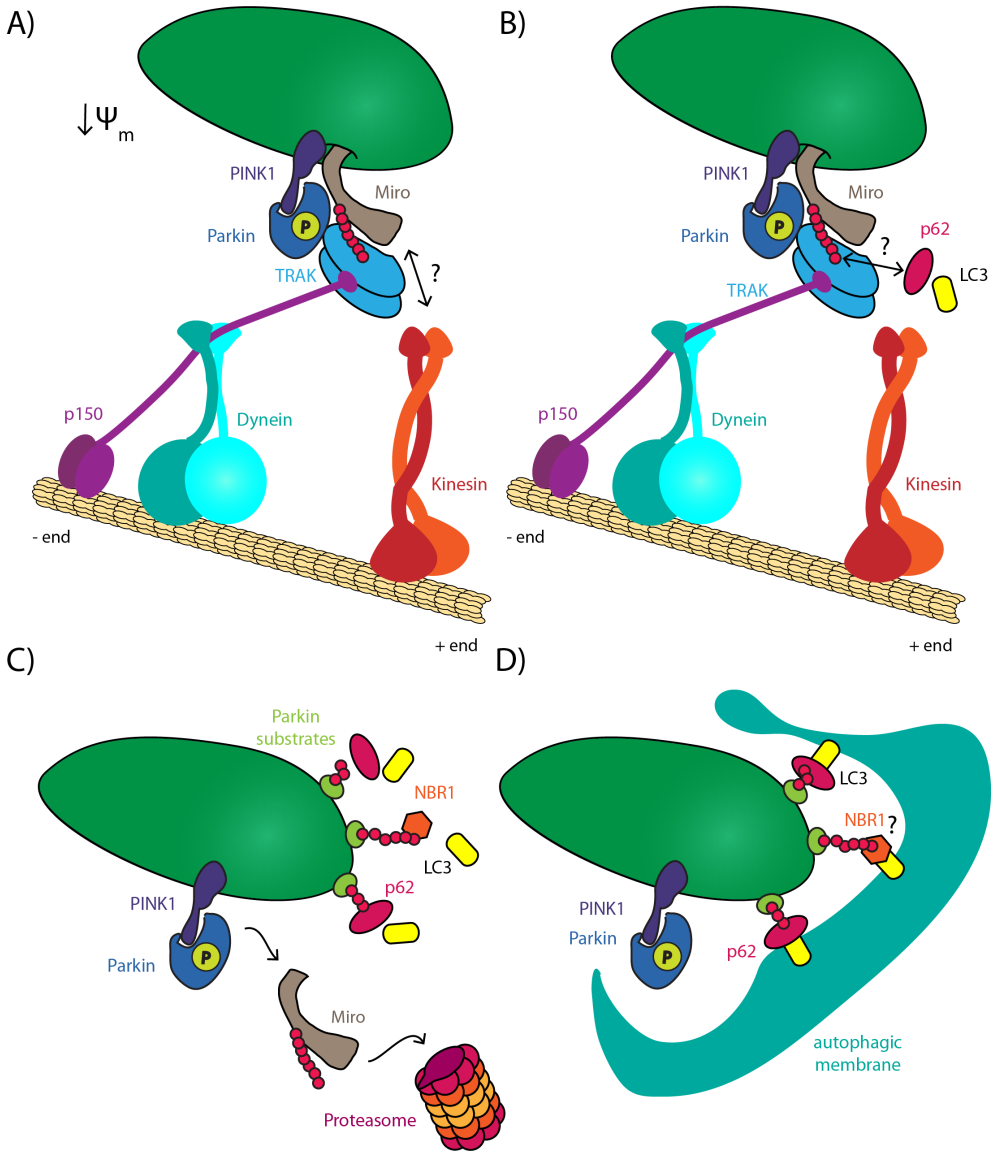

Figure 6.1: Model of damage-dependent Miro1 processing and mitophagy initiation.

(A) Mitochondrial depolarisation triggers PINK1-dependent Parkin translocation onto mitochondria and the formation of a complex with Miro. This leads to the ubiquitination of Miro by Parkin. Although interaction with TRAK2 increases, whether the ubiquitination of Miro influences its interaction with the kinesin motors is still not clear. (B) Ubiquitinated Miro on the OMM can serve as a acceptor of ubiquitin binding proteins involved in the autophagosome formation, such as p62. (C) At later time points Miro is extracted from the OMM and degraded by the proteasome, while other PINK/Parkin substrates, more stable on the OMM, further promote the recruitment of p62 and possibly NBR1 and their interactor LC3. (D) The recruitment of LC3 to damaged mitochondria promotes the formation of the autophagosome, that once mature will fuse with acidified lysosomes to degrade its contents.

would be interesting to reproduce this system in neurons, to investigate how targeting S65E Parkin/S65D ubiquitin influences mitochondrial trafficking.

Different types of mitophagy

Extensive mitochondrial damage promotes the induction of PINK1/Parkin-dependent mitophagy. Increasing evidence however, is showing that limited damage induces a localised activation of the PINK1/Parkin pathway to form small mitochondria-derived vesicles (MDV) that determine the selective degradation of damaged portions of mitochondria (Soubannier *et al.*, 2012; Mclelland *et al.*, 2014). Mitochondrial elimination needs to be coupled to biogenesis in order to support the cell metabolism, however this is likely to be a energetically costly process. It is plausible that MDV-mediated quality control serves as a constant repair mechanism to keep mitochondria functional. Whether the first steps of mitophagy actually comprise the production of MDV to then switch to a more global degradation of the organelle would be interesting to investigate.

FCCP model: advantages and disadvantages

The protonophores FCCP and CCCP, but also other mitochondrial uncouplers such as valinomycin, antimycin A and oligomycin, have been widely used to study mitochondrial damage. These drugs, however, cause an extensive mitochondrial damage that, if on one hand can be helpful for identifying regulators and modifiers of mitophagy, on the other hand they make the investigation of the fine regulation of mitochondrial damage in living cells and neurons challenging. In addition, proton ionophores have been reported to also affect other cellular components such as the microtubule cytoskeleton (Maro *et al.*, 1982), representing a clear caveat in the investigation of mitochondrial trafficking dynamics. More subtle, or locally defined ways of damaging mitochondria will be therefore needed for a finer dissection of this pathway. For example mito-KillerRed is a mitochondrially targeted protein that, when photo-activated, induces local ROS production leading to confined mitochondrial damage (Bulina *et al.*, 2006; Wang *et al.*, 2012). Moreover, mitochondrial damage triggered by more physiological stimuli, such as ischaemia, could be used to investigate mitochondrial dynamics.

Future directions

In the recent years remarkable advances have been made in the elucidation of the pathways underlying mitophagy. However, the signalling mechanisms controlling mitochondrial clearance and the role of mitochondrial trafficking in this process still remain to be fully elucidated. In this thesis, several aspects of PINK1/Parkin-dependent ubiquitination and degradation of the mitochondrial transport protein Miro1 have been analysed.

In Chapter 4 Miro was shown to be rapidly ubiquitinated, however the protein remained stable in its ubiquitinated form on the OMM for some time (at least one hour from the onset of mitochondrial damage) before being turned over by the proteasome. This suggests a signalling role for the protein, however whether ubiquitination of Miro regulates the transport of damaged mitochondria towards the cell soma or participates in the recruitment of the autophagic machinery on the OMM, still requires investigation. Ubiquitination-deficient Miro mutants might be of help to further dissect this pathway by separating the Parkin-dependent regulation of the protein from its trafficking role.

Analysis of the transport machinery composition will also shed light on the damage-dependent regulation of mitochondrial trafficking. Interestingly, increased levels of the TRAK2 adaptor, and of its interaction with Miro were described in Chapter 3. Experiments aimed to further understand the role of this protein in mitophagy might hint at exciting new perspectives on mitochondrial clearance.

According to the latest studies, phosphorylated ubiquitin further activates Parkin on the OMM. It is therefore possible that accumulation of phospho-mimic Parkin on the OMM (via the FRB/FKBP heterodimerisation) in the presence of phospho-mimic ubiquitin is sufficient to trigger OMM protein ubiquitination and the initiation of the mitophagic cascade. In this case, on one hand this system could be used to confirm that activation and localisation of Parkin on the OMM is sufficient to trigger mitophagy, and on the other hand it would allow the investigation of the consequences of OMM protein ubiquitination on mitochondrial trafficking and fission/fusion dynamics.

Mitochondrial uncouplers have been widely used to study mitophagy. These compounds, however, drastically depolarise all the mitochondrial network, challenging the cells to counteract such damage and degrade the organelles, thus resulting deprived of their

major energy source. Under physiological conditions mitophagy is thought to occur more seldomly, targeting few depolarised mitochondria while leaving the functional organelles unaffected. It would be therefore important to investigate mitochondrial dynamics and quality control following a more physiological, or spatially constricted damage in order to confirm and further analyse the mechanisms of mitochondrial clearance.

Most of the studies on mitochondrial quality control and mitophagy have been performed in cell lines and transgenic fibroblasts. However, since deficiencies in these pathways are likely to affect neuronal function and survival (in particular in PD), mitophagy should be examined in neurons, where, due to their extreme structural complexity, quality control mechanisms could be differently regulated or they could exhibit distinct spatial control.

Concluding remarks

To maintain a functional mitochondrial network cells need to identify and clear damaged organelles that cannot sustain the cells metabolism. Mitochondrial quality control systems are in place to recognise, isolate and target for degradation these impaired organelles. These pathways have been found to be affected in neurodegenerative disorders, such as Parkinson's disease, further highlighting their importance.

In this thesis the regulation of the mitochondrial transport protein Miro1 following mitochondrial damage has been investigated. Miro has been shown to be a substrate of the PINK1/Parkin mitochondrial quality control system. Interestingly, Parkin-dependent Miro1 ubiquitination was not found to induce immediate degradation of the protein, suggesting a signalling role for this modification in mitophagy. Moreover, Miro1 was shown to favour the translocation of Parkin phosphorylation mutants on the OMM, providing evidence of a new role for this trafficking protein in mitochondrial quality control.

A clearer understanding of the initiation, progress and regulation of mitophagy in neurons, will allow a better comprehension of how these pathways are affected in neurodegenerative disorders and in particular in Parkinson's disease, hopefully opening new avenues for improved targeting of drug therapies.

Bibliography

Akutsu, M., Ye, Y., Virdee, S., Chin, J. W. and Komander, D. Molecular basis for ubiquitin and ISG15 cross-reactivity in viral ovarian tumor domains. *Proceedings of the National Academy of Sciences of the United States of America* 108:2228–2233 (2011). ISSN 0027-8424.

Alberts, B. *Molecular biology of the cell*. Garland Science, New York, 5th edition (2008). ISBN 9780815341055 (hardcover) 0815341059 (hardcover) 0815341067 (pbk.) 9780815341062 (pbk.).

Allen, G. F. G., Toth, R., James, J. and Ganley, I. G. Loss of iron triggers PINK1/Parkin-independent mitophagy. *EMBO reports* 14(12):1127–35 (2013). ISSN 1469-3178.

Ardley, H. C., Scott, G. B., Rose, S. A., Tan, N. G., Markham, A. F. and Robinson, P. A. Inhibition of proteasomal activity causes inclusion formation in neuronal and non-neuronal cells overexpressing Parkin. *Molecular Biology of the Cell* 14(11):4541–4556 (2003).

Ashrafi, G., Schlehe, J. S., LaVoie, M. J. and Schwarz, T. L. Mitophagy of damaged mitochondria occurs locally in distal neuronal axons and requires PINK1 and Parkin. *The Journal of Cell Biology* (2014). ISSN 0021-9525.

Aslanukov, A., Bhowmick, R., Guruju, M., Oswald, J., Raz, D., Bush, R. a., Sieving, P. a., Lu, X., Bock, C. B. and Ferreira, P. a. RanBP2 modulates Cox11 and hexokinase I activities and haploinsufficiency of RanBP2 causes deficits in glucose metabolism. *PLoS genetics* 2(10):e177 (2006). ISSN 1553-7404.

Bartolome, F., Wu, H. C., Burchell, V. S., Preza, E., Wray, S., Mahoney, C. J., Fox, N. C., Calvo, A., Canosa, A., Moglia, C., Mandrioli, J., Chiò, A., Orrell, R. W., Houlden, H., Hardy, J., Abramov, A. Y. and Plun-Favreau, H. Pathogenic VCP Mutations Induce Mitochondrial Uncoupling and Reduced ATP Levels. *Neuron* 78:57–64 (2013). ISSN 08966273.

Baughman, J. M., Perocchi, F., Girgis, H. S., Plovanich, M., Belcher-Timme, C. a., Sancak, Y., Bao, X. R., Strittmatter, L., Goldberger, O., Bogorad, R. L., Koteliansky, V. and Mootha, V. K. Integrative genomics identifies MCU as an essential component of the mitochondrial calcium uniporter. *Nature* 476(7360):341–5 (2011). ISSN 1476-4687.

Beck, M., Brickley, K., Wilkinson, H. L., Sharma, S., Smith, M., Chazot, P. L., Pollard, S. and Stephenson, F. A. Identification, molecular cloning, and characterization of a novel GABAA receptor-associated protein, GRIF-1. *The Journal of biological chemistry* 277(33):30079–90 (2002). ISSN 0021-9258.

Berger, A. K., Cortese, G. P., Amodeo, K. D., Weihofen, A., Letai, A. and LaVoie, M. J. Parkin selectively alters the intrinsic threshold for mitochondrial cytochrome c release. *Human molecular genetics* 18(22):4317–28 (2009). ISSN 1460-2083.

Bernardi, P. Mitochondrial transport of cations: channels, exchangers, and permeability transition. *Physiological reviews* 79(4):1127–1155 (1999). ISSN 0031-9333.

Berridge, M. J., Lipp, P. and Bootman, M. D. The versatility and universality of calcium signalling. *Nature Reviews Molecular Cell Biology* 1(October):11–21 (2000).

Bingol, B., Tea, J. S., Phu, L., Reichelt, M., Bakalarski, C. E., Song, Q., Foreman, O., Kirkpatrick, D. S. and Sheng, M. The mitochondrial deubiquitinase USP30 opposes parkin-mediated mitophagy. *Nature* (2014). ISSN 0028-0836.

Blasius, T. L., Cai, D., Jih, G. T., Toret, C. P. and Verhey, K. J. Two binding partners cooperate to activate the molecular motor Kinesin-1. *The Journal of cell biology* 176(1):11–7 (2007). ISSN 0021-9525.

Brickley, K., Pozo, K. and Stephenson, F. A. N-acetylglucosamine transferase is an integral component of a kinesin-directed mitochondrial trafficking complex. *Biochimica et biophysica acta* 1813(1):269–281 (2011). ISSN 0006-3002.

Brickley, K., Smith, M. J., Beck, M. and Stephenson, F. A. GRIF-1 and OIP106, members of a novel gene family of coiled-coil domain proteins: association in vivo and in vitro with kinesin. *The Journal of biological chemistry* 280(15):14723–14732 (2005). ISSN 0021-9258.

Brickley, K. and Stephenson, F. A. Trafficking kinesin protein (TRAK)-mediated transport of mitochondria in axons of hippocampal neurons. *The Journal of biological chemistry* 286(20):18079–92 (2011). ISSN 1083-351X.

Bulina, M. E., Chudakov, D. M., Britanova, O. V., Yanushevich, Y. G., Staroverov, D. B., Chepurnykh, T. V., Merzlyak, E. M., Shkrob, M. A., Lukyanov, S. and Lukyanov, K. A. A genetically encoded photosensitizer. *Nature biotechnology* 24:95–99 (2006). ISSN 1087-0156.

Cai, Q., Gerwin, C. and Sheng, Z.-H. Syntabulin-mediated anterograde transport of mitochondria along neuronal processes. *The Journal of cell biology* 170(6):959–969 (2005). ISSN 0021-9525.

Cai, Q., Zakaria, H. M., Simone, A. and Sheng, Z. H. Spatial parkin translocation and degradation of damaged mitochondria via mitophagy in live cortical neurons. *Current Biology* 22(6):545–552 (2012).

Campanella, M., Casswell, E., Chong, S., Farah, Z., Wieckowski, M. R., Abramov, A. Y., Tinker, A. and Duchen, M. R. Regulation of mitochondrial structure and function by the F1Fo-ATPase inhibitor protein, IF1. *Cell metabolism* 8(1):13–25 (2008). ISSN 1932-7420.

Carter, S., Bischof, O., Dejean, A. and Vousden, K. H. C-terminal modifications regulate MDM2 dissociation and nuclear export of p53. *Nature cell biology* 9(4):428–35 (2007). ISSN 1465-7392.

Chada, S. R. and Hollenbeck, P. J. Nerve Growth Factor Signaling Regulates Motility and Docking of Axonal Mitochondria. *Current Biology* 14:1272–1276 (2004).

Chan, N. C., Salazar, A. M., Pham, A. H., Sweredoski, M. J., Kolawa, N. J., Graham, R. L. J., Hess, S. and Chan, D. C. Broad activation of the ubiquitin-proteasome system by Parkin is critical for mitophagy. *Human molecular genetics* 20(9):1726–1737 (2011). ISSN 1460-2083.

Chaugule, V. K., Burchell, L., Barber, K. R., Sidhu, A., Leslie, S. J., Shaw, G. S. and Walden, H. Autoregulation of Parkin activity through its ubiquitin-like domain. *EMBO Journal* 30(14):2853–2867 (2011).

Chen, H. and Chan, D. C. Mitochondrial dynamics-fusion, fission, movement, and mitophagy-in neurodegenerative diseases. *Human molecular genetics* 18(R2):R169–76 (2009). ISSN 1460-2083.

Chen, H., Chomyn, A. and Chan, D. C. Disruption of fusion results in mitochondrial heterogeneity and dysfunction. *The Journal of biological chemistry* 280(28):26185–92 (2005). ISSN 0021-9258.

Chen, H., Vermulst, M., Wang, Y. E., Chomyn, A., Prolla, T. a., McCaffery, J. M. and Chan, D. C. Mitochondrial fusion is required for mtDNA stability in skeletal muscle and tolerance of mtDNA mutations. *Cell* 141(2):280–9 (2010). ISSN 1097-4172.

Chen, Y. and Dorn II, G. W. PINK1-phosphorylated mitofusin 2 is a Parkin receptor for culling damaged mitochondria. *Science* 340(6131):471–475 (2013).

Chen, Y. and Sheng, Z.-H. Kinesin-1-syntaphilin coupling mediates activity-dependent regulation of axonal mitochondrial transport. *The Journal of cell biology* 202:351–64 (2013). ISSN 1540-8140.

Chen, Y.-M., Gerwin, C. and Sheng, Z.-H. Dynein light chain LC8 regulates syntaphilin-mediated mitochondrial docking in axons. *The Journal of neuroscience* 29:9429–9438 (2009). ISSN 0270-6474.

Chen, Z. J. and Sun, L. J. Nonproteolytic functions of ubiquitin in cell signaling. *Molecular cell* 33(3):275–286 (2009). ISSN 1097-4164.

Cho, D.-H., Nakamura, T., Fang, J., Cieplak, P., Godzik, A., Gu, Z. and Lipton, S. a. S-nitrosylation of Drp1 mediates beta-amyloid-related mitochondrial fission and neuronal injury. *Science* 324(5923):102–105 (2009). ISSN 1095-9203.

Cho, K.-i., Cai, Y., Yi, H., Yeh, A., Aslanukov, A. and Ferreira, P. a. Association of the kinesin-binding domain of RanBP2 to KIF5B and KIF5C determines mitochondria localization and function. *Traffic* 8(12):1722–1735 (2007). ISSN 1398-9219.

Choubey, V., Cagalinec, M., Liiv, J., Safiulina, D., Hickey, M. a., Kuum, M., Liiv, M., Anwar, T., Eskelinen, E.-L. and Kaasik, A. BECN1 is involved in the initiation of mitophagy: it facilitates PARK2 translocation to mitochondria. *Autophagy* 10(6):1105–1119 (2014). ISSN 1554-8635.

Clark, I. E., Dodson, M. W., Jiang, C., Cao, J. H., Huh, J. R., Seol, J. H., Yoo, S. J., Hay, B. a. and Guo, M. Drosophila pink1 is required for mitochondrial function and interacts genetically with parkin. *Nature* 441(7097):1162–6 (2006). ISSN 1476-4687.

Cornelissen, T., Haddad, D., Wauters, F., Van Humbeeck, C., Mandemakers, W., Koentjoro, B., Sue, C., Gevaert, K., De Strooper, B., Verstreken, P. and Vandenberghe, W. The deubiquitinase USP15 antagonizes Parkin-mediated mitochondrial ubiquitination and mitophagy. *Human molecular genetics* pages 1–16 (2014). ISSN 1460-2083.

Corti, O., Lesage, S. and Brice, A. What genetics tells us about the causes and mechanisms of Parkinson's disease. *Physiological reviews* 91(4):1161–218 (2011). ISSN 1522-1210.

Dagda, R. K., Pien, I., Wang, R., Zhu, J., Wang, K. Z. Q., Callio, J., Banerjee, T. D., Dagda, R. Y. and Chu, C. T. Beyond the mitochondrion: Cytosolic PINK1 remodels dendrites through Protein Kinase A. *Journal of Neurochemistry* 128:864–877 (2014). ISSN 14714159.

de Brito, O. M. and Scorrano, L. Mitofusin 2 tethers endoplasmic reticulum to mitochondria. *Nature* 456(7222):605–610 (2008). ISSN 1476-4687.

De Stefani, D., Raffaello, A., Teardo, E., Szabò, I. and Rizzuto, R. A forty-kilodalton protein of the inner membrane is the mitochondrial calcium uniporter. *Nature* 476(7360):336–40 (2011). ISSN 1476-4687.

De Stefani, D. and Rizzuto, R. Molecular control of mitochondrial calcium uptake. *Biochemical and Biophysical Research Communications* 449(4):373–376 (2014). ISSN 0006291X.

Deas, E., Plun-Favreau, H., Gandhi, S., Desmond, H., Kjaer, S., Loh, S. H., Renton, A. E., Harvey, R. J., Whitworth, A. J., Martins, L. M., Abramov, A. Y. and Wood, N. W. PINK1 cleavage at position A103 by the mitochondrial protease PARL. *Human molecular genetics* 20(5):867–879 (2011).

Deas, E., Plun-Favreau, H. and Wood, N. W. PINK1 function in health and disease. *EMBO molecular medicine* 1(3):152–165 (2009). ISSN 1757-4684.

DeLuca, H. F. and Engstrom, G. Calcium Uptake By Rat Kidney Mitochondria. *Proceedings of the National Academy of Sciences of the United States of America* pages 1744–1750 (1961).

Deng, H., Dodson, M. W., Huang, H. and Guo, M. The Parkinson's disease genes pink1 and parkin promote mitochondrial fission and/or inhibit fusion in Drosophila. *Proceedings of the National Academy of Sciences of the United States of America* 105(38):14503–8 (2008). ISSN 1091-6490.

Denison, S. R., Wang, F., Becker, N. A., Schüle, B., Kock, N., Phillips, L. A., Klein, C., Smith, D. I. and Schule, B. Alterations in the common fragile site gene Parkin in ovarian and other cancers. *Oncogene* 22(51):8370–8 (2003). ISSN 0950-9232.

Detmer, S. a. and Chan, D. C. Functions and dysfunctions of mitochondrial dynamics. *Nature reviews. Molecular cell biology* 8(11):870–9 (2007). ISSN 1471-0080.

Dice, J. F. Peptide sequences that target cytosolic proteins for lysosomal proteolysis. *Trends in biochemical sciences* 15:305–309 (1990). ISSN 09680004.

Duchen, M. R., Leyssens, a. and Crompton, M. Transient mitochondrial depolarizations reflect focal sarcoplasmic reticular calcium release in single rat cardiomyocytes. *The Journal of cell biology* 142(4):975–88 (1998). ISSN 0021-9525.

Exner, N., Lutz, A. K., Haass, C. and Winklhofer, K. F. Mitochondrial dysfunction in Parkinson's disease: molecular mechanisms and pathophysiological consequences. *The EMBO journal* 31(14):3038–3062 (2012). ISSN 1460-2075.

Fedorowicz, M. A., De Vries-Schneider, R. L. A., Ru'b, C., Becker, D., Huang, Y., Zhou, C., Wolken, D. M. A., Voos, W., Liu, Y. and Przedborski, S. Cytosolic cleaved PINK1 represses Parkin translocation to mitochondria and mitophagy. *EMBO Reports* 15(1):86–93 (2014).

Fransson, A., Ruusala, A., Aspenström, P. and Aspenstrom, P. Atypical Rho GTPases have roles in mitochondrial homeostasis and apoptosis. *The Journal of biological chemistry* 278(8):6495–6502 (2003). ISSN 0021-9258.

Fransson, S., Ruusala, A., Aspenström, P., Fransson, A. and Aspenstrom, P. The atypical Rho GTPases Miro-1 and Miro-2 have essential roles in mitochondrial trafficking. *Biochemical and biophysical research communications* 344(2):500–10 (2006). ISSN 0006-291X.

Friedman, J. R., Lackner, L. L., West, M., DiBenedetto, J. R., Nunnari, J. and Voeltz, G. K. ER Tubules Mark Sites of Mitochondrial Division. *Science* 334:358–362 (2011). ISSN 0036-8075.

Fu, M., St-Pierre, P., Shankar, J., Wang, P. T. C., Joshi, B. and Nabi, I. R. Regulation of mitophagy by the Gp78 E3 ubiquitin ligase. *Molecular biology of the cell* 24(8):1153–1162 (2013). ISSN 1939-4586.

Fujita, T., Maturana, A. D., Ikuta, J., Hamada, J., Walchli, S., Suzuki, T., Sawa, H., Wooten, M. W., Okajima, T., Tatematsu, K., Tanizawa, K. and Kuroda, S. Axonal guidance protein FEZ1 associates with tubulin and kinesin motor protein to transport mitochondria in neurites of NGF-stimulated PC12 cells. *Biochemical and biophysical research communications* 361(3):605–610 (2007). ISSN 0006-291X.

Gandhi, S., Wood-Kaczmar, A., Yao, Z., Plun-Favreau, H., Deas, E., Klupsch, K., Downward, J., Latchman, D. S., Tabrizi, S. J., Wood, N. W., Duchen, M. R. and Abramov, A. Y. PINK1-associated Parkinson's disease is caused by neuronal vulnerability to calcium-induced cell death. *Molecular Cell* 33(5):627–638 (2009). ISSN 1097-4164.

Gegg, M. E., Cooper, J. M., Chau, K. Y., Rojo, M., Schapira, A. H. and Taanman, J. W. Mitofusin 1 and mitofusin 2 are ubiquitinated in a PINK1/parkin-dependent manner upon induction of mitophagy. *Human molecular genetics* 19(24):4861–4870 (2010).

Geisler, S., Holmström, K. M., Skujat, D., Fiesel, F. C., Rothfuss, O. C., Kahle, P. J. and Springer, W. PINK1/Parkin-mediated mitophagy is dependent on VDAC1 and p62/SQSTM1. *Nature cell biology* 12(2):119–31 (2010). ISSN 1476-4679.

Glater, E. E., Megeath, L. J., Stowers, R. S. and Schwarz, T. L. Axonal transport of mitochondria requires milton to recruit kinesin heavy chain and is light chain independent. *The Journal of cell biology* 173(4):545–57 (2006). ISSN 0021-9525.

Glauser, L., Sonnay, S., Stafa, K. and Moore, D. J. Parkin promotes the ubiquitination and degradation of the mitochondrial fusion factor mitofusin 1. *Journal of neurochemistry* 118(4):636–45 (2011). ISSN 1471-4159.

Gomes, L. C., Di Benedetto, G. and Scorrano, L. During autophagy mitochondria elongate, are spared from degradation and sustain cell viability. *Nature cell biology* 13:589–598 (2011). ISSN 1465-7392.

Graham, F. L. and Van Der Eb, A. A New Technique for the Assay Adenovirus of Infectivity of Human Adenovirus 5 DNA. *Virology* 467:456–467 (1973).

Greene, A. W., Grenier, K., Aguileta, M. a., Muise, S., Farazifard, R., Haque, M. E., McBride, H. M., Park, D. S. and Fon, E. a. Mitochondrial processing peptidase regulates PINK1 processing, import and Parkin recruitment. *EMBO reports* 13(4):378–85 (2012). ISSN 1469-3178.

Greene, J. C., Whitworth, A. J., Kuo, I., Andrews, L. a., Feany, M. B. and Pallanck, L. J. Mitochondrial pathology and apoptotic muscle degeneration in Drosophila parkin mutants. *Proceedings of the National Academy of Sciences of the United States of America* 100(7):4078–83 (2003). ISSN 0027-8424.

Grishin, A., Li, H., Levitan, E. S. and Zaks-Makhina, E. Identification of gamma-aminobutyric acid receptor-interacting factor 1 (TRAK2) as a trafficking factor for the K+ channel Kir2.1. *The Journal of biological chemistry* 281:30104–30111 (2006). ISSN 0021-9258.

Guo, X., Macleod, G. T., Wellington, A., Hu, F., Panchumarthi, S., Schoenfield, M., Marin, L., Charlton, M. P., Atwood, H. L. and Zinsmaier, K. E. The GTPase dMiro is required for axonal transport of mitochondria to Drosophila synapses. *Neuron* 47(3):379–393 (2005). ISSN 0896-6273.

Guzman, J. N., Sanchez-Padilla, J., Wokosin, D., Kondapalli, J., Ilijic, E., Schumacker, P. T. and Surmeier, D. J. Oxidant stress evoked by pacemaking in dopaminergic neurons is attenuated by DJ-1. *Nature* 468(7324):696–700 (2010). ISSN 1476-4687.

Haglund, K., Di Fiore, P. P. and Dikic, I. Distinct monoubiquitin signals in receptor endocytosis. *Trends in biochemical sciences* 28(11):598–603 (2003a). ISSN 0968-0004.

Haglund, K., Sigismund, S., Polo, S., Szymkiewicz, I., Di Fiore, P. P. and Dikic, I. Multiple monoubiquitination of RTKs is sufficient for their endocytosis and degradation. *Nature cell biology* 5:461–466 (2003b). ISSN 1465-7392.

Han, X.-J., Lu, Y.-F., Li, S.-A., Kaitsuka, T., Sato, Y., Tomizawa, K., Nairn, A. C., Takei, K., Matsui, H. and Matsushita, M. CaM kinase I alpha-induced phosphorylation of Drp1 regulates mitochondrial morphology. *The Journal of cell biology* 182(3):573–585 (2008). ISSN 1540-8140.

Harder, Z., Zunino, R. and McBride, H. Sumo1 conjugates mitochondrial substrates and participates in mitochondrial fission. *Current biology : CB* 14(4):340–5 (2004). ISSN 0960-9822.

Hasson, S. a., Kane, L. a., Yamano, K., Huang, C.-H., Sliter, D. a., Buehler, E., Wang, C., Heman-Ackah, S. M., Hessa, T., Guha, R., Martin, S. E. and Youle, R. J. High-content genome-wide RNAi screens identify regulators of parkin upstream of mitophagy. *Nature* 504(7479):291–5 (2013). ISSN 1476-4687.

Helton, T. D., Otsuka, T., Lee, M.-C., Mu, Y. and Ehlers, M. D. Pruning and loss of excitatory synapses by the parkin ubiquitin ligase. *Proceedings of the National Academy of Sciences of the United States of America* 105(49):19492–19497 (2008). ISSN 1091-6490.

Hirokawa, N., Noda, Y., Tanaka, Y. and Niwa, S. Kinesin superfamily motor proteins and intracellular transport. *Nature reviews. Molecular cell biology* 10(10):682–96 (2009). ISSN 1471-0080.

Hirokawa, N., Sato-Yoshitake, R., Yoshida, T. and Kawashima, T. Brain dynein (MAP1C) localizes on both anterogradely and retrogradely transported membranous organelles in vivo. *The Journal of cell biology* 111(3):1027–1037 (1990). ISSN 0021-9525.

Hoege, C., Pfander, B., Moldovan, G.-L., Pyrowolakis, G. and Jentsch, S. RAD6-dependent DNA repair is linked to modification of PCNA by ubiquitin and SUMO. *Nature* 419:135–141 (2002). ISSN 0028-0836.

Hollenbeck, P. J. and Saxton, W. M. The axonal transport of mitochondria. *Journal of cell science* 118(23):5411–5419 (2005). ISSN 0021-9533.

Hollville, E., Carroll, R. G., Cullen, S. P. and Martin, S. J. Bcl-2 Family Proteins Participate in Mitochondrial Quality Control by Regulating Parkin/PINK1-Dependent Mitophagy. *Molecular Cell* (2014). ISSN 10972765.

Horiuchi, D., Barkus, R. V., Pilling, A. D., Gassman, A. and Saxton, W. M. APLIP1, a kinesin binding JIP-1/JNK scaffold protein, influences the axonal transport of both vesicles and mitochondria in Drosophila. *Current biology : CB* 15(23):2137–41 (2005). ISSN 0960-9822.

Horiuchi, D., Collins, C. a., Bhat, P., Barkus, R. V., Diantonio, A. and Saxton, W. M. Control of a kinesin-cargo linkage mechanism by JNK pathway kinases. *Current biology : CB* 17(15):1313–7 (2007). ISSN 0960-9822.

Iguchi, M., Kujuro, Y., Okatsu, K., Koyano, F., Kosako, H., Kimura, M., Suzuki, N., Uchiyama, S., Tanaka, K. and Matsuda, N. Parkin-catalyzed ubiquitin-ester transfer is triggered by PINK1-dependent phosphorylation. *The Journal of biological chemistry* 288(30):22019–22032 (2013). ISSN 1083-351X.

Ikuta, J., Maturana, A., Fujita, T., Okajima, T., Tatematsu, K., Tanizawa, K. and Kuroda, S. Fasciculation and elongation protein zeta-1 (FEZ1) participates in the polarization of hippocampal neuron by controlling the mitochondrial motility. *Biochemical and biophysical research communications* 353(1):127–132 (2007). ISSN 0006-291X.

Inoue, H., Nojima, H. and 0kayama, H. High efficiency transformation of Escherichia coli with plasmids. *Gene* 96:23–28 (1990).

Iyer, S. P. N., Akimoto, Y. and Hart, G. W. Identification and cloning of a novel family of coiled-coil domain proteins that interact with O-GlcNAc transferase. *The Journal of biological chemistry* 278(7):5399–409 (2003). ISSN 0021-9258.

Jin, S. M., Lazarou, M., Wang, C., Kane, L. A., Narendra, D. P. and Youle, R. J. Mitochondrial membrane potential regulates PINK1 import and proteolytic destabilization by PARL. *Journal of Cell Biology* 191(5):933–942 (2010). ISSN 1540-8140.

Jin, S. M. and Youle, R. J. The accumulation of misfolded proteins in the mitochondrial matrix is sensed by PINK1 to induce PARK2/Parkin-mediated mitophagy of polarized mitochondria. *Autophagy* 9:1750–7 (2013). ISSN 1554-8635.

Johnson, B. N., Berger, A. K., Cortese, G. P. and Lavoie, M. J. The ubiquitin E3 ligase parkin regulates the proapoptotic function of Bax. *Proceedings of the National Academy of Sciences of the United States of America* 109(16):6283–8 (2012). ISSN 1091-6490.

Kane, L. a., Lazarou, M., Fogel, A. I., Li, Y., Yamano, K., Sarraf, S. a., Banerjee, S. and Youle, R. J. PINK1 phosphorylates ubiquitin to activate Parkin E3 ubiquitin ligase activity. *Journal of Cell Biology* 205(2):143–53 (2014). ISSN 1540-8140.

Kang, J. S., Tian, J. H., Pan, P. Y., Zald, P., Li, C., Deng, C. and Sheng, Z. H. Docking of Axonal Mitochondria by Syntaphilin Controls Their Mobility and Affects Short-Term Facilitation. *Cell* 132:137–148 (2008). ISSN 00928674.

Karbowski, M., Jeong, S.-Y. and Youle, R. J. Endophilin B1 is required for the maintenance of mitochondrial morphology. *Journal of Cell Biology* 166:1027–1039 (2004). ISSN 0021-9525.

Kawaguchi, Y., Kovacs, J. J., McLaurin, A., Vance, J. M., Ito, A. and Yao, T. P. The deacetylase HDAC6 regulates aggresome formation and cell viability in response to misfolded protein stress. *Cell* 115(6):727–38 (2003). ISSN 0092-8674.

Kazlauskaite, A., Kelly, V., Johnson, C., Baillie, C., Hastie, C. J., Peggie, M., Macartney, T., Woodroof, H. I., Alessi, D. R., Pedrioli, P. G. a. and Muqit, M. M. K. Phosphorylation of Parkin at Serine65 is essential for activation: elaboration of a Miro1 substrate-based assay of Parkin E3 ligase activity. *Open biology* 4:130213 (2014a). ISSN 2046-2441.

Kazlauskaite, A., Kondapalli, C., Gourlay, R., Campbell, D. G., Ritorto, M. S., Hofmann, K., Alessi, D. R., Knebel, A., Trost, M. and Muqit, M. M. K. Parkin is activated by PINK1-dependent phosphorylation of ubiquitin at Ser65. *The Biochemical journal* 460(1):127–39 (2014b). ISSN 1470-8728.

Keusekotten, K., Elliott, P. R., Glockner, L., Fiil, B. K., Damgaard, R. B., Kulathu, Y., Wauer, T., Hospenthal, M. K., Gyrd-Hansen, M., Krappmann, D., Hofmann, K. and Komander, D. OTULIN antagonizes LUBAC signaling by specifically hydrolyzing Met1-linked polyubiquitin. *Cell* 153(6):1312–1326 (2013).

Kim, I., Rodriguez-Enriquez, S. and Lemasters, J. J. Selective degradation of mitochondria by mitophagy. *Archives of biochemistry and biophysics* 462(2):245–253 (2007). ISSN 0003-9861.

Kim, W., Bennett, E. J., Huttlin, E. L., Guo, A., Li, J., Possemato, A., Sowa, M. E., Rad, R., Rush, J., Comb, M. J., Harper, J. W. and Gygi, S. P. Systematic and quantitative assessment of the ubiquitin-modified proteome. *Molecular Cell* 44(2):325–340 (2011).

Kirk, E., Chin, L.-S. and Li, L. GRIF1 binds Hrs and is a new regulator of endosomal trafficking. *Journal of cell science* 119(Pt 22):4689–701 (2006). ISSN 0021-9533.

Kirkin, V., Lamark, T., Sou, Y.-S., Bjø rkøy, G., Nunn, J. L., Bruun, J.-A., Shvets, E., McEwan, D. G., Clausen, T. H., Wild, P., Bilusic, I., Theurillat, J.-P., Ø vervatn, A., Ishii, T., Elazar, Z., Komatsu, M., Dikic, I. and Johansen, T. A role for NBR1 in autophagosomal degradation of ubiquitinated substrates. *Molecular cell* 33(4):505–516 (2009). ISSN 1097-4164.

Kitada, T., Asakawa, S., Hattori, N., Matsumine, H., Yamamura, Y., Minoshima, S., Yokochi, M., Mizuno, Y. and Shimizu, N. Mutations in the parkin gene cause autosomal recessive juvenile parkinsonism. *Letters to Nature* 169(1993):166–169 (1998).

Komander, D. and Rape, M. The ubiquitin code. *Annu Rev Biochem* 81:203–229 (2012).

Kondapalli, C., Kazlauskaite, A., Zhang, N., Woodroof, H. I., Campbell, D. G., Gourlay, R., Burchell, L., Walden, H., Macartney, T. J., Deak, M., Knebel, A., Alessi, D. R. and Muqit, M. M. K. PINK1 is activated by mitochondrial membrane potential depolarization and stimulates Parkin E3 ligase activity by phosphorylating Serine 65. *Open Biology* 2(5):120080 (2012). ISSN 2046-2441.

Kotiadis, V. N., Duchen, M. R. and Osellame, L. D. Mitochondrial quality control and communications with the nucleus are important in maintaining mitochondrial function and cell health. *Biochimica et biophysica acta* 1840(4):1254–1265 (2014). ISSN 0006-3002.

Koyano, F., Okatsu, K., Kosako, H., Tamura, Y., Go, E., Kimura, M., Kimura, Y., Tsuchiya, H., Yoshihara, H., Hirokawa, T., Endo, T., Fon, E. a., Trempe, J.-F., Saeki, Y., Tanaka, K. and Matsuda, N. Ubiquitin is phosphorylated by PINK1 to activate parkin. *Nature* (2014). ISSN 0028-0836.

Kulathu, Y. and Komander, D. Atypical ubiquitylation - the unexplored world of polyubiquitin beyond Lys48 and Lys63 linkages. *Nature Reviews Molecular Cell Biology* 13(8):508–523 (2012). ISSN 1471-0072.

Langston, J. W., Irwin, I., Langston, E. B. and Forno, L. S. 1-Methyl-4-phenylpyridinium ion (MPP+): identification of a metabolite of MPTP, a toxin selective to the substantia nigra. *Neuroscience letters* 48:87–92 (1984). ISSN 03043940.

Lazarou, M., Jin, S. M., Kane, L. a. and Youle, R. J. Role of PINK1 binding to the TOM complex and alternate intracellular membranes in recruitment and activation of the E3 ligase Parkin. *Developmental cell* 22(2):320–333 (2012). ISSN 1878-1551.

Lazarou, M., Narendra, D. P., Jin, S. M., Tekle, E., Banerjee, S. and Youle, R. J. PINK1 drives Parkin self-association and HECT-like E3 activity upstream of mitochondrial binding. *The Journal of cell biology* 200(2):163–72 (2013). ISSN 1540-8140.

Lee, J.-Y., Koga, H., Kawaguchi, Y., Tang, W., Wong, E., Gao, Y.-S., Pandey, U. B., Kaushik, S., Tresse, E., Lu, J., Taylor, J. P., Cuervo, A. M. and Yao, T.-P. HDAC6 controls autophagosome maturation essential for ubiquitin-selective quality-control autophagy. *The EMBO journal* 29(5):969–80 (2010). ISSN 1460-2075.

Lefebvre, V., Du, Q., Baird, S., Ng, A. C.-H., Nascimento, M., Campanella, M., McBride, H. M. and Screaton, R. a. Genome-wide RNAi screen identifies ATPase inhibitory factor 1 (ATPIF1) as essential for PARK2 recruitment and mitophagy. *Autophagy* 9:1770–9 (2013). ISSN 1554-8635.

Lewis, M. and Lewis, W. Mitochondria in Tissue Culture Author. *Science* 39(1000):330–333 (1914).

Lewit-Bentley, A. and Réty, S. EF-hand calcium-binding proteins. *Current opinion in structural biology* pages 637–643 (2000).

Li, W., Bengtson, M. H., Ulbrich, A., Matsuda, A., Reddy, V. a., Orth, A., Chanda, S. K., Batalov, S. and Joazeiro, C. a. P. Genome-wide and functional annotation of human E3 ubiquitin ligases identifies MULAN, a mitochondrial E3 that regulates the organelle's dynamics and signaling. *PloS one* 3(1):e1487 (2008). ISSN 1932-6203.

Lim, K. L., Chew, K. C., Tan, J. M., Wang, C., Chung, K. K., Zhang, Y., Tanaka, Y., Smith, W., Engelender, S., Ross, C. A., Dawson, V. L. and Dawson, T. M. Parkin me-

diates nonclassical, proteasomal-independent ubiquitination of synphilin-1: implications for Lewy body formation. *The Journal of Neuroscience* 25(8):2002–2009 (2005).

Lin, W. and Kang, U. J. Characterization of PINK1 processing, stability, and subcellular localization. *Journal of Neurochemistry* 106(1):464–474 (2008). ISSN 00223042.

Liu, S., Sawada, T., Lee, S., Yu, W., Silverio, G., Alapatt, P., Millan, I., Shen, A., Saxton, W., Kanao, T., Takahashi, R., Hattori, N., Imai, Y. and Lu, B. Parkinson's disease-associated kinase PINK1 regulates Miro protein level and axonal transport of mitochondria. *PLoS genetics* 8(3):e1002537 (2012). ISSN 1553-7404.

Livingston, C. M., Ifrim, M. F., Cowan, A. E. and Weller, S. K. Virus-Induced Chaperone-Enriched (VICE) domains function as nuclear protein quality control centers during HSV-1 infection. *PLoS pathogens* 5:e1000619 (2009). ISSN 1553-7374.

López-Doménech, G., Serrat, R., Mirra, S., D'Aniello, S., Somorjai, I., Abad, A., Vitureira, N., García-Arumí, E., Alonso, M. T., Rodriguez-Prados, M., Burgaya, F., Andreu, A. L., García-Sancho, J., Trullas, R., Garcia-Fernàndez, J. and Soriano, E. The Eutherian Armcx genes regulate mitochondrial trafficking in neurons and interact with Miro and Trak2. *Nature communications* 3(May):814 (2012). ISSN 2041-1723.

Lorick, K. L., Jensen, J. P., Fang, S., Ong, a. M., Hatakeyama, S. and Weissman, a. M. RING fingers mediate ubiquitin-conjugating enzyme (E2)-dependent ubiquitination. *Proceedings of the National Academy of Sciences of the United States of America* 96(20):11364–11369 (1999). ISSN 0027-8424.

Mabb, A. M., Je, H. S., Wall, M. J., Robinson, C. G., Larsen, R. S., Qiang, Y., Corrêa, S. a. L. and Ehlers, M. D. Triad3A Regulates Synaptic Strength by Ubiquitination of Arc. *Neuron* 82(6):1299–316 (2014). ISSN 1097-4199.

MacAskill, A. F., Brickley, K., Stephenson, F. A. and Kittler, J. T. GTPase dependent recruitment of Grif-1 by Miro1 regulates mitochondrial trafficking in hippocampal neurons. *Molecular and cellular neurosciences* 40(3):301–312 (2009a). ISSN 1095-9327.

MacAskill, A. F. and Kittler, J. T. Control of mitochondrial transport and localization in neurons. *Trends in cell biology* 20(2):102–112 (2010). ISSN 1879-3088.

MacAskill, A. F., Rinholm, J. E., Twelvetrees, A. E., Arancibia-Carcamo, I. L., Muir, J., Fransson, A., Aspenstrom, P., Attwell, D. and Kittler, J. T. Miro1 is a calcium sensor for glutamate receptor-dependent localization of mitochondria at synapses. *Neuron* 61(4):541–555 (2009b).

Maday, S., Wallace, K. E. and Holzbaur, E. L. F. Autophagosomes initiate distally and mature during transport toward the cell soma in primary neurons. *The Journal of cell biology* 196(4):407–417 (2012). ISSN 1540-8140.

Mallette, F. A. and Richard, S. K48-linked ubiquitination and protein degradation regulate 53BP1 recruitment at DNA damage sites. *Cell Research* 22:1221–1223 (2012). ISSN 1001-0602.

Malli, R., Frieden, M., Trenker, M. and Graier, W. F. The role of mitochondria for Ca2+ refilling of the endoplasmic reticulum. *The Journal of biological chemistry* 280(13):12114–12122 (2005).

Mannella, C. a. Structure and dynamics of the mitochondrial inner membrane cristae. *Biochimica et biophysica acta* 1763(5-6):542–8 (2006). ISSN 0006-3002.

Maro, B., Marty, M. C. and Bornens, M. In vivo and in vitro effects of the mitochondrial uncoupler FCCP on microtubules. *The EMBO journal* 1:1347–1352 (1982). ISSN 0261-4189.

Martin, I., Dawson, V. L. and Dawson, T. M. Recent advances in the genetics of Parkinson's disease. *Annual review of genomics and human genetics* 12:301–325 (2011). ISSN 1545-293X.

Martin, M., Iyadurai, S. J., Gassman, A., Gindhart, J. G., Hays, T. S. and Saxton, W. M. Cytoplasmic dynein, the dynactin complex, and kinesin are interdependent and essential for fast axonal transport. *Molecular biology of the cell* 10(11):3717–3728 (1999). ISSN 1059-1524.

Martinez, T. N. and Greenamyre, J. T. Toxin models of mitochondrial dysfunction in Parkinson's disease. *Antioxidants & redox signaling* 16(9):920–934 (2012). ISSN 1557-7716.

Martinou, J. C., Desagher, S. and Antonsson, B. Cytochrome c release from mitochondria: all or nothing. *Nature cell biology* 2(3):E41–3 (2000). ISSN 1465-7392.

Mclelland, G.-l. L., Soubannier, V., Chen, C. X., McBride, H. M. and Fon, E. A. Parkin and PINK 1 function in a vesicular trafficking pathway regulating mitochondrial quality control. *EMBO Journal* 33(4):282–295 (2014).

Metzger, M. B., Hristova, V. a. and Weissman, A. M. HECT and RING finger families of E3 ubiquitin ligases at a glance. *Journal of cell science* 125(Pt 3):531–537 (2012). ISSN 1477-9137.

Mevissen, T. E. T., Hospenthal, M. K., Geurink, P. P., Elliott, P. R., Akutsu, M., Arnaudo, N., Ekkebus, R., Kulathu, Y., Wauer, T., El Oualid, F., Freund, S. M. V., Ovaa, H. and Komander, D. OTU deubiquitinases reveal mechanisms of linkage specificity and enable ubiquitin chain restriction analysis. *Cell* 154(1):169–84 (2013). ISSN 1097-4172.

Michiorri, S., Gelmetti, V., Giarda, E., Lombardi, F., Romano, F., Marongiu, R., Nerini-Molteni, S., Sale, P., Vago, R., Arena, G., Torosantucci, L., Cassina, L., Russo, M. a., Dallapiccola, B., Valente, E. M. and Casari, G. The Parkinson-associated protein PINK1 interacts with Beclin1 and promotes autophagy. *Cell death and differentiation* 17(6):962–74 (2010). ISSN 1476-5403.

Miller, K. E. and Sheetz, M. P. Axonal mitochondrial transport and potential are correlated. *Journal of cell science* 117(Pt 13):2791–804 (2004). ISSN 0021-9533.

Misko, A., Jiang, S., Wegorzewska, I., Milbrandt, J. and Baloh, R. H. Mitofusin 2 is necessary for transport of axonal mitochondria and interacts with the Miro/Milton complex. *The Journal of Neuroscience* 30(12):4232–4240 (2010). ISSN 1529-2401.

Mitchell, P. and Moyle, J. Chemiosmotic hypothesis of oxidative phosphorylation. *Nature* 213:137–139 (1967). ISSN 0028-0836.

Morais, V. A., Haddad, D., Craessaerts, K., De Bock, P.-J., Swerts, J., Vilain, S., Aerts, L., Overbergh, L., Grünewald, A., Seibler, P., Klein, C., Gevaert, K., Verstreken, P. and De Strooper, B. PINK1 loss-of-function mutations affect mitochondrial complex I activity via NdufA10 ubiquinone uncoupling. *Science* 344(6180):203–207 (2014). ISSN 1095-9203.

Morais, V. a., Verstreken, P., Roethig, A., Smet, J., Snellinx, A., Vanbrabant, M., Haddad, D., Frezza, C., Mandemakers, W., Vogt-Weisenhorn, D., Van Coster, R., Wurst,

W., Scorrano, L. and De Strooper, B. Parkinson's disease mutations in PINK1 result in decreased Complex I activity and deficient synaptic function. *EMBO molecular medicine* 1(2):99–111 (2009). ISSN 1757-4684.

Morlino, G., Barreiro, O., Baixauli, F., Robles-Valero, J., González-Granado, J. M., Villa-Bellosta, R., Cuenca, J., Sánchez-Sorzano, C. O., Veiga, E., Martín-Cófreces, N. B. and Sánchez-Madrid, F. Miro-1 links mitochondria and microtubule Dynein motors to control lymphocyte migration and polarity. *Molecular and cellular biology* 34(8):1412–1426 (2014). ISSN 1098-5549.

Mozdy, A. D., McCaffery, J. M. and Shaw, J. M. Dnm1p GTPase-mediated mitochondrial fission is a multi-step process requiring the novel integral membrane component Fis1p. *Jornal Cell Biology* 151(2):367–380 (2000).

Nangaku, M., Sato-Yoshitake, R., Okada, Y., Noda, Y., Takemura, R., Yamazaki, H. and Hirokawa, N. KIF1B, a novel microtubule plus end-directed monomeric motor protein for transport of mitochondria. *Cell* 79(7):1209–1220 (1994). ISSN 0092-8674.

Narendra, D., Kane, L. A., Hauser, D. N., Fearnley, I. M. and Youle, R. J. p62/SQSTM1 is required for Parkin-induced mitochondrial clustering but not mitophagy; VDAC1 is dispensable for both. *Autophagy* 6(8):1090–1106 (2010a).

Narendra, D., Tanaka, A., Suen, D. F. and Youle, R. J. Parkin is recruited selectively to impaired mitochondria and promotes their autophagy. *Journal Cell Biology* 183(5):795–803 (2008).

Narendra, D. P., Jin, S. M., Tanaka, A., Suen, D. F., Gautier, C. A., Shen, J., Cookson, M. R. and Youle, R. J. PINK1 is selectively stabilized on impaired mitochondria to activate Parkin. *PLoS Biology* 8(1):e1000298 (2010b).

Neuspiel, M., Schauss, A. C., Braschi, E., Zunino, R., Rippstein, P., Rachubinski, R. a., Andrade-Navarro, M. a. and McBride, H. M. Cargo-selected transport from the mitochondria to peroxisomes is mediated by vesicular carriers. *Current biology* 18(2):102–8 (2008). ISSN 0960-9822.

Overly, C. C., Rieff, H. I. and Hollenbeck, P. J. Organelle motility and metabolism in axons vs dendrites of cultured hippocampal neurons. *Journal of cell science* 109 (Pt 5:971–980 (1996). ISSN 0021-9533.

Palade, G. E. The fine structure of mitochondria. *The Anatomical record* 114(3):427–51 (1952). ISSN 0003-276X.

Park, J., Lee, S. B., Lee, S., Kim, Y., Song, S., Kim, S., Bae, E., Kim, J., Shong, M., Kim, J.-M. and Chung, J. Mitochondrial dysfunction in Drosophila PINK1 mutants is complemented by parkin. *Nature* 441(7097):1157–1161 (2006). ISSN 1476-4687.

Pekkurnaz, G., Trinidad, J. C., Wang, X., Kong, D. and Schwarz, T. L. Glucose Regulates Mitochondrial Motility via Milton Modification by O-GlcNAc Transferase. *Cell* 158(1):54–68 (2014). ISSN 1097-4172.

Piatkevich, K. D., Hulit, J., Subach, O. M., Wu, B., Abdulla, A., Segall, J. E. and Verkhusha, V. V. Monomeric red fluorescent proteins with a large Stokes shift. *Proceedings of the National Academy of Sciences of the United States of America* 107(12):5369–5374 (2010). ISSN 0027-8424.

Pilling, A. D., Horiuchi, D., Lively, C. M. and Saxton, W. M. Kinesin-1 and Dynein Are the Primary Motors for Fast Transport of Mitochondria in Drosophila Motor Axons. *Molecular Biology of the Cell* 17(April):2057–2068 (2006).

Plun-Favreau, H., Klupsch, K., Moisoi, N., Gandhi, S., Kjaer, S., Frith, D., Harvey, K., Deas, E., Harvey, R. J., McDonald, N., Wood, N. W., Martins, L. M. and Downward, J. The mitochondrial protease HtrA2 is regulated by Parkinson's disease-associated kinase PINK1. *Nature cell biology* 9(11):1243–1252 (2007). ISSN 1465-7392.

Pogson, J. H., Ivatt, R. M. and Whitworth, A. J. Molecular mechanisms of PINK1-related neurodegeneration. *Current neurology and neuroscience reports* 11(3):283–90 (2011). ISSN 1534-6293.

Polymeropoulos, M. H., Higgins, J. J., Golbe, L. I., Johnson, W. G., Ide, S. E., Di Iorio, G., Sanges, G., Stenroos, E. S., Pho, L. T., Schaffer, A. A., Lazzarini, A. M., Nussbaum, R. L. and Duvoisin, R. C. Mapping of a gene for Parkinson's disease to chromosome 4q21-q23. *Science* 274:1197–1199 (1996). ISSN 0036-8075.

Poole, A. C., Thomas, R. E., Andrews, L. a., McBride, H. M., Whitworth, A. J. and Pallanck, L. J. The PINK1/Parkin pathway regulates mitochondrial morphology. *Proceedings of the National Academy of Sciences of the United States of America* 105(5):1638–43 (2008). ISSN 1091-6490.

Poole, A. C., Thomas, R. E., Yu, S., Vincow, E. S. and Pallanck, L. The mitochondrial fusion-promoting factor mitofusin is a substrate of the PINK1/parkin pathway. *PLoS One* 5(4):e10054 (2010).

Pridgeon, J. W., Olzmann, J. a., Chin, L.-S. and Li, L. PINK1 protects against oxidative stress by phosphorylating mitochondrial chaperone TRAP1. *PLoS biology* 5(7):e172 (2007). ISSN 1545-7885.

Rakovic, A., Grünewald, A., Kottwitz, J., Brüggemann, N., Pramstaller, P. P., Lohmann, K. and Klein, C. Mutations in PINK1 and Parkin impair ubiquitination of Mitofusins in human fibroblasts. *PloS one* 6(3):e16746 (2011). ISSN 1932-6203.

Raturi, A. and Simmen, T. Where the endoplasmic reticulum and the mitochondrion tie the knot: the mitochondria-associated membrane (MAM). *Biochimica et biophysica acta* 1833(1):213–24 (2013). ISSN 0006-3002.

Rich, P. R. The molecular machinery of Keilin's respiratory chain. *Biochemical Society transactions* pages 1095–1105 (2003).

Riley, B. E., Lougheed, J. C., Callaway, K., Velasquez, M., Brecht, E., Nguyen, L., Shaler, T., Walker, D., Yang, Y., Regnstrom, K., Diep, L., Zhang, Z., Chiou, S., Bova, M., Artis, D. R., Yao, N., Baker, J., Yednock, T. and Johnston, J. A. Structure and function of Parkin E3 ubiquitin ligase reveals aspects of RING and HECT ligases. *Nature communications* 4:1982 (2013). ISSN 2041-1723.

Rintoul, G. L., Filiano, A. J., Brocard, J. B., Kress, G. J. and Reynolds, I. J. Glutamate decreases mitochondrial size and movement in primary forebrain neurons. *The Journal of neuroscience* 23(21):7881–7888 (2003). ISSN 1529-2401.

Rizzuto, R., Marchi, S., Bonora, M., Aguiari, P., Bononi, A., De Stefani, D., Giorgi, C., Leo, S., Rimessi, A., Siviero, R., Zecchini, E. and Pinton, P. Ca(2+) transfer from the ER to mitochondria: when, how and why. *Biochim Biophys Acta* 1787(11):1342–1351 (2009). ISSN 0006-3002.

Roberts, A. J., Kon, T., Knight, P. J., Sutoh, K. and Burgess, S. a. Functions and mechanics of dynein motor proteins. *Nature reviews. Molecular cell biology* 14(11):713–726 (2013). ISSN 1471-0080.

Russo, G. J., Louie, K., Wellington, A., Macleod, G. T., Hu, F., Panchumarthi, S. and Zinsmaier, K. E. Drosophila Miro is required for both anterograde and retrograde axonal mitochondrial transport. *The Journal of Neuroscience* 29(17):5443–5455 (2009).

Saotome, M., Safiulina, D., Szabadkai, G., Das, S., Fransson, A., Aspenstrom, P., Rizzuto, R. and Hajnoczky, G. Bidirectional Ca2+-dependent control of mitochondrial dynamics by the Miro GTPase. *Proceedings of the National Academy of Sciences of the United States of America* 105(52):20728–20733 (2008).

Sarraf, S. a., Raman, M., Guarani-Pereira, V., Sowa, M. E., Huttlin, E. L., Gygi, S. P. and Harper, J. W. Landscape of the PARKIN-dependent ubiquitylome in response to mitochondrial depolarization. *Nature* 496(7445):372–376 (2013). ISSN 1476-4687.

Schneider, J. L. and Cuervo, A. M. Autophagy and human disease: emerging themes. *Current opinion in genetics & development* 26C:16–23 (2014). ISSN 1879-0380.

Schwarzer, C., Barnikol-Watanabe, S., Thinnes, F. P. and Hilschmann, N. Voltage-dependent anion-selective channel (VDAC) interacts with the dynein light chain Tctex1 and the heat-shock protein PBP74. *The international journal of biochemistry & cell biology* 34(9):1059–70 (2002). ISSN 1357-2725.

Scorrano, L. Keeping mitochondria in shape: a matter of life and death. *European journal of clinical investigation* 43(8):886–893 (2013). ISSN 1365-2362.

Shiba-Fukushima, K., Imai, Y., Yoshida, S., Ishihama, Y., Kanao, T., Sato, S. and Hattori, N. PINK1-mediated phosphorylation of the Parkin ubiquitin-like domain primes mitochondrial translocation of Parkin and regulates mitophagy. *Scientific reports* 2:1002 (2012). ISSN 2045-2322.

Shiba-Fukushima, K., Inoshita, T., Hattori, N. and Imai, Y. PINK1-mediated phosphorylation of Parkin boosts Parkin activity in Drosophila. *PLoS genetics* 10(6):e1004391 (2014). ISSN 1553-7404.

Shin, J. H., Ko, H. S., Kang, H., Lee, Y., Lee, Y. I., Pletinkova, O., Troconso, J. C., Dawson, V. L. and Dawson, T. M. PARIS (ZNF746) repression of PGC-1a contributes to neurodegeneration in parkinson's disease. *Cell* 144:689–702 (2011). ISSN 00928674.

Sjostrand, F. Electron microscopy of mitochondria and cytoplasmic double membranes. *Nature* 171:30–31 (1953).

Slupe, A. M., Merrill, R. a., Flippo, K. H., Lobas, M. a., Houtman, J. C. D. and Strack, S. A calcineurin docking motif (LXVP) in dynamin-related protein 1 contributes to mitochondrial fragmentation and ischemic neuronal injury. *The Journal of biological chemistry* 288:12353–65 (2013). ISSN 1083-351X.

Smith, M. J., Pozo, K., Brickley, K. and Stephenson, F. A. Mapping the GRIF-1 binding domain of the kinesin, KIF5C, substantiates a role for GRIF-1 as an adaptor protein in the anterograde trafficking of cargoes. *The Journal of biological chemistry* 281(37):27216–27228 (2006). ISSN 0021-9258.

Soubannier, V., McLelland, G.-L., Zunino, R., Braschi, E., Rippstein, P., Fon, E. a. and McBride, H. M. A vesicular transport pathway shuttles cargo from mitochondria to lysosomes. *Current biology* 22(2):135–141 (2012). ISSN 1879-0445.

Staropoli, J. F., McDermott, C., Martinat, C., Schulman, B., Demireva, E. and Abeliovich, A. Parkin is a component of an SCF-like ubiquitin ligase complex and protects postmitotic neurons from kainate excitotoxicity. *Neuron* 37(5):735–49 (2003). ISSN 0896-6273.

Stowers, R. S., Megeath, L. J., Górska-Andrzejak, J., Meinertzhagen, I. a. and Schwarz, T. L. Axonal transport of mitochondria to synapses depends on milton, a novel Drosophila protein. *Neuron* 36(6):1063–1077 (2002). ISSN 0896-6273.

Su, Q., Cai, Q., Gerwin, C., Smith, C. L. and Sheng, Z.-H. Syntabulin is a microtubule-associated protein implicated in syntaxin transport in neurons. *Nature cell biology* 6(10):941–953 (2004). ISSN 1465-7392.

Sugiura, A., McLelland, G.-L., Fon, E. a. and McBride, H. M. A new pathway for mitochondrial quality control: mitochondrial-derived vesicles. *The EMBO journal* pages 1–15 (2014). ISSN 1460-2075.

Szabadkai, G. and Duchen, M. R. Mitochondria: the hub of cellular Ca2+ signaling. *Physiology (Bethesda, Md.)* 23:84–94 (2008). ISSN 1548-9213.

Tai, A. W., Chuang, J.-z., Bode, C., Wolfrum, U., Sung, C.-h. and Gutenberg-universita, J. Rhodopsin's Carboxy-Terminal Cytoplasmic Tail Acts as a Membrane Receptor for Cytoplasmic Dynein by Binding to the Dynein Light Chain Tctex-1. *Cell* 97:877–887 (1999).

Tanaka, A., Cleland, M. M., Xu, S., Narendra, D. P., Suen, D.-F. F., Karbowski, M. and Youle, R. J. Proteasome and p97 mediate mitophagy and degradation of mitofusins induced by Parkin. *The Journal of cell biology* 191(7):1367–80 (2010). ISSN 1540-8140.

Tanaka, K., Sugiura, Y., Ichishita, R., Mihara, K. and Oka, T. KLP6: a newly identified kinesin that regulates the morphology and transport of mitochondria in neuronal cells. *Journal of cell science* 124(14):2457–2465 (2011). ISSN 1477-9137.

Tanaka, Y., Kanai, Y., Okada, Y., Nonaka, S., Takeda, S., Harada, a. and Hirokawa, N. Targeted disruption of mouse conventional kinesin heavy chain, kif5B, results in abnormal perinuclear clustering of mitochondria. *Cell* 93(7):1147–58 (1998). ISSN 0092-8674.

Tasaki, T., Sriram, S. M., Park, K. S. and Kwon, Y. T. The N-end rule pathway. *Annual review of biochemistry* 81:261–289 (2012). ISSN 1545-4509.

Tondera, D., Czauderna, F., Paulick, K., Schwarzer, R., Kaufmann, J. and Santel, A. The mitochondrial protein MTP18 contributes to mitochondrial fission in mammalian cells. *J Cell Sci* 118(Pt 14):3049–3059 (2005).

Trancikova, A., Tsika, E. and Moore, D. J. Mitochondrial dysfunction in genetic animal models of Parkinson's disease. *Antioxidants & redox signaling* 16(9):896–919 (2012). ISSN 1557-7716.

Trempe, J.-F., Sauvé, V., Grenier, K., Seirafi, M., Tang, M. Y., Ménade, M., Al-Abdul-Wahid, S., Krett, J., Wong, K., Kozlov, G., Nagar, B., Fon, E. a. and Gehring, K. Structure of parkin reveals mechanisms for ubiquitin ligase activation. *Science (New York, N.Y.)* 340:1451–5 (2013). ISSN 1095-9203.

Trinidad, J. C., Barkan, D. T., Gulledge, B. F., Thalhammer, A., Sali, A., Schoepfer, R. and Burlingame, A. L. Global identification and characterization of both O-GlcNAcylation and phosphorylation at the murine synapse. *Molecular & cellular proteomics : MCP* 11(8):215–29 (2012). ISSN 1535-9484.

Twig, G., Elorza, A., Molina, A. J. a., Mohamed, H., Wikstrom, J. D., Walzer, G., Stiles, L., Haigh, S. E., Katz, S., Las, G., Alroy, J., Wu, M., Py, B. F., Yuan, J., Deeney, J. T., Corkey, B. E. and Shirihai, O. S. Fission and selective fusion govern mitochondrial segregation and elimination by autophagy. *The EMBO journal* 27(2):433–446 (2008). ISSN 1460-2075.

Valente, E. M., Abou-Sleiman, P. M., Caputo, V., Muqit, M. M. K., Harvey, K., Gispert, S., Ali, Z., Del Turco, D., Bentivoglio, A. R., Healy, D. G., Albanese, A., Nussbaum, R., González-Maldonado, R., Deller, T., Salvi, S., Cortelli, P., Gilks, W. P., Latchman, D. S., Harvey, R. J., Dallapiccola, B., Auburger, G. and Wood, N. W. Hereditary early-onset Parkinson's disease caused by mutations in PINK1. *Science (New York, N.Y.)* 304(5674):1158–1160 (2004). ISSN 1095-9203.

Van Humbeeck, C., Cornelissen, T., Hofkens, H., Mandemakers, W., Gevaert, K., De Strooper, B. and Vandenberghe, W. Parkin interacts with Ambra1 to induce mitophagy. *The Journal of neuroscience* 31(28):10249–61 (2011). ISSN 1529-2401.

van Spronsen, M., Mikhaylova, M., Lipka, J., Schlager, M. a., van den Heuvel, D. J., Kuijpers, M., Wulf, P. S., Keijzer, N., Demmers, J., Kapitein, L. C., Jaarsma, D., Gerritsen, H. C., Akhmanova, A. and Hoogenraad, C. C. TRAK/Milton motor-adaptor proteins steer mitochondrial trafficking to axons and dendrites. *Neuron* 77(3):485–502 (2013). ISSN 1097-4199.

Wagner, O. I., Lifshitz, J., Janmey, P. a., Linden, M., McIntosh, T. K. and Leterrier, J.-F. Mechanisms of mitochondria-neurofilament interactions. *The Journal of neuroscience* 23(27):9046–9058 (2003). ISSN 1529-2401.

Wagner, S. A., Beli, P., Weinert, B. T., Nielsen, M. L., Cox, J., Mann, M. and Choudhary, C. A Proteome-wide, Quantitative Survey of In Vivo Ubiquitylation Sites Reveals Widespread Regulatory Roles. *Molecular & Cellular Proteomics* 10:M111.013284–M111.013284 (2011). ISSN 1535-9476.

Wang, H., Song, P., Du, L., Tian, W., Yue, W., Liu, M., Li, D., Wang, B., Zhu, Y., Cao, C., Zhou, J. and Chen, Q. Parkin ubiquitinates Drp1 for proteasome-dependent degradation: implication of dysregulated mitochondrial dynamics in Parkinson disease. *The Journal of biological chemistry* 286(13):11649–11658 (2011a). ISSN 1083-351X.

Wang, H. J., Guay, G., Pogan, L., Sauvé, R. and Nabi, I. R. Calcium regulates the association between mitochondria and a smooth subdomain of the endoplasmic reticulum. *The Journal of cell biology* 150(6):1489–1498 (2000). ISSN 0021-9525.

Wang, X. and Schwarz, T. L. The mechanism of Ca2+ -dependent regulation of kinesin-mediated mitochondrial motility. *Cell* 136(1):163–74 (2009). ISSN 1097-4172.

Wang, X., Winter, D., Ashrafi, G., Schlehe, J., Wong, Y. L., Selkoe, D., Rice, S., Steen, J., Lavoie, M. J. and Schwarz, T. L. PINK1 and Parkin Target Miro for Phosphorylation and Degradation to Arrest Mitochondrial Motility. *Cell* 147(4):893–906 (2011b). ISSN 00928674.

Wang, Y., Nartiss, Y., Steipe, B., McQuibban, G. A. and Kim, P. K. ROS-induced mitochondrial depolarization initiates PARK2/PARKIN-dependent mitochondrial degradation by autophagy. *Autophagy* 8(10):1462–76 (2012). ISSN 1554-8635.

Waterman-Storer, C. M., Karki, S. B., Kuznetsov, S. a., Tabb, J. S., Weiss, D. G., Langford, G. M. and Holzbaur, E. L. The interaction between cytoplasmic dynein and dynactin is required for fast axonal transport. *Proceedings of the National Academy of Sciences of the United States of America* 94(22):12180–12185 (1997). ISSN 0027-8424.

Wauer, T. and Komander, D. Structure of the human Parkin ligase domain in an autoinhibited state. *The EMBO journal* 32(15):2099–2112 (2013). ISSN 1460-2075.

Webber, E., Li, L. and Chin, L.-S. Hypertonia-associated protein Trak1 is a novel regulator of endosome-to-lysosome trafficking. *Journal of molecular biology* 382(3):638–51 (2008). ISSN 1089-8638.

Weihofen, A., Thomas, K. J., Ostaszewski, B. L., Cookson, M. R. and Selkoe, D. J. Pink1 forms a multiprotein complex with Miro and Milton, linking Pink1 function to mitochondrial trafficking. *Biochemistry* 48(9):2045–2052 (2009).

Wells, L., Whalen, S. A. and Hart, G. W. O-GlcNAc: A regulatory post-translational modification (2003).

Westermann, B. Mitochondrial fusion and fission in cell life and death. *Nature Reviews Molecular Cell Biology* 11(12):872–884 (2010).

Winter, L., Abrahamsberg, C. and Wiche, G. Plectin isoform 1b mediates mitochondrion-intermediate filament network linkage and controls organelle shape. *The Journal of cell biology* 181(6):903–11 (2008). ISSN 1540-8140.

Wood-Kaczmar, A., Gandhi, S., Yao, Z., Abramov, A. Y., Miljan, E. A., Keen, G., Stanyer, L., Hargreaves, I., Klupsch, K., Deas, E., Downward, J., Mansfield, L., Jat, P., Taylor, J., Heales, S., Duchen, M. R., Latchman, D., Tabrizi, S. J. and Wood,

N. W. PINK1 is necessary for long term survival and mitochondrial function in human dopaminergic neurons. *PLoS One* 3(6):e2455 (2008).

Yamano, K., Fogel, A. I., Wang, C., van der Bliek, A. M. and Youle, R. J. Mitochondrial Rab GAPs govern autophagosome biogenesis during mitophagy. *eLife* 3:e01612 (2014). ISSN 2050-084X.

Yamano, K. and Youle, R. J. PINK1 is degraded through the N-end rule pathway. *Autophagy* 9(11):1758–1769 (2013). ISSN 1554-8635.

Yang, Y., Gehrke, S., Imai, Y., Huang, Z., Ouyang, Y., Wang, J.-W., Yang, L., Beal, M. F., Vogel, H. and Lu, B. Mitochondrial pathology and muscle and dopaminergic neuron degeneration caused by inactivation of Drosophila Pink1 is rescued by Parkin. *Proceedings of the National Academy of Sciences of the United States of America* 103(28):10793–10798 (2006). ISSN 0027-8424.

Yang, Y., Ouyang, Y., Yang, L., Beal, M. F., Mcquibban, A., Vogel, H. and Lu, B. Pink1 regulates mitochon- drial dynamics through interaction with the fission/fusion machinery. *Proceedings of the National Academy of Sciences of the United States of America* 105(45) (2008).

Ye, Y., Akutsu, M., Reyes-Turcu, F., Enchev, R. I., Wilkinson, K. D. and Komander, D. Polyubiquitin binding and cross-reactivity in the USP domain deubiquitinase USP21. *EMBO Rep* 12(4):350–357 (2011).

Yi, M., Weaver, D. and Hajnóczky, G. Control of mitochondrial motility and distribution by the calcium signal: a homeostatic circuit. *The Journal of cell biology* 167(4):661–672 (2004). ISSN 0021-9525.

Yokoyama, N., Hayashi, N., Seki, T., Pante, N., Ohba, T., Nishii, K., Kuma, K., Hayashida, T., Miyata, T., Aebi, U., Fukui, M. and Nishimoto, T. A giant nucleopore protein that binds Ran/TC4. *Letters to Nature* 376:184–188 (1995).

Yoshii, S. R., Kishi, C., Ishihara, N. and Mizushima, N. Parkin mediates proteasome-dependent protein degradation and rupture of the outer mitochondrial membrane. *The Journal of biological chemistry* 286(22):19630–19640 (2011).

Youle, R. J. and Narendra, D. P. Mechanisms of mitophagy. *Nature reviews. Molecular cell biology* 12(1):9–14 (2011). ISSN 1471-0080.

Zhang, C., Lee, S., Peng, Y., Bunker, E., Giaime, E., Shen, J., Zhou, Z. and Liu, X. PINK1 Triggers Autocatalytic Activation of Parkin to Specify Cell Fate Decisions. *Current biology : CB* 24(16):1854–1865 (2014). ISSN 1879-0445.

Zhang, Y., Gao, J., Chung, K. K., Huang, H., Dawson, V. L. and Dawson, T. M. Parkin functions as an E2-dependent ubiquitin- protein ligase and promotes the degradation of the synaptic vesicle-associated protein, CDCrel-1. *Proceedings of the National Academy of Sciences of the United States of America* 97(24):13354–13359 (2000).

Zhou, C., Huang, Y. and Przedborski, S. Oxidative stress in Parkinson's disease: A mechanism of pathogenic and therapeutic significance. In *Annals of the New York Academy of Sciences*, volume 1147, pages 93–104 (2008a). ISBN 9781573317139. ISSN 00778923.

Zhou, C., Huang, Y., Shao, Y., May, J., Prou, D., Perier, C., Dauer, W., Schon, E. A. and Przedborski, S. The kinase domain of mitochondrial PINK1 faces the cytoplasm. *Proceedings of the National Academy of Sciences of the United States of America* (2008b).

Ziviani, E., Tao, R. N. and Whitworth, A. J. Drosophila parkin requires PINK1 for mitochondrial translocation and ubiquitinates mitofusin. *Proceedings of the National Academy of Sciences of the United States of America* 107(11):5018–5023 (2010).